

Molecular Analysis of the Unconventional
Export Machinery of HASPB,
a component of the surface coat of
Leishmania parasites

Dissertation submitted to the
Combined Faculties for the Natural Sciences and for Mathematics
of the Ruperto Carola University of Heidelberg, Germany

for the degree of
Doctor of Natural Sciences

presented by

Diplom-Biologin Carolin Stegmayer
born in Bad Kreuznach

DISSERTATION

submitted to the
Combined Faculties for the Natural Sciences and for Mathematics
of the Ruperto Carola University of Heidelberg, Germany



for the degree of
Doctor of Natural Sciences

presented by

Diplom-Biologin Carolin Stegmayer
born in Bad Kreuznach

Oral examination:

Molecular Analysis of the Unconventional
Export Machinery of HASPB,
a component of the surface coat of
Leishmania parasites

Referees:

Prof. Dr. rer. nat. Walter Nickel

Prof. Dr. rer. nat. Michael Brunner

List of Publications

Engling, A., Backhaus, R., Stegmayer, C., Zehe, C., Seelenmeyer, C., Kehlenbach, A., Schwappach, B., Wegehlingel, S., and Nickel, W. (2002). Biosynthetic FGF-2 is targeted to non-lipid raft microdomains following translocation to the extracellular surface of CHO cells. *J Cell Sci* *115*, 3619-3631.

Stegmayer, C., Kehlenbach, A., Tournaviti, S., Wegehlingel, S., Zehe, C., Denny, P., Smith, D. F., Schwappach, B., and Nickel, W. (2005). Direct transport across the plasma membrane of mammalian cells of Leishmania HASPB as revealed by a CHO export mutant. *J Cell Sci* *118*, 517-527.

Tournaviti, S., Hannemann, S., Terjung, S., Kitzing, T. M., Stegmayer, C., Ritzerfeld, J., Grosse, R., Nickel, W., and Fackler, O. T. (2006 submitted). SH4 Domain-induced Plasma Membrane Blebbing Implicated in 3D Cell Motility.

Contents

| | |
|---|-----------|
| ABBREVIATION | 1 |
| ZUSAMMENFASSUNG..... | 5 |
| SUMMARY | 7 |
| 1 INTRODUCTION | 9 |
| 1.1 CLASSICAL OR ER-GOLGI-MEDIATED PROTEIN SECRETION..... | 10 |
| 1.2 NON-CLASSICAL OR UNCONVENTIONAL PROTEIN SECRETION..... | 17 |
| 1.3 HYDROPHILIC ACYLATED SURFACE PROTEIN B (HASPB) | 21 |
| 1.3.1 <i>Dual acylation mediated by myristoylation and palmitoylation</i> | 22 |
| 1.3.2 <i>Leishmania parasites</i> | 26 |
| 1.3.3 <i>Life Cycle of Leishmania parasites</i> | 27 |
| 1.3.4 <i>Composition and assembly of the Leishmania surface coat</i> | 29 |
| 1.3.5 <i>Non-classical export of HASPB</i> | 31 |
| 1.3.6 <i>HASPB is of exceptional biomedical relevance</i> | 36 |
| 1.4 FIBROBLAST GROWTH FACTOR-1 AND- 2 (FGF-1 AND -2) | 37 |
| 1.5 GALECTIN-1..... | 40 |
| 1.6 AIM OF THE CURRENT STUDY | 43 |
| 2 MATERIAL AND METHODS..... | 44 |
| 2.1 MATERIAL..... | 44 |
| 2.1.1 <i>Chemicals</i> | 44 |
| 2.1.2 <i>Plasmids</i> | 48 |
| 2.1.3 <i>DNA modifying enzymes</i> | 49 |
| 2.1.4 <i>Primers and oligonucleotides</i> | 49 |
| 2.1.5 <i>Bacteria and bacterial media</i> | 51 |
| 2.1.6 <i>Eukaryotic cell lines</i> | 52 |
| 2.1.7 <i>Eukaryotic cell culture media (Wilson et al., 1994)</i> | 52 |
| 2.1.8 <i>Primary antibodies</i> | 53 |
| 2.1.9 <i>Secondary antibodies</i> | 54 |
| 2.2 MOLECULAR BIOLOGICAL METHODS | 54 |
| 2.2.1 <i>Bacterial transformation</i> | 54 |
| 2.2.2 <i>Selection and amplification of plasmids</i> | 55 |
| 2.2.3 <i>Plasmid preparation</i> | 55 |
| 2.2.4 <i>Isolation of genomic DNA from cultured cells</i> | 56 |
| 2.2.5 <i>Isolation of RNA from cultured cells</i> | 56 |
| 2.2.6 <i>Determination of DNA/RNA concentrations</i> | 57 |
| 2.2.7 <i>Agarose gel electrophoresis</i> | 58 |
| 2.2.8 <i>DNA sample buffer/loading buffer</i> | 59 |

| | | |
|--------|---|----|
| 2.2.9 | DNA marker | 59 |
| 2.2.10 | Polymerase chain reaction | 60 |
| 2.2.11 | RT-PCR..... | 62 |
| 2.2.12 | PCR purification | 64 |
| 2.2.13 | Gel extraction of DNA fragments | 64 |
| 2.2.14 | Restriction digests..... | 65 |
| 2.2.15 | Elongation of DNA using the Klenow fragment..... | 65 |
| 2.2.16 | DNA dephosphorylation..... | 66 |
| 2.2.17 | Ligation of DNA fragments | 66 |
| 2.2.18 | DNA sequencing | 67 |
| 2.2.19 | Short interfering RNAs (siRNAs) in mammalian cells | 67 |
| 2.3 | EUKARYOTIC CELL CULTURE TECHNIQUES | 68 |
| 2.3.1 | Maintaining cell lines..... | 68 |
| 2.3.2 | Freezing of eukaryotic cells | 69 |
| 2.3.3 | Thawing of eukaryotic cells | 70 |
| 2.3.4 | Retroviral transduction | 70 |
| 2.3.5 | Doxycycline-dependent protein expression..... | 72 |
| 2.4 | BIOCHEMICAL METHODS | 72 |
| 2.4.1 | Generation of cell lines expressing various HASPB-GFP fusion proteins | 72 |
| 2.4.2 | Sample preparation for SDS polyacrylamide gel electrophoresis (SDS-PAGE) | 73 |
| 2.4.3 | SDS polyacrylamide gel electrophoresis | 73 |
| 2.4.4 | SDS-PAGE protein molecular weight standards..... | 75 |
| 2.4.5 | Silver staining | 76 |
| 2.4.6 | Western blot analysis..... | 77 |
| 2.4.7 | Immunochemical protein detection using the ECL system | 78 |
| 2.4.8 | Immunochemical protein detection using the LICOR system | 79 |
| 2.4.9 | Preparation of cell lysates..... | 80 |
| 2.4.10 | Biotinylation of cell surface proteins | 80 |
| 2.4.11 | Biochemical analysis of membrane association of HASPB-GFP fusion proteins | 82 |
| 2.4.12 | Metabolic labeling of CHO cells using ³ [H]myristate and ³ [H]palmitate..... | 83 |
| 2.4.13 | Biochemical analysis of the subcellular distribution of HASPB-GFP in CHO cells using subcellular fractionation | 84 |
| 2.4.14 | Biochemical analysis of HASPB export from CHO cells using immunoprecipitation from cell culture supernatants | 85 |
| 2.4.15 | Precipitation of HASPB-GFP fusion proteins using TCA | 86 |
| 2.4.16 | Biochemical analysis of membrane sediments containing various GFP fusion proteins using ultracentrifugation of cell culture supernatants..... | 87 |
| 2.4.17 | Biochemical analysis of extracellular vesicles containing various GFP fusion proteins using flotation in Nycodenz gradients | 87 |

| | | |
|----------|--|-----------|
| 2.4.18 | <i>Biochemical analysis of extracellular vesicles containing various GFP fusion proteins using continuous sucrose gradients</i> | 88 |
| 2.4.19 | <i>Biochemical analysis of the localization of HASPB-GFP in extracellular vesicles using protease protection experiments</i> | 89 |
| 2.5 | FLOW CYTOMETRY | 90 |
| 2.5.1 | <i>Fluorescence activated cell sorting (FACS)</i> | 90 |
| 2.5.2 | <i>FACS-sorting</i> | 91 |
| 2.5.3 | <i>Retroviral insertion mutagenesis and FACS-based isolation of HASPB export mutants</i> | 92 |
| 2.6 | CONFOCAL MICROSCOPY | 92 |
| 2.6.1 | <i>Confocal microscopy using fixed cells</i> | 92 |
| 2.6.2 | <i>Live confocal imaging</i> | 93 |
| 2.7 | ELECTRON MICROSCOPY | 93 |
| 2.7.1 | <i>Electron microscopy using microsections of membrane sediments containing HASPB-GFP</i> | 93 |
| 3 | RESULTS | 95 |
| A. | DIRECT TRANSPORT ACROSS THE PLASMA MEMBRANE OF MAMMALIAN CELLS OF LEISHMANIA HASPB AS REVEALED BY A CHO EXPORT MUTANT | 95 |
| 3.1 | GENERATION OF MODEL CELL LINES TO STUDY HASPB EXPORT FROM MAMMALIAN CELLS | 96 |
| 3.1.1 | <i>Retroviral transduction of HASPB-N18-GFP reporter molecules in pRevTRE2</i> | 96 |
| 3.1.2 | <i>Sorting of doxycycline-inducible single clones</i> | 97 |
| 3.1.3 | <i>Characterization of HASPB fusion protein-expressing cell lines</i> | 98 |
| 3.1.4 | <i>Subcellular distribution of HASPB-N18-GFP fusion proteins as determined by confocal microscopy</i> | 99 |
| 3.1.5 | <i>Functional analysis of HASPB-N18-GFP export from CHO cells based on quantitative flow cytometry</i> | 101 |
| 3.1.6 | <i>Biochemical analysis of HASPB-N18-GFP export to the outer leaflet of the plasma membrane of CHO cells</i> | 103 |
| 3.1.7 | <i>Membrane association of HASPB-N18-GFP fusion proteins expressed in CHO cells</i> | 104 |
| 3.2 | RANDOM SOMATIC MUTAGENESIS BY RETROVIRAL INSERTION IN ORDER TO GENERATE CHO MUTANTS DEFECTIVE IN HASPB EXPORT | 106 |
| 3.2.1 | <i>Random somatic mutagenesis by retroviral insertion</i> | 106 |
| 3.2.2 | <i>Screening for somatic CHO mutants characterized by a defect in HASPB export</i> | 108 |
| 3.2.3 | <i>Sequence analysis of HASPB-N18-GFP in CHO wild-type and CHO K3 cell lines</i> | 110 |
| 3.2.4 | <i>Characterization of HASPB-N18-GFP export from CHO wild-type cells compared to CHO K3 mutant cells employing FACS-analysis and Biotinylation</i> | 112 |

| | | |
|-------|--|-----|
| 3.2.5 | <i>Expression level, membrane association and post-translational acylation of HASPB-N18-GFP in CHO wild-type cells and mutant K3 cells</i> | 114 |
| 3.2.6 | <i>HASPB-N18-GFP localizes to the plasma membrane in CHO K3 cells</i> | 116 |
| 3.2.7 | <i>An FGF-2-GFP reporter molecule is exported from CHO wild-type and K3 mutant cells at similar levels</i> | 118 |
| 3.2.8 | <i>Secretion of Galectin-1 from CHO K3 cells occurs as efficiently as from parental CHO wild-type cells</i> | 119 |
| 3.3 | ANALYSIS OF THE PHENOTYPE OBSERVED IN THE CHO K3 MUTANT CELL LINE | 121 |
| 3.3.1 | <i>Identification of the chemokine-orphan-receptor 1 (cmkor 1) in the CHO K3 mutant cell line</i> | 121 |
| 3.3.2 | <i>Sequence analysis of the chemokine orphan receptor 1 expressed in CHO cells</i> | 125 |
| 3.3.3 | <i>HASPB-N18-GFP export from CHO wild-type is not affected by downregulation of cmkor 1</i> | 125 |
| 3.3.4 | <i>Overexpression of cmkor 1 in CHO wild-type and CHO K3 cell lines</i> | 127 |
| 3.3.5 | <i>HASPB-N18-GFP export from CHO K3 cell line cannot be restored by overexpression of cmkor 1</i> | 129 |
| 3.3.6 | <i>Quantitative analysis of cell surface localized HASPB-N18-GFP fusion proteins exported from cmkor 1 transduced CHO wild-type and CHO K3 cell lines</i> | 131 |
| B. | THE SH4 PROTEIN HASPB IS RELEASED IN EXTRACELLULAR VESICLES IN A PALMITOYLATION-DEPENDENT MANNER | 133 |
| 3.4 | CHARACTERIZATION OF HASPB-MEDIATED PLASMA MEMBRANE BLEB FORMATION | 134 |
| 3.4.1 | <i>Heterologous expression of an HASPB-N18-GFP fusion protein induces curvature of the plasma membrane resulting in the formation of highly dynamic, non-apoptotic plasma membrane blebs</i> | 134 |
| 3.4.2 | <i>The Leishmania protein HASPB can be found in extracellular vesicles following ultracentrifugation of cell culture supernatants from growing HASPB-N18-GFP expressing cells</i> | 135 |
| 3.4.3 | <i>Flotation of HASPB-containing vesicles in Nycodenz gradients</i> | 137 |
| 3.4.4 | <i>Characterization of the floated material using different exosomes markers</i> | 139 |
| 3.4.5 | <i>HASPB-N18-GFP is localized in the lumen of extracellular vesicles as revealed by protease protection experiments</i> | 141 |
| 3.4.6 | <i>Quantitative analysis of extracellular vesicles containing various HASPB reporter molecules</i> | 142 |
| 3.4.7 | <i>Quantitative analysis of extracellular vesicles containing FGF-2 and Galectin-1</i> | 143 |
| 3.4.8 | <i>Extracellular HASPB-containing vesicles have an apparent density similar to that of exosomes</i> | 145 |
| 3.5 | THE ROLE OF ROCK KINASE ON HASPB-N18-GFP-INDUCED PLASMA MEMBRANE BLEBBING AND VESICLE-ASSOCIATED HASPB-N18-GFP | 147 |

| | | |
|----------|---|------------|
| 3.5.1 | <i>HASPB-N18-GFP mediated plasma membrane blebbing is blocked in the presence of Rock inhibitor</i> | 147 |
| 3.5.2 | <i>Levels of HASPB-containing extracellular vesicles only partially decrease in the presence of Rock inhibitor</i> | 148 |
| 3.6 | CHARACTERIZATION OF SRC, FYN, YES AND LCK REGARDING PLASMA MEMBRANE BLEBBING AND EXTRACELLULAR VESICLES | 150 |
| 3.6.1 | <i>Plasma membrane blebs are also induced by Src, Fyn, Yes and Lck</i> | 150 |
| 3.6.2 | <i>Quantitative analysis of extracellular vesicles containing Src, Fyn, Yes and Lck</i> | 152 |
| 3.6.3 | <i>The extracellular vesicle populations containing Src, Fyn, Yes and Lck are notably reduced in presence of Rock inhibitor compared to the HASPB-containing vesicle population</i> | 154 |
| 3.7 | CHARACTERIZATION OF HASPB-CONTAINING VESICLES DERIVED FROM HELa CELL LINES | 157 |
| 3.7.1 | <i>HASPB-N18-GFP mediated plasma membrane blebbing is notably reduced in HeLa cells compared to CHO cells</i> | 157 |
| 3.7.2 | <i>Flotation of HASPB-containing extracellular vesicles derived from HeLa cells in Nycodenz gradients</i> | 158 |
| 3.7.3 | <i>HASPB-containing extracellular vesicles derived from HeLa cells have an apparent density similar to that of exosomes</i> | 159 |
| 3.7.4 | <i>Confocal images of extracellular vesicles containing various reporter molecules</i> | 161 |
| 3.7.5 | <i>Ultrastructural analysis of extracellular vesicles employing electron microscopy</i> | 163 |
| 3.8 | SUPPLEMENTARY FIGURES | 164 |
| 4 | DISCUSSION | 170 |
| | A. DIRECT TRANSPORT ACROSS THE PLASMA MEMBRANE OF MAMMALIAN CELLS OF LEISHMANIA HASPB AS REVEALED BY A CHO EXPORT MUTANT | 171 |
| 4.1 | TRANSDUCE CHO CELLS STABLY EXPRESSING HASPB-N18-GFP EXPORT THE FUSION PROTEIN TO THE CELL SURFACE | 172 |
| 4.2 | HASPB-N18-GFP EXPRESSED IN CHO K3 MUTANT CELLS IS STABLY ASSOCIATED WITH THE PLASMA MEMBRANE, BUT GETS EXPORTED TO REDUCED LEVELS AS COMPARED TO CHO WILD-TYPE CELLS | 173 |
| 4.3 | THE INTEGRATION OF THE RETROVIRUS INTO THE GENOME OF CHO K3 CELLS DOES NOT CAUSE THE PERTURBED HASPB MEMBRANE TRANSLOCATION | 175 |

| | |
|---|------------|
| B. THE SH4 PROTEIN HASPB IS RELEASED IN EXTRACELLULAR VESICLES IN A PALMITOYLATION-DEPENDENT MANNER..... | 177 |
| 4.4 HASPB-N18-GFP-EXPRESSING CHO CELL LINES INDUCE BLEB FORMATION AND RELEASE HASPB-CONTAINING VESICLES INTO THE EXTRACELLULAR SPACE | 179 |
| 4.5 THE ROCK INHIBITOR BLOCKS THE FORMATION OF BLEBS BUT ONLY PARTIALLY REDUCES THE AMOUNT OF HASPB-CONTAINING VESICLES..... | 181 |
| 4.6 SRC, FYN, YES AND LCK MEDIATE PLASMA MEMBRANE BLEBBING, HOWEVER LESS AMOUNTS OF THE REPORTER MOLECULES COMPARED TO HASPB ARE FOUND IN EXTRACELLULAR VESICLES..... | 182 |
| 4.7 HASPB-N18-GFP EXPRESSED IN HELa CELL LINES CAN BE FOUND ASSOCIATED WITH EXTRACELLULAR VESICLES, HOWEVER PLASMA MEMBRANE BLEBBING IS LARGELY REDUCED | 183 |
| 4.8 MODELS FOR THE UNCONVENTIONAL SECRETION OF HASPB..... | 185 |
| REFERENCES | 190 |
| ACKNOWLEDGEMENT | 210 |

Abbreviation

| Abbreviation | |
|--------------|--|
| ABC | ATP binding cassette |
| APC | allophycocyanin |
| AP | Adaptor protein |
| APS | ammonium peroxo disulphate |
| ARF | ADP-ribosylation factor 1 |
| ATP | adenosin triphosphate |
| BFA | brefeldin A |
| bp | basepairs |
| cDNA | complementary DNA |
| CDB | cell dissociation buffer |
| CHO | Chinese hamster ovary (cells) |
| CRD | carbohydrate recognition domain |
| COP | Coat proteine |
| C-terminal | carboxy terminal |
| DAG | Diacylglycerin |
| DMSO | dimethyl sulphoxide |
| DNA | desoxyribonucleic acid |
| E.coli | Escherichia coli |
| e.g. | exempli gratia |
| ECL | enhanced chemoluminescence |
| ECM | Extracellular matrix |
| EDTA | ethylenediaminetetraacetic acid |
| EGF | epidermal growth factor |
| En2 | engrailed 2 |
| ER | endoplasmatic reticulum |
| ERGIC | ER-Golgi intermediate compartment |
| ESCRT | endosomal complex required for transport |
| et al. | et alii |
| FACS | fluorescence activated cell sorting |

| | |
|-----------------|--|
| FCS | fetal calf serum |
| FGF2 | fibroblast growth factor 2 |
| FGFR | fibroblast growth factor receptor |
| FV | Foamy virus |
| g_{av} | Average gravitation |
| GAG | glycosaminoglycans |
| Gal-1 | galectin-1 |
| GEF | guanine nucleotide exchange factor |
| GFP | green fluorescence protein |
| GM1 | Ganglioside GM1 |
| GPI | glycosyl phosphatidyl inositol |
| GTP | guanosine triphosphate |
| h | hour |
| HASPB | hydrophilic acylated surface protein B |
| HCl | hydrochlorid acid |
| HEK 293T | human endothelial kidney (cells) |
| HeLa | Henrietta Lacks (cells) |
| HIV | human immunodeficiency virus |
| HMGB | high mobility group protein |
| HRP | horse raddish peroxidase |
| HS | heparan sulfate |
| HSPG | heparan sulfate proteoglycans |
| i.e. | id est |
| IgG | Immunoglobulin G |
| IL | interleukin |
| IP ₃ | inositol triphosphate |
| IRES | internal ribosome entry side |
| kDa | kilo Dalton |
| LB | Luria Bertani |
| LTR | long terminal repeat |
| MCAT | Mouse cationic amino acid transporter |
| MIF | migration inhibitory factor |
| MVB | multivesicular body |

| | |
|--------------|---|
| MVE | multivesicular endosome |
| MVT | multivesicular tubule |
| nm | Nanometer (wavelength) |
| NMT | N-myristoyl transferase |
| NSF | N-ethylmaleimide sensitive factor |
| N-terminal | Amino terminal |
| ORF | open reading frame |
| PAGE | polyacrylamide gel electrophoresis |
| PBS | phosphate buffered saline |
| PCR | polymerase chain reaction |
| PE | phycoerythrin |
| PKC | Proteinkinase C |
| PLC γ | Phospholipase C γ |
| PS | phosphatidylserine |
| PVDF | polyvinyliden fluoride |
| RNA | ribonucleic acid |
| RT | Room temperature |
| RT-PCR | Reverse transcriptase-PCR |
| SDS | sodium dodecyl sulfate |
| SHERP | small hydrophilic endoplasmic reticulum (ER)- associated protein |
| SNAP | Soluble NSF attachment protein |
| SNARE | SNAP receptors |
| SRP | signal recognition particle |
| Tat | HIV transactivator protein |
| TEMED | N,N;N',N'-tetramethylethylenediamine |
| TRAM | Translocation chain associating membrane |
| Tris | Tris[hydroxymethyl]aminoethane |
| Tween 20 | polyoxethylene sorbitane monolaureate |
| U | units (enzyme activity) |
| UDP | Uridine diphosphate |
| v/v | volume/volume relationship |
| VEGF | vascular endothelial growth factor |

| | |
|---------------|--|
| vps | vacuolar protein sorting |
| w/v | weight/volume relationship |
| α -MEM | α -modification of Minimal Essential Medium |

Amino Acids

| Abbreviation | Abbreviation | Amino acid |
|--------------|--------------|---------------|
| A | Ala | Alanine |
| C | Cys | Cysteine |
| D | Asp | Aspartic acid |
| E | Glu | Glutamic acid |
| F | Phe | Phenylalanine |
| G | Gly | Glycine |
| H | His | Histidine |
| I | Ile | Isoleucine |
| K | Lys | Lysine |
| L | Leu | Leucine |
| M | Met | Methionine |
| N | Asn | Asparagine |
| P | Pro | Proline |
| Q | Gln | Glutamine |
| R | Arg | Arginine |
| S | Ser | Serine |
| T | Thr | Threonine |
| V | Val | Valine |
| W | Trp | Tryptophan |
| Y | Tyr | Tyrosine |

Zusammenfassung

Leishmania HASPB ist ein Lipoprotein, das unkonventionell sowohl von *Leishmania* Parasiten als auch von Säugetierzellen exportiert wird (Denny et al., 2000; Stegmayer et al., 2005). Exportiertes HASPB bleibt aufgrund einer Myristoylierung und einer Palmitoylierung in der N-terminalen SH4 Domäne auf der extrazellulären Oberfläche der Plasmamembran verankert (Denny et al., 2000; Stegmayer et al., 2005). Diese SH4-spezifische Acylierung erfolgt an intrazellulären Membranen und ist die Voraussetzung für den Transport von HASPB zur Plasmamembran. Zum heutigen Standpunkt jedoch ist der Exportweg von HASPB noch ungeklärt, im speziellen der subzelluläre Ort der HASPB Membrantranslokation. Zudem sind mögliche molekulare Maschinen für den Export von HASPB noch nicht bekannt. Aus diesem Grund wurden mittels somatischer Mutagenese klonale CHO Mutanten generiert, die sich durch einen Defekt im HASPB Export auszeichneten. HASPB war in einer solchen Mutante (CHO K3) sowohl myristoyliert als auch palmitoyliert und konnte assoziiert mit der Plasmamembran nachgewiesen werden, wie konfokale Mikroskopie und subzelluläre Fraktionierung gezeigt haben. Im Gegensatz dazu war der Transport von HASPB an die extrazelluläre Oberfläche der Plasmamembran, trotz eines mit dem Wildtyp übereinstimmenden Expressionslevels, in CHO K3 Zellen stark reduziert. Dies wurde sowohl mittels Durchflusszytometrie als auch biochemischer Zelloberflächenbiotinylierung nachgewiesen. Daraus resultierend scheint die Plasmamembran der subzelluläre Ort der HASPB Membrantranslokation zu sein. Dies wird durch die Akkumulation des Fusionsproteins an dieser Stelle im Falle eines Exportdefekts bestätigt. Anhand dieser Daten kann ein Exportmodell aufgestellt werden, in dem, im ersten Schritt, die SH4 Acylierung den intrazellulären Transport von HASPB an die Plasmamembran vermittelt. Dort wird dann im zweiten Schritt die Translokation von HASPB über eine Plasmamembran-lokalisierte Maschinerie, welche in CHO K3 Zellen defekt zu sein scheint, ermöglicht. Interessanterweise werden FGF-2 und Galectin-1, beides unkonventionell sezernierte Proteine, in CHO K3 Zellen an die Oberfläche der

Plasmamembran transloziert. Dies beweist, dass die entsprechende Komponente, die in der Exportmaschinerie von CHO K3 Zellen defekt ist, eine wichtige Funktion spezifisch im Export von HASPB einnimmt. Der in CHO K3 Zellen identifizierte Chemokine Orphan Rezeptor 1 konnte als Ursache für den HASPB Exportdefekt dieser Zellen ausgeschlossen werden.

Im zweiten Teil dieser Arbeit konnte gezeigt werden, dass das SH4 Protein HASPB, neben seiner Lokalisation an der Zelloberfläche, zudem noch mit extrazellulären Vesikeln assoziiert ist. An der Plasmamembran lokalisiertes HASPB führt zur Bildung von dynamischen nicht-apoptotischen Ausstülpungen (Tournaviti et al., 2006 submitted). Aus diesem Grund wurde der Zellkulturüberstand von HASPB-exprimierenden Zellen auf sedimentierbares Material mittels Ultrazentrifugation untersucht. Darin konnte in Nycodenz Flotationsgradienten eine HASPB-assoziierte Vesikelfraktion nachgewiesen werden. Interessanterweise konnten andere SH4 Proteine wie Src, Fyn, Yes and Lck nicht in extrazellulären Vesikeln gefunden werden. Aufgrund der Tatsache, dass diese Ausstülpungen der Plasmamembran in diesen Zelllinien beobachtet werden konnten, kann angenommen werden, dass die extrazellulären HASPB-assoziierten Vesikel nicht durch das Abschnüren dieser verursacht wurden. Bestätigt wird diese Beobachtung durch die Analyse von HeLa Zellen, bei denen HASPB-assoziierte Vesikel nachweisbar waren, jedoch Ausstülpungen der Plasmamembran nur in gerigem Maße beobachtet wurden. Wie mit Proteaseschutz-Experimenten bewiesen werden konnte, ist HASPB im Lumen dieser extrazellulären Vesikel lokalisiert. Kollokalisationsexperimente mit verschiedenen Exosomenmarkern bestätigte des weiteren, das HASPB, vermittelt durch die MVB Maschinerie, in Vesikeln exportiert wird. Diese Aussage konnte mit den Ergebnissen von linearen Sucrosegradienten und mittels Elektronenmikroskopie noch bekräftigt werden. HASPB-assoziierte Vesikel liegen mit einer Dichte von 1,15 g/ml (Heijnen et al., 1999) im Dichtebereich von Exosomen und besitzen, ebenso wie Exosomen, einen Durchmesser von weniger als 100 nm (Stoorvogel et al., 2002). Zusammenfassend kann ein zweites Exportmodell aufgestellt werden, in dem vollständig acyliertes HASPB, welches an der cytoplasmatischen Seite der Plasmamembran lokalisiert ist, Zutritt zur MVB Maschinerie gewährt wird und schließlich in Vesikeln exportiert wird.

Summary

Leishmania HASPB is a lipoprotein that is exported to the extracellular space from both *Leishmania* parasites and mammalian cells via an unconventional secretory pathway (Denny et al., 2000; Stegmayer et al., 2005). Exported HASPB remains anchored in the outer leaflet of the plasma membrane mediated by myristate and palmitate residues covalently attached to the N-terminal SH4 domain of HASPB (Denny et al., 2000; Stegmayer et al., 2005). HASPB targeting to the plasma membrane depends on SH4 acylation, which occurs at intracellular membranes. How acylated HASPB is targeted to the plasma membrane and, in particular the subcellular site of HASPB membrane translocation is unknown. Furthermore, possible secretory mechanisms for HASPB are not yet clarified in molecular terms.

In order to address this issue, a screening for clonal CHO mutants derived from somatic mutagenesis that are incapable of exporting HASPB, was performed. In such a CHO mutant cell line HASPB was myristoylated and palmitoylated and was mainly localized to the plasma membrane as judged by confocal microscopy and subcellular fractionation. However, based on a quantitative flow cytometry assay and a biochemical biotinylation assay of surface proteins, HASPB transport to the outer leaflet of the plasma membrane was largely reduced in this mutant despite a normal expression level of the HASPB reporter molecule compared to CHO wild-type cells. These findings indicate that the subcellular site of HASPB membrane translocation is the plasma membrane as the reporter molecule accumulates in this location when export is blocked. Hence, based on these results a two-step process of HASPB cell surface biogenesis can be defined, in which SH4 acylation of HASPB mediates intracellular targeting to the plasma membrane. In a second step, the plasma membrane-resident machinery that is apparently disrupted in the CHO mutant cell line, mediates membrane translocation of HASPB. Intriguingly, the angiogenic growth factor FGF-2 and Galectin-1, a lectin of the extracellular matrix, proteins secreted by unconventional means, were shown to be secreted normally from the HASPB export mutant cell line.

These observations demonstrate that the export machinery component defective in the export mutant cell line functions specifically in the HASPB export pathway. However, as revealed from the mutagenesis analysis the identified chemokine orphan receptor 1 was not the reason for the perturbed HASPB membrane localization in CHO K3 cells since its expression did not seem to be affected in CHO K3 cells.

In the second chapter of this thesis, the SH4 protein HASPB, besides being localized to the cell surface, was found to be associated with extracellular vesicles. HASPB induces curvature of the plasma membrane resulting in the formation of highly-dynamic non-apoptotic plasma membrane blebs (Tournaviti et al., 2006 submitted). Based on these observations cell culture supernatants from HASPB expressing CHO cells were analyzed. As revealed by flotation analysis the detected sedimentable material contained a vesicle-associated HASPB population. Importantly, other SH4 proteins such as Src, Fyn, Yes and Lck were not detectable in extracellular vesicles. Since these proteins were able to induce the formation of plasma membrane blebs, the extracellular HASPB vesicle population was shown not to be a consequence of plasma membrane blebbing, a process promoting the shedding of plasma membrane-derived vesicles that are released into the extracellular space. This observation was confirmed by results obtained from HeLa cells that were able to produce HASPB-containing vesicles. Importantly, the formation of plasma membrane blebs was largely reduced in this cell line. As judged by protease protection experiments HASPB was shown to be located on the inner leaflet of the vesicle membrane. Colocalization analysis with different exosomes markers further confirmed that HASPB might be exported via vesicles being released by the MVB sorting machinery. Furthermore employing linear sucrose gradients and electron microscopy, these vesicles corresponded to the reported density of 1.15 g/ml for exosomes (Heijnen et al., 1999) as well as to the exosomal size with diameters <100 nm (Stoorvogel et al., 2002). Together, these findings strongly suggest that dually acylated HASPB localized on the inner leaflet of the plasma membrane is delivered into vesicles that are released by the MVB sorting machinery into the extracellular space.

1 Introduction

In eukaryotic cells, internal membranes create compartments and organelles into which different metabolic processes are segregated (Gal and Raikhel, 1993; Lee et al., 2004). Besides other functions, this elaborate membrane system makes up the secretory pathway. It consists of a number of independent organelles that function sequentially to mediate protein secretion to the extracellular environment. Each compartment provides a specialized environment that facilitates the various stages of protein biogenesis, such as posttranslational modifications, sorting, and ultimately, secretion (Gal and Raikhel, 1993; Lee et al., 2004).

Cells that secrete proteins by exocytosis in large amounts are characterized by a permanent turnover of transport vesicles (Gruenberg and Clague, 1992). Proteins destined for export are synthesized in the ER followed by a transport to the Golgi via various kinds of transport vesicles (Bonifacino and Glick, 2004; Rothman, 1990; Rothman and Orci, 1992). In the Golgi proteins get modified and packed into vesicles for further transport to the target organelle, i.e. the plasma membrane (Keller and Simons, 1997). Upon fusion of the vesicle membrane with the plasma membrane its content is released into the extracellular space. Vesicles also bud from the plasma membrane transporting proteins into the cell. Based on this balance between exo- and endocytosis, the size of the plasma membrane does not vary (Pryer et al., 1992). Moreover, based on this permanent recycling of membranes, the ER gets regenerated. Similarly, this process regenerates plasma membranes, which have a high throughput of endocytosed material (Hong and Tang, 1993). The fusion of membranes and different compartments is termed membrane flow and represents the dynamics of cells (Bennett, 1956). With the exception of mitochondria, plastids and peroxisomes, the ER, Golgi, lysosomes and the plasma membrane are involved in this process. In case of the nucleus, only the outer membrane, which is identical to the membrane of the rough ER is studded with ribosomes engaged in protein synthesis (Dingwall and Laskey, 1992; Newport and Forbes, 1987). The proteins made on these ribosomes are transported into the space between the inner and

outer nuclear membranes (the perinuclear space), which is continuous with the ER lumen (Dingwall and Laskey, 1992; Newport and Forbes, 1987). In the first step on a pathway to another destination proteins enter the ER followed by a transport to the Golgi network. (Pryer et al., 1992). Transport from the ER to the Golgi network and from the Golgi to other compartments of the endomembrane system is carried out by the continuous budding and fusion of transport vesicles containing newly made proteins (Bonifacino and Glick, 2004). The accurate delivery of proteins to the correct target organelle e.g. for secretion from the cell, is therefore necessary for a cell to be able to grow, divide and function properly (Lee et al., 2004; Sudhof, 2004).

1.1 *Classical or ER-Golgi-mediated protein secretion*

The endoplasmic reticulum (ER) is the most extensive membrane system in eukaryotic cells and serves as an entry point for proteins destined for other organelles, as well as for the ER itself (Depierre and Dallner, 1975; Lee and Chen, 1988). Proteins will then be ferried by transport vesicles from organelle to organelle and, in some cases, from organelles to the plasma membrane or the cell exterior (Rapoport, 1992). The ER exists in two different forms, the rough ER and the smooth ER (Borgese et al., 1974; Jones and Fawcett, 1966). The region termed rough ER contains membrane-bound ribosomes, which synthesize proteins being translocated into the ER. These proteins are destined for export, for lysosomes or for transport to the plasma membrane (Borgese et al., 1974; Jones and Fawcett, 1966; Rapoport, 1992; Vertel et al., 1992). Free ribosomes are not associated with membranes and synthesize all of the other proteins encoded by the nuclear DNA. Membrane-bound ribosomes and free ribosomes are structurally and functionally identical, they differ only in the proteins they are making at any given time (Borgese et al., 1974; Jones and Fawcett, 1966; Rapoport, 1992; Vertel et al., 1992). When a protein is translated on a ribosome with an ER signal sequence, the signal sequence, a segment of hydrophobic amino acids, directs the ribosome to the ER membrane (Blobel and Dobberstein, 1975a; Blobel and Dobberstein, 1975b; Rapoport et al., 1992; Walter et al., 1984). This process is supported

by the **signal recognition particle** (SRP) present in the cytosol that binds to the ER signal sequence exposed on the ribosome (Tajima et al., 1986). In parallel, the SRP receptor, an α/β -dimer consisting of two G-proteins, embedded in the membrane of the ER, recognizes SRP (Gilmore, 1993; Siegel, 1995; Walter and Lingappa, 1986). Binding of SRP to a signal sequence causes protein synthesis by the ribosome to slow down until the ribosome and its bound SRP bind to an SRP receptor (Gilmore, 1993; Siegel, 1995; Tajima et al., 1986; Walter and Lingappa, 1986). At the same time, exchange of SRP-bound GDP for GTP is stimulated. The contact between SRP and its receptor facilitates the binding of the ribosome to the Sec61 complex, a translocase providing a hydrophilic channel with an aqueous milieu (High et al., 1991; Powers and Walter, 1996; Rapoport, 1992). This cycle, termed the SRP-cycle, is completed upon hydrolysis of GTP by SRP and its receptor, leading to the dissociation of SRP from the ER membrane (Blobel and Dobberstein, 1975a; Blobel and Dobberstein, 1975b; Gilmore, 1993; Siegel, 1995; Tajima et al., 1986; Walter and Lingappa, 1986). The channel of the Sec61 complex opens into the direction of the ER luminal side, followed by an association of the signal sequence to the TRAM-protein (**translocating chain associating membrane**), an integral transmembrane protein (High et al., 1991; Powers and Walter, 1996). Upon continuation of translation, the polypeptide is being threaded into the lumen of the ER. The signal sequence not only directs proteins to the ER but also functions to open the translocation channel. It remains bound to the channel while the rest of the protein chain is threaded through the membrane (Crowley et al., 1993; Dalbey and Von Heijne, 1992; Goerlich et al., 1992). During translocation, the signal sequence is cleaved off by a signal peptidase located on the luminal side of the ER membrane (Blobel and Dobberstein, 1975a; Blobel and Dobberstein, 1975b; Dalbey and Von Heijne, 1992). The signal peptide is then released from the translocation channel and rapidly degraded to amino acids (Blobel and Dobberstein, 1975a; Blobel and Dobberstein, 1975b; Dalbey and Von Heijne, 1992). Once the C-terminus of the protein has passed through the membrane, the protein is released into the ER lumen (Blobel and Dobberstein, 1975a; Blobel and Dobberstein, 1975b; Dalbey and Von Heijne, 1992). Additionally proteins also remain embedded in the ER membrane as

integral transmembrane proteins. The N-terminal signal sequence initiates translocation, but the transfer process is halted by a stop-transfer sequence, an additional sequence of hydrophobic amino acids, within the polypeptide chain (High and Dobberstein, 1992; Singer, 1990; Thrift et al., 1991). The stop-transfer sequence is released from the translocation channel and drifts into the plane of the lipid bilayer, where it forms an alpha-helical membrane-spanning segment anchoring the protein in the membrane (High and Dobberstein, 1992; Singer, 1990; Thrift et al., 1991). Simultaneously, the N-terminal signal sequence is also released from the channel into the lipid bilayer and is cleaved off. As a result, the translocated protein ends up as a transmembrane protein inserted into the membrane with a defined orientation, the N-terminus on the luminal side and the C-terminus on the cytosolic side of the lipid bilayer (High and Dobberstein, 1992; Singer, 1990; Thrift et al., 1991). As opposed to type I transmembrane proteins, proteins containing the N-terminus on the cytosolic side and the C-terminus on the luminal side of the lipid bilayer represent type II transmembrane proteins. Once inserted into the membrane, a transmembrane protein does not change its orientation, which is retained throughout any subsequent vesicle budding and fusion events (Hartmann et al., 1989; Kyte and Doolittle, 1982).

Vesicular trafficking between membrane-enclosed compartments of the endomembrane system is highly organized (Lee et al., 2004). The secretory pathway starts with the biosynthesis of proteins on the ER membrane and their entry into the ER. Proteins are sorted in the trans Golgi network and are transported in vesicles to their final destinations. In the absence of specific targeting signals, proteins are carried to the plasma membrane by constitutive secretion. Alternatively, proteins can be diverted from the constitutive secretion pathway and targeted to other destinations such as lysosomes or secretory granules destined for regulated secretion (Fig. 1) (Balch, 1990; Rothman and Orci, 1992).

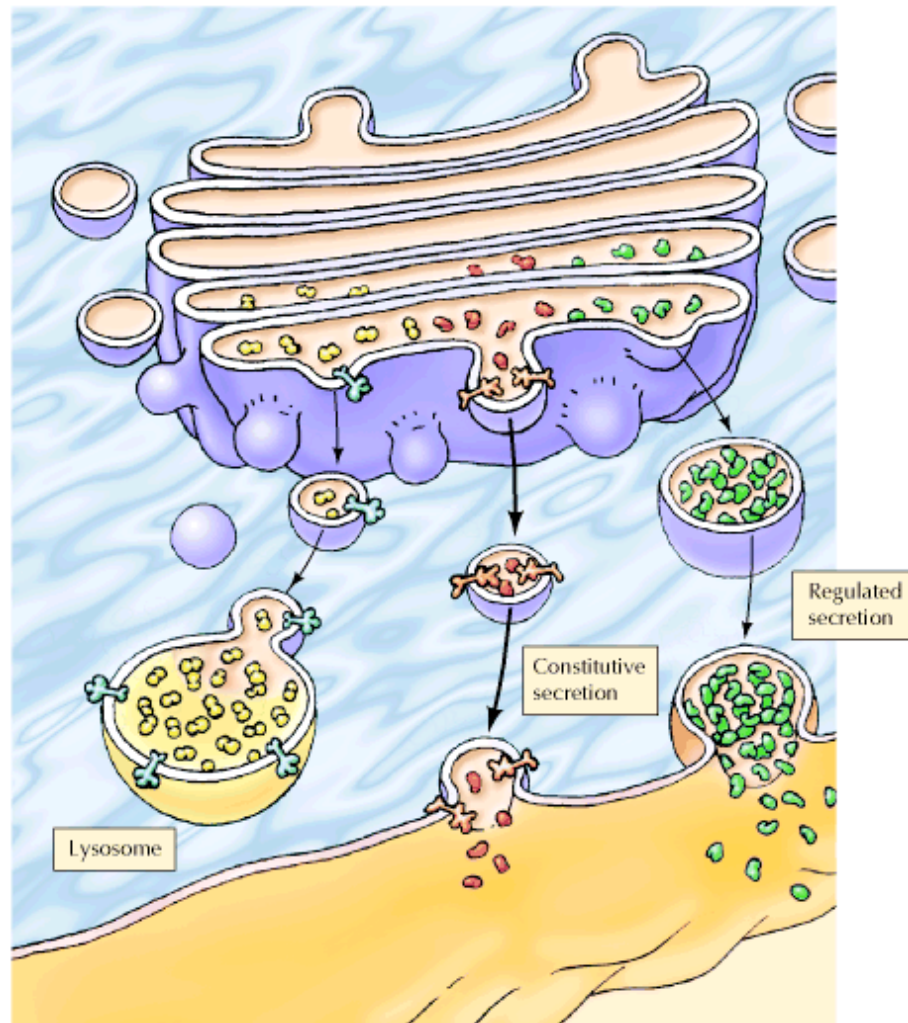


Fig. 1 Intercellular transport pathways. For details, see main text.

Usually the Golgi is located near the cell nucleus and consists of a collection of flattened, membrane-enclosed sacs (cisternae). They are piled like stacks of plates. (Mollenhauer and Morre, 1991; Rambourg and Clermont, 1990). The Golgi is an assymetrical, polar structure containing two distinct faces (Mollenhauer and Morre, 1991; Rambourg and Clermont, 1990). The cis-side or entry side is typically orientated towards the ER, from where transport vesicles containing proteins derived from the ER enter the Golgi (Warren and Malhotra, 1998). The proteins travel through the cisternae in sequence by means of transport vesicles which bud from one cisternae and fuse with the next. Proteins packed in transport vesicles exit the trans-Golgi network destined for either the cell surface or for lysosomes (Hong and Tang, 1993). Vesicles that bud from membranes are usually covered with a coat on their

surface, therefore termed coated vesicles (Kirchhausen, 2000; Robinson, 1987). COPII-coated-vesicles (COPII, COP is shorthand for coat protein) mediate anterograde transport from the ER to the Golgi network (Barlowe, 1998; Lee et al., 2004; Rothman, 1994; Rothman and Orci, 1992). COPII coat assembly is initiated by the ER resident protein, Sec12, which serves as a guanine nucleotide exchange factor (GEF) for the small GTPase Sar1 (Barlowe et al., 1993). GTP binding by Sar1 exposes an amphiphatic α -helix that facilitates association with the ER membrane (Bielli et al., 2005). Membrane-associated Sar1 recruits the Sec23-24 heterodimer and this complex interacts with cargo proteins via specific sorting signals (Matsuoka et al., 1998). The Sar1-Sec23-Sec24 complex then recruits the Sec13-31 heterotetramer leading to polymerization and membrane deformation to yield a COPII vesicle (Schekman and Orci, 1996). After budding from its parent organelle, the vesicle sheds its coat, allowing its membrane to interact directly with the target membrane (Barlowe, 1998). Besides COPII-coated-vesicles, COPI-coated-vesicles (COPI) are necessary to transport ER-specific proteins as well as cargo from the membrane of the cis-side of the Golgi to the ER, termed retrograde transport (Cosson and Letourneur, 1994; Letourneur et al., 1994; Nickel et al., 2002; Orci et al., 1997; Sonnichsen et al., 1996). Alternatively, COPI vesicles mediate transport between various Golgi cisternae (Orci et al., 1997). COPI coat assembly is initiated by GDP-GTP exchange onto Arf1, mediated by the Arf GEF, Gea1 (Peyroche et al., 1996). Membrane-bound Arf1 then recruits the preassembled coatomer complex, which contains seven subunits: the $\alpha/\beta'/\epsilon$ complex and the $\beta/\gamma/\delta/\zeta$ complex (Pavel et al., 1998) to the p24 receptor-family in the membrane (Bonifacino and Glick, 2004). The COPI coatomer complex likely contains multiple cargo recognition sites on separate subunits that mediate recruitment of cargo proteins (Austin et al., 2000). Ultimately, the coat is polymerized and membrane curvature may facilitate the recruitment of an Arf GTPase-activating protein (Arf GAP), stimulating GTP hydrolysis on Arf and subsequent dissociation from the membrane (Goldberg, 1998; Goldberg, 1999). Brefeldin A, an antibiotic from *Penicillium procumbens* targets the complex between a domain in Arf GEF and GDP-bound Arf. As a result the

fungal metabolite disrupt Arf1-dependent trafficking (Helms and Rothman, 1992; Mossessova et al., 2003b; Orci et al., 1991; Robineau et al., 2000). In mammalian cells the selective and efficient capture of cargo proteins into COPI vesicles also takes place in an additional membrane-bound compartment, the **ER-Golgi** intermediate compartment (ERGIC). The ERGIC is a site for concentrating retrograde cargo into COPI vesicles for delivery back to the ER. The ERGIC is delivered en bloc to the Golgi in a microtubule-dependent manner. This compartment is thought to arise from the homotypic fusion of COPII vesicles and is the main sorting station for the retrieval of escaped ER resident proteins (Lee et al., 2004; Martinez-Menarguez et al., 1999).

Besides COPI and COPII vesicles there are clathrin-coated vesicles budding from the Golgi apparatus on the outward secretory pathway and from the plasma membrane on the inward endocytic pathway (Brodsky, 1988; Morris et al., 1989). Clathrin (190 kDa) is able to assemble as trimers into a basket like network (triskelions) on the cytosolic surface of the membrane (Pearse et al., 2000). After the formation of clathrin-coated pits the assembly process starts shaping the membrane into a vesicle (Ahle et al., 1988; Cupers et al., 1994). Binding of clathrin coats to the membrane is mediated by heterotetrameric adaptor proteins that secure the clathrin coat to the vesicle membrane and help to select cargo molecules for transport (Pearse and Robinson, 1990). AP-1 functions on the membrane of the trans-Golgi network (Stamnes and Rothman, 1993), whereas AP-2 is necessary for the binding of clathrin coats on the plasma membrane (Traub et al., 1996). Together with the small G-proteins Rab5A, 5B and 5C (Bucci et al., 1992), recruited to the neck of the vesicle, the GTP-binding protein dynamin causes the ring to constrict, resulting in the release of the vesicle from the membrane. Subsequently, an uncoating ATPase, a chaperon of the Hsp70-family and auxilin are required for the dissociation of the vesicle coat upon destabilization of the clathrin molecules that are recycled into the cytoplasm (Takel et al., 1995; Warnock et al., 1996).

In addition to their role in vesicle formation, coat proteins also drive the selective capture of proteins into vesicles by interacting with specific signals present on the cytoplasmic domains of membrane proteins (Goldberg, 2000;

Lee et al., 2004; Mossessova et al., 2003a; Pelham, 1990). The polymerized coat thus acts as an affinity matrix to cluster selected cargo proteins into forming vesicle buds. Soluble proteins within the lumen of the parental organelles can in turn be selected by binding to the luminal domains of certain membrane cargo proteins (e.g. KDEL signal sequence and KDEL receptor) (Lewis and Pelham, 1992). The combination of coat recruitment to the correct donor membrane and signal-specific interactions between the coat and the cargo proteins contributes to the directionality and fidelity of vesicular transport (Lippincott-Schwartz, 1993; Pelham, 1991).

To deliver its contents to its correct destination a transport vesicle has to recognize and dock to the target organelle. Only then, fusion of the vesicle membrane with the target membrane and unloading of the vesicle's cargo is guaranteed (Jahn and Grubmuller, 2002; Rothman and Wieland, 1996; Schekman and Orci, 1996). The impressive specificity of vesicular transport is mediated by a family of related transmembrane proteins termed SNAREs (Söllner et al., 1993; Söllner and Rothman, 1996). The SNARE family consists of compartment-specific type II membrane proteins (Bock et al., 2001). SNAREs on vesicles (v-SNARE) are recognized specifically by complementary t-SNAREs on the cytosolic surface of the target membrane (t-SNARE) (Ungar and Hughson, 2003; Weber et al., 1998). At the structural level, a fully assembled v-/t-SNARE complex consists of a four-helix-bundle, with the v-SNARE contributing one helix and the t-SNARE contributing three helices (Sutton et al., 1998). The assembled trimeric t-SNARE provides the folding template for the v-SNARE. These reactions appear to occur in a zipper-like fashion progressing towards the membrane (Söllner, 2002; Söllner and Rothman, 1996). Following membrane fusion, v/t-SNARE cis-complexes that are extremely stable become the substrate for cytosolic SNAPs (**s**oluble **N**SF **a**ttachment **p**roteins) and the hexameric ATPase NSF (**N**-ethylmaleimide-**s**ensitive **f**actor, belongs to the family of AAA-type ATPases). ATPase hydrolysis by NSF disassembles SNARE complexes (Söllner et al., 1993). Free v-SNAREs are recycled by retrograde-oriented COPI-vesicles back to the donor organelle, while t-SNAREs remain in the target membrane for further fusion events (Jahn and Grubmuller, 2002; Jahn and Sudhof, 1999). In a following budding and fusion event, v-SNAREs are specifically recognized

by coat proteins. Binding and structural analysis further suggest that the vesicle coat proteins select the fusion competent conformation of SNAREs (Mossessova et al., 2003a). The direct coupling of vesicle budding and specific SNARE packaging ensures the production of fusion-competent vesicles (Lee et al., 2004; Sollner, 2002; Söllner and Rothman, 1996). Besides the delivery of cargo from the vesicle into the interior of the target organelle, fusion also leads to the addition of the vesicle membrane to the membrane of the corresponding organelle. Each organelle as well as each type of transport vesicle carries a unique SNARE, resulting in two types of fusion events, a heterotypic and a homotypic fusion event since interactions are restricted to complementary SNAREs. Only then transport vesicles can fuse with the correct membrane (Lee et al., 2004; Sollner, 2002; Söllner and Rothman, 1996).

1.2 *Non-classical or Unconventional protein secretion*

As opposed to classical secretion (section 1.1) where proteins contain an N-terminal signal peptide (Walter, 1992) that mediates translocation into the lumen of the ER followed by ER-Golgi-dependent vesicular transport to the cell surface (Mellman and Warren, 2000; Nickel et al., 1998; Rothman and Wieland, 1996; Schatz and Dobberstein, 1996), soluble factors with defined extracellular functions exist that get exported via an ER/Golgi-independent pathway (Hughes, 1999). This pathway has been termed non-classical or unconventional secretion (Cleves, 1997; Hughes, 1999; Muesch et al., 1990; Nickel, 2003; Prudovsky et al., 2003; Rubartelli and Sitia, 1991). As illustrated in Fig. 2, the most prominent examples are the angiogenic growth factors FGF-1 (Jackson et al., 1992; Jackson et al., 1995; Landriscina et al., 2001; LaVallee et al., 1998; Mandinova et al., 2003; Prudovsky et al., 2002; Shin et al., 1996; Tarantini et al., 1998) and FGF-2 (Engling et al., 2002; Florkiewicz et al., 1995; Mignatti et al., 1992; Mignatti and Rifkin, 1991; Trudel et al., 2000), cytokines like interleukin-1 β (IL1- β) (Andrei et al., 1999; Andrei et al., 2004; Rubartelli et al., 1990) and migration inhibitory factor MIF (Flieger et al., 2003) as well as the galectin protein family, lectins of the extracellular

matrix (Cleves et al., 1996; Cooper and Barondes, 1990; Lutomski et al., 1997). Also viral proteins such as Herpes simplex tegument protein VP22 (Elliott and O'Hare, 1997), Human immunodeficiency virus (HIV) Tat protein (Ensoli et al., 1993) and Foamy virus Bet protein (Lecellier et al., 2002) are released by non-classical export. Another quite remarkable example of nonclassical protein export from eukaryotic cells is the mechanism of cell surface expression of *Leishmania* HASPB which is found associated with the outer leaflet of the plasma membrane only in infectious stages of the parasite lifecycle (Alce et al., 1999; Denny et al., 2000; Flinn et al., 1994; McKean et al., 2001; Pimenta et al., 1994). These and other unconventional secretory proteins are characterized by the lack of a signal peptide and therefore are rejected by the ER translocation machinery (Cleves, 1997; Hughes, 1999; Prudovsky et al., 2003). These proteins are not found in subcellular compartments that belong to the ER/Golgi-dependent pathway (Cleves, 1997; Hughes, 1999). Despite bearing multiple consensus sites for glycosylation, all proteins have been reported not to contain this post-translational modification (Cleves, 1997; Hughes, 1999). Furthermore, their export mechanism is fully functional in the presence of brefeldin A, a drug that blocks ER/Golgi-dependent protein transport (section 1.1) (Lippincott-Schwartz et al., 1989; Misumi et al., 1986; Orci et al., 1991). The secretory proteins discussed here are soluble factors synthesized on free ribosomes in the cytoplasm and are found in the extracellular space. These observations led to the postulation of alternative secretory mechanisms in eukaryotic cells and therefore have been termed unconventional secretory processes. However, the molecular machineries mediating these processes are still not known in molecular terms (Cleves, 1997; Hughes, 1999).

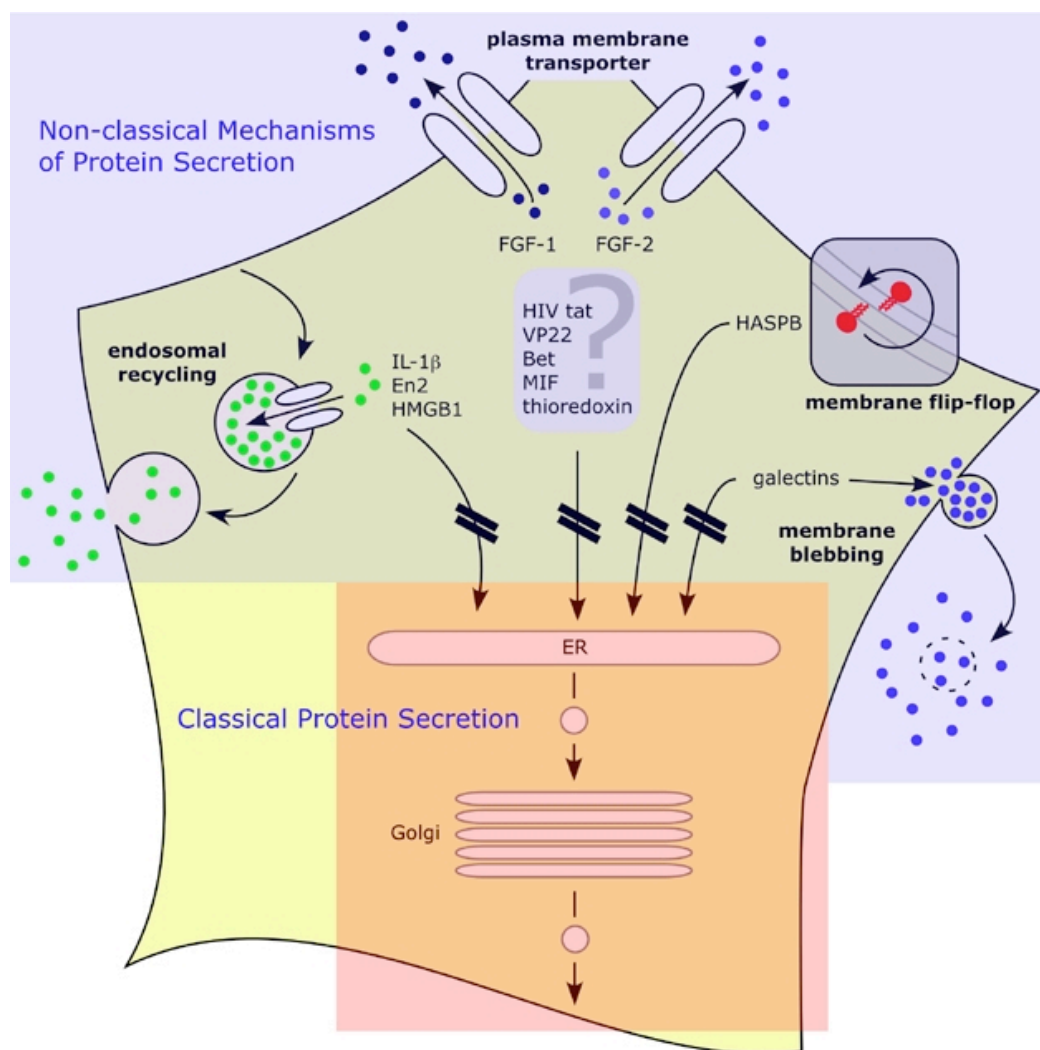


Fig. 2 Overview about unconventionally secreted proteins and their suggested export routes. Four different plasma membrane translocation processes involved in non-classical export can be distinguished. FGF-1 and FGF-2 are directly translocated across the plasma membrane using plasma membrane resident transporters. *Leishmania* SH4 protein HASPB is also directly translocated across the plasma membrane potentially involving a flip-flop mechanism since the protein is membrane anchored via its dual acylation at the extreme N-terminus. Galectins are exported by membrane blebbing, a process promoting the shedding of plasma membrane-derived microvesicles that are released into the extracellular space. IL-1 β , En2 and HMGB1 exit the cell packaged into intracellular vesicles originating from multivesicular endosomes or secretory lysosomes. (Courtesy of Walter Nickel (Nickel, 2003))

It has generally been assumed that proteins like FGF-2 are released following cell death and the disruption of plasma membrane integrity (McNeil et al., 1989; Muthukrishnan et al., 1991). However, nonconventional protein

secretion was shown to be dependent on both energy and temperature, is stimulated or inhibited by various treatments (Cleves, 1997; Hughes, 1999). Moreover, nonconventional protein secretion was shown to be regulated for example by cell differentiation (Cooper and Barondes, 1990; Lutonski et al., 1997), NF- κ B-dependent signaling pathways (Wakisaka et al., 2002), and post-translational modifications such as phosphorylation (Maizel et al., 2002). Based on these observations, it has to be concluded that the secretory proteins exit eukaryotic cells in a controlled manner mediated by proteinaceous machineries. As depicted in Fig. 3, four potential mechanism of unconventional protein export have been discussed in the literature to mediate translocation of cytosolic factors into the extracellular space (Hughes, 1999).

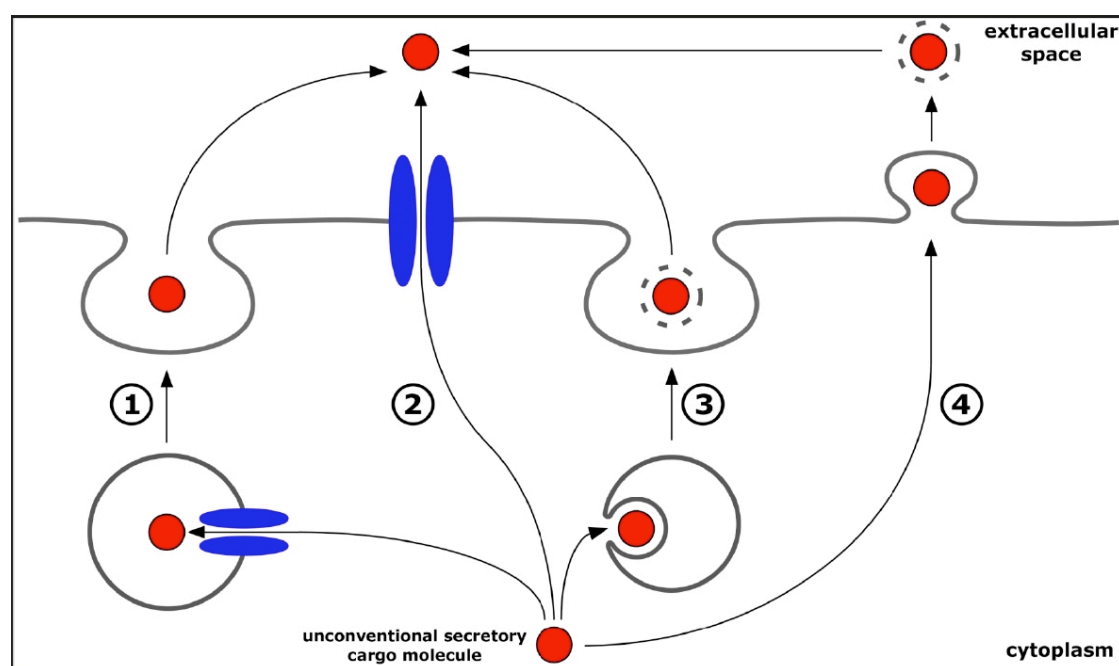


Fig. 3 Vesicular and non-vesicular pathways involved in unconventional secretory processes. (1) Export by secretory lysosomes (2) Export mediated by plasma membrane-resident transporters (3) export through the release of exosomes derived from multi-vesicular bodies (4) Export mediated by plasma membrane shedding of microvesicles. For details, see main text.

Two of these involve intracellular vesicles of the endocytic membrane system, such as secretory lysosomes (Clark and Griffiths, 2003; Stinchcombe et al.,

2004) and exosomes (Stoorvogel et al., 2002). In the first case export involves secretory lysosomes, which upon fusion of the plasma membrane release their contents into the extracellular space (Fig. 3, mechanism 1), a mechanism known for cytotoxic T lymphocytes for example as well as for melanocytes (Clark and Griffiths, 2003; Stinchcombe et al., 2004). In case of melanocytes, vesicles that fuse with the plasma membrane are then termed melanosomes (Stinchcombe et al., 2004). The second mechanism involving intracellular vesicles of the endocytic membrane system is characterized by an export through the release of exosomes derived from multi-vesicular bodies (MVBs) (Fig. 3, mechanism 3) (Stoorvogel et al., 2002).

Two alternative unconventional secretory mechanisms are characterized by a direct translocation of cytosolic factors across the plasma membrane using either membrane systems such as ABC transporters (Fig. 3, mechanism 2) (Cleves et al., 1996) or a process called membrane blebbing (Fig. 3, mechanism 4). In the latter case cells shed plasma membrane-derived microvesicles into the extracellular space (Freyssinet, 2003; Hugel et al., 2005; Martinez et al., 2005). Overall, these mechanisms give an idea of unconventional secretory mechanisms, however, further research is required to bring much more light into the phenomenon of unconventional protein secretion in the future.

1.3 Hydrophilic acylated surface protein B (HASP B)

Hydrophilic Acylated Cell Surface Proteins (HASPs) are components of the cell surface coat of *Leishmania* parasites (Alce et al., 1999; Flinn et al., 1994; McKean et al., 1997). *Leishmania* HASPB is an unconventional secretory protein and is exclusively expressed in infective parasites in both extracellular metacyclics and intracellular amastigotes of *L. major* and *L. donovani* (Alce et al., 1999; McKean et al., 2001; McKean et al., 1997; Rangarajan et al., 1995) suggesting a role in parasite virulence (McKean et al., 2001). Intriguingly, following heterologous expression dually acylated HASPB is also externalized by mammalian cells (Denny et al., 2000; Stegmayer et al., 2005) suggesting that endogenous factors exist in higher eukaryotes that are

exported in a mechanistically similar manner. The characteristics of HASPB are discussed in more detail in the following sections since HASPB is the main focus of the present study. Furthermore, FGF-2 as well as Galectin-1 will be described as these proteins were used in various experimental approaches as examples for other unconventionally secreted proteins.

1.3.1 Dual acylation mediated by myristoylation and palmitoylation

Peripheral membrane proteins are often anchored in a membrane via a covalent lipid modification (Resh, 1999). However association with a membrane mediated by only one fatty acid is not really tight (Bijlmakers and Marsh, 2003). Addition of a second lipid anchor or electrostatic interactions between basic amino acid residues and acidic phospholipids allow for a stable interaction of lipoproteins with membranes (Bhatnagar and Gordon, 1997). This covalent attachment is a widely recognized form of protein modification. Proteins containing fatty acids play key roles in regulating cellular structure and function (Bhatnagar and Gordon, 1997; Resh, 1999).

As noted above HASPB is an unconventionally secreted protein (Denny et al., 2000). One of its characteristics represents the dual acylation of its N-terminal SH4 domain, which mediates a stable association of the protein with the plasma membrane (Denny et al., 2000). HASPB is myristoylated at glycine 2 and palmitoylated at cysteine 5 (Denny et al., 2000).

Myristoylation is characterized by an amide bond between an N-terminal glycine residue with myristate, a 14-carbon saturated fatty acid (Fig. 4, left hand side) (Resh, 1999). All proteins destined for myristoylation start with the amino acids methionine, which is cotranslationally removed during the reaction followed by glycine (Resh, 1999). N-myristoylation is catalyzed by **N-myristoyl transferase (NMT)** and starts with the binding of myristoyl CoA to NMT (Rudnick et al., 1990). In a second step the peptide substrate binds to NMT and myristate is transferred to the N-terminal glycine of the peptide (Deichaite et al., 1988). Finally, both CoA and the myristoyl-peptide are released from the enzyme (Wilcox et al., 1987). N-myristoylation is a cotranslational process that occurs while the nascent polypeptide chain is still

attached to the ribosome (Resh, 1999; Rudnick et al., 1990; Wilcox et al., 1987). A number of proteins including the human immunodeficiency virus type 1 Nef protein (Bentham et al., 2006), the alpha subunit of trimeric G-proteins (Resh, 1999) as well as tyrosine kinases of the Src-family (Liang et al., 2004; Yasuda et al., 2000; Hirsch et al., 2005; Chou et al., 2002) are myristoylated at their N-terminal glycine.

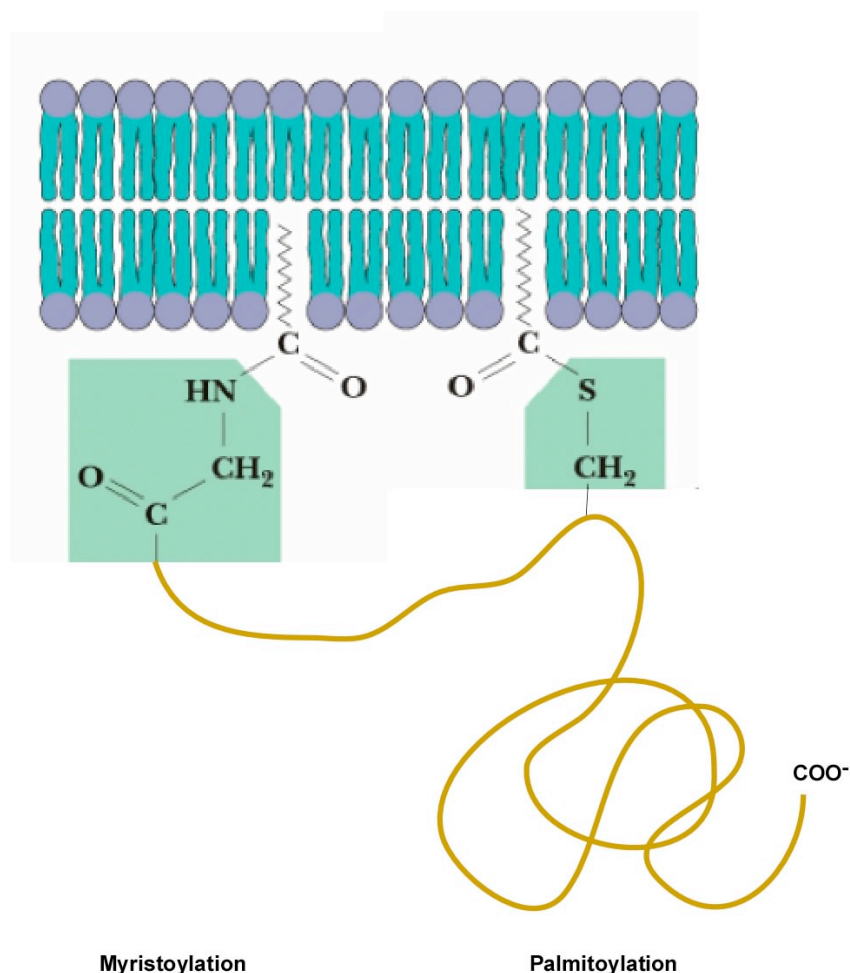


Fig. 4 Fatty acylation of protein modification. Myristoylation and palmitoylation facilitates stable membrane association. For details, see main text.

Palmitoylated proteins are acylated by a thioester linkage of the sulfhydryl group of cysteine to palmitate, a 16-carbon saturated fatty acid (Fig. 4, right hand side) (Bijlmakers and Marsh, 2003). This attachment occurs post-translationally and is localized near the N- or C-termini of proteins or near transmembrane domains. The reaction is catalyzed by a membrane-bound enzyme, **palmitoyltransferase** (PAT), which exhibits a preference for

myristoylated protein substrates and for palmitoyl-CoA over other acyl CoA substrates (Resh, 1999). To this end, PAT activity has been detected at the plasma membrane (Dunphy et al., 1996; Schroeder et al., 1997), the intermediate compartment (Bonatti et al., 1989), Golgi complex (Dunphy et al., 1996; Solimena et al., 1993) and mitochondria (Dunphy et al., 1996). However, the further characterization of their specificities and subcellular distributions will be important steps forward (Bijlmakers and Marsh, 2003). Furthermore, it has been shown that two cytosolic proteins, SNAP25 and GAP43 are not palmitoylated in presence of brefeldin A. This suggests that palmitoylation of these proteins requires functional Golgi membranes either to deliver the proteins to a specific location or, perhaps, to facilitate the reaction itself (Gonzalo and Linder, 1998). By contrast, palmitoylation of several viral proteins is insensitive to brefeldin A (Veit and Schmidt, 1993). Proteins containing this kind of lipid modification are for example the transferrin receptor (Resh, 1999), rhodopsin (Bijlmakers and Marsh, 2003), ankyrin in erythrocytes (Resh, 1999) as well as members of the Src family (Bijlmakers and Marsh, 2003). Both myristoylation and palmitoylation can be dynamically regulated: the myristate moiety can be sequestered through the use of myristoyl switches, while palmitate can be removed by protein palmitoyl thioesterases (Resh, 1999).

While myristoylation is clearly necessary for membrane binding of some proteins, it is not sufficient (Resh, 1999). A second signal within the N-myristoylated protein is therefore required for efficient membrane binding (Peitzsch and McLaughlin, 1993). Interestingly, myristoylation is absolutely required for a protein to get palmitoylated (Bijlmakers and Marsh, 2003). Domains containing one or both lipid modifications are termed SH4 domains (Chou et al., 2002; Hirsch et al., 2005; Rudd et al., 1993; Yasuda et al., 2000). This short conserved NH₂-terminal region is found in HASPB and in Src-family kinases such as Src, Yes, Fyn, Lck, Fgr, Hck, Blk, Lyn and Yrk, respectively (Rudd et al., 1993) (Fig. 5).

HASPB N- M **G** S S **C** T K D S A K E P Q K R A D -C

Src family of tyrosine protein kinases

Src N- M **G** S S K S K P K D P S Q R R R -C

Yes N- M **G** **C** I K S K E D K G P A M K Y -C

Fyn N- M **G** **C** V Q **C** K D K E A T K L T E -C

Lyn N- M **G** **C** I K S K R K D N L N D D E -C

Lck N- M **G** **C** V C S S N P E D D W M E N -C

Hck N- M **G** **C** M K S K F L Q V G G N T G -C

Fgr N- M **G** **C** V F **C** K K L E P V A T A K -C

Yrk N- M **G** **C** V H **C** K E K I S G K G Q G -C

Blk N- M **G** L L S S K R Q V S E K G K G -C

Fig. 5 N-terminal sequences of various SH4 proteins. Myristoylation and palmitoylation sites are highlighted in red and green, respectively. For details, see main text.

Besides myristoylation and palmitoylation two other forms of lipid modification have been described: the carboxy (C)-terminal isoprenylation of cytoplasmic proteins and the modification of plasma membrane proteins with glycosylphosphatidylinositol (GPI)-anchors (Bijlmakers and Marsh, 2003). The first one is characterized by a thioether-linkage of a cysteine residue in the C-terminal region of a protein with the farnesyl (C₁₅) or geranylgeranyl (C₂₀) isoprenoid (Bhatnagar and Gordon, 1997; Rocks et al., 2005). It can be found on heterotrimeric G-proteins (Bhatnagar and Gordon, 1997) and GTP-binding Ras proteins (Rocks et al., 2005). As opposed to all other lipid modifications the covalent attachment of the phospholipid phosphatidylinositol to the C-terminal of a protein via a glycan chain and ethanolamine is localized on the extracellular site (Fevrier et al., 2005; Ilgoutz and McConville, 2001; Naderer et al., 2004; Resh, 1999). This form of lipid attachment, also termed shortly GPI-anchor (**g**lycosyl**p**hosphatidylinositol) is found on various surface proteins of trypanosomes (Ilgoutz and McConville, 2001; Naderer et al., 2004), on

alkaline phosphatases (Resh, 1999) as well as on prion proteins (Fevrier et al., 2005).

1.3.2 *Leishmania* parasites

The Trypanosomatids, or Kinetoplastids, are a widespread group of flagellated protozoa (Shlomai, 2004). The major distinguishing feature of this group is a subcellular structure known as the kinetoplast, which is distinct from the nucleus. In fact, it is a distinct region of mitochondria containing extranuclear DNA (Shlomai, 2004). Members of this group parasitize virtually in all animal groups as well as plants and insects. Three distinct trypanosomatids cause human disease: *Leishmania* species (Fig. 6) (Leishmaniasis), *Trypanosoma brucei* complex (African sleeping sickness) and *Trypanosoma cruzi* (Chagas disease) (Schuster and Sullivan, 2002). They are parasites of the blood and/or tissues of the human host and are transmitted by arthropod vectors (Rittig and Bogdan, 2000; Schuster and Sullivan, 2002).

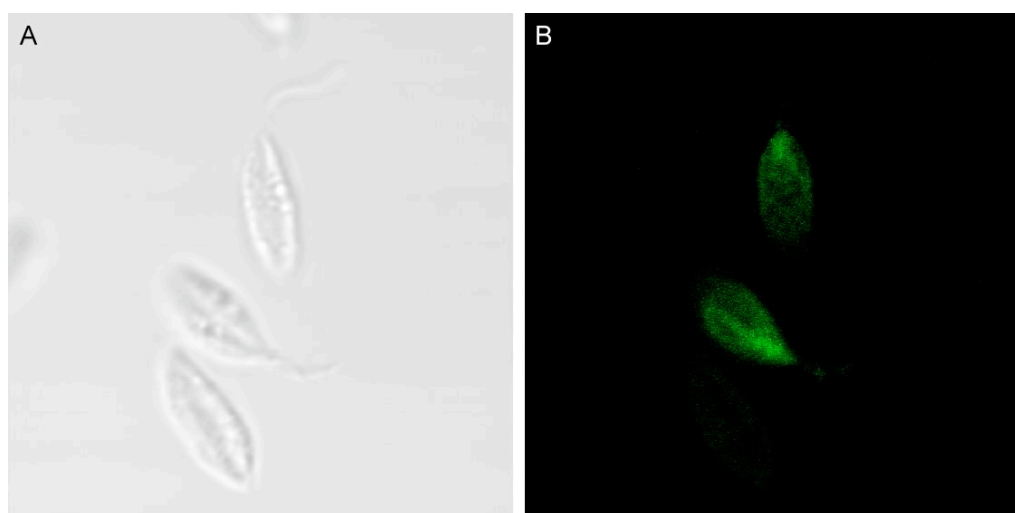


Fig. 6 Subcellular distribution of HASPB-N18-GFP fusion proteins expressed in *Leishmania* parasites as determined by confocal microscopy. Confocal images of *L. mexicana* expressing HASPB-N18-GFP. (A) Nomarski image (B) GFP-derived fluorescence was viewed with a Zeiss LSM 510 confocal microscope.

Leishmania species are sandfly-transmitted protozoan parasites that cause disease in more than 12 million people world-wide and 2 million new cases are diagnosed per year (Ilgoutz and McConville, 2001). Depending on the species and host genetics, infection with *Leishmania* parasites can result in cutaneous infections (one or more skin ulcers), mucocutaneous leishmaniasis (involving extensive destruction of mucous membranes) and visceral leishmaniasis (kala azar) that is invariably lethal unless treated (Schuster and Sullivan, 2002). At present there are no defined vaccines against leishmaniasis and only a limited number of drugs are available for treatment (Croft et al., 1996; Davies et al., 2003).

1.3.3 Life Cycle of *Leishmania* parasites

The lifecycle (Fig. 7) of *Leishmania* parasites relies upon transmission of a hematophagous arthropod (Peters et al., 1987). Two different genera of sandflies transmit *Leishmania*: *Phlebotomus* (Old World) and *Lutzomyia* (New World), which only house tropic and subtropic climates (Schuster and Sullivan, 2002).

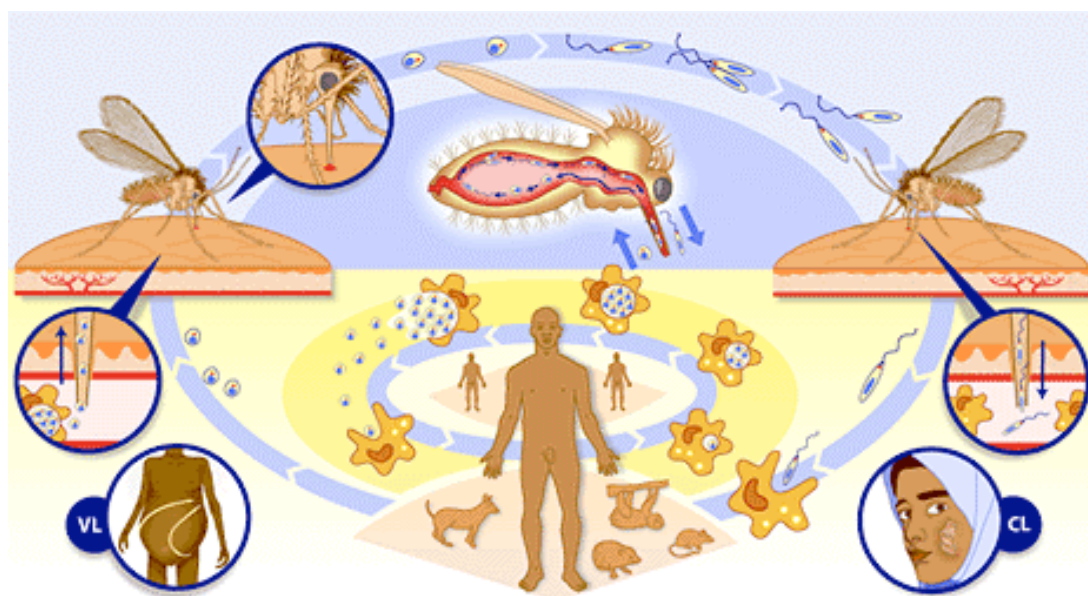


Fig. 7 Lifecycle of *Leishmania*. For details, see main text.

In the sandfly the parasites live as flagellated promastigotes within the midgut where they undergo developmental changes and become highly virulent upon migration to the mouthparts, especially the pharynx of the sandfly (Sacks, 1989; Sacks et al., 1983). The differentiation from non-infective procyclics into infective metacyclic parasites is also called metacyclogenesis and is a prerequisite for resistance to complement-mediated lysis as well as intracellular survival (Franke et al., 1985; Sacks, 1989). These promastigotes are then transferred to the vertebrate host during feeding (Franke et al., 1985; Sacks, 1989). Because of their high density promastigotes plug the pharynx and the sandfly must regurgitate to take a blood meal resulting in the expulsion of promastigotes into the bite wound and accordingly to the transfer in the bloodstream of the mammalian host (Franke et al., 1985; Sacks, 1989). Within the vertebrate host the promastigotes are phagocytosed by macrophages (Peters et al., 1987). This parasite-containing phagosome fuses with a lysosome (Rittig and Bogdan, 2000). Normally the pathogen is destroyed in the resulting phagolysosome, but *Leishmania* parasites are resistant to the acidic pH and hydrolytic enzymes present in the phagolysosome (Rittig and Bogdan, 2000). Additionally, the parasite shuts down the generation of reactive oxygen intermediates by the macrophage (Rittig and Bogdan, 2000). The promastigotes differentiate into non-flagellated amastigotes within the phagolysosome, which replicate by binary fission and fill up the infected macrophage (Peters et al., 1987; Rittig and Bogdan, 2000). When the macrophage cell ruptures, amastigotes are released from the host cell and are taken up by another macrophage leading to another round of replication. Alternatively, released amastigotes are taken up by the sandfly vector in a subsequent blood meal (Peters et al., 1987; Rittig and Bogdan, 2000). The release of the amastigotes is generally described as a bursting of the host cell (Rittig and Bogdan, 2000). However, the parasitophorous vacuoles containing amastigotes have been reported to accumulate at the periphery of the infected cell and amastigotes are continuously released over several hours (Rittig and Bogdan, 2000). Accordingly, release of amastigotes resembles an exocytosis-like process involving the fusion of the parasitophorous vacuolar membrane with the host cell plasma membrane (Rittig and Bogdan, 2000). Finally, the lifecycle is completed when the amastigotes differentiate back into

flagellated promastigotes in the sandfly midgut (Coulson and Smith, 1990; Ilgoutz and McConville, 2001; Peters et al., 1987; Rittig and Bogdan, 2000).

1.3.4 Composition and assembly of the *Leishmania* surface coat

The cell surface of all trypanosomatids is dominated by glycosylphosphatidylinositol (GPI)-anchored proteins and/or free GPI glycolipids (Ferguson et al., 1994; Smith et al., 1994). These molecules form a protective surface coat, which also mediates essential host-parasite interactions (Ilgoutz and McConville, 2001; Smith et al., 1994). Based on biochemical studies, the best characterized virulence determinants of *Leishmania* parasites are cell surface components such as GPI-anchored glycoproteins, heavily glycosylated GPI-anchored proteophosphoglycans and complex protein-free lipophosphoglycans (Ilgoutz and McConville, 2001; Smith et al., 1994). Other virulence determinants are the zinc metalloprotease GP63, also termed leishmanolysin (Bordier, 1987; Brittingham et al., 1995) on the parasite surface as well as specific cysteine proteases (Mottram et al., 1998). Their expression is upregulated in metacyclics (Ramamoorthy et al., 1992; Turco and Descoteaux, 1992). Together, these surface molecules facilitate resistance to complement-mediated lysis that results in a successful parasite infection within host macrophages (Joshi et al., 1998; Mosser and Brittingham, 1997). Additionally, a family of novel hydrophilic proteins encoded by the LmcDNA 16 gene locus on chromosome 23 of *Leishmania major* (Flinn and Smith, 1992; Knuepfer et al., 2001; McKean et al., 1997) has been identified. Two of the five genes in this array, SHERP1 and SHERP 2 (**s**mall **h**ydrophilic **e**ndoplasmic **r**eticulum (ER)-associated **p**rotein) (Fig. 8) encode for small non-integral membrane proteins. They localize to the endoplasmic reticulum and the outer mitochondrial membrane only in extracellular metacyclics (Knuepfer et al., 2001). The two SHERP genes show a high homology with 98.8% identity and are conserved across the *Leishmania* genus (Knuepfer et al., 2001). SHERP transcripts are upregulated in infective metacyclic parasites and its expression may be a specific

requirement for organellar function during *Leishmania* differentiation, an essential process for vector transmission (Knuepfer et al., 2001).

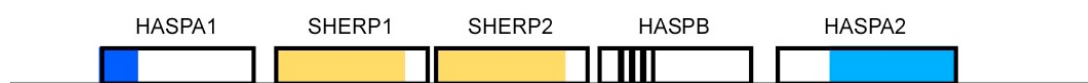


Fig. 8 Schematic representation of the LmcDNA 16 locus. LmcDNA 16 genes are represented as boxes, with colors and vertical bars to indicate unique or shared sequences. For details, see main text.

Moreover, within the LmcDNA 16 locus, genes encoding hydrophilic acylated surface proteins (HASPs) have been identified representing a novel family of components of the *Leishmania* surface coat (Fig. 8) (Coulson and Smith, 1990; Flinn et al., 1994). The HASP protein family consists of three closely related isoforms termed HASPA-1, HASPA-2 and HASPB, encoded by the LmcDNA 16 gene locus (Denny et al., 2000; McKean et al., 2001; Stager et al., 2000). They are a family of stage-regulated genes that are expressed exclusively in the infective forms of *Leishmania* parasites (metacyclics and amastigotes) (McKean et al., 2001). HASPA1 and HASPB mRNAs derived from the polycistronically transcribed LmcDNA 16 locus are detected only in metacyclic and amastigote stages, whereas HASPA2 mRNA is present at low level in procyclics, more abundant in metacyclics but absent from amastigotes (Knuepfer et al., 2001). The HASP family was originally found following a differential cDNA library screen for the identification of genes upregulated or uniquely-expressed in infective extracellular (metacyclics) stages of *Leishmania major* (Coulson and Smith, 1990). Interestingly, based on homology searches HASPs appear to be unique factors of *Leishmania* parasites as similar open reading frames could not even be found in closely related parasites such as trypanosomes (McKean et al., 2001). However, these observations do not rule out the presence of functional homologues of HASPs in trypanosomes or other related parasites. There are only limited sequence variations between various *Leishmania* species (Alce et al., 1999; McKean et al., 2001; McKean et al., 1997). The HASP surface molecules contain highly conserved N- and C-terminal domains and more divergent

central repetitive regions (McKean et al., 2001; McKean et al., 1997). In *L.major*, HASPB has an extensive region of repeats between the N- and C-terminal conserved regions while HASPA, the smallest member, has only 17 additional amino acids. This structural similarity between family members is conserved in all *Leishmania* species (Alce et al., 1999; Bhatia et al., 1999; McKean et al., 1997). Interestingly, their attachment to the surface is not via a GPI anchor, rather their N-terminal 18 amino acids are both myristoylated and palmitoylated (Denny et al., 2000). Collectively, these components form an effective macromolecular diffusion barrier in that they protect promastigotes from complement-mediated lysis, oxygen radicals and hydrolases in the mammalian and insect host environments (McConville et al., 1992; Turco and Descoteaux, 1992).

1.3.5 Non-classical export of HASPB

The HASPB protein family members are characterized by large internal repetitive regions containing mainly charged amino acids, interspersed with proline residues (Flinn et al., 1994). Similar repeats are found in HASPs from different *Leishmania* species, although their number and composition show inter- and intraspecific variation (Alce et al., 1999; McKean et al., 1997). HASPs contain an N-terminal SH4 domain that undergoes dual acylation at glycine 2 (co-translational myristoylation) and cysteine 5 (post-translational palmitoylation). These modifications are essential for HASPB transport to the cell surface (Denny et al., 2000). A palmitoylation-deficient HASPB mutant in which cysteine 5 has been changed to alanine has been demonstrated to localize to the cytoplasmic leaflet of the Golgi (Denny et al., 2000). These findings indicate that the palmitoylacyltransferase (PAT, section 1.3.1) represents a Golgi-resident enzyme. The 18 N-terminal amino acids representing the SH4 domain are sufficient to target a reporter molecule such as GFP to the cell surface of parasites (Denny et al., 2000). At this location, at least a proportion of HASPB molecules are displayed on the external surface, as shown by both high resolution microscopy and biochemical analyses (Denny et al., 2000; Pimenta et al., 1994). Intriguingly, heterologous

expression of HASPB in mammalian cells results in cell surface localization as well, suggesting that the corresponding translocation machinery is conserved among eukaryotes (Denny et al., 2000; Stegmayer et al., 2005). Brefeldin A, a drug that causes a collapse of the Golgi into the ER in mammalian cells (Lippincott-Schwartz et al., 1989), does not interfere with the appearance of HASPB at the plasma membrane of CHO cells (Denny et al., 2000). Based on these observations HASPB has been termed an unconventional secretory protein as it gets access to the extracellular space under conditions where the functional integrity of the ER/Golgi system has been perturbed (Denny et al., 2000). Consistently, HASPB does not contain a classical signal peptide, which would allow translocation across the membrane of the endoplasmic reticulum. Furthermore, the protein is not glycosylated, a modification that starts cotranslationally in the ER and continues in the Golgi (Denny et al., 2000). Based on these facts, export of fully acylated HASPB is likely to rely on plasma membrane-resident transporters (Fig. 3, mechanism 2). Interestingly, current evidence suggests that endosome sorting is an essential process for differentiation and virulence of *Leishmania major* (Besteiro et al., 2006). In this study the function of multivesicular bodies (MVBs) in *Leishmania major* has been investigated by characterizing the leishmanial Vps4 homologue, an AAA-ATPase involved in the MVB sorting machinery (Besteiro et al., 2006). They reported that a dominant-negative Vps4 mutant (Vps4^{E235Q}) accumulated the mutated protein around vesicular structures of the endocytic system and showed a defect in transport to the MVT (Multi vesicular tubule)-lysosome. Indeed, although this unusual lysosomal compartment has been shown to be downstream of an MVB-like network of vesicular endosomes that surrounds the flagellar pocket (Mullin et al., 2001), very little is known about them in *Leishmania* parasites. Thus, the findings described above are similar to what has been observed in yeast and mammalian Vps4 mutants, suggesting a conserved role for this protein in MVB architecture from the early branching kinetoplastid flagellate lineage to mammals. Moreover, *L. major*-overexpressing Vps4^{E235Q} were impaired in their differentiation in culture and their resistance to starvation, suggesting a crucial role for Vps4 and the MVB compartment in these processes (Besteiro et al., 2006). Accordingly, export of HASPB through the release of exosomes derived from multi-vesicular bodies

(MVB) might be another potential mechanism as indicated in Fig. 3, mechanism 3. Multivesicular bodies (MVB), also called multivesicular endosomes (MVE) represent endocytic intermediates, which are formed through invagination and pinching-off of the endosomal membrane (Stoorvogel et al., 2002). Since this vesicle budding process occurs in the opposite orientation compared with other budding events of cellular membranes, i.e. outwards from the cytosol, this molecular mechanism must be different from coated vesicle budding at the plasma membrane or at the Golgi (Raiborg et al., 2003; Stoorvogel et al., 2002). For the formation of MVBs three different complexes termed ESCRT-I-III (**E**ndosomal **S**orting **C**omplex **R**equired for **T**ransport) are necessary (Fig. 9) (Babst et al., 2002; Bache et al., 2003; Katzmann et al., 2001). They contain several subcomplexes, small coiled-coil proteins known as Vps class E proteins. The Vps27 protein initiates the MVB-sorting process. It is targeted to endosomal membranes via its FYVE domain that bind PI(3)P, and its UIM domains (short helical motifs that bind ubiquitin with low affinity), which bind ubiquitinated cargo such as carboxypeptidase S (CPS). Vps27 subsequently recruits and activates the ESCRT-I complex via the P(S/T)XP motif in the C-terminal domain of Vps27 that interacts with the UEV (ubiquitin E2 variant) domain of Vps 23 in ESCRT-I. ESCRT-I, consisting of the three subunits Vps 23, Vps28 and Vps37 recognizes ubiquitinated cargo via binding to the UEV domain of Vps23. However, it should be noted, that not all proteins require ubiquitination for their sorting into the MVB pathway (Reggiori and Pelham, 2001). This process is followed by the recruitment of ESCRT-II (Vps22, Vps25 and Vps36) and ESCRT-III (Snf7-Vps20 and Vps2-Vps24) to endosomal membranes. ESCRT-III seems to function in the concentration of cargoes into MVBs and coordinates the association of accessory factors such as Bro1/Alix and the Doa-4-deubiquitinating enzyme that removes ubiquitin from cargo. Finally, the membrane dissociation of the ESCRT complexes is controlled by the AAA-type ATPase Vps4 (Ahle et al., 1988; Babst, 2005; Babst et al., 2002; Greco et al., 2001; Gruenberg and Stenmark, 2004; Hurley and Emr, 2006; Raiborg et al., 2003; Thery et al., 2001; Thery et al., 2002; van Niel et al., 2006). For all class Vps (**v**acuolar **p**rotein **s**orting) E proteins, with the exception of Vps37, mammalian equivalents have been identified indicating that these complexes have conserved function (Raiborg et al.,

2003). TSG101, for example, identified as one of the major components of the ESCRT-1 complex is the human homologue of Vps23. This protein is found on endosomes and is required for lysosomal trafficking of endocytosed EGF (Babst et al., 2000; Bishop et al., 2002; Garrus et al., 2001; Pisitkun et al., 2004). Bro1/Alix, a protein involved in apoptosis and inducing cytoplasmic vacuolization functions as an ESCRT-III binding partner (Chatellard-Causse et al., 2002).

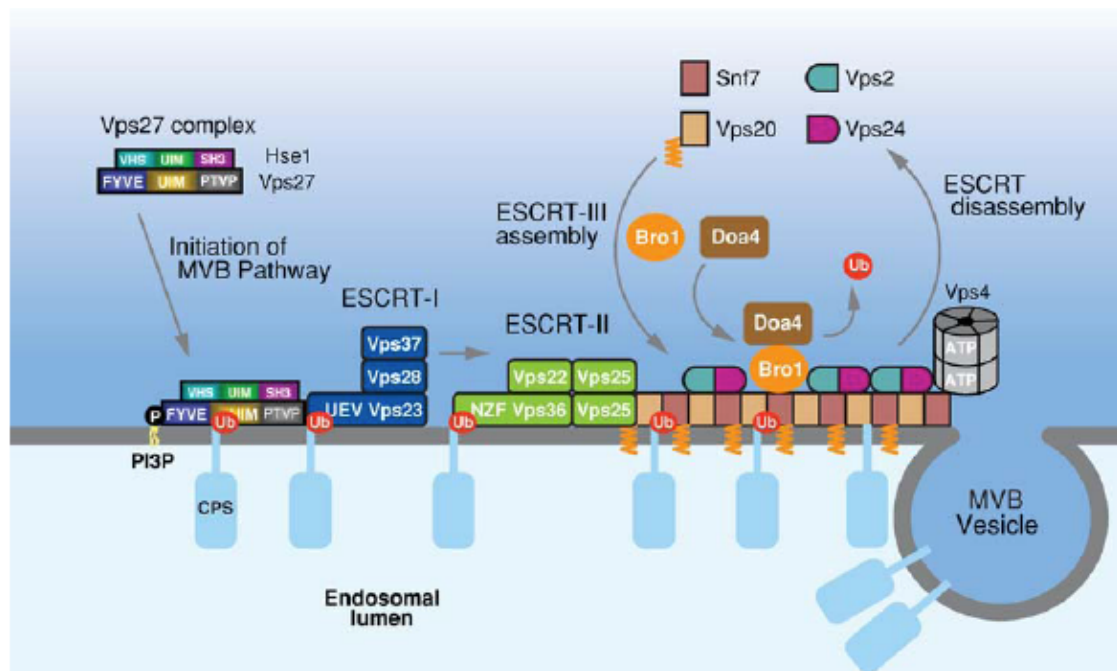


Fig. 9 The ESCRT complexes in MVB sorting (Hurley and Emr, 2006). For details, see main text.

These kinds of intraluminal vesicles have been proposed to serve several important functions: i) transmembrane proteins in the intraluminal membrane will be susceptible to degradation by lysosomal hydrolases, ii) intraluminal vesicles might represent storage vehicles for transmembrane proteins that are to be released to the extracellular space via these vesicles (Raiborg et al., 2003) or iii) they can participate in receptor signaling, which might be possible from the limiting membranes of MVBs, but not from the membranes of intraluminal vesicles. This means that sorting into MVBs can determine both the delivery of transmembrane proteins to lysosomes and the extracellular

space, and also the ability of endocytosed receptors to transmit signals (Raiborg et al., 2003; Stoorvogel et al., 2002; van Niel et al., 2006).

In addition to the observations described above HASPB induces curvature of the plasma membrane resulting in the formation of highly dynamic tubules and plasma membrane blebs (Tournaviti et al., 2006 submitted). Plasma membrane blebs are cell protrusions generated by the osmotic pressure of the cell interior upon localized destabilization of the cortical actin network at the plasma membrane (Charras et al., 2005; Cunningham, 1995; Sheetz et al., 2006). These reorganizations of the plasma membrane require the membrane association of the SH4 domain depend on the integrity of F-actin as well as microtubule architecture and are regulated by the activities of Rock kinase and Myosin-II ATPase (Tournaviti et al., 2006 submitted). Furthermore as revealed by RNAi analysis, the actin and microtubule regulating diaphanous related formin (DRF) FHOD1 has been identified as a factor that facilitates plasma membrane bleb formation (Tournaviti et al., 2006 submitted). Based on these findings, export mediated by plasma membrane shedding of microvesicles might also be an alternative secretory mechanism for HASPB (Fig. 3, mechanism 4) (Freyssinet, 2003; Hugel et al., 2005; Martinez et al., 2005). Microvesicles are fragments shed almost spontaneously from the plasma membrane blebs of virtually all cell types when submitted to a number of stress conditions, including apoptosis. Vesicle release is an integral part of the membrane-remodeling process resulting in the occurrence of phosphatidylserine (PS) in the exoplasmic leaflet that generally is located mainly in the inner (cytoplasmic) leaflet of the plasma membrane. Translocation of PS to the outer leaflet of the plasma membrane is a hallmark of programmed cell death. In this location PS acts as a peripheral membrane protein that links activated/apoptotic cells to phagocytes (Freyssinet, 2003; Hugel et al., 2005; Martinez et al., 2005). However, HASPB-induced membrane blebbing could be observed over hours without apparent damage of cells. Consistent with this observation, these cells were strictly negative for markers of apoptotic events such as cell surface exposure of phosphatidylserine or nuclear fragmentation (Tournaviti et al., 2006 submitted). Based on these observations HASPB secretion might not involve shedding of plasma membrane vesicles.

1.3.6 HASPB is of exceptional biomedical relevance

HASPB is expressed exclusively in infective parasites (both extracellular metacyclics and intracellular amastigotes of *L. major* and *L. donovani*) (Alce et al., 1999; Flinn et al., 1994; Rangarajan et al., 1995). In *L. mexicana*, expression is low in metacyclics but high in amastigotes (Nugent et al., 2004). Deletion of the *Leishmania* LmcDNA 16 locus containing all isoforms of HASP proteins has been demonstrated to cause changes in cell surface coat structure resulting in an increased sensitivity to complement-mediated lysis (McKean et al., 2001). This phenotype is similar to non-infective procyclics that do not express HASP proteins. HASP null mutants have been shown to remain infectious, however, this has so far only been tested in high dose experiments in highly susceptible mouse mutant strains (McKean et al., 2001). Therefore, it remains to be established whether HASP-deficient parasites are infectious under physiological conditions, i.e. in experiments using sandfly-mediated low dose infections into a wild-type host background. Additionally, overexpression of the gene products of the LmcDNA 16 locus results in avirulence (McKean et al., 2001). Together, these findings confirm that HASPs are critical determinants of both virulence and parasite survival within the vertebrate host and targets suited for the development of a novel class of anti-parasitic drugs.

In addition to these observations HASPB is recognized by human sera collected in endemic regions with high specificity and sensitivity (Jensen et al., 1999) and shows promise as a target vaccine antigen for visceral leishmaniasis (Stager et al., 2003; Stager et al., 2000). Recent data have demonstrated that *L. donovani* HASPB is able to protect against infection *in vivo* via a novel immune mechanism involving natural antibodies and complement (Stager et al., 2003). Whether the cell surface localization of HASPB contributes to this immune response is currently unclear. However, recent experiments using the N-terminal acylated HASPB domain to target a model antigen, ovalbumin, to the parasite plasma membrane have clearly demonstrated that HASPB in this location is presented preferentially to the immune system *in vivo* (Prickett et al., 2006). Therefore the elucidation of the

molecular apparatus catalyzing HASPB export might pave the way for the development of a novel class of anti-parasitic drugs causing alterations in the coat structure of *Leishmania* parasites potentially inducing avirulence and/or lability towards the host immune system.

1.4 Fibroblast Growth Factor-1 and- 2 (FGF-1 and -2)

FGFs belong to a large family of heparin-binding growth factors, which, apart from their mitogenic activity (Burgess and Maciag, 1989; Schweigerer et al., 1987), are key stimulators of tumor-induced angiogenesis (Christofori and Luef, 1997). Although acidic and basic fibroblast growth factors (aFGF1, bFGF2) are often regarded as prototypic members of the FGF family, neither one has a classical leader sequence that might explain their presence outside cells (Bikfalvi et al., 1997; Szebenyi and Fallon, 1999). Accordingly, they belong to the unusual class of unconventionally secreted proteins (Cleves, 1997; Nickel, 2003). FGF-2 was first identified as an 146-amino acid protein isolated from the pituitary (Bohlen et al., 1984). Upon expression of the FGF-2 cDNA, five isoforms could be identified with molecular masses ranging from 18, 22, 22,5 and 24 kDa that arise from a single mRNA transcript as a result of alternate utilization of AUG or CUG translation start sites (Florkiewicz and Sommer, 1989; Prats et al., 1989). The longer forms of 22, 22.5 and 24 kDa, initiated by CUG codons are localized in the nucleus, whereas the AUG-initiated 18kDa form is localized to the cytoplasm (Florkiewicz et al., 1995; Florkiewicz and Sommer, 1989) and has been shown to be secreted by unconventional means (Jackson et al., 1992; Mignatti et al., 1992; Trudel et al., 2000). Using recombinant FGF-2, several groups have determined the three-dimensional structure of the 18-kDa form of FGF-2 (Eriksson et al., 1991; Zhu et al., 1991). FGF-2 contains 12 anti-parallel β -sheets organized into a trigonal pyramidal structure (Baird et al., 1988). This FGF-prototype has pleiotropic effects in different cells and organ systems. FGF-2 is a potent angiogenic molecule *in vivo* and *in vitro* stimulates smooth muscle cell growth, wound healing, and tissue repair (Basilico and Moscatelli, 1992; Schwartz and Liaw, 1993). In addition FGF-2 may stimulate hematopoieses (Allouche and

Bikfalvi, 1995; Bikfalvi et al., 1995) and may play an important role in differentiation and/or function of the nervous system (Baird, 1994; Logan et al., 1991; Unsicker et al., 1992), the eye (McAvoy et al., 1991), and the skeleton (Fallon et al., 1994; Riley et al., 1993).

FGF-2 is able to initiate differentiation, i.e. the transformation of fibroblasts to adipocytes (Rogelj et al., 1989). By contrast, FGF-2 blocks the differentiation of myoblasts in the muscle and thereby prevents apoptosis (Rogelj et al., 1989). FGF-2 is involved in mitogenesis by inducing the synthesis of DNA in various cells (Gospodarowicz et al., 1987). It stimulates the secretion of proteases, for example plasminogenactivator, collagenases and gelatinases upon receptor-mediated signaling (Ye et al., 1988). As a result of the activation of plasminogenactivator, the protease plasmin arises upon scission of peptides by plasminogen and is able to digest basal membranes that usually prevent the migration of cells (Ye et al., 1988). All FGF-2-forms entail high affinity interactions with tyrosine kinase FGF receptors and low-affinity interactions with proteoglycans (HSPGs) containing heparan sulfate polysaccharides (Johnson and Williams, 1993; Rusnati et al., 2002). Binding of soluble FGF-2 to heparanproteoglycans of cells induces oligomerization (Gleizes et al., 1995). The oligomerization of FGFs triggered by binding to heparan sulfates promotes the recruitment of several FGFRs leading to receptor dimerization and activation (Powers et al., 2000). Dimerization of FGFRs induces autophosphorylation of cytosolic tyrosine residues, which, in turn, activates phospholipase C γ (PLC γ), a protein found to be associated with FGFRs (Burgess and Maciag, 1989; Burgess et al., 1990). PLC γ cleaves phosphatidyl-inositol-4,5-bisphosphate (PIP₂) to inositol triphosphate (IP₃) and diacylglycerol (DAG) leading to an increase of the intracellular concentration of Ca²⁺-ions by release from the ER reservoir in response to the stimulus by IP₃. Ca²⁺-ions function as second messengers that induce numerous cellular responses and additionally DAG together with the released Ca²⁺-ions activates protein kinase C (PKC) (Clapham and Sneyd, 1995). Another signalling pathway, which can be activated by FGFR dimerization is Ras/MAP-kinase signalling (Marshall, 1995).

These signaling cascades mediated by FGF-2 represent the basis for its function as tumor-producing direct acting stimulator of angiogenesis, a process that is essential for tumor growth and metastasis (Bikfalvi et al., 1995). Upon growing of endothelial cells, new blood vessels are formed that regulate the exchange between blood stream and the surrounding tissue (Ferrara, 1999; Mignatti and Rifkin, 1991). Upon release of FGF-2, endothelial cells, organized as monolayer in blood vessels form capillary tubes, secrete proteases, proliferate and form new capillaries (Ferrara, 1999; Mignatti and Rifkin, 1991). As a result, the extracellular matrix (ECM) gets degraded by the proteases and the endothelial cells grow towards the tumor (Ferrara, 1999; Mignatti and Rifkin, 1991). Based on this neovascularisation, a connection of the tumor cell to the blood vessel and thereby to the whole blood system is guaranteed representing the prerequisite for tumor growth and metastasis (Liekens et al., 2001).

Besides the common functions of FGF-1 and FGF-2, there exists a lot of differences, as the secretion of FGF-2 is blocked upon heat shock treatment (Jackson et al., 1992; Mignatti and Rifkin, 1991) while FGF-1 secretion is not influenced by stress conditions such as heat shock (Hughes, 1997; Jackson et al., 1992; Lindquist, 1986; Tsay et al., 1999). In case of FGF-1, export requires the formation of a Cys30-mediated FGF-1 homodimer (Jackson et al., 1995; Tarantini et al., 1995) as well as the association of FGF-1 with the extravesicular p40 fragment of p65 Syt1, an integral transmembrane protein participating in secretory vesicle docking (LaVallee et al., 1998; Tarantini et al., 1998). Additionally, S100A13, a member of the family of intracellular calcium-binding S100 proteins is implicated in this multiprotein release complex (Landriscina et al., 2001; Mouta Carreira et al., 1998). Furthermore, serum starvation has been reported to inhibit export of FGF-2 (Mignatti et al., 1992) while it was found to induce secretion of FGF-1 (Shin et al., 1996). Similarly, methylamine has an effect only regarding FGF-2 export (Jackson et al., 1995). FGF-2 secretion is blocked in presence of ouabain (Florkiewicz et al., 1998). Ouabain binds to the alpha-subunit of the Na/K-ATPase and prevents FGF-2 secretion suggesting that the Na/K-ATPase regulates FGF-2 secretion. This observation is confirmed by experiments with an ouabain-resistant mutant expressing the alpha subunit of the ATPase since FGF-2

export can be restored (Dahl et al., 2000). Despite the apparent mechanistically differences in the export modes of FGF-1 and FGF-2, it appears quite likely that FGF-1, alike FGF-2, is exported by a direct translocation across the plasma membrane of mammalian cells (Fig. 3, mechanism 2). This is consistent with earlier findings in that FGF-2 is capable of crossing the membrane of plasma membrane-derived inside-out vesicles *in vitro* (Schäfer et al., 2004). Additionally, current evidence suggests that HSPGs are essential components of the FGF-2 export machinery, thereby acting as FGF-2 export receptors (Zehe et al., 2006). The specific binding of FGF-2 to heparan sulfate proteoglycans (HSPG) (Faham et al., 1996; Faham et al., 1998; Raman et al., 2003) requires a functional structure that seems to be the case upon export as FGF-2 membrane translocation occurs in a folded state (Backhaus et al., 2004). Collectively, translocation of FGF-2 might be coupled to a mechanism that ensures secretion only of functional FGF-2 implicating that exported FGF-2 has passed quality control measures (Backhaus et al., 2004).

As recently reported (Taverna et al., 2003), the shedding of plasma membrane vesicles has also been proposed as a main mechanism of FGF-2 secretion (Fig. 3, mechanism 4). This work was initiated based on the previous findings that following secretion FGF-2-GFP concentrates in heparan sulfate proteoglycans (HSPG)-containing clusters on the outer leaflet of the plasma membrane (Engling et al., 2002). These structures were interpreted as potential exovesicles originating from the plasma membrane (Taverna et al., 2003). However, further work is needed to establish a role for this mechanism in the release of FGF-2 from mammalian cells, especially because in the absence of various forms of cell activation. FGF-2 export has been found to occur in a constitutive manner from many cells (Prudovsky et al., 2003).

1.5 Galectin-1

Galectin-1 belongs to a family of β -galactoside-binding lectins expressed in distinct patterns during development and in differentiated tissues (Hughes,

1999). These lectins are associated with components of the extracellular matrix (ECM) and counter receptors on the cell surface of mammalian cells (Liu and Rabinovich, 2005). Due to the β -galactoside-binding capability, galectins can be clustered through interactions with glycoproteins and glycolipids representing a key event in galectin signal transmission to downstream targets (Brewer et al., 2002). Cell surface association of galectins is mediated by both N- and O-glycosylated β -galactose-terminated oligosaccharide side chains of glycoproteins (Hughes, 1997; Perillo et al., 1998) as well as by galactose-containing glycolipids such as GM1 (Kopitz et al., 1998; Perillo et al., 1995). Regarding Galectin-1 it is involved in tumor-mediated immune response, promoting immune suppression by inducing apoptosis of activated T cells upon secretion from tumor cells (He and Baum, 2004; Perillo et al., 1995). Accordingly, galectins have been implicated in a wide range of physiological processes such as apoptosis, tumor progression, inflammation and cell adhesion (Liu and Rabinovich, 2005; Perillo et al., 1995; Rabinovich et al., 2002). Each galectin contains one or two highly conserved carbohydrate recognition domains (CRDs) made up of about 135 amino acid residues and great varieties concerning their carbohydrate-binding specificities (Hughes, 1999). Most galectin CRDs have similar affinities for lactose or N-acetylglucosamine. Moreover, they have highly conserved amino acid residues in the primary carbohydrate site responsible for binding to β -galactosides (Henrick et al., 1998; Seetharaman et al., 1998). Interestingly, Galectin-3 has an extended binding site for accommodation of longer oligosaccharides such as polylactosamines, suggesting that the differences in carbohydrate-binding-specificities are important for specific downstream effects (Henrick et al., 1998; Lukyanov et al., 2005; Seetharaman et al., 1998). Each galectin may interact with a discrete spectrum of glycoconjugate receptors leading to consequent downstream signaling (Henrick et al., 1998; Seetharaman et al., 1998). Galectin-1, a homodimeric lactose-binding lectin, is highly expressed in muscle cells, thymus, kidney, placenta and motor and sensory neurons and export of galectin-1 from these tissues can both promote and inhibit cell adhesion (Barondes et al., 1994). In early studies (Lindstedt et al., 1993; Sato et al., 1993), it has been proven that galectin secretion does not abrogate in presence of brefeldin A, indicating that they exit the cells

through an alternative, non-classical route, the unconventional secretion (Cleves et al., 1996). For galectins, different pathways have been proposed according to the structure of the lectin, the cell type and its polarity (Hughes, 1999). It seems likely that part of the diversity in secretory pathways used by galectins lies in interaction with different sets of intracellular proteins that direct them to specific sites during their secretion (Hughes, 1999). This also implicates the translocation through a limiting membrane of a vesicular compartment or at the cell surface (Hughes, 1999). The association of galectins with actin (Huflejt et al., 1997; Joubert et al., 1992) and cytokeratins (Goletz et al., 1997) could be involved in focal concentration of the protein at specialized regions of the cytoskeleton (Hughes, 1999). Galectin-1 was reported to accumulate in such evaginations of the plasma membrane as revealed by immunolocalization studies at intermediate stages of the differentiation process (Cooper and Barondes, 1990). The protein has been found in the extracellular space upon differentiation of muscle cells from myoblasts to myotubes (Cooper and Barondes, 1990). Furthermore, Galectin-1 was detected in exovesicles apparently in the process of detaching from the plasma membrane (Cooper and Barondes, 1990), suggesting an export mediated by plasma membrane shedding of microvesicles (Fig. 3, mechanism 4). Besides Galectin-1, Galectin-3 has been proposed to get exported via membrane shedding of labile vesicles into the supernatant of COS cells (Mehul and Hughes, 1997). Intriguingly, Galectin-3 has been identified as a major component of exosomes, which were isolated from cell culture supernatants of dendritic cells (Thery et al., 2001) suggesting that the shedded exovesicles are derived from multivesicular bodies (MVB) (Fig. 3, mechanism 3) rather than by membrane blebbing. Moreover, it has been reported, that Galectin-1 is capable of translocating across the membrane of plasma membrane-derived inside-out vesicles (Schäfer et al., 2004) suggesting an export via mechanism 2 (Fig. 3). Based on this result, plasma membrane derived transporters could be implicated in Galectin-1 secretion (Seelenmeyer et al., 2005). So far, the idea of an interaction of galectins with their counter receptors such as laminin, fibronectin, lamp1 and 2 or GM1 glycolipid was not operated. However, current evidence suggests that these interactions have been shown to be an integral part of the export mechanism

itself (Seelenmeyer et al., 2005) proving that the elusive targeting motif of Galectin-1 is primarily defined by its β -galactoside-specific carbohydrate recognition domain (Seelenmeyer et al., 2005). Their ligands such as β -galactoside-containing glycolipids act as cargo receptors, which either act at an intracellular level or at an extracellular level, both resulting into a directional transport of galectins across the plasma membrane (Seelenmeyer et al., 2005).

1.6 Aim of the current study

The specific aim of this thesis was to analyze the molecular mechanism of HASPB targeting to the plasma membrane. In this regard, there is also a complete lack of knowledge about the subcellular site of HASPB membrane translocation, a process that eventually allows HASPB exposure on the cell surface of eukaryotic cells. Therefore, a novel experimental system was planned to be established that permits the precise quantification of HASPB export from mammalian cells based on flow cytometry. Using this assay, the aim was to screen somatic CHO mutants that are incapable of exporting HASPB-GFP fusion proteins employing retroviral insertion mutagenesis. Based on a detailed biochemical and morphological characterization of mutants with this phenotype, the site of HASPB membrane translocation was studied. Moreover, based on the mutagenesis strategy used, the analysis of the component that might be potentially involved in the unconventional secretion process of HASPB export mutants was aimed.

In the second chapter of this thesis, the aim was to analyze whether HASPB-mediated plasma membrane blebbing (Tournaviti et al., 2006 submitted) results in shedding of plasma membrane-derived HASPB-containing vesicles into the extracellular space (section 1.3.5). Based on various biochemical approaches the analysis of cell culture supernatants from HASPB-N18-GFP expressing CHO cells was planned. Using these methods, a major aim was to analyze and characterize alternative secretory mechanisms that potentially might drive export of the unconventionally secreted protein HASPB.

2 Material and Methods

2.1 *Material*

2.1.1 *Chemicals*

| Chemicals | Manufacturer |
|--|--|
| AEBSF | Sigma-Aldrich Chemie GmbH, Steinheim |
| Agar | Becton Dickinson, Le Pont de Claix, France |
| Agarose electrophoresis grade | Invitrogen Ltd., Paisley, UK |
| alpha-MEM | Biochrom AG, Berlin |
| Ammonium chloride | Carl Roth GmbH, Karlsruhe |
| Ampicillin sodium salt | Gerbu Biotechnik GmbH, Gaiberg |
| APS (Ammonium peroxo disulfate) | Carl Roth GmbH, Karlsruhe |
| β -Mercaptoethanol | Merck, Darmstadt |
| EZ-Link Sulfo-NHS-SS-Biotin | Pierce, Perbio Sciences, Bonn |
| Bromphenol Blue Na-salt | Serva Electrophoresis GmbH, Heidelberg |
| BSA (Bovine serum albumine, Albumin fraction V) | Carl Roth GmbH, Karlsruhe |
| Calcium chloride dihydrate | Applichem, Darmstadt |
| Cell dissociation buffer (CDB) | Invitrogen, Paisley, UK |
| Chloroquine | Sigma-Aldrich Chemie GmbH, Steinheim |
| CL-4B Sepharose (Beads) | Amersham Biosciences Pharmacia, Uppsala, Sweden |
| Clear Nail Protector | Wet'n Wild USA, North Arlington, USA |
| Complete Mini (Protease Inhibitor Cocktail Tablets) | Roche Diagnostics, Mannheim |

| | |
|---|---|
| Deoxycholic acid sodium salt | Sigma-Aldrich Chemie GmbH, Steinheim |
| DMEM | Biochrom AG, Berlin |
| DMSO (Dimethyl sulfoxide) | J.T. Baker, Deventer, USA |
| DNA ladder (1 kb and 100 bp) | New England Biolabs, Frankfurt |
| dNTP-Mix | Peqlab, Erlangen |
| Doxycycline | Clontech, Palo Alto, USA |
| ECL Western Blotting Detection Reagent | Amersham Biosciences Pharmacia, Uppsala, Sweden |
| EDTA (Ethylene diamine tetraacetic acid) | Merck, Darmstadt |
| Ethanol pro analysi | Riedel-de Haën, Seelze |
| FCS (Fetal Calf Serum) | PAA Laboratories GmbH, Linz, Austria |
| Fluoromount G | Southern Biotechnologies Associa- tion Inc., Birmingham, USA |
| Glycerol | Carl Roth GmbH, Karlsruhe |
| Glycine | Applichem, Darmstadt |
| Hepes | Carl Roth GmbH, Karlsruhe |
| ImProm-II TM Reverse Transcription System | Promega |
| Isopropanol | Merck, Darmstadt |
| Kanamycin sulfate | Gerbu Biotechnik GmbH, Gaiberg |
| L-Glutamine | Biochrom AG, Berlin |
| Magnesium chloride hexahydrate | Applichem, Darmstadt |
| Methanol pro analysi | Merck, Darmstadt |
| Milk Powder | Carl Roth GmbH, Karlsruhe |
| Nonidet P40 (NP-40) | Roche, Mannheim |
| Nycodenz | Axis Shield |
| Paraformaldehyde | Electron Microscope Sciences, Hatfield, UK |
| Penicillin/Streptomycin for cell culture | Biochrom AG, Berlin |

| | |
|---|--|
| Ponceau S | Serva Electrophoresis GmbH, Heidelberg |
| Potassium dihydrogen carbonate | Carl Roth GmbH, Karlsruhe |
| Potassium hydroxide | J.T.Baker, Deventer, USA |
| Protein A-Sepharose (Beads) | Amersham Biosciences Pharmacia, Uppsala, Sweden |
| PVDF Membrane Immobilon P | Millipore Corporation, Bedford |
| PVDF Membrane Immobilon FL | Millipore Corporation, Bedford |
| Rotiphorese Gel 30 (37.5:1) | Carl Roth GmbH, Karlsruhe |
| Sodium chloride | J.T. Baker, Deventer, USA |
| Sodium dodecyl sulfate | Serva Electrophoreis GmbH, Heidelberg |
| Sodium hydrogen carbonate | J.T. Baker, Deventer, USA |
| Sodium hydroxide | J.T. Baker, Deventer, USA |
| Sucrose | J.T. Baker, Deventer, USA |
| TEMED (N,N,N',N'-tetramethyl- ethylenediamine) | Bio-Rad, München |
| Trichloroacetic acid | Carl Roth GmbH, Karlsruhe |
| Tris | Carl Roth GmbH, Karlsruhe |
| Triton X-100 | Roche, Mannheim |
| Trypsin/EDTA for cell culture | Biochrom AG, Berlin |
| Trypsin | Sigma-Aldrich Chemie GmbH, Steinheim |
| Tryptone | Becton Dickinson, Le Pont de Claix, France |
| Tween 20 (Polyoxyethylene- sorbitan monolaurate) | Carl Roth GmbH, Karlsruhe |
| UltraLink immobilized streptavidin (Beads) | Pierce, Perbio Sciences, Bonn |
| Whatman MM | Whatman AG, Würzburg |
| Xylencyanol FF | Serva Electrophoresis GmbH, Heidelberg |

| | |
|---------------|--|
| Yeast Extract | Beckton Dickinson, Le Pont de Claix, France |
|---------------|--|

| Technical devices | Manufacturer |
|--|---------------------------------------|
| Anthos 2001 Microplate Photometer | Anthos, Hombrechtikon, Switzerland |
| Bacterial Incubator Infors HT ITE | Infors AG, Einsbach |
| Bacterial Shaker Centromat R | Braun, Melsungen |
| Centrifuge 5415 R | Eppendorf, Hamburg |
| Centrifuge 5417 R | Eppendorf, Hamburg |
| Centrifuge Avanti J-25 | Beckman Coulter, Krefeld |
| Centrifuge Megafuge 1.0 R | Kendro, Langenselbold |
| Centrifuge Optima TLX Ultracentrifuge | Beckman Coulter, Krefeld |
| Centrifuge Rotor Sorvall SS-34 | Kendro, Langenselbold |
| Centrifuge Sorvall Evolution RC | Kendro, Langenselbold |
| Centrifuge Sorvall RC 6 | Kendro, Langenselbold |
| Ultracentrifuge Rotor TLA-45 | Beckman Coulter, Krefeld |
| Ultracentrifuge | Beckman Coulter, Krefeld |
| FACSAria | Becton Dickinson, Heidelberg |
| FACSVantage | Becton Dickinson, Heidelberg |
| FACSCalibur | Becton Dickinson, Heidelberg |
| Gel Doc 2000 | Bio-Rad, München |
| Incubator Heraeus CO ₂ -Auto-Zero | Kendro, Langenselbold |
| LKB Ultraspec III | Amersham Biosciences, Freiburg |
| Microscope Axiovert 40 C | Zeiss, Göttingen |
| Microscope LSM 510 Meta Confocal | Zeiss, Göttingen |
| Mini Trans-Blot Cell | Bio-Rad, München |
| Mini-PROTEAN 3 Electrophoresis System | Bio-Rad, München |
| Nanodrop ND-1000 Spectrophotometer | Peqlab, Erlangen |
| Odyssey Infrared Imaging System | LI-COR Biosciences, Bad Homburg |

| | |
|---------------------------------|--|
| PCR Primus Advanced 25 and 96 | Peqlab, Erlangen |
| pH-Meter 766 Calimatic | Knick, Egelsbach |
| Power Pack 200 and 300 | Bio-Rad, München |
| Roto-Shake Genie | Scientific Industries, Bohemia, USA |
| Sonorex Super RK 103 h | Bandelin, Berlin |
| Thermomixer compact and comfort | Eppendorf, Hamburg |
| Tricorn 5/150 Column | Amersham Biosciences, Freiburg |

2.1.2 Plasmids

| Name | Origin |
|---------------------------------------|---------------------------------|
| pRevTRE2-HASPB-N18-GFP | AG Nickel, BZH, Heidelberg |
| pRevTRE2- Δ palm-HASPB-N18-GFP | AG Nickel, BZH, Heidelberg |
| pRevTRE2- Δ myr-HASPB-N18-GFP | AG Nickel, BZH, Heidelberg |
| pRevTRE2-Src-GFP-IgG | AG Nickel, BZH, Heidelberg |
| pRevTRE2-Yes-GFP-IgG | AG Nickel, BZH, Heidelberg |
| pRevTRE2-Fyn-GFP-IgG | AG Nickel, BZH, Heidelberg |
| pRevTRE2-Lck-GFP-IgG | AG Nickel, BZH, Heidelberg |
| pGEM-T | Promega, Madison, USA |
| pGEM-T-cmkor | AG Nickel, BZH, Heidelberg |
| pRTi-cmkor-IRES-CD8 | AG Nickel, BZH, Heidelberg |
| pBICD4 | AG Schwappach, ZMBH, Heidelberg |
| pRevTRE2 | Clontech, Mountain View, USA |
| pRevTRE2-GFP | AG Nickel, BZH, Heidelberg |
| pcDNA 16- Δ palm-HASPB-N18-GFP | Deborah Smith, York, UK |
| pcDNA 16- Δ myr-HASPB-N18-GFP | Deborah Smith, York, UK |
| pcDNA 16-HASPB full length | Deborah Smith, York, UK |
| pFB-hrGFP | Stratagene, La Jolla, USA |
| pVPack-Eco | Stratagene, La Jolla, USA |
| pVPack-GP | Stratagene, La Jolla, USA |

2.1.3 DNA modifying enzymes

| Enzyme | Manufacturer |
|-----------------------------------|---------------------------------------|
| AmpliTaq Polymerase | Perkin Elmer (Roche), Branchburg, USA |
| PfuTurbo Polymerase | Stratagene, La Jolla, USA |
| Age I | New England Biolabs, Frankfurt |
| BamH I | New England Biolabs, Frankfurt |
| EcoR I | New England Biolabs, Frankfurt |
| Nde I | New England Biolabs, Frankfurt |
| Not I | New England Biolabs, Frankfurt |
| Pac I | New England Biolabs, Frankfurt |
| Pme I | New England Biolabs, Frankfurt |
| Xba I | New England Biolabs, Frankfurt |
| Calf Intestinal Phosphatase (CIP) | New England Biolabs, Frankfurt |
| Klenow | New England Biolabs, Frankfurt |

2.1.4 Primers and oligonucleotides

Primers and oligonucleotides were purchased from Thermo Electron Company.

PCR primers for HASPB-N18 and eGFP:

5'-primer for HASPB-N18 (pRevTRE2-GFP), BamHI-restriction-site:

5'-GATCCCGCCACCATGGGAAGTTCTTGTACAAAGGACTCCGCAAAGG
AGCCCCAGAAGCGTGCTGATGGA - 3'

3'-primer for HASPB-N18 (pRevTRE2-GFP), AgeI-restriction-site:

5'-CCGGTCCATCAGCACGCTTCTGGGGCTCCTTTGCGGAGTCCTTTGT
ACAAGAACTTCCCATGGTGGCGG - 3'

PCR primers for cmkor 1-RT-PCR:**5'-primer for cmkor 1 (No.1):**

5' - AACAGCAGCGACTGCATTGTGGTGGACAC - 3'

3'-primer for cmkor 1 (No.1):

5' - CCTGTTTTGGCCGAGTACTTGAAGATGAAGGC- 3'

5'-primer for cmkor 1 (No.2):

5' - ATGGATGTGCACTTGTGTTGACTATGCAGAGCC- 3'

3'-primer for cmkor 1 (No.2):

5' - TCACTTGGTGTCTGTTCCAGGGCAGAGTACTC- 3'

PCR primers for pRTi-cmkor 1-IRES-CD8:**5'-primer for cmkor (pRTi-cmkor 1-IRES-CD8), BamHI-restriction-site:**

5' - CGGATCCATGGATGTGCACTTGTGTTGACTATGCAGAGCCTGGG - 3'

3'-primer for cmkor (pRTi-cmkor 1-IRES-CD8), PacI-restriction-site:

5' - CCTTAATTAATCACTTGGTGTCTGTTCCAGGGCAGAGTACTCCG- 3'

PCR primers for pRTi-sequencing:**5'-primer for pRTi:**

5' - CCACGCTGTTTTGACCTCCA - 3'

3'-primer for pRTi:

5' - CGCACACCGGCCTTATTCC- 3'

siRNA oligonucleotides directed against cmkor 1 (CHO):**No.1 Sense:**

5'-CGCUCUCCUUCAUCUACAUtt -3'

No.1 Antisense:

5'-AUGUAGAUGAAGGAGAGCGtg -3'

No.2 Sense:

5'-CCUUUUCGGGAGCAUCUUCtt -3'

No.2 Antisense:

5'-GAAGAUGCUCGCGAAAAGGtt -3'

No.3 Sense:

5'-GCUCACAUGCAAGGUCACAtt -3'

No.3 Antisense:

5'-UGUGACCUUGCAUGUGAGCtc-3'

2.1.5 Bacteria and bacterial media

Transformation and plasmid amplification were performed with competent DH5a cells (Invitrogen). They were grown in LB medium (Luria Bertani) or on LB agar plates supplied with ampicillin in a final concentration of 100 µg/ml in order to select for successfully transformed cells carrying plasmids containing a resistance gene.

Bacteria: subcloning efficiency DH5α competent cells, Genotype:
 F⁻ φ80d/*lacZ*ΔM15 Δ(*lacZYA-argF*) U169 *recA1 endA1 hsdR17*
 (*r_k*⁻, *m_k*⁺) *phoA supE44 λ⁻ thi-1 gyrA96 relA1*

| | | |
|------------|------------|---------------|
| LB medium: | 0.5% (v/w) | NaCl |
| | 1% (w/v) | Tryptone |
| | 0.5% (w/v) | Yeast extract |

| | | |
|-----------------|------------|---------------|
| LB agar plates: | 0.5% (w/v) | NaCl |
| | 1% (w/v) | Tryptone |
| | 0.5% (w/v) | Yeast extract |
| | 1.6% (w/v) | Agar |

2.1.6 Eukaryotic cell lines

In order to produce stable packaging cell lines the 293 cell derivative 293T HEK (Human Embryonic Kidney) cell line allowed the production of high-titer viral supernatants following transient cotransfection of the viral vector together with expression vectors encoding the *gag*, *pol* and *env* genes.

CHO (Chinese Hamster Ovary) cells and HeLa (Henrietta Lacks) cells were used as target cell lines for retroviral transduction. Upon incubation of viral supernatant with the target cells a stable transduction with cDNA constructs was achieved. Retroviral transduced cell lines expressing various reporter molecules were used in *in vivo* systems to study proteins in an eukaryotic living cell environment.

Eukaryotic cell lines: HEK 293T cells (ATCC CRL-11268)
 CHO cells (ECACC 85050302)
 HeLa cells (ATCC CCL-2.1)

2.1.7 Eukaryotic cell culture media (Wilson et al., 1994)

α Modification of the Minimal Essential Medium (α MEM)

α MEM (F0925, Biochrom AG) was used for the cultivation of CHO cells.

To produce 5 l α MEM dry powder was dissolved in H₂O_{MilliQ} and 10 g of sodium hydrogencarbonate was added to adjust the pH to 7.4. The prepared medium was sterile filtered into autoclaved bottles and stored at 4°C. Before incubation of cells with α MEM, 10% (v/v) fetal calf serum (FCS), 100 µg/ml Streptomycin/Penicillin and 2 mM L-Glutamine, only after storage over 4 weeks, was supplemented.

Dulbecco's Modified Eagle Medium (DMEM)

DMEM (F0415, Biochrom AG) was used for the cultivation of HEK 293T and HeLa cells.

To produce 5 l DMEM dry medium was dissolved in H₂O_{MilliQ} and 10 g of sodium hydrogencarbonate were added to adjust the pH to 7.4. The prepared medium was sterile filtered into autoclaved bottles and stored at 4°C. Before incubation of cells with DMEM, 10% (v/v) FCS, 100 µg/ml Streptomycin/Penicillin and, 2 mM L-Glutamine, only after storage over 4 weeks, was supplemented.

2.1.8 Primary antibodies

Anti-GFP antibodies were generated by immunization of rabbits with recombinant

N-terminally His₆-tagged eGFP expressed in E.coli. The resulting anti-serum was incubated with His₆-tagged eGFP coupled to Epoxy-sepharose (Amersham Pharmacia). Bound antibodies were eluted under acidic and basic conditions according to standard procedures.

Monoclonal antibodies against the CD4 epitope and CD8 epitope were derived from the hybridoma Okt 4 (ATCC CRL-8002) and Okt 8 (Hoffmann, 1980) cells, respectively.

Antibodies directed against the transferrin receptor were from Zymed, antibodies directed against GM130 were purchased from BD Transduction Laboratories and were both kind gifts of Felix Wieland (Biochemiezentrum Heidelberg).

Antibodies directed against TSG101 (1:500) were from Gene Tex, antibodies directed against Hsc70 (1:750) were purchased from Stressgen. Antibodies directed against GAPDH (1:4000) were obtained from Ambion. Antibodies directed against Alix were the kind gifts of Oliver Fackler (Hygieneinstitut Heidelberg).

To detect GFP-containing reporter constructs affinity-purified anti-GFP antibodies (Pineda Antibodies, acidic elution) were used (Engling et al., 2002). They were applied in a 1:300 dilution for Western blot and in a 1:200 dilution for FACS analysis.

In immunoprecipitation experiments 20 μ l of affinity-purified anti-GFP antibodies (Pineda Antibodies, basic elution, (Engling et al., 2002)) were coupled to 20 μ l Protein A sepharose: CL4B beads per reaction.

2.1.9 Secondary antibodies

HRP-coupled goat anti-rabbit (1:5,000) and goat anti-mouse (1:5,000) IgG antibodies used for Western blot analysis were from Biorad.

Alexa 680-coupled goat anti-rabbit (1:20,000), goat anti-mouse (1:10,000) and goat anti-rat (1:10,000) IgG antibodies used for western blot analysis were obtained from Molecular Probes.

APC (Allophycocyanin)-conjugated anti-rabbit and anti-mouse IgG antibodies used for FACS analysis were from Molecular Probes and used in a 1:750 dilution.

2.2 Molecular biological methods

2.2.1 Bacterial transformation

For the transformation of chemically competent DH5 α cells 1 to 5 μ l (1-10 ng DNA) or 5 μ l of each ligation reaction were directly added to 45 μ l competent cells, mixed by tapping gently and incubated for 30 minutes on ice. After heat-shock for exactly 20 seconds at 37°C and placing for further incubation period of 2 minutes on ice, 900 to 950 μ l of pre-warmed medium (w/o ampicillin) were added to each vial followed by an incubation at 37°C for exactly 1 hour at 225 rpm in a shaking incubator.

From each transformation vial 20 to 200 µl were spread on separate, labelled LB agar plates supplemented with 100 µg/ml ampicillin and incubated at 37°C for 12 to 16 h.

2.2.2 Selection and amplification of plasmids

Bacteria grown on agar plates form colonies originating from a single bacterium. In order to obtain genetically identical plasmids a single colony was selected and transferred to 10 ml LB medium supplemented with the respective antibiotic by using a 20 µl pipet tip. After incubation at 37°C overnight at 280 rpm in a shaking incubator the selection for bacteria carrying plasmids containing a resistance gene is guaranteed.

2.2.3 Plasmid preparation

Plasmids were prepared from overnight LB medium cultures of transformed bacteria by the application of Qiagen or Macherey Nagel DNA purification kits. The appropriate kit was chosen in dependence on the volume of the overnight culture.

| <i>Volume of bacterial culture</i> | <i>Qiagen Kit</i> | <i>Macherey Nagel Kit</i> |
|------------------------------------|---------------------------|---------------------------|
| 5 - 10 ml | QIAprep Spin Miniprep Kit | Nucleospin Plasmid |
| 20 – 150 ml | QIAGEN Plasmid Midi Kit | Nucleobond-PC 100 |
| More than 150 ml | QIAGEN Plasmid Maxi Kit | Nucleobond-PC 500 |

Purification was performed following the manufacturer's manual employing alkaline lysis and binding of DNA to silica membranes or anion-exchange resins, respectively. Elution of the DNA was performed using appropriate volumes of H₂O_{MilliQ}.

2.2.4 Isolation of genomic DNA from cultured cells

In eukaryotes the genomic DNA is located in the nucleus and consists of chromosomes varying in number due to different organisms. Isolated genomic DNA represents a collection of all genes within an organism. The isolation of genomic DNA from cultured cells was prepared by the application of the DNeasy Tissue kit (Quiagen). Cells grown in 10 cm plates were washed with PBS, scratched from the plates and spinned for 3 min at 300 g. Following incubation in an appropriate volume of proteinase K buffer at 70°C for 10 minutes and further washing steps, genomic DNA was eluted with buffer provided by the kit. Since storage at -20°C can cause shearing of genomic DNA, the genomic DNA isolated from cultured cells were stored at 4°C.

2.2.5 Isolation of RNA from cultured cells

The isolation of RNA from cultured cell was performed employing the RNeasy kit (Quiagen). Due to further applications total or cytoplasmic RNA was isolated with the RNeasy Micro kit or the RNeasy Midi/Maxi kit, respectively. Since the cytoplasm contains RNA in its mature form, the isolation of cytoplasmic RNA from cultured cells is particularly advantageous in applications where unspliced or partially spliced RNA is not desirable. In applications such as RT-PCR where the absence of DNA contamination is critical, traces of DNA were removed either by centrifugation for cytoplasmic RNA isolation or by DNase treatment for total RNA isolation, respectively. To isolate cytoplasmic RNA cultured cells were lysed in a buffer containing a non-ionic detergent. Nuclei remain intact during the lysis procedure and were removed by centrifugation. Following extensive washing optimal conditions for selective binding of the RNA to the silica gel membrane were provided. Contaminants were efficiently washed away and high quality RNA was eluted in RNase-free water and stored at -70°C. Cytoplasmic RNA accounts for 85% of total cellular RNA. Similarly, total RNA from cultured cells was isolated. Traces of DNA that may copurify were removed by DNase treatment on the RNeasy spin column. DNase and any contaminants were removed by washing and high-quality total

RNA was eluted in RNase-free water and stored at -70°C . This procedure enriches for mRNA since most RNAs smaller than 200 nucleotides such as 5.8S rRNA, 5S rRNA and tRNAs (which together make up 15-20% of total RNA) are selectively excluded.

2.2.6 Determination of DNA/RNA concentrations

The concentration of a given DNA was determined upon a photometrically measurement of the optical density (OD) at a wavelength of 260 nm. In a photometer with UV-lamp the absorption of the diluted DNA solution transferred to a quartz- cuvette was performed. An optical density (OD) of 1 corresponds to a concentration of 50 $\mu\text{g/ml}$ of double stranded DNA. Using this DNA-specific multiplication factor, the dilution and the OD at 260 nm, the exact concentration of the DNA was calculated. The OD value should range between 0.1 and 1.0 to ensure optimal measurement.

Alternatively, the concentration was measured by directly pipetting 1 μl of the DNA solution in a Nanodrop photometer.

The ratio $\text{OD}_{260}/\text{OD}_{280}$ represents the grade of purity since pure DNA shows a value between 1.8 and 2.0. An $\text{OD}_{260}/\text{OD}_{280}$ below 1.8 indicate that the preparation is contaminated with proteins and aromatic substances (e.g. phenol). In contrast, an $\text{OD}_{260}/\text{OD}_{280}$ above 2 indicate a possible contamination with RNA.

Analogous to the determination of DNA concentration the concentration of RNA was performed using a conventional UV-containing photometer or the Nanodrop photometer, respectively.

Concerning RNA an optical density (OD) of 1 corresponds to a concentration of 40 $\mu\text{g/ml}$ of ssRNA. To obtain pure RNA the ratio $\text{OD}_{260}/\text{OD}_{280}$ should be between 1.9 and 2.1 in 10 mM Tris buffer. An $\text{OD}_{260}/\text{OD}_{280}$ smaller than 2.0 indicate, that the preparation is contaminated with proteins and aromatic substances.

2.2.7 Agarose gel electrophoresis

Agarose gel electrophoresis was used to separate and identify DNA-fragments of 0.5 to 25 kb in length. An appropriate amount of agarose was solved in electrophoresis buffer (TAE) upon heating. In order to make the DNA visible ethidiumbromide was added and a gel with pockets was poured. After curing, the DNA solution was transferred into the pockets and electricity was subjected that leads to the migration of the negatively charged DNA fragments towards the anode. The migratory behaviour of DNA fragments depends on their size and is limited by the pore size of the gel, which is defined by the amount of agarose used. To achieve a good separation of DNA fragments between 300 and 5000 bp generally agarose concentrations of 0.8-2% were used.

Agarose gels were prepared by dissolution of 1% agarose (w/v) in TAE buffer upon heating. After cooling, ethidiumbromide was added in a final concentration of 0.5 µg/ml and the solution was poured into an agarose gel-casting chamber containing a plastic comb forming the loading pockets. Following completely curing the gel was stored at 4°C until use.

Electrophoresis was performed upon transfer of the gel into an agarose gel running chamber and addition of TAE. DNA samples containing DNA sample buffer in a 1:5 dilution were transferred into the pockets and electrophoresis was performed at 100 V until sufficient separation was reached visualized by the migration behaviour of the blue bromphenol marker front. Agarose gels were documented using the Gel Doc 2000 imaging system (Bio-Rad).

| | | |
|-------------------|---------|------------------------------------|
| TAE buffer (50x): | 242 g | Tris |
| | 57.1 ml | Glacial acidic acid |
| | 100 ml | 0.5 M EDTA, pH 8 |
| | ad 1 l | H ₂ O _{MilliQ} |

2.2.8 DNA sample buffer/loading buffer

Since DNA solutions have a density similar to that of electrophoresis buffer, transfer of DNA-containing samples into the pockets of an agarose gel is not possible. Upon addition of sample buffer to the DNA solution, which in turn results in increasing of the density, the loading of the samples was achieved. To visualize the DNA sample during electrophoresis generally dyes such as Xylencyanol, Bromphenol Blue or Orange G are added.

| | |
|-------------------------|-----------------------------|
| DNA sample buffer (5x): | 0.25% (w/v) Bromphenol Blue |
| | 0.25% (w/v) Xylencyanol FF |
| | 30% (w/v) Glycerol |

2.2.9 DNA marker

To determine the size of a loaded DNA sample DNA ladders were used as size standard. They contain DNA-fragments in a regular distance, the 1 kb DNA ladder (New England Biolabs) containing DNA fragments ranging from sizes of 500 to 10,000 bp was used to calculate large inserts and vectors. To analyze smaller DNA fragments the 100 bp DNA ladder (New England Biolabs) containing DNA fragments of defined sizes ranging from 100 to 1,500 bp was used.

The markers were applied by loading 10 μ l of a stock solution containing 0.05 μ g/ μ l DNA in DNA sample buffer. Besides the determination of the size of a given DNA sample, the marker can be used to approximate the mass of DNA of an unknown sample. Since each band of the marker contains a defined amount of DNA the determination of the mass of the unknown sample was achieved by comparing band intensities visually.

2.2.10 Polymerase chain reaction

To amplify genes or DNA fragments a polymerase chain reaction (PCR) was performed (Lawyer et al., 1989; Saiki et al., 1988).

Using this method a DNA template defined by a forward and reverse oligonucleotide primer was amplified in high amounts and could be used for further cloning to generate desired reporter constructs. The amplification reaction was mediated by the thermostable DNA-polymerase, *AmpliTaq* polymerase (Perkin Elmer) an enzyme generating adenosine overhangs at the 3'-ends. Based on this 3'-overhangs ligation of PCR products into the pGEM-T vector containing thymidine overhangs at its 3'-ends was achieved and used for further cloning.

The following reaction mix was used for PCRs.

Sample reaction (total 100 µl):

- 10 µl 10x reaction buffer
- 2 µl (10 ng) dsDNA template
- 1 µl (25 pmol) oligonucleotide forward primer
- 1 µl (25 pmol) oligonucleotide reverse primer
- 10 µl (10 mM) dNTP mix
- 5.9 µl (25 mM) MgCl₂
- 69.1 µl H₂O_{MilliQ}
- 1 µl of *AmpliTaq* DNA Polymerase (2.5 U/µl)

The PCR reaction was performed employing a Primus Advance Thermocycler (PeqLab). In principle the PCR contains three main steps, denaturation, annealing and elongation. At 94°C, the double-stranded DNA is denatured and both strands get divided. In a second step the temperature is dropped to 55°C resulting in hybridisation of the oligonucleotide primers to the single-stranded DNA. Upon increase of the temperature back to 72 °C, the temperature optimum of the *AmpliTaq* polymerase, elongation of the primers is achieved. As a result double-stranded DNA was produced that corresponds exactly to the used template-DNA. Since the complementation is performed

on both DNA strands the amount of template DNA is doubled in one PCR-cycle. Upon repeating of a cycle the amount increases to a four fold and continues by using some rounds of cycles. The following program was used to amplify DNA.

Cycling parameters:

| | | |
|------------------------------|--|---|
| Denaturation | 2 min, 95°C | |
| Amplification (30 cycles) | 45 sec, 94°C 1 min, $T < T_m$ of primers 1 min, 72°C | Denaturation Hybridization Elongation |
| Elongation | 10 min, 72°C | |
| Store | ∞, 4°C | |

The annealing temperature was determined depending on the melting temperatures (T_m) of the used primers. It was chosen after subtracting 5°C from the T_m of the primer having the lower T_m ($T = T_m - 5^\circ\text{C}$). Generally melting temperatures were defined depending on the amount of the bases guanine (G) and cytosine (C) and were calculated for each individual primer according to the following equation.

$$T_m = 81.5 + 16.6 \times \log [\text{Na}^+] + 41 \times \% \text{GC} - \frac{675}{N}$$

$$[\text{Na}^+] = 0.05 \text{ M}$$

% GC = GC content of annealing sequence

N = number of annealing bases

As Mg^{2+} influences the annealing of the primers, the separation of the DNA strands during denaturation and the specificity of the product the concentration of MgCl_2 needs to be optimized for each PCR reaction.

Furthermore the enzyme needs free Mg^{2+} -ions for its optimal activity. Therefore perfect Mg^{2+} concentrations are a prerequisite for an optimal PCR reaction. Additionally, dimethyl sulfoxide (DMSO) until 10% (v/v) and Formamid until 5% (v/v) increase the specificity and facilitates the amplification of sequences containing high amounts of GC. To accelerate the reaction Glycerin, PEG 6000 and Tween 20 can be used.

2.2.11 RT-PCR

To detect the transcription of a gene in cells, the reverse transcriptase-polymerase chain reaction (RT-PCR) was performed. RNA isolated from cells was used for the synthesis of cDNA in the RT reaction that in turn was used as template for the PCR reaction. In the reverse transcription reaction gene-specific primers (section 2.1.5) were used.

The RT-PCR was performed by the application of ImProm-IITM Reverse Transcription Sytem kit (Promega).

The following steps were used for the synthesis of cDNA from RNA (RT):

A. Target RNA and primer combination and denaturation:

up to 1 µg RNA template

20 pmol gene-specific primer

Nuclease-free water to a final volume of 5 µl

This mixture was placed into a preheated 70°C heat block for 5 minutes. Immediately the sample was chilled in ice-water for at least 5 minutes and spinned for 10 seconds in a microcentrifuge.

B. Reverse Transcription:

Reverse Transcription mix (total volume 15 µl):

3.7 µl Nuclease-free water

4.0 µl ImProm-II™ 5xReaction Buffer

4.8 µl (25 mM) MgCl₂

1.0 µl (10 mM) dNTP mix

0.5 µl Recombinant RNasin Ribonuclease inhibitor

1.0 µl ImProm-II™ Reverse Transcriptase

After vortexing, the reverse transcription mix was added to the RNA and primer mix (step A) resulting to a final reaction volume of 20 µl per tube. Analogous to the PCR-reaction the reverse transcription was performed in the following steps.

Annealing: The tubes were placed in a controlled temperature heat block equilibrated at 25 °C and incubated for 5 minutes.

Extension: The tubes were incubated for 1 hour in a controlled temperature heat block at 42 °C

Inactivation of the reverse transcriptase: To proceed with the PCR, the reverse transcriptase was thermally inactivated prior to amplification. The tubes were incubated in a controlled temperature block at 70°C for 15 minutes.

C. PCR Amplification

The following reaction mix was used for the PCR amplification.

PCR mix (total 80 µl):

62.4 ml Nuclease-free water

8 µl 10x thermophilic polymerase reaction buffer (w/o MgCl₂)

5.6 µl (25 mM) MgCl₂

1 µl (10 mM) dNTP mix

1 µl (1 µM) oligonucleotide forward primer

1 µl (1 µM) oligonucleotide reverse primer

1 µl of *Taq* DNA Polymerase (5.0 U/µl)

The PCR mix was combined with the cDNA sample (20 µl) to a final volume of 100 µl and amplified by the following programme.

Cycling parameters:

| | | |
|------------------------------|---|---|
| Denaturation | 2 min, 94°C | |
| Amplification (25 cycles) | 1 min, 94°C 1 min, 60°C 2 min, 72°C | Denaturation Hybridization/Annealing Elongation |
| Elongation | 5 min, 72°C | |
| Store | ∞, 4°C | |

The PCR products were analyzed by agarose gel electrophoresis using approximately 10% of the total reaction. The amplification product obtained using the positive control RNA (1.2 kb Kanamycin positive control RNA, 0.5 µg/ml) with the upstream and downstream control primers applied with the ImProm-II™ Reverse Transcription Sytem kit, is 323bp long.

2.2.12 PCR purification

PCR products were purified for further analysis in order to remove primers and reaction mix components employing a PCR purification kit (QiaQuick PCR purification kit, Qiagen). Under high salt conditions the amplified DNA was bound to a silica membrane and eluted after washing with an appropriate volume of H₂O_{MilliQ}.

2.2.13 Gel extraction of DNA fragments

To isolate pure DNA after a restriction digest the reaction mix was separated on a 1% agarose gel. DNA fragments were transiently visualized with an UV lamp (366 nm) and the desired DNA fragment was cut out of the gel with a sharp blade. To separate the agarose gel from the DNA and to purify the DNA

the samples were processed using a gel extraction kit (Qiagen). Upon incubation of the samples in lysis containing buffer at 50°C the agarose was melted. The samples were transferred to column tubes applied by the manufacturer and DNA was bound to a silica membrane under high salt conditions. Elution was performed after a washing step in an appropriate volume of H₂O_{MilliQ}.

2.2.14 Restriction digests

To digest DNA for further cloning experiments restriction enzymes or restriction endonucleases (New England Biolab) were used. These enzymes recognise a specific target sequence within the DNA mostly ranging four to eight nucleotides and digest DNA at exactly specific base pairs resulting in sticky or blunt ends. Restriction digests were performed according to the manufacturer's manual. DNA, H₂O_{MilliQ}, an appropriate enzyme and buffer optimized for the given enzyme were incubated for at least 2 hours at 37°C. In the case of a double digest a buffer was chosen that provides the highest cleavage efficiency for both enzymes or the digest was performed sequentially for an appropriate time followed by combining both samples. Depending on the enzyme and the quality of the DNA 1 to 5 U/μg DNA were used in a restriction digest.

2.2.15 Elongation of DNA using the Klenow fragment

To elongate digested DNA in order to generate blunt ends for further cloning the Klenow fragment (New England Biolab) was used. The Klenow fragment is the big subunit of the DNA Polymerase I of E. coli and functions as 5'-3' polymerase. Synthesis of DNA was performed according to the manufacturer's manual. Klenow, H₂O_{MilliQ}, dNTPs and buffer were added to the digested DNA and incubated for 15 minutes at 25°C. For the synthesis of 3 basepairs 1 U/μg Klenow was used.

2.2.16 DNA dephosphorylation

Digested DNA contains phosphates at its 5'-ends that are necessary for further cloning such as ligation. In order to prevent self-ligation of the vector based on these phosphates, the dephosphorylation of the vector was achieved using the *Calf Intestinal Phosphatase* (CIP, New England Biolabs). The enzyme was added to the reaction mix in a concentration of 1 U/μg DNA for 30 min at 37°C and in turn was heat inactivated by incubation at 70°C for 10 min.

2.2.17 Ligation of DNA fragments

The ligation of PCR products or other DNA fragments to each other or into linearized vectors was performed using a ligation kit (Takara Bio Inc.). Digestion of the ligation partners with the same restriction enzymes providing compatible ends is a prerequisite for ligation reactions. Based on the application of the manufacturer, 50 ng of vector DNA were used and the amount of insert (digested DNA or annealed oligonucleotides) was calculated according to the following equation.

$$\frac{\text{amount vector [ng]} \times \text{number of basepairs insert [bp]}}{\text{number of basepairs vector [bp]}} = \text{amount insert [ng]}$$

The DNA sample was combined with 5 μl of Takara Solution 1 containing the standard enzyme for ligations (T4 DNA ligase) as well as an optimized buffer in a 2-fold concentration. The reaction was filled to a total volume of 10 μl, mixed and incubated for 2 h at 37°C or for at least 16 h at 4°C. To stop the ligation reaction the mix was heat inactivated by incubation at 65°C for 10 min.

2.2.18 DNA sequencing

For further use of cloned products the sequence of cloned inserts or cDNA constructs in different plasmids were analyzed by sequencing to rule out mutations and to verify the correct sequence. Plasmid samples and appropriate primers were sent to commercial sequencing companies (Seqlab, Göttingen or GATC, Konstanz). Sequenced data was analyzed employing the Lasergene software suite (Lasergene, DNASTar) or the 'align 2 sequences' function of the BLAST project:

<http://www.ncbi.nlm.nih.gov/blast/bl2seq/wblast2.cgi>

2.2.19 Short interfering RNAs (siRNAs) in mammalian cells

Short interfering RNAs or simply RNA interference were used to inactivate genes in cell culture lines in order to study gene function. RNAi is an effective tool for shutting down genes individually based on controlling gene expression. Double stranded RNA molecules, whose nucleotide sequence matches that of the gene to be inactivated, were introduced into a cell. The RNA molecule was hybridized with the mRNA produced by the target gene and directs its degradation. Small fragments of this degraded RNA were subsequently used by the cell to produce more double-stranded RNA that directs the continued elimination of the target mRNA. Since these short RNA fragments were passed on to progeny cells, RNAi can cause heritable changes in gene expression.

In order to achieve a specific silencing of target genes, siRNA target sites are typically chosen by scanning the mRNA sequence of interest for AA dinucleotides, recording the 19 nucleotides downstream of AA. Subsequently the potential siRNA target sequences were compared with an appropriate genome database to eliminate any sequences with significant homology to other genes. To generate siRNAs the siRNA Target Finder and Design Tool[®] provided by Ambion was used:

http://www.ambion.com/techlib/misc/siRNA_finder.html

The three different siRNAs obtained were transfected into CHO cells using Oligofectamine. An appropriate amount of siRNA was mixed with Opti-MEM I Reduced Serum Medium and combined to a mixture of Oligofectamine and opti-MEM I Medium (1:4). Following incubation for 20 minutes at room temperature to form siRNA:Oligofectamine complexes, the mixture was added to the cells that in turn were placed back into the CO₂-incubator at 37°C. After 24-72 hours the cells were used for gene knock down assays.

2.3 *Eukaryotic cell culture techniques*

2.3.1 *Maintaining cell lines*

Optimized growth conditions of adherent cells were achieved on culture dishes in fresh media supplemented with some constituents necessary for growth (section 2.1.8). The cells were grown at 37°C in a CO₂-incubator at 100% humidity. Since cell physiology is highly sensitive to pH variations CO₂ is needed to control pH and was optimized to 5% CO₂ for the used media. Based on the density, the cells were splitted every 3-5 days by washing with PBS and addition of 0.125% (w/v) Trypsin/EDTA in PBS. Following incubation for 1 minute, Trypsin was removed and the cells were resuspended in an appropriate volume of medium used for the corresponding culture dish. Subsequently, cells were seeded in the desired dilution on new culture dishes containing fresh medium. Since cell lines tend to be unstable and features may change with time in culture, cells were cultured for four to six weeks depending on their passage number. Additionally due to mycoplasma contamination, one of the major problems in biological research using cultured cells, freshly thawed cells were treated with Mycoplasma Removal Agent (MRA) (MP formerly ICN Biomedicals, Inc.). MRA was added in a 1:100 (0.5 µg/ml) dilution to the medium and was removed after an incubation time for 1 week.

| | | |
|--------------------------------|--------------------|----------------------------------|
| PBS (Phosphate buffer saline): | 140 mM | NaCl |
| | 2.7 mM | KCl |
| | 10 mM | Na ₂ HPO ₄ |
| | 1.8 mM | KH ₂ PO ₄ |
| Trypsin/EDTA: | 0.5 mM | EDTA |
| | 0.125% (w/v) | Trypsin |
| | up to final volume | PBS |

2.3.2 Freezing of eukaryotic cells

Since cells should not be kept in culture for a period longer than 6 weeks, cells were frozen for long-term storage. In order to prepare frozen stocks, the cells were grown to about 100% confluency. After washing once with PBS cells were detached using 0.125% (w/v) Trypsin/EDTA in PBS. Following resuspending in normal growth medium and transfer to a 15 ml tube, the cells were collected by centrifugation (200 g_{av}, 5 min, 4°C). The sediment was carefully resuspended in 2 ml freeze medium and transferred to 1.8 ml cryo-vial (Greiner). Alternatively, cells were resuspended directly in freeze medium after detaching. Prepared cryo-vials were stored at -80°C in special cryo-boxes that ensure a temperature decrease of 1°C per minute. After incubation for at least 24 hours, frozen cryo-vials were transferred to liquid nitrogen tanks in order to guarantee long-term storage.

| | | |
|----------------|--------------------|-------------------------|
| Freeze Medium: | 20% (v/v) | FCS |
| | 10% (v/v) | DMSO |
| | 100 µg/ml | Streptomycin/Penicillin |
| | up to final volume | αMEM or DMEM |

2.3.3 Thawing of eukaryotic cells

To unfreeze cells, the cryo-vials were removed from liquid nitrogen and immediately thawed in a water bath at 37°C. Following transfer of the cell suspension to 20 ml fresh, pre-warmed culture medium in a 50 ml tube, cells were sedimented by centrifugation (200 g_{av}, 5 min, 4°C). After removing of the DMSO-containing medium, the cell sediment was resuspended in fresh culture medium. Subsequently, cells were seeded on corresponding culture dishes used for preparing the frozen stocks and incubated at 37°C with 5% CO₂.

2.3.4 Retroviral transduction

In order to generate genetically modified reporter cell lines the stable integration of vector DNA containing reporter genes into the genome of target cells was performed employing the MBS Mammalian Transfection Kit (Stratagene). According to the instructions of the manufacturer's manual the production of high titer recombinant retrovirus that are capable of infecting a virtually limitless range of cell types was achieved. Using an MMLV-based expressing vector and the pVPack vector system applied by the manufacturer, viral supernatant was produced. The vectors include a *gag-pol*-expressing vector (pVPack-GP) that is cotransfected with the retroviral expression vector containing the gene of interest and an *env*-expressing vector (pVPack-Eco). Within four days the production of retroviral particles using HEK 293T as host cells and the infection of target cells were performed. As target cell lines CHO_{MCAT-TAM2} (Engling et al., 2002) and HeLa_{MCAT-TAM2} cells expressing the murine cationic transporter MCAT-1 (Albritton et al., 1989; Davey et al., 1997) on the cell surface were chosen facilitating recognition by the virus and mediating docking and uptake. All constructs were cloned into the retroviral expression vector pRev-TRE2 that contains the constitutively expressed doxycycline-sensitive transactivator rtTA2-M2 (Urlinger et al., 2000) and guarantees the production of reporter proteins in a doxycycline-dependent manner (Engling et al., 2002). Besides pRev-TRE2 that allows doxycycline-

dependent protein synthesis due to a doxycycline transactivator responsive element mediating mRNA formation, pFB and pRTI-CD8 vectors were used as expression vectors. The retroviral expression vector pRTi-CD8 promotes the doxycycline-dependent expression of CD8 and simultaneously, due to an IRES element (Jang et al., 1988; Liu et al., 2000), the doxycycline-dependent expression of the gene of interest (cmk α 1). In case of pFB, GFP was constitutively expressed after successful transduction and used as control in various experimental approaches.

On the first day of the retroviral transduction the corresponding DNA mixture was precipitated using 1 ml 100% (v/v) ethanol and 0.1x volume 3 M sodium acetate. After incubation at -80°C for 30 minutes, the DNA sediment was collected by centrifugation at 12,000 g_{av} for 10 minutes. The supernatant was discarded and 1 ml 70% (v/v) ethanol was added. Following centrifugation (12,000 g_{av} , 4°C, 5 min) the supernatant was discarded and the wet sediment was stored at 4°C overnight. In parallel, the virus producing HEK 293T cells were seeded on freshly prepared culture dishes in an appropriate density facilitating a successful transfection on the following day.

HEK 293T cells were transfected with the precipitated DNA pellets prepared the day before according to the manual of the MBS mammalian transfection kit and incubated for 48 h at 37°C to produce retroviral particles. Alternatively, if virus was to be harvested 72 hours post-transfection, all steps from day four were performed on the following day.

On the third day, the medium from the HEK 293T cells was removed and replaced by fresh medium. Additionally, the target cells, CHO_{M α TCAT-TAM2} or HeLa_{M α TCAT-TAM2} cells, respectively, were seeded on culture dishes in an appropriate density useful for transduction 24 h later.

Finally, on day four, the viral supernatants were harvested from transfected HEK 293T cells and passed through a sterile 0.45 μ m filter. Subsequently, the viral supernatant supplemented with 25 μ M chloroquin was transferred to the target cells. After 3 hours growth medium was added and the cells were incubated for two days in order to allow successful transduction efficiency. Residual viral supernatant was frozen in liquid nitrogen and stored at -80°C for further use.

Transduction was achieved by virus mediated gene transfer generating stable integration of the construct into the genome of the target cell. Transduced cells were used for further applications such as flow cytometry or biochemical assays, respectively. The transduction efficiency was controlled measuring GFP positive cells transduced with pFB-hrGFP by flow cytometry.

| | | |
|----------|------------|---|
| Vectors: | pVPack-GP | (Stratagene) |
| | pVPack-Eco | (Stratagene) |
| | pFB-hrGFP | (Clontech) derived from Moloney Murine Leukemia Virus (MMLV) |
| | pRevTRE2 | (Clontech) derived from MMLV, contains tet-response element (TRE) |

2.3.5 Doxycycline-dependent protein expression

In order to induce the expression of the various reporter constructs by the retroviral expression vector pRev-TRE2 containing the tetracycline/doxycycline-responsive element, doxycycline (Clontech) was added to the culture medium used for growth of the reporter cell lines. The stock solution of 1 mg/ml in PBS was diluted 1:1,000 with culture medium to obtain a final concentration of 1 µg/ml. Depending on the used cell line, doxycycline was added for different time periods, ranging from 12 to 48 hours.

2.4 Biochemical methods

2.4.1 Generation of cell lines expressing various HASPB-GFP fusion proteins

All HASPB fusion proteins used in this study are based on enhanced GFP (Clontech). The 18 N-terminal amino acids (MGSSCTKDSAKEPQKRAD) of HASPB were fused to the N-terminus of eGFP through a short linker sequence (GPVAT). In case of Δ myr-HASPB-N18-GFP and Δ palm-HASPB-

N18-GFP, two single amino acid changes were introduced to prevent myristoylation and palmitoylation (G2A), and palmitoylation (C5S), respectively. All constructs were cloned into the retroviral expression vector pRev-TRE2 that contains a doxycycline-dependent promotor. Generation of CHO cell lines and HeLa cell lines expressing the various HASPB fusion proteins and GFP alone employing retroviral transduction was performed as described (section 2.3.4).

2.4.2 Sample preparation for SDS polyacrylamide gel electrophoresis (SDS-PAGE)

In order to allow separation of proteins for SDS-gel electrophoresis, samples were mixed with SDS sample buffer in a ratio of 3:1 followed by an incubation at 95°C for 5-10 minutes. Following centrifugation (5,000 g_{av}, 4°C, 1 min) the samples were loaded into the pockets of the SDS-gel.

| | | |
|-------------------------|------------|-------------------|
| SDS sample buffer (4x): | 200 mM | Tris-HCl, pH 6.8 |
| | 25% (w/v) | Glycerol |
| | 2% (w/v) | SDS |
| | 0.2% (w/v) | Bromphenol Blue |
| | 0.7 M | β-Mercaptoethanol |

2.4.3 SDS polyacrylamide gel electrophoresis

Proteins are amphoteric macromolecules and contain different amounts of positively (lysine, arginine) and negatively charged (aspartic acid, glutamic acid) as well as ionic (histidine, cysteine) amino acid residues. To separate proteins exclusively in size a treatment with the anionic detergent sodium dodecyl sulfate (SDS) together with reagents (β-mercaptoethanol) breaking sulfur-bridges was performed. Using this method, proteins were denatured and dissociate into their subunits. Hydrophobic interactions between the polypeptides and the negatively charged SDS lead to an overlapping of the

proteins self-charge. As a result proteins have a constant ratio of charge to mass and can be electrophoretically separated by their relative molecular masses using gel-matrices.

To separate SDS denatured proteins according to their size SDS polyacrylamide gel electrophoresis was performed as described (Laemmli et al., 1970) using the Mini PROTEAN III Electrophoresis System (Bio-Rad). The separating gel solution containing 13% acrylamide was poured between to glass plates fixed in a casting frame and in turn was overlaid with isopropanol to obtain an well-balanced surface. After polymerization, isopropanol was removed completely followed by pouring the stacking gel solution into the gel cassette. Subsequently, a plastic comb was inserted from the top necessary to form the loading wells. After polymerization the gel with dimensions of 80 x 73 mm and a thickness of 0.75 mm was wrapped in wet towels and stored at 4°C for further use.

Electrophoresis was performed using the PROTEAN III system. The gel was placed into the electrode assembly and electrophoresis-running buffer was added to the inner and outer chamber of the tank. The comb was carefully removed and the samples were transferred into the wells of the stacking gel using extra-long loading pipet tips. Electrophoresis was performed at 200 V for ~55 minutes and stopped before emerging of the Bromphenol Blue front of the SDS sample buffer out of the separating gel.

| | | |
|--------------------------|----------------|------------------------------------|
| Separating Gel Solution: | <u>13% Gel</u> | |
| | 1.25 ml | 1.5 M Tris-HCl, pH 8.8 |
| | 50 µl | 10% (w/v) SDS |
| | 2 ml | 30% (w/v) Acrylamide/Bis |
| | 25 µl | 10% (w/v) APS |
| | 2.5 µl | TEMED |
| | 1.68 ml | H ₂ O _{MilliQ} |

| | | |
|---------------------------------|-----------------|------------------------------------|
| Stacking Gel Solution: | <u>4.8% Gel</u> | |
| | 0.625 ml | 0.5 M Tris-HCl, pH 6.8 |
| | 25 μ l | 10% (w/v) SDS |
| | 335 μ l | 30% (w/v) Acrylamide/Bis |
| | 12.5 μ l | 10 % (w/v) APS |
| | 2.5 μ l | TEMED |
| | 1.53 ml | H ₂ O _{MilliQ} |
| | | |
| Electrophoresis running buffer: | 25 mM | Tris-HCl, pH 8.3 |
| | 192 mM | Glycine |
| | 0.1% | SDS |

Alternatively, Novex NuPAGE 10% Bis-Tris-HCl Polyacrylamide-gels (pH 6.4) were used according to the manufacturer's manual. To separate proteins under reducing conditions, 0.5 ml Antioxidant (Novex) was added to the MES running buffer into the inner chamber of the XCELL II™ MINI-CELL apparatus. Electrophoresis was performed at 200 V for approximately 35 min.

MES (Morpholineethanesulfonic acid)-running buffer (20 x):

| | |
|---------|-----------|
| 1 M | MES |
| 1 M | Tris Base |
| 69.3 mM | SDS |
| 20.5 mM | EDTA |

2.4.4 SDS-PAGE protein molecular weight standards

In order to calculate the size of proteins following electrophoresis, protein molecular weight standards peqGOLD Protein-Marker I (PeqLab) or Odyssey Protein Molecular Weight Marker (LICOR) were used, respectively. The peqGold marker, ranging from sizes of 14 to 116 kDa, was loaded analyzing gels by Western blot using the ECL detection method. The Odyssey marker, ranging from sizes of 10 to 250 kDa, was applied performing the analysis in an *Odyssey infrared imaging system*. Using this system the protein markers

are prestained with Coomassie and can be visualized. SDS-PAGE protein molecular weight standards were applied by loading 1 to 5 μ l of the premixed solutions.

2.4.5 Silver staining

Silver staining was performed in order to impregnate proteins fixed in the SDS-gel by generating complexes of silver nitrate in presence of sodium thiosulfate. Gels were incubated for 1 hour in staining solution 1. Following three washing steps (20 minutes) in ethanol and incubation for 1 minute in sodium thiosulfate (staining solution 2), the gel was washed again three times with $\text{H}_2\text{O}_{\text{MilliQ}}$ for 20 seconds and stained for 20 min in silver nitrate containing solution (staining solution 3). Subsequently, the gel was washed twice (20 seconds with $\text{H}_2\text{O}_{\text{MilliQ}}$) and stained with sodium thiosulfate solution (staining solution 4) until staining of proteins were visible (1-2 minutes). After fixing for 10 minutes in acetic acid the gel was stored in $\text{H}_2\text{O}_{\text{MilliQ}}$.

| | | |
|----------------------|--------------------|--------------------------------------|
| Staining solution 1: | 50% | MetOH |
| | 12% | CH_3COOH |
| | 50 μ l | Formaldehyde |
| | up to final volume | $\text{H}_2\text{O}_{\text{MilliQ}}$ |
| Staining solution 2: | 20 mg | $\text{Na}_2\text{S}_2\text{O}_3$ |
| | up to 100 ml | $\text{H}_2\text{O}_{\text{MilliQ}}$ |
| Staining solution 3: | 200 mg | AgNO_3 |
| | 75 μ l | Formaldehyde |
| | up to 100 ml | $\text{H}_2\text{O}_{\text{MilliQ}}$ |
| Staining solution 4: | 6 g | NaCO_3 |
| | 50 μ l | Formaldehyde |
| | 0.4 mg | $\text{Na}_2\text{S}_2\text{O}_3$ |
| | up to 100 ml | $\text{H}_2\text{O}_{\text{MilliQ}}$ |

| | | |
|------------------|--------------------|------------------------------------|
| Washing buffer: | 50% | EtOH |
| | up to final volume | H ₂ O _{MilliQ} |
| Fixing solution: | 7% | CH ₃ COOH |
| | up to final volume | H ₂ O _{MilliQ} |

For long-term storage, gels were dried employing the gel drying solution (Invitrogen). SDS-gels, stored in H₂O_{MilliQ} were incubated for 20 minutes in gel drying solution. Subsequently, the gels were placed between two sheets of cellophane equilibrated with gel drying solution and fitted into a plastic frame. Following incubation overnight at room temperature dried gels were taken out of the frame and residual cellophane was removed by cutting.

2.4.6 Western blot analysis

Since proteins contain various different antigenic determinants (epitopes), antibodies directed against these epitopes can bind to proteins based on their corresponding binding sites (paratopes). In order to identify antigens using specific antibodies western blot analysis were performed. Proteins separated by SDS-PAGE were transferred to a polyvinylidene fluoride (PVDF) membrane for further analysis (Towbin et al., 1979) using a wet blot transfer device (Mini Trans-Blot Cell, Bio-Rad). To prepare PVDF membranes for western blotting analysis membranes were activated by incubation in 100% methanol for 1 min. Subsequently, membranes and filter papers (Whatman 3MM, Whatman AG), cut to the size similar of the gels as well as sponges and sandwich-blotting cassettes were equilibrated in blotting buffer. All components were assembled into layers avoiding air bubbles as depicted in the following figure.

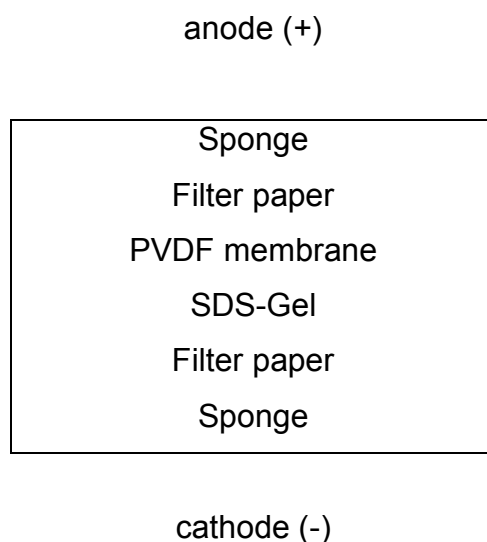


Fig. 10 Schematic overview: Assembly of a Western blot sandwich cassette.

After transfer of the assembled blotting cassette into the blotting tank, an ice block was added for cooling and the tank was filled with blotting buffer. Protein transfer was achieved at 100 V for 1 h under constant stirring.

| | | |
|------------------|-----------|--------------|
| Blotting buffer: | 192 mM | Glycine |
| | 25 mM | Tris, pH 8.4 |
| | 20% (v/v) | MetOH |

2.4.7 Immunochemical protein detection using the ECL system

Following western blotting as described above (section 2.4.6) Immobilon-P PVDF membranes (Millipore Corporation) were incubated in blocking buffer for 1 h at room temperature or at 4°C overnight on a shaker. After washing with PBS-T, membranes were incubated with primary antibodies directed against the protein of interest in the desired dilution for 1 hour at room temperature on a shaker. Following washing (3x 5 min) with PBS-T, membranes were incubated with secondary goat anti-rabbit IgG or goat anti-mouse IgG antibodies coupled to HRP in a 1:5000 dilution. Membranes were washed again (3x 5 min) with PBS-T on a shaker and subsequently, were incubated with ECL solution for 1 min at room temperature employing the enhanced

chemiluminescence system (ECL, Amersham Pharmacia). Using this system chemiluminescence was detected using medical x-ray films (Super RX Medical X ray film, Fuji).

| | | |
|----------------------------|--------------------|--------------|
| Blocking buffer: | 5% (w/v) | Milk powder |
| | up to final volume | PBS-T |
| Primary antibody buffer: | 3% (w/v) | BSA |
| | 0.02% (w/v) | Sodium azide |
| | up to final volume | PBS-T |
| Secondary antibody buffer: | 3% (w/v) | Milk powder |
| | up to final volume | PBS-T |

2.4.8 Immunochemical protein detection using the LICOR system

Alternatively, following western blotting as described (section 2.4.6), the LICOR system was performed. Upon using Immobilon-FL PVDF membranes (Millipore Corporation) optimized for the detection of fluorescence, membranes were incubated in blocking buffer for 1 h at room temperature on a shaker. Analogous to the procedure described above, membranes were washed and incubated with the primary antibody solution. As secondary antibody goat anti-rabbit IgG (1:10,000), goat anti-mouse IgG (1:5,000) or goat anti-rat IgG (1:10,000) antibodies coupled to the fluorophor Alexa 680 were used, respectively. Following incubation for 30 min at room temperature under constant shaking in the dark, membranes were washed three times and incubated in PBS (w/o Tween 20) for at least 5 minutes. Visualization was performed using the *Odyssey infrared imaging system*.

| | | |
|------------------|--------------------|-------------|
| Blocking buffer: | 5% (w/v) | Milk powder |
| | up to final volume | PBS |

| | | |
|----------------------------|--------------------|--------------|
| Primary antibody buffer: | 3% (w/v) | BSA |
| | 0.02% (w/v) | Sodium azide |
| | 0.1% (w/v) | Tween 20 |
| | up to final volume | PBS |
| Secondary antibody buffer: | 3% (w/v) | Milk powder |
| | 0.01% (w/v) | SDS |
| | 0.1% (w/v) | Tween 20 |
| | up to final volume | PBS |

2.4.9 Preparation of cell lysates

Expression of the various fusion proteins in CHO or HeLa cells were performed by cultivating cells in the presence of doxycycline (1 µg/ml) for 48 h at 37°C. Following detachment of cells from the culture dishes using PBS, 0.5 mM EDTA pH 8.0 (10 min, 37°C), an appropriate amount of cells was mixed with SDS-sample buffer and incubated for 10 minutes at 95°C before analyzed employing the SDS-gel electrophoresis (section 2.4.4).

2.4.10 Biotinylation of cell surface proteins

The biochemical analysis of cell-surface-associated proteins was performed using the biotinylation assay. The membrane impermeable biotinylation reagent added to cells binds covalently to all free ε-amino groups of lysines present in surface-associated proteins. After quenching and removing excess amounts of the biotinylation reagent, cells were lysed and subjected to streptavidin affinity chromatography to separate biotinylated (cell surface) from non-biotinylated (intracellular) proteins.

CHO cells expressing various fusion proteins were grown in six-well plates in presence of 1 µg/ml doxycycline for 48 h at 37°C. Following removal of the medium, the cells were washed twice with PBS containing Ca²⁺ and Mg²⁺ (2 mM each). A membrane-impermeable biotinylation reagent (EZ-Link Sulfo-

NHS-SS-biotin; Pierce) dissolved in 10 mM triethanolamine, 150 mM NaCl and 2mM CaCl_2 (pH 9) was added to a final concentration of 0,5 mg/ml. Following incubation for 30 minutes at 4°C quenching of excess amounts of biotinylation reagent was achieved by adding 100 mM PBS/glycine. Cells were then washed twice with PBS (without Ca^{2+} and Mg^{2+}). Cell lysates were prepared by adding PBS containing NP-40, followed by sonication (water bath for 3 min). Cell lysates were cleared by centrifugation (18,000 g_{av} , 10 min, 4°C) and biotinylated and non-biotinylated proteins were separated by streptavidin affinity chromatography. After incubation for 1 hour at room temperature under constant rotation, these streptavidin beads were washed three times with washing buffer 1 and two times with washing buffer 2. Sedimentation of the beads was performed by centrifugation (3,000 g_{av} , 4°C, 1 min). After the last washing step the supernatant was carefully discarded and bound material was eluted by incubation with SDS sample buffer for 10 min at 95°C. The biotinylated and non-biotinylated fractions were probed for the presence of the desired fusion proteins using SDS-PAGE (section 2.4.3) and western blotting (section 2.4.6) using affinity-purified anti-GFP antibodies.

| | | |
|---------------------------------------|--------------------|-------------------------------------|
| PBS $\text{Ca}^{2+}/\text{Mg}^{2+}$: | 1 mM | MgCl_2 |
| | 0.1 mM | CaCl_2 |
| | up to final volume | PBS |
| Incubation buffer: | 150 mM | MgCl_2 |
| | 10 mM | Triethanolamine, pH 9 |
| | 2 mM | CaCl_2 |
| Quenching buffer : | 100 mM | Glycine |
| | up to final volume | PBS $\text{Ca}^{2+}/\text{Mg}^{2+}$ |
| Lysis buffer: | 62.5 mM | EDTA |
| | 50 mM | Tris-HCl, pH 7.5 |
| | 0.4% (w/v) | Deoxycholate |
| | 1/10 ml | Protease Inhibitor tablet (mini) |

| | | |
|-------------------|------------|------------------|
| Washing buffer 1: | 62.5 mM | EDTA |
| | 50 mM | Tris-HCl, pH 7.5 |
| | 0.4% (w/v) | Deoxycholate |
| | 1% (w/v) | NP-40 |
| | 0.5 M | NaCl |
| Washing buffer 2: | 62.5 mM | EDTA |
| | 50 mM | Tris-HCl, pH 7.5 |
| | 0.4% (w/v) | Deoxycholate |
| | 0.1% (w/v) | NP-40 |
| | 0.5 M | NaCl |

2.4.11 Biochemical analysis of membrane association of HASPB-GFP fusion proteins

In order to determine whether an integral membrane protein has achieved stable insertion into the bilayer carbonate extraction analysis was performed. Using this biochemical assay, membrane association of HASPB-GFP fusion proteins were analyzed. Basically treatment with sodium carbonate at pH 11.5 results in disruption of protein-protein interactions. However, protein-lipid interactions remain and the bilayer is otherwise intact. Thus, cytosolic, cisternal and peripheral membrane proteins are retained to sediment with the membrane remnants.

CHO cells expressing the various kinds of HASPB-GFP fusion proteins were cultured in 10 cm plates for 2 days at 37°C in the presence of doxycycline (1 µg/ml). Following detachment using PBS/EDTA (10 min at 37°C), cells were sedimented by centrifugation (500 g_{av}, 5 minutes, 4°C) and resuspended in PBS/sucrose (500 µl) homogenization buffer. Cells were lysed by sonication (3 times a 20 seconds) and then subjected to ultracentrifugation for 60 minutes at 100,000 g_{av}. The resulting supernatant was defined as the cytosolic fraction (fraction 1), the sediment was resuspended in homogenization buffer (250 µl) and defined as the membrane fraction (fraction 2). For carbonate extraction experiments, membranes were again collected by

ultracentrifugation (20 minutes, 100,000 g_{av} , 4°C). Following resuspension in 250 μ l Na_2CO_3 (0.1 M, pH 11.5), the samples were incubated for 30 minutes at 4°C. Membranes were re-isolated by ultracentrifugation (30 min, 100,000 g_{av} , 4°C) and separated into supernatant (peripheral membrane proteins, fraction 3) and membrane sediment (integral and tightly associated proteins, fraction 4). 5% of each fraction was combined with SDS sample buffer and analyzed for HASPB-GFP fusion proteins by SDS-PAGE (section 2.4.3) following western blotting (section 2.4.6) using affinity-purified anti-GFP antibodies.

| | | |
|-----------------------|--------------------|---------|
| Homogenizationbuffer: | 10% (w/v) | Sucrose |
| | up to final volume | PBS |

| | | |
|--------------------------|--------------------|----------------------|
| Sodium carbonate buffer: | 100 mM | Na_2CO_3 , pH 11.5 |
| | up to final volume | PBS |

2.4.12 Metabolic labeling of CHO cells using $^3[H]$ myristate and $^3[H]$ palmitate

To investigate whether myristoylation and palmitoylation is present in the N-terminal SH4 domain of HASPB-GFP fusion proteins, metabolic labeling of CHO cells using $^3[H]$ myristate and $^3[H]$ palmitate was performed. CHO cells expressing HASPB-GFP fusion proteins were grown in six-well plates for 48 hours at 37°C in the presence of doxycycline (1 μ g/ml) to about 80% confluency. Following two hours of incubation in FCS-free medium, cells were incubated in FCS-free medium containing either 250 μ Ci $^3[H]$ palmitic or 100 μ Ci $^3[H]$ myristic acid. After three hours of incubation in labeling medium at 37°C, cells were washed and lysed in buffer containing detergent by sonication. Following removal of insoluble material by centrifugation (14,000 g_{av} , 10 minutes), the lysates were subjected to immunoprecipitation of HASPB-GFP fusion proteins employing affinity-purified anti-GFP antibodies. Antibody-bound protein was eluted with SDS-sample buffer and subjected to SDS-PAGE (section 2.4.3). For this purpose, the samples were split into two

fractions in order to analyze the eluted proteins by both fluorography and silver staining. For fluorography, SDS-gels were treated with NAMP100 amplifier solution (Amersham) and then dried for exposure using Hyperfilm™ (Amersham). Typically, SDS-gels containing $^3\text{[H]}$ myristic acid-labeled proteins were exposed for about two weeks whereas SDS-gels containing $^3\text{[H]}$ palmitic acid-labeled proteins were exposed for up to six weeks.

2.4.13 Biochemical analysis of the subcellular distribution of HASPB-GFP in CHO cells using subcellular fractionation

Subcellular fractionation of CHO cells was performed as described in (Schäfer et al., 2004). CHO cells were grown in 15 cm plates in the presence of doxycycline (1 $\mu\text{g/ml}$) for 48 hours at 37°C. Cells from five plates were washed with PBS and detached with PBS/EDTA (3 ml, 10 minutes at 37°C). Subsequently, the cells were combined and centrifuged at 500 g_{av} for 10 minutes at 4°C. The cell sediment was lysed in 7 ml of hypotonic buffer supplemented with protease inhibitor mixture (Roche Applied Science). Following incubation for 2 hours at 4°C (fraction 1), the cell lysate was centrifuged at 100,000 g_{av} for 40 min at 4°C. The sediment was resuspended in 1 ml of hypotonic buffer and homogenized by passing 15 times through a 24-gauge needle and 10 times by a 27-gauge needle. Following dilution in incubation buffer in a ratio of 1:2, the lysate was centrifuged for 10 min at 12,000 g_{av} at 4°C. The sediment was resuspended in 500 μl of incubation buffer and again subjected to the procedure described. Postnuclear supernatants from both steps were combined (fraction 2) and subjected to ultracentrifugation at 100,000 g_{av} for 40 min at 4°C. The resulting sediment was resuspended in 700 μl of incubation buffer and manually homogenized as described above (fraction 3). The resulting membrane suspension was layered on top of a 9.5 ml 38% (w/v) sucrose solution. Following centrifugation at 280,000 g_{av} for 2 hours in a Beckman SW41 swing-out rotor, membranes in the 0/38% interface were collected. This suspension was again homogenized with a 27- and 24-gauge needle followed by ultracentrifugation at 100,000 g_{av} for 40 min at 4°C. The corresponding sediment was resuspended in 50 μl SDS-sample buffer and

equal amounts were analyzed by SDS-PAGE (section 2.4.3) following western blotting (section 2.4.6).

| | | |
|--------------------|--------------|--------------------------------|
| Hypotonic buffer: | 0.5 mM | NaPO ₄ , pH 8 |
| | 0.1 mM | EDTA |
| | (1 Tab/10 ml | Protease-inhibitor, EDTA-free) |
| Incubation buffer: | 10 mM | Tris-HCl, pH7.4 |
| | 250 mM | Sucrose |
| | (1 Tab/10 ml | Protease-inhibitor, EDTA-free) |

Sucrose solution in 5 mM HEPES-KOH pH 7.4

2.4.14 Biochemical analysis of HASPB export from CHO cells using immunoprecipitation from cell culture supernatants

To immunoprecipitate GFP fusion proteins a mixture of Protein A-Sepharose beads, CL-4B beads (Amersham Pharmacia) and 20% ethanol (1:1:2) were prepared and 40 µl slurry beads (corresponding to 20 µl packed beads) per sample were used. Beads were washed three times with IP-Buffer 1 and sedimented at 800 g_{av} for 3 min at 4°C. Affinity-purified anti-GFP antibodies were coupled to beads by incubation with 20 µl anti-GFP antibodies (basic elution) in 180 µl buffer 1 overnight at 4°C on a rotation wheel. Subsequently, the beads were washed three times using IP-buffer 2. After sedimentation and removal of the buffer, the beads were ready for the incubation with the sample containing GFP fusion proteins. Cell culture supernatants (1 ml, supplemented with and w/o 1% trypsin) obtained from the respective reporter cell line grown in six-well plates in presence of doxycycline (1 µg/ml) were combined with the beads followed by an 2 to 4 h incubation at 4°C. After this incubation period, the beads were washed three times with IP-buffer 0. Bound material was eluted by addition of 15-30 µl SDS sample buffer and incubation at 95°C for 10 minutes.

| | | |
|--------------|------------|------------------|
| IP-buffer 0: | 25 mM | Tris-HCl, pH 7,4 |
| | 150 mM | NaCl |
| | 1 mM | EDTA |
| IP-buffer 1: | 25 mM | Tris-HCl, pH 7,4 |
| | 150 mM | NaCl |
| | 1 mM | EDTA |
| | 0.5% (w/v) | NP-40 |
| IP-buffer 2: | 25 mM | Tris-HCl, pH 7,4 |
| | 150 mM | NaCl |
| | 1 mM | EDTA |

2.4.15 Precipitation of HASPB-GFP fusion proteins using TCA

To precipitate proteins from diluted solutions, trichloroacetic acid (TCA) was used. Samples containing proteins obtained from various experimental approaches were mixed with 2% DOC (deoxycholate, 1/10 volume) followed by 100% TCA (1/10 volume). After incubation for 15 minutes on ice, samples were centrifuged (21,000 g_{av} (14,000 rpm), 15 min, 4°C) and the resulting sediments were evaporated with ammonia (NH₃)-steam and resuspended in appropriate amounts of SDS-sample buffer. Following incubation at 95°C for 10 minutes, samples were probed for the desired proteins employing SDS-PAGE (section 2.4.3) and western blotting (section 2.4.6) using the corresponding antibodies.

2.4.16 Biochemical analysis of membrane sediments containing various GFP fusion proteins using ultracentrifugation of cell culture supernatants

To investigate the presence of various fusion proteins in cell culture supernatants of CHO or HeLa cells, respectively, membrane sediments were generated by ultracentrifugation of the corresponding cell culture supernatants. CHO or HeLa cell lines expressing the various fusion proteins were grown in 10 cm plates in the presence of doxycycline (1 µg/ml) for 48 hours at 37 °C in 3.5 ml of the corresponding medium. After centrifugation (1000 g_{av} for 20 min at 4°C) in order to remove dead cells, the supernatants were centrifuged at 100,000 g_{av} for 1 hour at 4°C. Following ultracentrifugation, the supernatants were removed and the resulting membrane sediments were either resuspended in SDS-sample buffer to analyze total material using SDS-PAGE or were subjected to Nycodenz flotation gradients (section 2.4.17) or linear sucrose gradients (section 2.4.18) for further analysis, respectively.

2.4.17 Biochemical analysis of extracellular vesicles containing various GFP fusion proteins using flotation in Nycodenz gradients

To discriminate vesicles from aggregates, the membrane sediments (section 2.4.16) were recovered and concentrated by flotation in a Nycodenz (Axis Shield) step gradient as described in (Weber et al., 1998). Membrane sediments obtained after ultracentrifugation were resuspended in 150 µl reconstitution buffer supplemented with protease-inhibitors and were mixed with 150 µl of 80% (w/v) Nycodenz dissolved in reconstitution buffer. This mixture was transferred into a 5x41 mm ultraclear centrifuge tube and overloaded with 250 µl 30% (w/v) Nycodenz solution followed by 50 µl reconstitution buffer. Samples were then centrifuged in an SW55 rotor (Beckman) with the appropriate adaptors at 48,000 rpm (218,438 g_{av}) for 4 hours at 4°C. Vesicles were harvested from the 0/30% Nycodenz interphase in 50 µl aliquots generating three fractions containing ~100 µl, 150 µl and 350 µl. Subsequently, proteins in each fraction were subjected to precipitation

using TCA (section 2.4.15) and analyzed by SDS-PAGE (section 2.4.3) followed by western blotting (section 2.4.6) using affinity-purified anti-GFP antibodies.

In order to determine the density of each fraction, refractive indices (σ) were measured using a refractometer. Densities were then calculated using the following equation:

$$\text{Density [g/ml]} = (\sigma \times 3.287) - 3.383$$

| | | |
|------------------------|--------------|---------------------|
| Reconstitution buffer: | 25 mM | Hepes-KOH, pH 7,4 |
| | 100 mM | KCl |
| | 10% (w/v) | Sucrose |
| | 1mM | DTT |
| | (1 Tab/10 ml | Protease-inhibitor) |

2.4.18 Biochemical analysis of extracellular vesicles containing various GFP fusion proteins using continuous sucrose gradients

To generate a more precise separation of vesicles continuous sucrose gradients were performed. Membrane sediments obtained following ultracentrifugation of cell culture supernatants (section 2.4.16) from CHO cells or HeLa cells expressing the various fusion proteins were resuspended in 150 μ l reconstitution buffer supplemented with protease inhibitors. The mixtures were loaded on top of a five-step sucrose gradient, containing 2 M, 1.6 M, 1.2 M, 0.8 M and 0.4 M sucrose dissolved in reconstitution buffer. Following centrifugation in a SW55 rotor with the appropriate adaptors at 26,000 rpm (65,000 g_{av}) for 16 hours at 4°C, 60 μ l aliquots were generated. Proteins in each fraction were precipitated using TCA (section 2.4.15) and samples were analyzed by SDS-PAGE (section 2.4.3) following western blotting (section 2.4.6) using affinity-purified anti-GFP antibodies. In order to confirm the linearity of the used gradient, refractive indices were measured employing a refractometer. Densities were determined using the data on the following web-page:

<http://homepages.gac.edu/~cellab/chpts/chpt3/table3-2.html>

| | | |
|------------------------|--------------|--------------------------------|
| Reconstitution buffer: | 25 mM | Hepes-KOH, pH 7,4 |
| | 100 mM | KCl |
| | 10% (w/v) | Sucrose |
| | 1mM | DTT |
| | (1 Tab/10 ml | Protease-inhibitor, EDTA-free) |

2.4.19 Biochemical analysis of the localization of HASPB-GFP in extracellular vesicles using protease protection experiments

To analyze the localization of HASPB-GFP fusion proteins in vesicles protease protection experiments were performed. CHO cells expressing HASPB-GFP fusion proteins were grown in 10 cm plates in the presence of doxycycline (1µg/ml) for 48 hours at 37°C. Cell culture supernatants (3.5 ml) were centrifuged at 1000 g_{av} for 20 minutes at 4°C in order to remove dead cells. Subsequently, supernatants were centrifuged at 100,000 g_{av} for 1 hour at 4°C and the resulting membrane sediments (section 2.4.16) were subjected to protease treatment following resuspension in TNE-buffer. Trypsin (0.5 µg) was added in the presence and absence of the detergent NP-40 by adding the corresponding buffers (1x trypsin-buffer with and w/o NP-40). Following incubation for 30 minutes at room temperature, the protease was inactivated by adding AEBSF. After addition of SDS-sample buffer, the samples (100%) were analyzed by SDS-PAGE (section 2.4.3) following western blotting (section 2.4.6) using affinity-purified anti-GFP antibodies.

| | | |
|-----------------|----------|-------------------|
| TNE-buffer: | 10 mM | Tris, pH 7,4 |
| | 100 mM | NaCl |
| | 1 mM | EDTA |
| Trypsin buffer: | 50 mM | Tris, pH 8 |
| | 10 mM | CaCl ₂ |
| | 1 mM | DTT |
| | 1% (w/v) | NP-40 |

2.5 Flow cytometry

2.5.1 Fluorescence activated cell sorting (FACS)

To analyze GFP fluorescence and exported reporter proteins in living cells by specific antibody cell surface staining, cells were processed according to the following protocol and analyzed via fluorescence-activated cell sorting (FACS).

CHO cells expressing the various fusion proteins were grown in six-well plates to a confluency of about 80% in the absence or presence of doxycycline (1 µg/ml) to obtain samples used as negative and positive controls regarding expression of the reporter constructs. In order to detach the cells from the culture plates without using protease-based protocols, 500 µl cell dissociation buffer (Life Technologies) or PBS/EDTA, respectively, were used to generate a cell suspension devoid of cell aggregates. Following incubation of 10 min at 37°C, cells were softly removed from the culture dishes by resuspension. Where indicated, cells were treated with 300 µl affinity-purified anti-GFP antibodies in the desired dilution for 1 hour at 4°C on a rotating wheel. Wash procedures with growth medium were carried out by sedimenting the cells at 200 g_{av} for 3 minutes at 4°C. Primary antibodies were detected with 300 µl goat anti-rabbit secondary antibodies coupled to allophycocyanin (APC; Molecular Probes) in a 1:750 dilution for 30 minutes at 4°C on a rotating wheel in the dark. Cells were washed once as described above and the resulting sediments were resuspended in 500 µl sorting medium. Prior to FACS analysis, propidium iodide (1 µg/ml) was added in order to detect damaged cells. GFP-and APC-derived fluorescence was analyzed using a Becton Dickinson FACSCalibur flow cytometer. Autofluorescence was determined by measuring non-induced cells that were treated with primary and APC-coupled secondary antibodies.

| | | |
|-----------|--------------------|------|
| PBS/EDTA: | 0.5 mM | EDTA |
| | up to final volume | PBS |

| | | |
|-----------------------|---|----------------------|
| Primary antibodies: | α MEM supplemented with FCS (10% (v/v)) Affinity-purified anti-GFP antibodies (acidic elution) 1:200 Monoclonal anti-CD4 antibodies (1:10) Monoclonal anti-CD8 antibodies (1:50) | |
| Secondary antibodies: | α MEM supplemented with FCS (10% (v/v)) goat anti-rabbit IgG APC-coupled antibodies 1:750 goat anti-mouse IgG APC-coupled antibodies 1:750 | |
| Sorting Medium: | 5% (v/v) | CDB |
| | 0.2% (v/v) | FCS |
| | up to final volume | α MEM w/o FCS |

2.5.2 FACS-sorting

FACS-based isolation of cell populations and single clones was performed using a Becton Dickinson FACS cell sorter in collaboration with Dr. Blanche Schwappach from the *Center of Molecular Biology Heidelberg* (ZMBH).

The procedure used for FACS sorting was carried out under sterile conditions. Cells were grown in presence or absence of doxycycline for 48 h due to further analysis. Following washing with PBS cells were detached from culture dishes using CDB (Invitrogen). The resulting cell suspensions were added to 5 ml cell culture medium. After centrifugation (200 g_{av}, 4°C, 5 min) supernatants were discarded and the sediments were carefully resuspended in sorting medium (section 2.5.1). Cells were transferred through cell strainer caps (Becton Dickinson) into 5 ml round bottom FACS tubes (Becton Dickinson) and propidium iodide was added to a final concentration of 1 µg/ml. Subsequently, cells were sorted using a FACSVantage or FACS Aria sorting device obtaining pools ranging from 30.000 to 100.000 cells into six-well plates. Alternatively, individual cells were sorted into 96-well plates in order to generate single cell lines.

2.5.3 *Retroviral insertion mutagenesis and FACS-based isolation of HASPB export mutants*

To randomly mutate CHO cells, retroviral particles were prepared encoding the cell surface protein CD4 (pBI-CD4) (Liu et al., 2000) using the Viraport system (Stratagene) (section 2.3.4). CHO cells expressing HASPB-N18-GFP were transduced according to standard procedures (section 2.3.4). Following three days of incubation at 37°C CD4-positive cells were selected by FACS sorting. In order to isolate HASPB export mutants CD4-positive cells were subjected to multiple rounds of FACS sorting, selecting for cells with high GFP fluorescence and low cell surface staining. In the third round of FACS sorting, individual cells were collected and further propagated in 96-well plates at 37°C. The corresponding mutant clonal cell line (CHO K3) was then characterized as described in the first section (section A) of the current thesis.

2.6 *Confocal microscopy*

2.6.1 *Confocal microscopy using fixed cells*

To visualize cells by confocal microscopy, cells were grown on glass coverslips to about 70% confluency in 24-well plates for 48 hours in the presence of doxycycline (1 µg/ml). Following extensive washing with PBS on ice, 300 µl Paraformaldehyde (PFA) dissolved in PBS was added (3% (w/v)) for 20 min at 4°C in order to fix cells. Following washing with PBS, quenching of PFA was achieved by adding 50 mM NH₄Cl for 10 minutes. Cells were washed four times with PBS. The specimens were then mounted in Fluoromount G (Southern Biotechnology Associates) and incubated overnight at room temperature in the dark. For long-term storage clear nail polish was used to seal the edges of the cover slip. GFP-derived fluorescence was viewed with a Zeiss LSM 510 Meta confocal microscope.

| | | |
|----------------------------|--------------------|--------------------|
| PFA in PBS: | 3% (w/v) | PFA |
| | up to final volume | PBS |
| NH ₄ Cl in PBS: | 50 mM | NH ₄ Cl |
| | up to final volume | PBS |

2.6.2 Live confocal imaging

To analyze cells in a live status, cells were grown in appropriate cell culture dishes in the presence of doxycycline (1 µg/ml) for 48 hours at 37°C. Using 3 cm plates (Nunc) or 8-chamber plates (Nunc), respectively, GFP-derived fluorescence was directly viewed with a Zeiss LSM 510 Meta confocal microscope.

2.7 Electron microscopy

2.7.1 Electron microscopy using microsections of membrane sediments containing HASPB-GFP

To visualize extracellular vesicles derived from HASPB-GFP expressing CHO cells, electron microscopy analysis were performed in collaboration with Prof. Zentgraf (DKFZ). CHO cells expressing HASPB-GFP fusion proteins were grown in 10 cm plates in the presence of 1 µg/ml doxycycline for 48 hours at 37°C. Cell culture supernatants were centrifuged (1000 g_{av} for 20 minutes) in order to remove dead cells. The corresponding supernatants were ultracentrifuged (100,000 g_{av} for 1 hour at 4°C, section 2.4.16) and the resulting membrane sediments were directly fixed using 2% glutar aldehyde in sodium cacodylate buffer (0.1 M sodium cocadylate, pH 7.2) for 30 minutes at 4°C. Following repeating washing steps using cold 0.05 M sodium cacodylate buffer (pH 7.2), samples were incubated for 2 hours using 2% (w/v) osmium tetroxide (OsO₄) in 0.05 M sodium cocadylate buffer (pH 7.2). Subsequently,

samples were washed using H₂O_{MilliQ} and dehydrated by incubation in various ethanol concentrations for 30 minutes. Following two incubation steps in 100% ethanol, samples were transferred in propylene oxide and embedded in Epon 812 (Ciba). Microsections were generated using the ultramicrotome OmU2 (Leica) and stained using uranyl acetate (4% w/v) and lead citrate upon washing steps in CO₂-free H₂O.

3 Results

A. *Direct transport across the plasma membrane of mammalian cells of Leishmania HASPB as revealed by a CHO export mutant*

The unconventionally secreted *Leishmania* protein HASPB is a component of the surface coat of *Leishmania* parasites (Alce et al., 1999; Flinn et al., 1994; McKean et al., 2001). HASPB is expressed on the cell surface of *Leishmania* parasites (Denny et al., 2000). Only in infectious stages of the parasite lifecycle HASPB is associated with the outer leaflet of the plasma membrane (Flinn et al., 1994; Pimenta et al., 1994). The N-terminal SH4 domain of HASPB containing a myristoylation and a palmitoylation is the molecular basis of how HASPB is anchored in the membrane in *Leishmania* parasites and mammalian cells (Denny et al., 2000). Mutational analysis revealed that a HASPB construct lacking the palmitoylation site is associated with the cytoplasmic surface of the Golgi (Denny et al., 2000). Furthermore mutants lacking both acylations have been found redistributed in the cytosol (Denny et al., 2000). Based on these observations, HASPB is transferred from the cytoplasm to the outer leaflet of the Golgi membrane, from where it is transported to the plasma membrane and in turn translocated across the membrane, resulting in the insertion of the two acyl chains in the outer leaflet of the plasma membrane. This unconventional cell-surface expression of HASPB by *Leishmania* parasites appears to be tightly correlated with host cell infection (Flinn et al., 1994; Pimenta et al., 1994) and, therefore, the HASPB export pathway might be an excellent target for the development of drugs against tropical and subtropical diseases termed the leishmaniasis. The identification of inhibitors that do not interfere with the essential function of the classical secretory pathway might be therefore a great step forward towards the prevention of such diseases, which can be fatal unless treated. Notably, after synthesizing on free ribosomes in the cytoplasm, HASPB can be found in the extracellular space. However, the mechanism of this transport process is completely unknown. There is also a complete lack of knowledge about the

subcellular site of membrane translocation of HASPB, a process that eventually allows HASPB exposure on the cell surface of eukaryotic cells. Therefore the elucidation of the molecular machinery controlling this nonclassical export might provide a whole variety of novel target proteins suitable for drug design. In the current study a novel experimental system was established that permits the precise quantification of HASPB export from mammalian cells based on flow cytometry. Using this assay, a genetic screen was used to identify mutants with a defect in HASPB in order to identify components involved in this pathway.

3.1 Generation of model cell lines to study HASPB export from mammalian cells

3.1.1 Retroviral transduction of HASPB-N18-GFP reporter molecules in pRevTRE2

The HASPB export process appears to be a unique mechanism of eukaryotic protein secretion as the corresponding targeting motif depends on dual acylation within a SH4 domain comprising 18 amino acids at the extreme N-terminus (Denny et al., 2000) (Fig. 11A). When transferred to a reporter molecule such as GFP, the corresponding fusion protein has shown to be exported from both *Leishmania* parasites and mammalian cells (Denny et al., 2000; Stegmayer et al., 2005). As control, Δ palm-HASPB-N18-GFP (C5S), Δ myr-HASPB-N18-GFP (G2A) and GFP were generated. In order to study the export mechanism of HASPB on a quantitative basis in mammalian cells, HASPB-GFP fusion proteins were expressed from a retroviral vector containing a doxycycline/transactivator-sensitive element. Following transduction of CHO_{MCAT-TAM2} cells that constitutively express both an ecotropic retrovirus receptor and a doxycycline-sensitive transactivator, it was possible to precisely quantify (Fig. 11B) HASPB membrane translocation by simultaneous measurements of HASPB cell surface presentation (antibody staining) and the expression level of the reporter molecule (GFP-derived fluorescence).

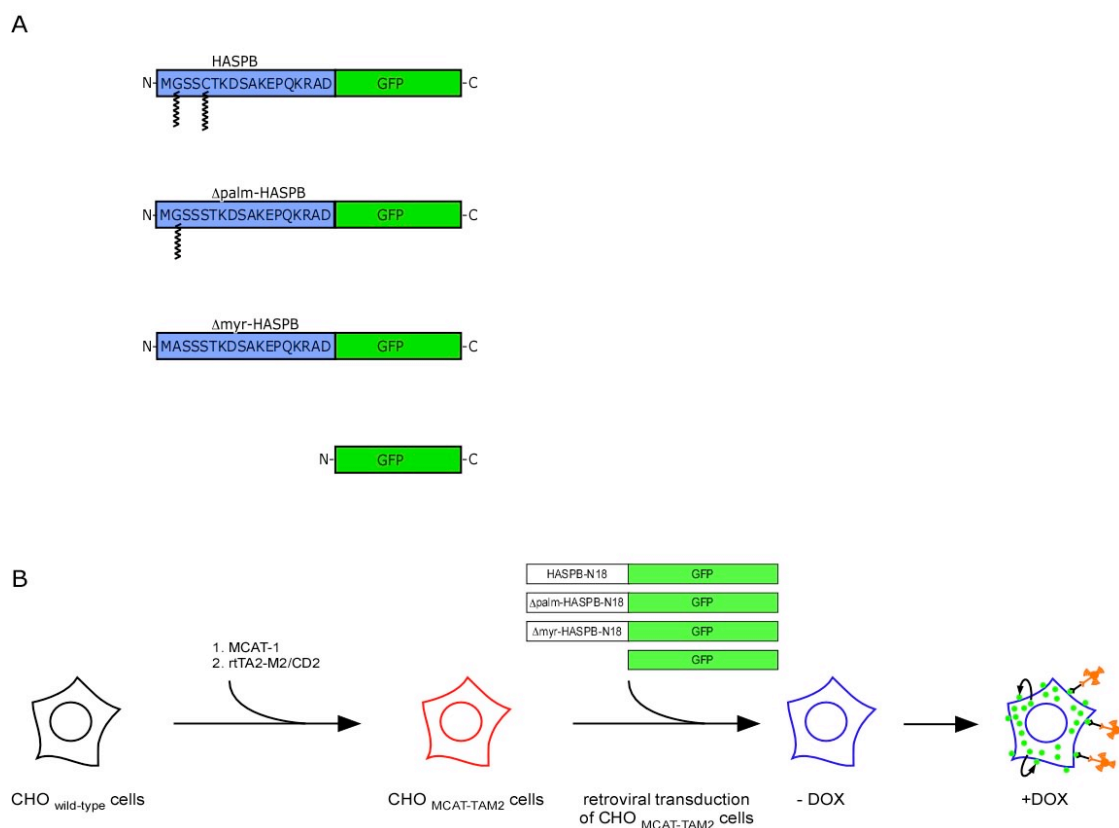


Fig. 11 Schematic description of HASPB reporter molecules and general model system to generate reporter cell lines. (A) Overview about the various HASPB-GFP containing reporter constructs as well as of GFP alone. (B) In order to generate CHO cell lines expressing the various reporter molecules shown in A, CHO cells were transfected with an ecotropic retrovirus receptor (MCAT-1) and a doxycycline-sensitive transactivator (rtTA2-M2/CD2), followed by the transduction of the various fusion proteins. With this general model system, doxycycline-dependent HASPB-N18-GFP export was quantified by FACS analysis using affinity-purified anti-GFP antibodies and APC-derived secondary antibodies.

3.1.2 Sorting of doxycycline-inducible single clones

Using the described general model system (section 3.1.1) CHO cells were generated, expressing various kinds of HASPB-GFP fusion proteins in a doxycycline-dependent manner. Following transduction of CHO_{MCAT-TAM2} cells GFP-positive cells were isolated by three rounds of FACS sorting in the presence and absence of doxycycline (Fig. 12, HASPB-N18-GFP as example for the sorting procedure). In the third round single cells were selected

characterized by GFP-derived fluorescence only after the addition of doxycycline.

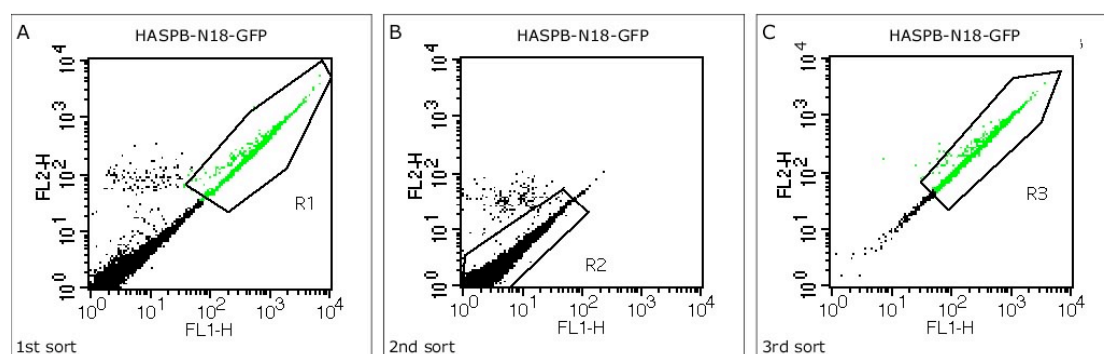


Fig. 12 Sorting of doxycycline-inducible single clones. HASPB-N18-GFP-transduced CHO cells were grown for 48 hours in the presence of 1 $\mu\text{g/ml}$ doxycycline at 37°C and subjected to three rounds of FACS sorting. (A) GFP-positive cell pools were isolated as illustrated on the x-axis by FL-1 that represents the green channel measuring GFP fluorescence. (B) In absence of doxycycline GFP-negative cell pools were isolated. (C) In presence of doxycycline, single clones, showing a high GFP expression, were isolated.

3.1.3 Characterization of HASPB fusion protein-expressing cell lines

As illustrated in Fig. 13 clonal cell lines genetically modified with HASPB-N18-GFP or other constructs were found to express the reporter molecules only following incubation of the cells with doxycycline as analyzed by western blotting employing anti-GFP antibodies.

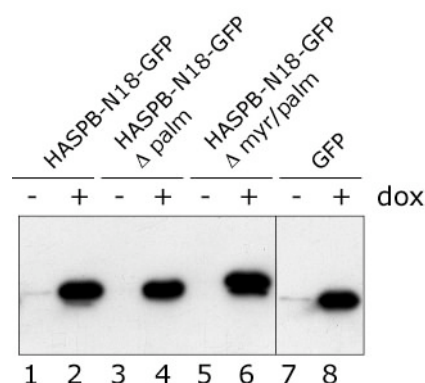


Fig. 13 Doxycycline-dependent expression of HASPB-GFP fusion proteins in CHO cells.

CHO cells expressing HASPB-GFP fusion proteins as indicated were grown in six-well plates in the absence (lanes 1, 3, 5 and 7) or presence (lanes 2, 4, 6 and 8) of 1 μ g/ml doxycycline (dox). Cells were detached and collected by centrifugation followed by lysis in SDS sample buffer. 1% of each lysate corresponding to cells from one well were subjected to SDS-PAGE. Following SDS-PAGE and western blotting HASPB-GFP fusion proteins were detected using affinity-purified anti-GFP antibodies.

3.1.4 Subcellular distribution of HASPB-N18-GFP fusion proteins as determined by confocal microscopy

In order to characterize the subcellular distribution of various HASPB-N18-GFP fusion proteins confocal microscopy was performed. When compared to the staining pattern of GFP without modification (cytoplasmic and nuclear staining, Fig. 14, panel D), a dramatic change in the subcellular localization was observed when HASPB-N18-GFP was transferred to the N-terminus of GFP (Fig. 14, panel A). Evidently, the N-terminal targeting motif directed the fusion protein to the plasma membrane, which in turn resulted to a localization mainly to the plasma membrane as well as to droplet-like structures that were typically located in close proximity to the plasma membrane. By contrast, mutations that either prevented palmitoylation or both myristoylation and palmitoylation caused mislocalization of the reporter molecule. Δ palm-HASPB-N18-GFP was not at all associated with the plasma membrane but was rather localized on intracellular membranes showing a perinuclear staining (Fig. 14, panel B). As expected, Δ myr-HASPB-N18-GFP was found

exclusively, like GFP, in the cytoplasm (Fig. 14, panel C). Thus, membrane association of HASPB-N18-GFP depends on dual acylation of the HASPB N-terminal SH4 domain. These results are consistent with previous studies analyzing similar constructs in *Leishmania* parasites (Denny et al., 2000).

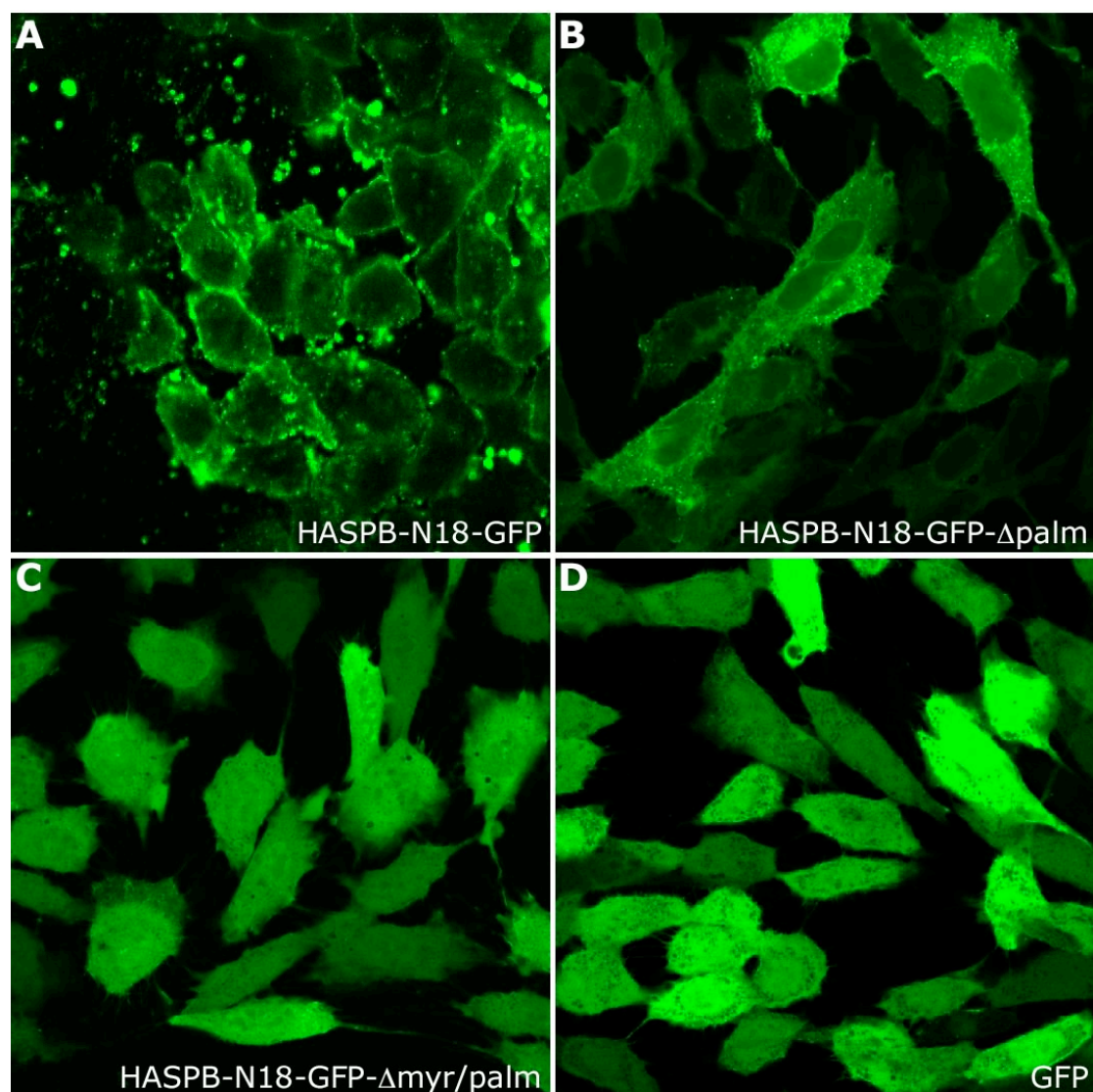


Fig. 14 Subcellular distribution of HASPB-GFP fusion proteins as determined by confocal microscopy. Cells were grown on glass coverslips in the presence of 1 μ g/ml doxycycline for 48 hours at 37°C. GFP-derived fluorescence was viewed with a Zeiss LSM 510 confocal microscope. (A) HASPB-N18-GFP; (B) Δ palm-HASPB-N18-GFP; (C) Δ myr/ Δ palm-HASPB-N18-GFP; (D) GFP

3.1.5 Functional analysis of HASPB-N18-GFP export from CHO cells based on quantitative flow cytometry

Based on previous observations (Denny et al., 2000), an export assay was developed that simultaneously measures both the expression level of a given HASPB-GFP fusion protein and its export to the outer leaflet of the plasma membrane on a quantitative basis. Following translocation to the surface of *Leishmania* parasites, HASPs remain membrane-anchored via their N-terminal acyl chains. Therefore, similar to FGF-2 and Galectin-1 export assays (Engling et al., 2002; Seelenmeyer et al., 2003), the extracellular population can be decorated with affinity-purified anti-GFP antibodies to assess a potential cell surface localization of HASPB-N18-GFP. This subpopulation is then specifically detected using APC-conjugated secondary antibodies. Employing flow cytometry GFP- and APC-derived fluorescence monitored by the expression levels of the various reporter molecules and by the exported population, respectively, can be measured simultaneously. All three HASPB-GFP fusion proteins as well as GFP lacking a N-terminal HASPB tag were expressed at similar levels by titration with doxycycline (Fig. 15, panel A). As demonstrated in Fig. 15 panel B (shown in dark blue) only the HASPB-N18-GFP reporter molecule could be detected on the cell surface. No signal could be observed under control conditions (without doxycycline; shown in light blue) and with the control molecules Δ palm-HASPB-N18-GFP, Δ myr-HASPB-N18-GFP and GFP. Again, these data are consistent with previous observations made in parasites (Denny et al., 2000) in which the export to the extracellular leaflet of the plasma membrane of mammalian cells is critically dependent on dual acylation of the SH4 N-terminus of HASPB. The *in vivo* assay introduced in Fig. 15 allows for a precise quantification of HASPB export under normalized conditions with respect to the expression level of a given HASPB-GFP fusion protein.

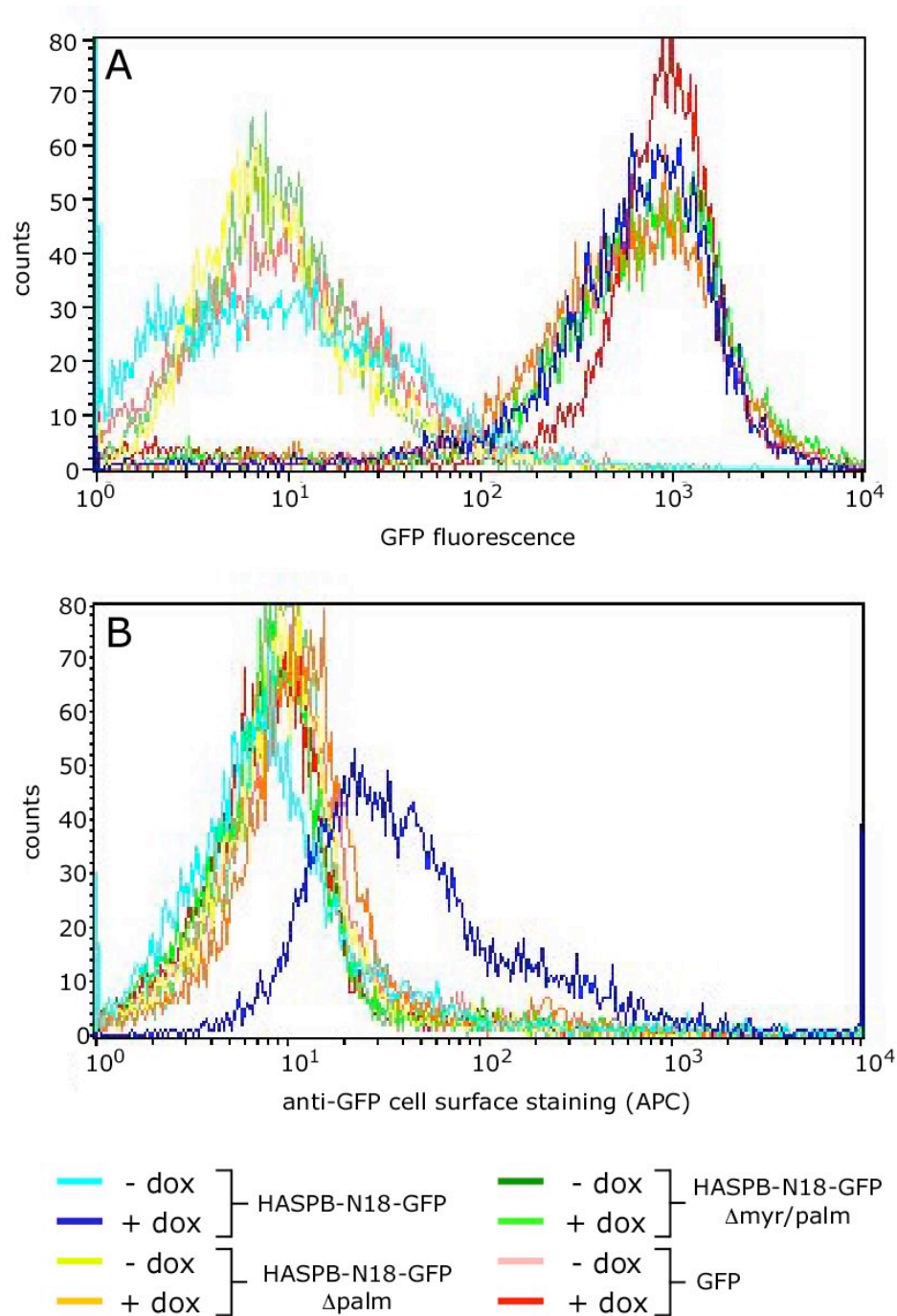


Fig. 15 Quantitative analysis of cell surface localized HASPB-GFP fusion proteins using flow cytometry. (A) GFP-derived fluorescence (expression level). (B) APC-derived fluorescence (cell surface staining). Cells were incubated in the presence and absence of 1 μ g/ml doxycycline as indicated followed by processing for FACS sorting. HASPB-N18-GFP, light and dark blue curves; Δ palm-HASPB-N18-GFP, yellow and orange curves; Δ myr/ Δ palm-HASPB-N18-GFP, light and dark green curves; GFP, light and dark red curves.

3.1.6 Biochemical analysis of HASPB-N18-GFP export to the outer leaflet of the plasma membrane of CHO cells

To demonstrate by means of an independent method that an external population of HASPB-N18-GFP is associated with the outer leaflet of the plasma membrane biotinylation experiments were carried out employing a membrane-impermeable biotinylation reagent. Cells were incubated in the presence of doxycycline, the cell culture supernatant was removed followed by treatment with the biotinylation reagent. After quenching and removing excess amounts of the biotinylation reagent, cells were lysed in a detergent. The lysate was then subjected to streptavidin affinity chromatography to separate biotinylated (cell surface) from non-biotinylated (intracellular) proteins.

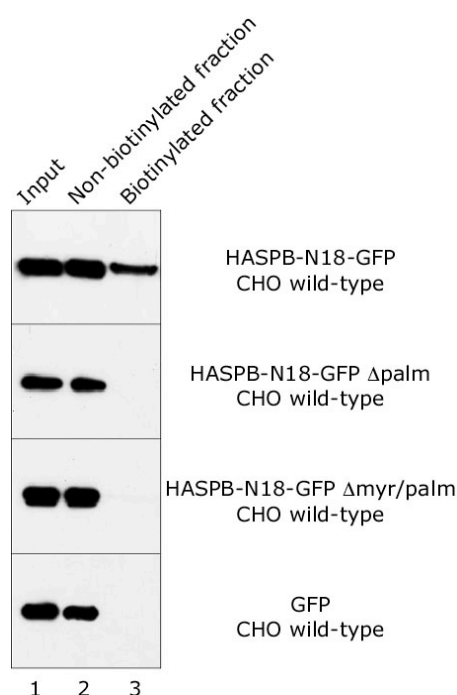


Fig. 16 Biochemical quantification of cell surface localized HASPB-GFP fusion proteins. CHO cells expressing HASPB-GFP fusion proteins as indicated were treated with a membrane-impermeable biotinylation reagent. Cell lysates were generated and biotin-labeled and biotin-unlabeled proteins were separated by streptavidin affinity chromatography. Input material (lane 1; 2%), streptavidin supernatant (non-biotinylated proteins, lane 2; 2%) and streptavidin-bound proteins (biotinylated proteins, lane 3, 50%) were separated by SDS-PAGE followed by western blotting using affinity-purified anti-GFP antibodies.

HASPB-N18-GFP could be detected in the fraction eluted from streptavidin beads (Fig. 16 lane 3) whereas Δ palm-HASPB-N18-GFP, Δ myr-HASPB-N18-GFP and GFP alone were absent from this fraction. These results demonstrate that the biotinylation reagent does not traverse the plasma membrane and, therefore, the positive signal for HASPB-N18-GFP in the fraction of biotinylated proteins represents an exported population located on the cell surface of these cells.

3.1.7 Membrane association of HASPB-N18-GFP fusion proteins expressed in CHO cells

The SH4 domain of the N-terminus of HASPB-N18-GFP is required and sufficient to target the fusion protein to the plasma membrane where it is anchored via dual acylation at the extreme N-terminus. To analyze the overall membrane association of the various HASPB fusion proteins, a soluble pool representing the cytosol (Fig. 17, lane 1) and a membrane fraction (Fig. 17, lane 2) were generated by subcellular fractionation. Additionally, the membrane fraction was subjected to carbonate extraction (Fujiki et al., 1982) to discriminate loosely attached material (Fig. 17, lane 3) from protein tightly associated with membranes (Fig. 17, lane 4). Typically roughly equal amounts of HASPB-N18-GFP were found in the cytosolic and the membrane fractions. About two thirds of the membrane-bound material was found to be resistant to carbonate treatment. In the case of Δ palm-HASPB-N18-GFP (C5S), as expected, the population found in the cytosolic fraction was significantly larger than that present in the membrane fraction (Fig. 17). About 50% of membrane-associated Δ palm-HASPB-N18-GFP was found to be resistant to carbonate treatment. The vast majority of Δ myr-HASPB-N18-GFP (G2A), a mutant that lacks both myristoylation and palmitoylation, was found in the cytosolic fraction. The same applied to GFP lacking the SH4 N-terminal region of HASPB (Fig. 17). Consequently, subcellular fractionation combined with carbonate extraction allows to distinguish between different forms of HASPB fusion proteins with regard to their acylation status.

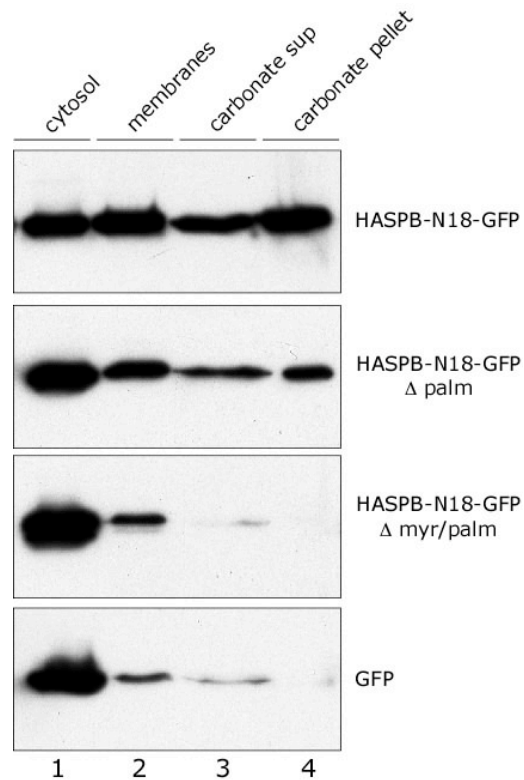


Fig. 17 Membrane association of HASPB-GFP fusion proteins expressed in CHO cells.

CHO cells expressing HASPB-GFP fusion proteins as indicated were separated into a cytosolic (lane 1) and a membrane fraction (lane 2). Additionally, the membrane fraction was subjected to carbonate extraction resulting in a carbonate pellet containing proteins tightly associated with membranes (lane 4). Each fraction (5%) was combined with SDS sample buffer and proteins were separated by SDS-PAGE. Following western blotting, HASPB-GFP fusion proteins were detected with affinity-purified anti-GFP antibodies.

3.2 *Random somatic mutagenesis by retroviral insertion in order to generate CHO mutants defective in HASPB export*

3.2.1 *Random somatic mutagenesis by retroviral insertion*

The principal aim of this study was to establish a genetic screening procedure for molecular components of the HASPB export machinery. CHO cells were initially chosen because they have been reported to export HASPB (Denny et al., 2000). Additionally, since they are pseudo-diploid (Robbins and Roff, 1987) CHO cells were an ideal choice for somatic mutagenesis studies as mutation of genes with a specific function in a given pathway directly resulted in a phenotype due to no functional compensation by a second intact allele. In order to develop a FACS-based screening procedure to identify and isolate export-deficient CHO mutant cells, it was necessary to demonstrate the system's ability to detect a mutant phenotype of individual cells among a vast excess of wild-type cells. To simulate such a scenario, it was tested whether HASPB-N18-GFP-expressing and non-expressing cells present in a mixed culture, treated with doxycycline and subjected to a FACS analysis measuring GFP- and APC-derived cell surface fluorescence could be distinguished from each other with regard to HASPB-N18-GFP cell surface staining. As shown in Fig. 18, panel A, following individual gating of the two populations in the FACS setup based on GFP-derived fluorescence HASPB-N18-GFP-expressing (shown in blue) and non-expressing cells (shown in green) clearly differed in cell surface staining by a factor of about 3 to 4. However, cell surface staining of HASPB-N18-GFP-non-expressing cells was in fact significantly higher than the autofluorescence background defined by antibody-treated CHO_{MCA-TAM2} cells (Fig. 18, panel A red curve) suggesting that a certain amount of HASPB-N18-GFP was transferred from HASPB-N18-GFP-expressing cells to non-expressing cells.

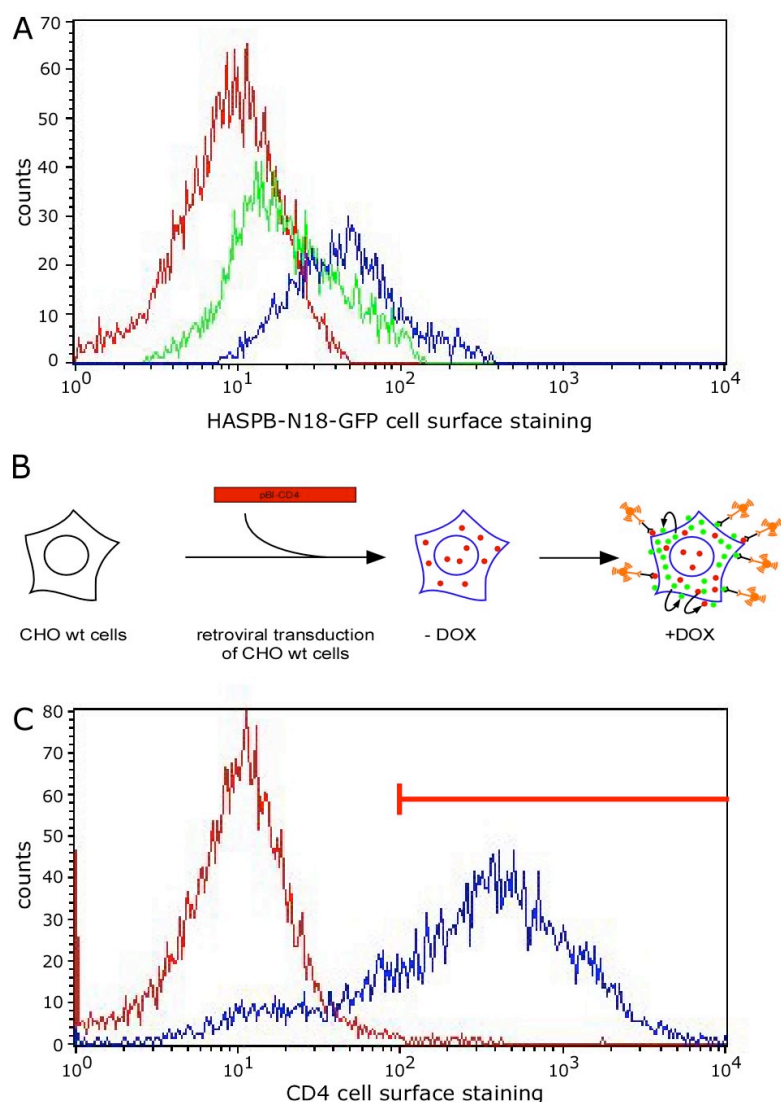


Fig. 18 Retroviral insertion mutagenesis of CHO cells. (A) Intercellular spreading was monitored by growing CHO_{MCAT-TAM2} cells ('CHO wild-type') with CHO_{MCAT-TAM2} cells retrovirally transduced with the HASPB-N18-GFP construct in a mixed culture. HASPB-N18-GFP expression was induced by 1 µg/ml doxycycline for 48 hours at 37°C. CHO_{MCAT-TAM2} cells and CHO_{MCAT-TAM2} cells expressing HASPB-N18-GFP were gated based on GFP fluorescence and APC-derived fluorescence of CHO_{MCAT-TAM2} cells (green curve) and CHO_{MCAT-TAM2} cells expressing HASPB-N18-GFP (blue curve) was measured as depicted in the histogram. Autofluorescence was measured using CHO_{MCAT-TAM2} cells treated with antibodies. (B) Schematic overview of the insertion mutagenesis achieved by a retroviral transduction of CHO_{MCAT-TAM2} cells expressing HASPB-N18-GFP with the pBI-CD4 plasmid in order to generate HASPB-N18-GFP export mutants. (C) CHO_{MCAT-TAM2} cells expressing HASPB-N18-GFP were treated with retroviral particles encoding the cell surface protein CD4. Following transduction, CD4-positive cells were selected based on anti-CD4 cell surface staining employing FACS-sorting.

This result was actually not necessarily expected since substantial amounts of intercellular spreading for both FGF-2 and Galectin-1 following export from CHO cells (Engling et al., 2002; Seelenmeyer et al., 2003) could be observed (Supplementary Fig. 53). In this case, it was virtually impossible to identify and isolate for example FGF-2 export deficient mutant cells in the presence of wild-type cells. In conclusion, this observation emphasizes the results from the experiments shown in Fig. 15 and Fig. 16. The extracellular population of HASPB-N18-GFP could be defined by its appearance on the surface of cells that were incapable of expressing the reporter molecule when mixed with HASPB-N18-GFP-expressing cells. With regard to the mutagenesis strategy, however, these experiments demonstrate that HASPB-N18-GFP exported from CHO wild-type cells is largely retained on the cell surface of the secreting cells. This result, in turn, allows for the identification and isolation of export-deficient CHO mutant cells based on FACS sorting (Fig. 18, panel A), even in the presence of a large excess of wild-type cells. To address this point clonal CHO mutants were randomly generated by retroviral insertion mutagenesis that were characterized by a negative HASPB export phenotype. As illustrated in Fig. 18B, CHO cells carrying the HASPB-N18-GFP reporter gene were transduced with retroviral particles encoding the open reading frame of the integral plasma membrane protein CD4 (Liu et al., 2000). In this context, CD4 was used as a marker for mutagenized cells that were subsequently enriched by FACS (Fig. 18, panel C, horizontal bar above the blue curve).

3.2.2 Screening for somatic CHO mutants characterized by a defect in HASPB export

The pool of CD4-positive mutagenized cells, enriched by the procedure described in section 3.2.1, was subjected to a selection of CHO mutants expressing the HASPB-N18-GFP reporter molecule at a level compared to wild-type cells, however, did not present the fusion protein on their surface.

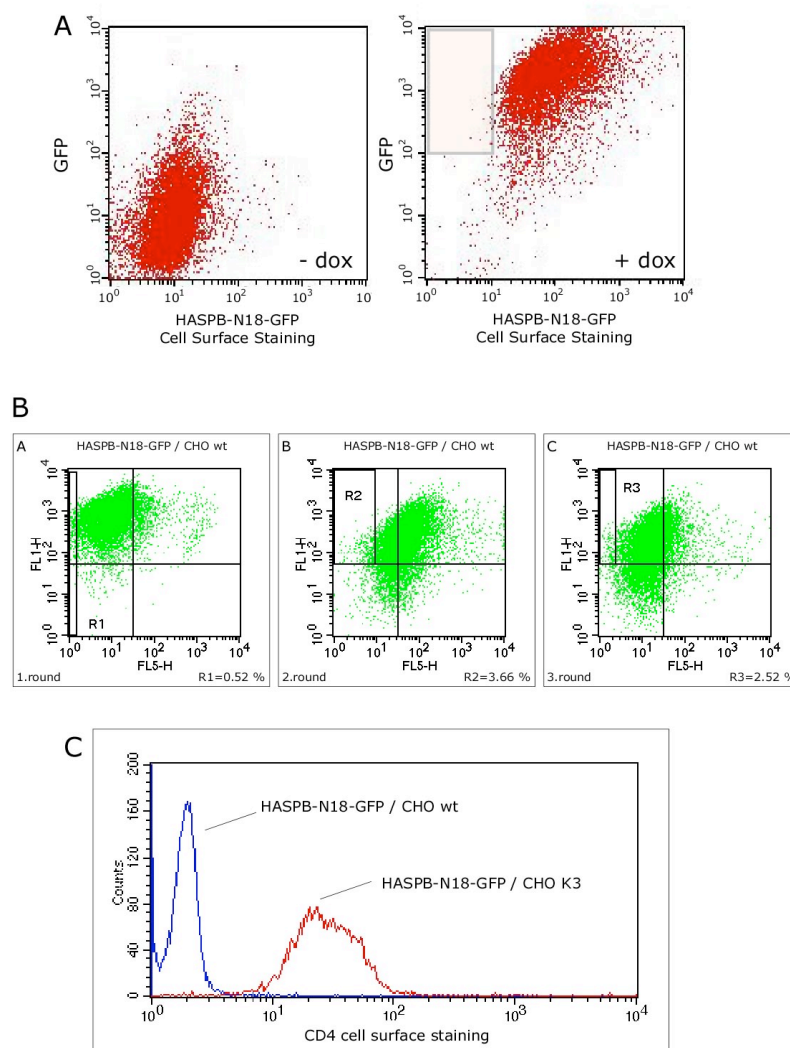


Fig. 19 Genetic screening for HASPB export mutants. (A) CD4-positive cells as enriched in the FACS experiment depicted in Fig. 18, panel C were subjected to FACS sorting as shown by an example for the sorting strategy. Cells were monitored in dot blot mode with GFP-derived fluorescence shown on the y-axis and HASPB-N18-GFP cell surface staining shown on the x-axis. The left-hand panel shows the population grown in the absence of doxycycline. To select for HASPB export mutants the sorting window was adjusted as depicted in the right-hand panel (in presence of 1 μ g/ml doxycycline) to isolate cells characterized by high GFP fluorescence and low APC cell surface staining. (B) CD4-positive cells were subjected to three rounds of FACS sorting as depicted in panel A. In the first two rounds of FACS sorting 0.52% and 3.66% of HASPB-N18-GFP expressing cells with a negative export phenotype were isolated. In the third round 2.52% of HASPB-N18-GFP expressing cells were isolated as single clones. (C) The mutant CHO K3 cell line showing a negative export phenotype was positive for CD4 cell surface staining due to the retroviral transduction while the CHO wild-type cell line showed no CD4 cell surface staining using anti CD4 antibodies in the FACS measurement.

For this purpose, cells were viewed in the FACS setup in a dot blot modus and a sorting window was defined to select for the phenotype described as shown in panel A of Fig. 19. Cells isolated from this sorting window in the first round of selection procedure (Fig. 19B, panel A) were negative for HASPB cell surface staining. About 0.5% of the total population were propagated and subjected to a second round of cell sorting in which 3.66% (Fig. 19 B, panel B) of the selected population displayed the desired phenotype. Finally, in the third round, single cells were selected in the sorting window that was defined as described in panel C of Fig. 19B (2.52%). From this selection procedure a clonal CHO cell line (from here on referred to as “K3”) was isolated that was positive for successful mutagenesis as indicated by CD4 staining (Fig. 19, panel C, red curve) employing flow cytometry. As expected, the parental cell line HASPB-N18-GFP CHO wild-type (Fig. 19, panel C, blue curve) was negative for the integral plasma membrane protein CD4.

3.2.3 Sequence analysis of HASPB-N18-GFP in CHO wild-type and CHO K3 cell lines

As the somatic mutagenesis might result in a mutation of the reporter molecule itself, sequence analysis of the fusion protein expressed in the clonal CHO K3 cell line was performed (Stella Tournaviti). Genomic DNA was isolated followed by amplification of the HASPB-N18-GFP open reading frame. As shown by sequencing of the corresponding PCR products, the sequence of the N-terminal SH4 domain of the reporter molecule was confirmed to be unchanged compared to the parental CHO wild-type cells (Fig. 20).

```

BamHI   Kozak                                     HASPB-N18
Query: 1  gatcccgccaccatgggaagttcttgtacaaaggactccgcaaaggagccccagaagcgt 60
          |||||
Sbjct: 41  gatcccgccaccatgggaagttcttgtacaaaggactccgcaaaggagccccagaagcgt 100
          MetGlySerSerCysThrLysAspSerAlaLysGluProGlnLysArg

          AgeI   Linker   GFP
Query: 61  gctgatggaccggtcgccaccatggtgagcaagggcgaggagctgttcaccgggtgtg 120
          |||||
Sbjct: 101 gctgatggaccggtcgccaccatggtgagcaagggcgaggagctgttcaccgggtgtg 160
          AlaAspGlyProValAlaThrMetValSerLysGlyGluGluLeuPheThrGlyValVal

Query: 121  cccatcctggtcgagctggacggcgacgtaaacggccacaagttcagcgtgtccggcgag 180
          |||||
Sbjct: 161  cccatcctggtcgagctggacggcgacgtaaacggccacaagttcagcgtgtccggcgag 220
          ProIleLeuValGluLeuAspGlyAspValAsnGlyHisLysPheSerValSerGlyGlu

Query: 181  ggcgagggcgatgccacctacggcaagctgacctgaagttcatctgcaccaccggcaag 240
          |||||
Sbjct: 221  ggcgagggcgatgccacctacggcaagctgacctgaagttcatctgcaccaccggcaag 280
          GlyGluGlyAspAlaThrTyrGlyLysLeuThrLeuLysPheIleCysThrThrGlyLys

Query: 241  ctgcccggtgccctggccaccctcgtgaccacctgacctacggcgtgcagtgttcagc 300
          |||||
Sbjct: 281  ctgcccggtgccctggccaccctcgtgaccacctgacctacggcgtgcagtgttcagc 340
          LeuProValProTrpProThrLeuValThrThrLeuThrTyrGlyValGlnCysPheSer

Query: 301  cgctaccccgaccacatgaagcagcagcacttcttcaagtcgcccatgccgaaggctac 360
          |||||
Sbjct: 341  cgctaccccgaccacatgaagcagcagcacttcttcaagtcgcccatgccgaaggctac 400
          ArgTyrProAspHisMetLysGlnHisAspPhePheLysSerAlaMetProGluGlyTyr

Query: 361  gtccaggagcgcaccatcttcttcaaggacgacggcaactacaagaccgcgccgaggtg 420
          |||||
Sbjct: 401  gtccaggagcgcaccatcttcttcaaggacgacggcaactacaagaccgcgccgaggtg 460
          ValGlnGluArgThrIlePhePheLysAspAspGlyAsnTyrLysThrArgAlaGluVal

Query: 421  aagttcgagggcgacaccctggtgaaccgcatcgagctgaaggcatcgacttcaaggag 480
          |||||
Sbjct: 461  aagttcgagggcgacaccctggtgaaccgcatcgagctgaaggcatcgacttcaaggag 520
          LysPheGluGlyAspThrLeuValAsnArgIleGluLeuLysGlyIleAspPheLysGlu

Query: 481  gacggcaacatcctggggcacaagctggagtacaactacaagccacaacgtctatc 540
          |||||
Sbjct: 521  gacggcaacatcctggggcacaagctggagtacaactacaagccacaacgtctatc 580
          AspGlyAsnIleLeuGlyHisLysLeuGluTyrAsnTyrAsnSerHisAsnValTyrIle

Query: 541  atggccgacaagcagaagaacggcatcaaggtgaacttcaagatccgccacaacatcgag 600
          |||||
Sbjct: 581  atggccgacaagcagaagaacggcatcaaggtgaacttcaagatccgccacaacatcgag 640
          MetAlaAspLysGlnLysAsnGlyIleLysValAsnPheLysIleArgHisAsnIleGlu

Query: 601  gacggcagcgtgcagctcgccgaccactaccagcagaacacccccatc 648
          |||||
Sbjct: 641  gacggcagcgtgcagctcgccgaccactaccagcagaacacccccatc 688
          AspGlySerValGlnLeuAlaAspHisTyrGlnGlnAsnThrProIle

```

Fig. 20 Sequence analysis of HASPB-N18-GFP in CHO wild-type and CHO K3 cells.

Genomic DNA of CHO wild-type and CHO K3 cells were isolated and subjected to PCR-amplification using vector-specific primers. The resulting PCR products were sequenced and aligned. The cloning sites (marked in red) used for integration into the doxycycline-dependent vector (pRevTRE2) are indicated. The HASPB-N18 sequence (yellow) containing a Kozak region (blue) was spaced by a short linker from the GFP sequence (green).

3.2.4 Characterization of HASPB-N18-GFP export from CHO wild-type cells compared to CHO K3 mutant cells employing FACS-analysis and Biotinylation

In order to analyze the CHO K3 mutant cell line regarding HASPB cell surface localization compared to CHO wild-type cells flow cytometry as well as the biochemical biotinylation assay were performed. Based on GFP-fluorescence, the expression level of HASPB-N18-GFP did not significantly differ between wild-type and K3 mutant cells as analyzed by FACS (Fig. 21, panel A, blue bars). However, HASPB-N18-GFP cell surface staining was largely reduced to about 30% as compared to wild-type levels (Fig. 21, panel A, red bars). These data were confirmed by a biochemical assessment of the extracellular population of HASPB-N18-GFP in wild-type versus K3 mutant cells using a membrane-impermeable biotinylation reagent and streptavidin-based immunopurification of factors exposed on the cell surface. As illustrated in Fig. 21 panel B, the amount of biotinylated cell surface HASPB-N18-GFP (lower box, lane 3) derived from K3 cells was largely reduced to about 30% as compared to CHO wild-type cells (upper box, lane 3). As expected, the control proteins Δ palm-HASPB-N18-GFP, Δ myr-HASPB-N18-GFP and GFP were not detectable on the cell surface.

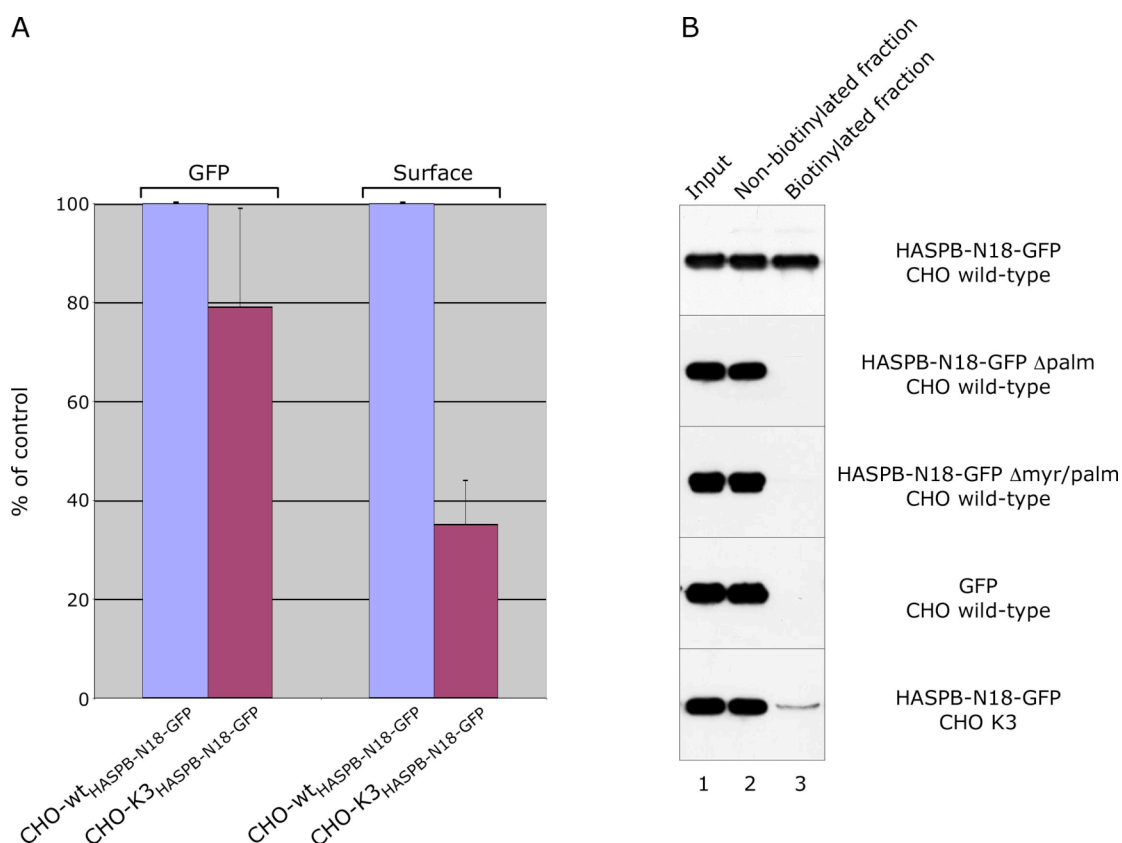


Fig. 21 Characterization of HASPB-N18-GFP export from CHO wild-type cells compared to CHO K3 mutant cells. (A) FACS analysis. CHO wild-type cells and CHO K3 cells were grown for 48 hours at 37°C in the presence of doxycycline (1 μ g/ml). Cells were processed for FACS sorting using affinity-purified anti-GFP antibodies and APC-coupled secondary antibodies to detect exported HASPB-N18-GFP by cell surface staining. For a statistical analysis of four independent experiments, GFP-derived fluorescence and APC-derived cell surface staining of CHO wild-type cells expressing HASPB-N18-GFP was set to 100%, respectively. (B) Biochemical analysis of exported HASPB-N18-GFP in CHO wild-type cells, CHO K3 cells and various control cell lines using cell surface biotinylation. The experiment was conducted exactly as described in the 'Material and Methods' section. Input material (lane 1, 2%), streptavidin supernatant (non-biotinylated proteins, lane 2, 2%) and streptavidin-bound proteins (biotinylated proteins, lane 3, 50%) were separated by SDS-PAGE followed by western blotting using affinity-purified anti-GFP antibodies.

3.2.5 Expression level, membrane association and post-translational acylation of HASPB-N18-GFP in CHO wild-type cells and mutant K3 cells

As dual acylation of HASPB-N18-GFP is a critical determinant for plasma membrane targeting and export, it was important to analyze whether the reporter molecule HASPB-N18-GFP itself was properly modified in K3 cells. Therefore, in a first set of experiments, overall membrane association of HASPB-N18-GFP was tested in CHO K3 cells by a carbonate extraction analysis. The input material of HASPB-N18-GFP was comparable in wild-type CHO and K3 cells, which was consistent with the FACS experiment shown in Fig. 21, demonstrating that the expression level of HASPB-N18-GFP does not differ significantly in the two cell lines (Fig. 22, panel A). Similarly there were no apparent differences in the distribution of HASPB-N18-GFP between cytosol and membranes when CHO wild-type and K3 cells were compared (Fig. 22B, lanes 1 and 2). Finally, when the membrane fractions of wild-type and K3 cells were subjected to carbonate extraction, the distribution of HASPB-N18-GFP between the membrane-associated and the soluble pool was identical between the two cell types (Fig. 22B, lanes 3 and 4). These data indicate that the acylation status of HASPB-N18-GFP does not differ between CHO wild-type and K3 cells.

This conclusion was confirmed by metabolic labeling of HASPB-N18-GFP in wild-type and K3 cells using [^3H]-labeled myristate and [^3H]-labeled palmitate (performed by Stella Tournaviti). Incorporation of both fatty acids into HASPB-N18-GFP could be detected in both wild-type and K3 cells whereas the corresponding negative controls were either labeled with [^3H]-myristate alone (in case of Δpalm -HASPB-N18-GFP) or not labeled at all (for Δmyr -HASPB-N18-GFP and GFP) (Fig. 22, panel C). Together, these results strongly suggest that HASPB-N18-GFP gets normally acylated in the CHO K3 mutant cell line. Therefore, the lack of HASPB-N18-GFP present on the cell surface of these cells must be due to the translocation machinery itself from which at least one component is apparently disrupted in K3 cells.

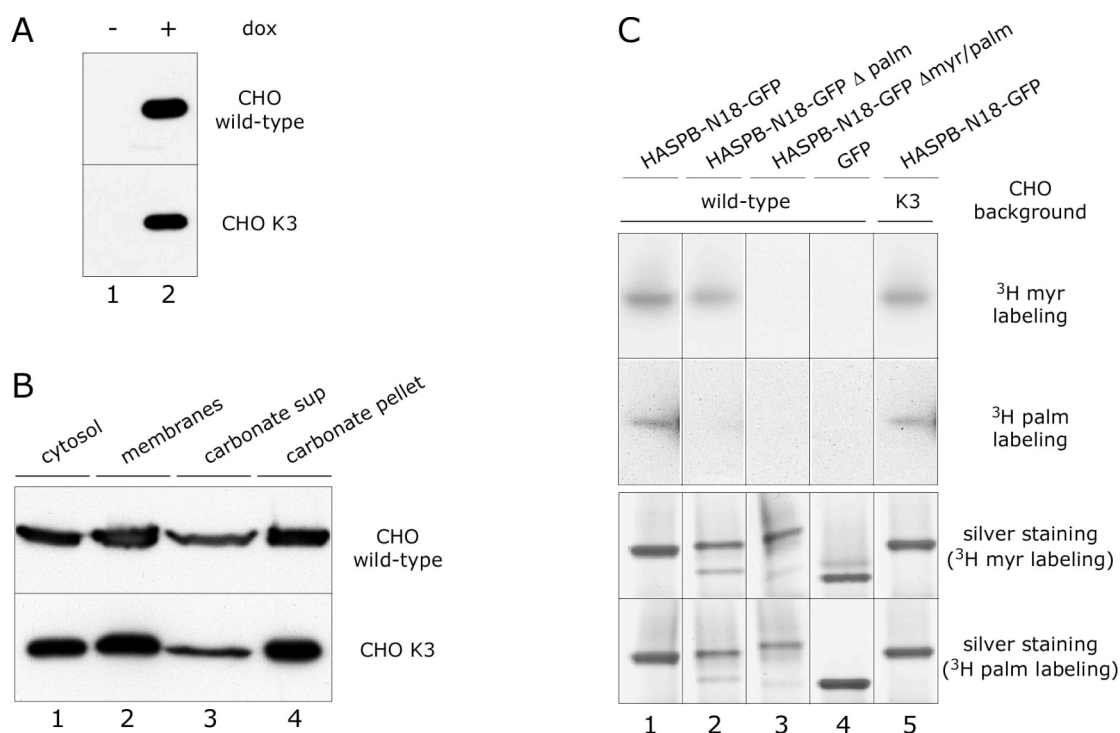


Fig. 22 Expression level, membrane association and acylation of HASPB-N18-GFP in CHO wild-type cells and CHO mutant K3 cells. (A) CHO wild-type cells and CHO K3 cells (both expressing HASPB-N18-GFP) were grown in six-well plates to about 80% confluency in the absence (lane 1) or presence (lane 2) of doxycycline (1 $\mu\text{g}/\text{ml}$) for 48 hours at 37°C. Cells were detached with PBS/EDTA, collected by centrifugation and lysed in SDS sample buffer. 1% of each lysate, corresponding to cells from one well, were subjected to SDS-PAGE. HASPB-N18-GFP was detected by western blotting using affinity-purified anti-GFP antibodies. (B) CHO wild-type cells and CHO K3 cells (both expressing HASPB-N18-GFP) were grown in six-well plates to about 80% confluency in the presence of 1 $\mu\text{g}/\text{ml}$ doxycycline for 48 hours at 37°C. Subcellular fractionation and carbonate extraction of membranes were performed and 5% of each fraction was combined with SDS sample buffer and proteins were separated by SDS-PAGE. Following western blotting, HASPB-GFP fusion proteins were detected with affinity-purified anti-GFP antibodies. (C) CHO wild-type cells, CHO K3 cells (both expressing HASPB-N18-GFP) as well as control cell lines expressing Δmyr -HASPB-N18-GFP and Δpalm -HASPB-N18-GFP, respectively, were grown in six-well plates to about 80% confluency in the presence of 1 $\mu\text{g}/\text{ml}$ doxycycline for 48 hours at 37°C and labeled with [^3H]-myristate and [^3H]-palmitate. Cell lysates were prepared and subjected to immunoprecipitation using affinity-purified anti-GFP antibodies. Immunopurified fractions were split into two samples, separated by SDS-PAGE and either processed by fluorography (upper panel) or silver staining (lower panel).

3.2.6 *HASPB-N18-GFP localizes to the plasma membrane in CHO K3 cells*

To this point the experiments have shown that HASPB export was largely reduced in the CHO K3 mutant cell line as compared to CHO wild-type cells. Intriguingly, similar to CHO wild-type cells, HASPB-N18-GFP expressed in CHO K3 was stably associated with the plasma membrane. In order to define the subcellular site of HASPB-N18-GFP membrane translocation, the precise localization in CHO wild-type cells versus CHO K3 cells was analyzed employing confocal microscopy and subcellular distribution. There was virtually no difference in the subcellular distribution of HASPB-N18-GFP in the two cell types and in both cases the majority of the material was localized to the plasma membrane (Fig. 23, panel A and B). These morphological data were confirmed by a biochemical analysis employing subcellular fractionation (Fig. 23, panel C). After purification of plasma membrane-derived vesicles (Schäfer et al., 2004) the enrichment of the HASPB-N18-GFP reporter molecule in plasma membranes of CHO wild-type cells (Fig. 23C, lanes 1-4) and CHO K3 cells (Fig. 23C, lanes 5-8) was compared, respectively. Compared to the homogenate (lanes 1 and 5), HASPB-N18-GFP was found to be enriched in gradient-purified plasma membrane vesicles using the plasma membrane marker transferrin receptor (TfR) (Futter et al., 1998) in both CHO wild-type and CHO K3 cells (lanes 4 and 8, respectively). Using the Golgi marker GM130 (Nakamura et al., 1995), the plasma membrane vesicle fraction was depleted of Golgi membranes demonstrating the significance of the findings described above. The association of HASPB-N18-GFP with plasma membranes in both CHO wild-type cells and K3 cells was considered to be quite striking, as it demonstrated a defect in CHO K3 cells directly in the translocation machinery rather than some kind of intracellular segregation of HASPB-N18-GFP. In the latter case, access to the site of membrane translocation would be prevented. Together, these findings confirm that the HASPB-N18-GFP translocation apparatus is a plasma membrane-resident machinery.

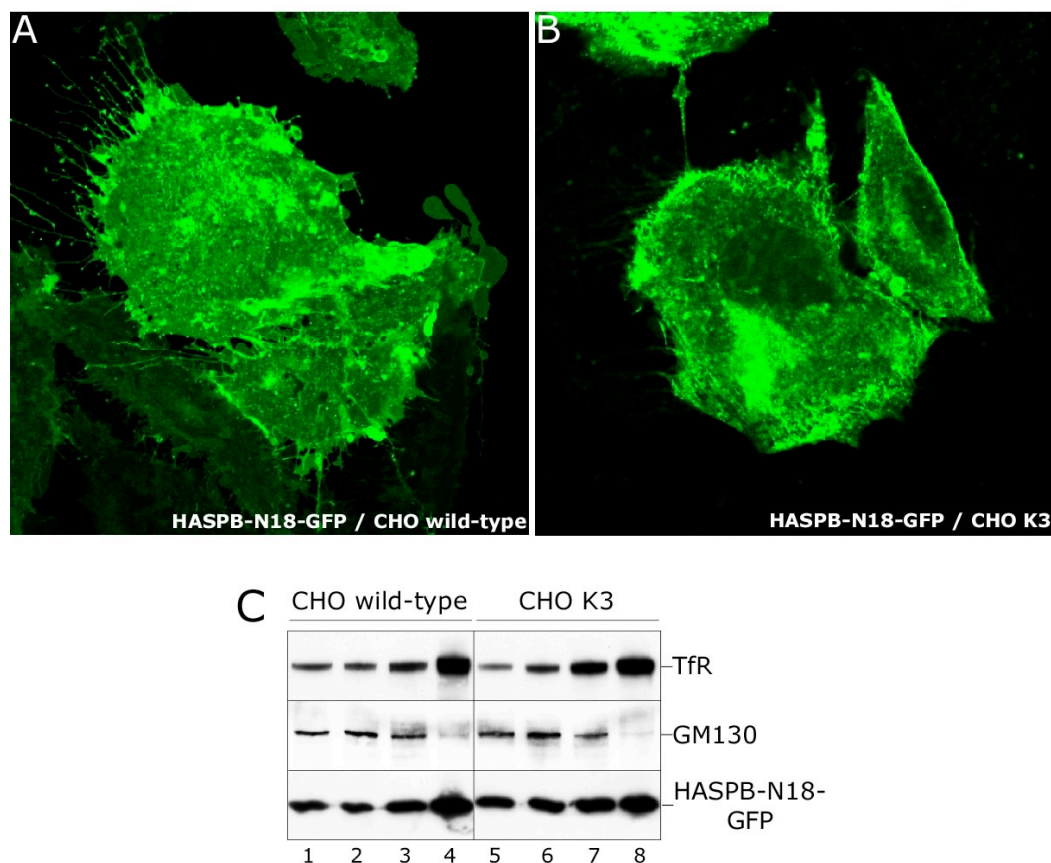


Fig. 23 Subcellular localization of HASPB-N18-GFP in CHO wild-type and CHO K3 mutant cells as determined by confocal microscopy and subcellular fractionation. (A) HASPB-N18-GFP expressed in CHO wild-type cells. (B) HASPB-N18-GFP expressed in CHO K3 mutant cells. Cells were grown on glass coverslips in the presence of 1 $\mu\text{g/ml}$ doxycycline for 48 hours at 37°C and processed for confocal microscopy. GFP-derived fluorescence was viewed with a Zeiss LSM 510 confocal microscope. (C) Subcellular fractionation of CHO wild-type cells and CHO K3 cells was conducted as described earlier (Schäfer et al., 2004). To identify plasma membranes, antibodies directed against the transferrin receptor were used (Futter et al., 1998). To detect Golgi membranes, antibodies directed against GM130 were used (Nakamura et al., 1995). Four fractions were generated and analyzed for each cell line: a hypotonic lysate (lanes 1 and 5), a post-mitochondrial supernatant (lanes 2 and 6), a microsomal membrane fraction (lanes 3 and 7) and gradient-purified plasma membranes (lanes 4 and 8). For each fraction 15 μg total protein were separated by SDS-PAGE and analyzed by western blotting using the antibodies indicated.

3.2.7 An FGF-2-GFP reporter molecule is exported from CHO wild-type and K3 mutant cells at similar levels

In CHO K3 mutant cells, as revealed from the somatic mutagenesis screen, a component essential for HASPB export might be disrupted since the fusion protein expressed in CHO K3 is transported and associated to the plasma membrane, however, its translocation to the outer cell surface is blocked. To assess whether the disrupted export component in CHO K3 cells is a specific factor for HASPB export or rather a general component for non-classical secretory processes, the export of FGF-2 from CHO K3 cells, a classical example for unconventional secretory proteins (Florkiewicz et al., 1995; Mignatti et al., 1992; Mignatti and Rifkin, 1991; Nickel, 2003), was analyzed. For this purpose, both CHO K3 and the parental CHO wild-type cells expressing the HASPB-N18-GFP fusion protein were transduced with retroviral particles encoding an FGF-2-GFP fusion protein (Backhaus et al., 2004; Engling et al., 2002). Owing to the different molecular weights (25 and 45 kDa, respectively), the two reporter molecules could be easily distinguished in the cell surface biotinylation assay (Figs. 16 and 21). There was no difference in FGF-2 cell surface expression between CHO wild-type and CHO K3 cells (Fig. 24, compare lanes 3 and 6, upper panels), respectively. By contrast, HASPB-N18-GFP analyzed from the same cell preparations was exported only from CHO wild-type cells (compare lanes 3 and 6, lower panels). Overall, the experiment show that the component disrupted in CHO K3 cells is a specific component of the HASPB export pathway.

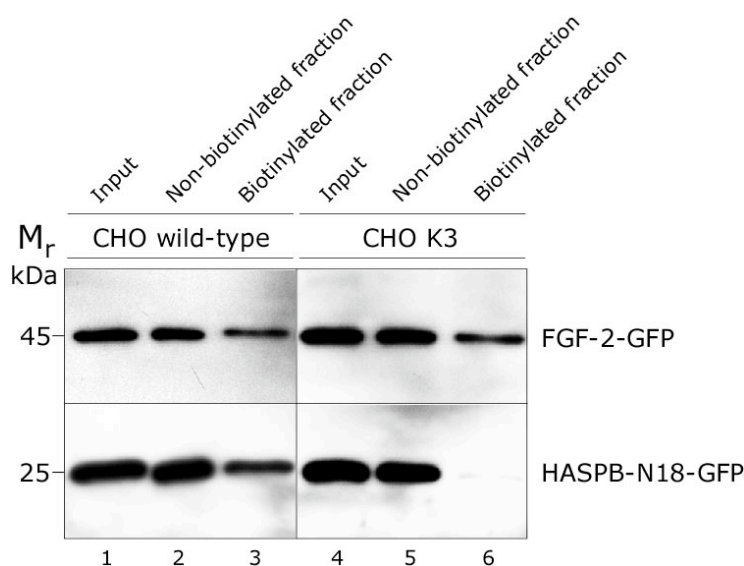


Fig. 24 Export of an FGF-2-GFP reporter molecule from CHO wild-type and CHO K3 cells. Parental CHO wild-type (lanes 1-3) and CHO K3 mutant cells (lanes 4-6) expressing HASPB-N18-GFP were transduced with retroviral particles containing the FGF-2-GFP open reading frame controlled by a doxycycline-dependent element. Transduction efficiency was about 65% as determined by GFP-derived fluorescence. Both cell types were treated with a membrane-impermeable biotinylation reagent. Cell lysates were generated and biotinylated and non-biotinylated proteins were separated by streptavidin affinity chromatography. Input material (lane 1 and 4; 4%), streptavidin supernatant (non-biotinylated proteins, lanes 2 and 5; 4%) and streptavidin-bound proteins (biotinylated proteins, lanes 3 and 6; 50%) were separated by SDS-PAGE followed by western blotting using affinity-purified anti-GFP antibodies.

3.2.8 Secretion of Galectin-1 from CHO K3 cells occurs as efficiently as from parental CHO wild-type cells

Interestingly coincident with FGF-2 (Schäfer et al., 2004; Zehe et al., 2006), Galectin-1 (Seelenmeyer et al., 2005) was reported to translocate directly across the plasma membrane. Moreover, as described previously, Galectin-1 was shown to accumulate in evaginations of the plasma membrane followed by an export mechanism that appears to involve the formation of membrane-bound vesicles (Cooper and Barondes, 1990; Hughes, 1999; Mehul and Hughes, 1997; Sato et al., 1993). To assess the relevance of Galectin-1 export in the context of the compromised export mutant K3, the biochemical

assessment of the extracellular population of HASP-N18-GFP and Galectin-1-GFP in the wild-type compared to K3 mutant cells was analyzed. Employing the biotinylation assay (compare Fig. 24), Galectin-1 and HASPB fusion proteins could be distinguished based on their molecular sizes (40.5 kDa for Galectin-1-GFP and 25 kDa for HASPB-N18-GFP).

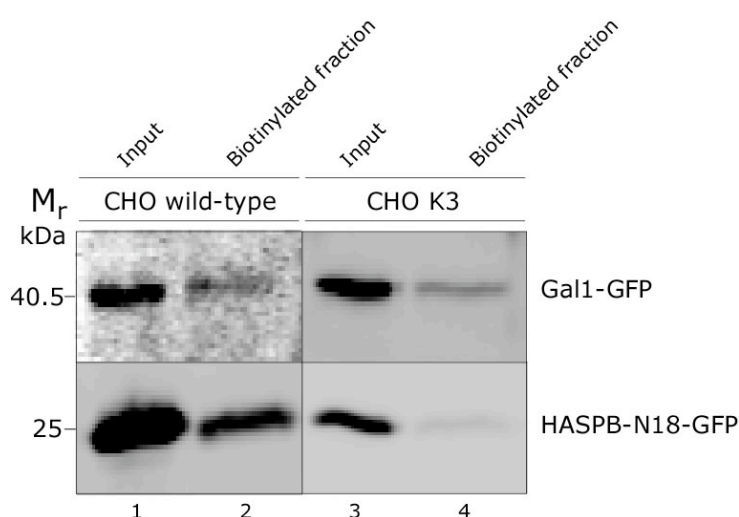


Fig. 25 Export of a Gal-1-GFP reporter molecule from CHO wild-type and CHO K3 cells.

Parental CHO wild-type (lanes 1 and 2) and CHO K3 mutant cells (3 and 4) expressing HASPB-N18-GFP were transduced with retroviral particles containing the Gal-1-GFP open reading frame controlled by a doxycycline-dependent element. Transduction efficiency was about 30% as determined by GFP-derived fluorescence. Both cell types were treated with a membrane-impermeable biotinylation reagent as described in the 'Materials and Methods' section and streptavidin-bound proteins (biotinylated proteins, lanes 2 and 4; 50%) were separated by SDS-PAGE followed by western blotting using affinity-purified anti-GFP antibodies.

As expected, HASPB-N18-GFP was exported only from CHO wild-type cells (Fig. 25, lanes 2 and 4, lower panel). By contrast, Galectin-1-GFP was exported from CHO wild-type as efficiently as from the mutant K3 cell line (Fig. 25, lanes 2 and 4, upper panel). This observation confirms previous findings indicating that the defect in the mutant CHO K3 cell line is specific for HASPB-N18-GFP export and not a general component of non-classical secretory processes.

3.3 Analysis of the phenotype observed in the CHO K3 mutant cell line

3.3.1 Identification of the chemokine-orphan-receptor 1 (*cmkor 1*) in the CHO K3 mutant cell line

To identify the disrupted component in the CHO K3 mutant cell line, a LAM (linear amplification mediated)-PCR was performed (GATC).

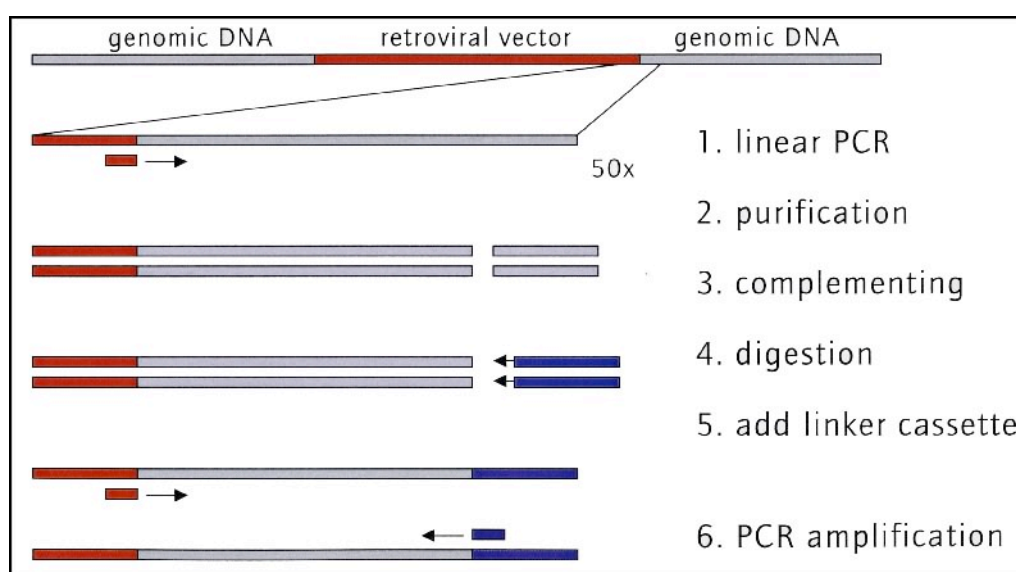
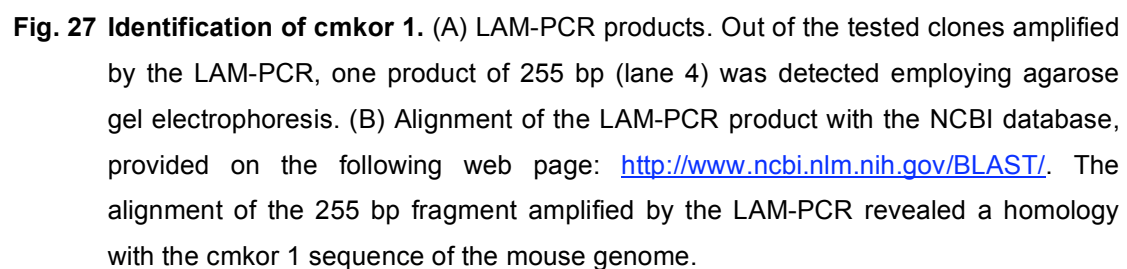


Fig. 26 LAM-PCR. Genomic DNA was amplified using vector-specific primers to obtain a linear PCR-product. After purification and complementation the product was digested using an enzyme generating blunt ends followed by addition of a linker cassette. Due to the known sequence of the added linker cassette, PCR amplification was possible.

As illustrated in Fig. 26, the insertion site of the retroviral vector was amplified performing a LAM-PCR followed by sequencing of the corresponding products. Since CD4 was used as a marker for mutagenized cells (section 3.2.1), one integration site was found employing the LAM-PCR of genomic DNA isolated from the K3 mutant CHO cell line by using CD4-specific primers.



Interestingly the identified 255 bp fragment (Fig. 27, panel A) aligned with a specific mouse sequence (Fig. 27, panel B) located on chromosome 1 (Fig. 28, panel A) of the mouse genome. In this regard, the retrovirus integrated into a non-coding region, an intron flanked by two exons (Fig. 28, panel B, red box). The gene, chemokine orphan receptor 1, belongs to a family of G-protein coupled receptors, which includes hormones, neuro-

transmitter and light receptors, all of which transduce extracellular signals through interaction with guanine nucleotide (G) binding proteins (Shimizu et al., 2000). Upon binding of their respective chemokines they play a pivotal role in diseases such as autoimmune and allergic inflammatory disorders, cancer and organ transplant where excessive cellular recruitment plays a deleterious role. Their function is not limited to recruitment, since they also play a role in cellular activation, differentiation, degranulation and in processes such as organ development, angiogenesis, lymphogenesis and wound repair (Bruhl et al., 2001; Rot and von Andrian, 2004). As described recently the protein seems to function as a coreceptor for human immunodeficiency viruses (HIV) (Shimizu et al., 2000). However, at this stage its endogenous ligand has not yet been identified (Shimizu et al., 2000; Tilakaratne and Sexton, 2005). Together, these findings strongly suggest that cmk1 might be an important component necessary for HASPB export from mammalian cells.

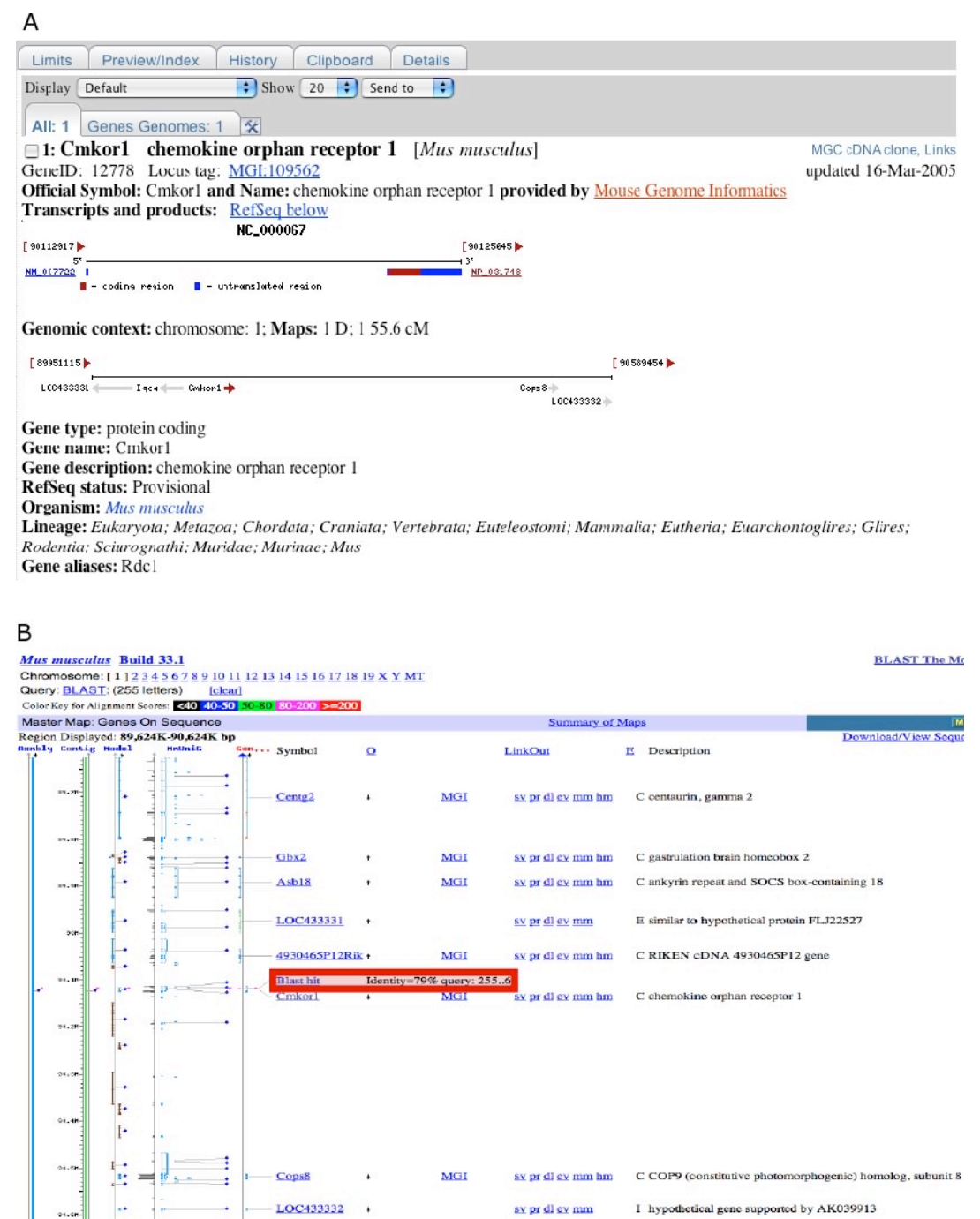


Fig. 28 Localization of cmkor 1. (A) NCBI, the provided database, identified the 255 bp fragment as the chemokine orphan receptor 1 located on chromosome 1 of the mouse genome. (B) Mouse genome informatics. Employing NCBI database, the retrovirus integrated into a non-coding region, an intron, located between two exons within the chemokine orphan receptor 1 (red box).

3.3.2 *Sequence analysis of the chemokine orphan receptor 1 expressed in CHO cells*

To validate the link between the expression of cmkor 1 and the HASPB export defect in the mutant K3 cell line RNA interference experiments were planned. For this kind of experiments it was crucial to analyze the sequence of the chemokine orphan receptor 1 expressed in CHO cells. Therefore, RNA from CHO wild-type cells was isolated. The following RT-PCR was performed with two cmkor 1-specific primer pairs flanking conserved regions of the mouse and the human cmkor 1-sequences (Supplementary Fig. 54, purple and blue boxes). The resulting PCR products were introduced into a vector and following amplification five positive clones were identified. After sequencing, the CHO sequence of the chemokine orphan receptor 1 (Supplementary Fig. 55) was used for the design of three different siRNAs.

3.3.3 *HASPB-N18-GFP export from CHO wild-type is not affected by downregulation of cmkor 1*

To this point the experiments showed that HASPB-N18-GFP export from the mutant CHO K3 cell line was not as efficient as in CHO wild-type cells. To verify whether the reduced HASPB export in the mutant CHO K3 cell line was due to the integration of the retrovirus inserted into the genome of CHO K3 cells RNA interference experiments were performed. CHO wild-type and K3 cells were transfected with three different cmkor-specific siRNA oligos in two different molar ratios by using Oligofectamine as transfection reagent. Following isolation of the corresponding RNA and reverse transcription-PCR, the amplified products were separated on agarose gel electrophoresis. As illustrated in Fig. 29A, lanes 1-6, a cmkor 1 knockdown was observed (Fig. 29A, lanes 5 and 6) only by using siRNA oligo 2 and 3 in low concentrations (80 nM) during the transfection procedure. However, a parallel experiment using only the transfection reagent (Fig. 29, lane 7) revealed the same result. This was not expected, as cmkor 1 mRNA should not get down-

regulated under control conditions. Additionally, *cmkor* 1 mRNA was detectable in both CHO wild-type and, quite strikingly, in CHO K3 cells as shown by the analysis of cytoplasmic and total RNA (Fig. 29B, lanes 1-4). In contrast to these paradox results, the RT-PCR was shown to be functional (Fig. 29C, lanes 1 and 2). Moreover the cells were strongly affected regarding growth due to the transfection procedure.

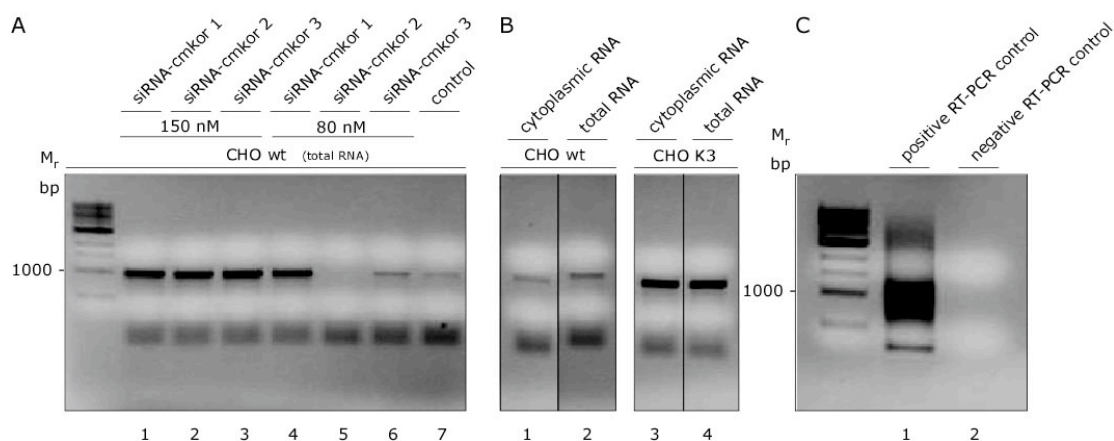


Fig. 29 Cmkor downregulation in CHO wild-type cells. (A) CHO wild-type cells were transfected with three different *cmkor* 1-specific siRNAs (lanes 1-6) in two different molar ratios (lanes 1-3 and 4-6) using Oligofectamine. As control CHO wild-type cells were treated only with Oligofectamine. After RNA isolation a RT-PCR was performed. (B) Cytoplasmic and total RNA from CHO wild-type (lanes 1 and 2) and CHO K3 cells (lanes 3 and 4) were isolated and subjected to RT-PCR. (C) Positive RT-PCR control (lane 1) and negative RT-PCR control (lane 2) as given by the RT-PCR manual. All samples were separated by agarose gel electrophoresis.

To further assess the relevance of *cmkor* 1 in the context of the perturbed HASPB membrane translocation in CHO K3 cells RT-PCR products obtained from isolation of cytoplasmic and total RNA from CHO wild-type and CHO K3 cells, respectively, were sequenced. As illustrated in the alignment (Supplementary Fig. 56, red parts indicate homology with the *cmkor* 1 sequence) both cell types contained *cmkor* 1 mRNA. Overall, the experiment showed that *cmkor* 1 has no influence on the HASPB export defect in CHO K3 cells as HASPB export from CHO wild-type cells was not blocked employing RNA interference. Since *cmkor* 1 mRNA was detectable especially

in CHO K3 cells the expression of chemokine orphan receptor 1 seems not affected in the CHO K3 mutant cell line.

3.3.4 Overexpression of *cmkor 1* in CHO wild-type and CHO K3 cell lines

To monitor a possible effect of the chemokine orphan receptor 1 on HASPB export, overexpression of the *cmkor 1* gene in CHO wild-type as well as in CHO K3 cells was performed. The *cmkor 1* sequence was introduced into an expression vector encoding the cell surface protein CD8 (Hoffmann, 1980) as marker protein. Since the vector contained an IRES element (Jang et al., 1988; Liu et al., 2000) a simultaneous expression of *cmkor 1* as well as CD8 was achieved. Following retroviral transduction of the *cmkor 1* clones 4 (Fig. 30, panel A, B, E and F) and 9 (Fig. 30, panel C, D, G and H) into CHO wild-type and CHO K3 cells, the cell lines were sorted twice in order to select for *cmkor 1*-expressing cells represented by CD8 cell surface staining (Fig. 30, shown on the y-axis by CD8 cell surface staining). The enrichment of *cmkor 1*-positive cells could be achieved in a second round of sorting as shown in Fig. 30, panel B, D, F and H.

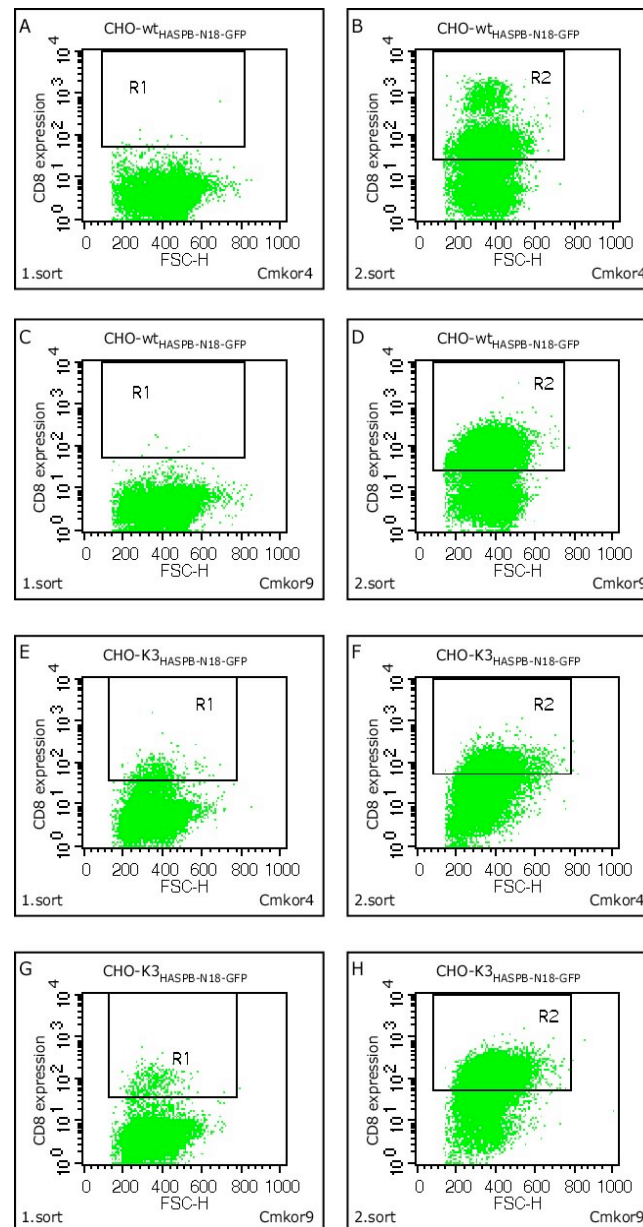


Fig. 30 Generation of cmkor-expressing CHO wild-type and CHO K3 cell lines.

CHO wild-type and CHO K3 cells were retrovirally transfected with a vector containing an IRES element allowing for simultaneous expression of cmkor 1 as well as CD8. CD8 was used as a marker protein in order to select for cmkor 1-positive cells by two rounds of FACS sorting (first round: left hand panels; second round: right hand panels, FSC-H represents the size of the cells). CHO wild-type cells (A-D) and CHO K3 (E-H) cells were transduced with two different cmkor 1 clones, 4 and 9, respectively.

3.3.5 *HASPB-N18-GFP export from CHO K3 cell line cannot be restored by overexpression of cmkor 1*

In order to analyze whether HASPB export from CHO K3 cells can be restored by overexpression of cmkor 1 or rather can be blocked in CHO wild-type cells, HASPB-N18-GFP cell surface staining was monitored by flow cytometry. As shown in the quantitative analysis in Fig. 31, the expression level of HASPB-N18-GFP in CHO K3 cells was only slightly reduced compared to wild-type levels (Fig. 31, panel A, green bars). However, as expected (compared to Fig. 15), the HASPB-N18-GFP cell surface staining was largely reduced to about 60% (Fig. 31, panel A, blue bars). By contrast, overexpressing the cmkor 1 gene, HASPB-N18-GFP cell surface staining of the mutant CHO K3 cell line could not be restored to wild-type levels. Moreover, due to overexpression, HASPB export could not be blocked in CHO wild-type cells (Fig. 31, panel A, blue bars). To verify the expression of cmkor 1, both cell lines were analyzed regarding CD8 cell surface expression. As illustrated in Fig. 31, panel B, CHO wild-type and CHO K3 cells, respectively, were successfully transduced with cmkor 1 as shown by positive staining for CD8. Together, these results strongly suggest that the chemokine orphan receptor 1 has no influence on HASPB export.

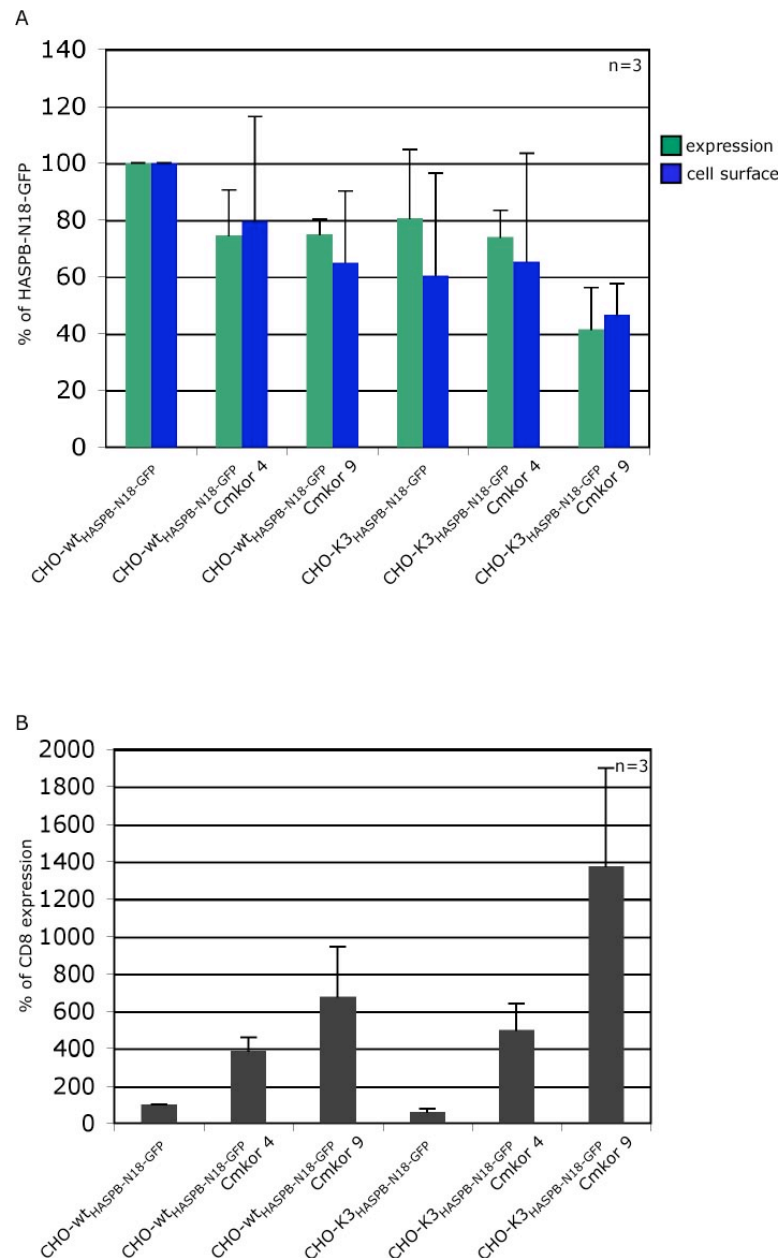


Fig. 31 Characterization of HASPB-N18-GFP export from cmk1 transduced CHO wild-type and CHO K3 cells as analyzed by FACS. (A) Cmk1 transduced CHO wild-type and CHO K3 cells as well as their corresponding parental cell lines were grown for 48 hours at 37°C in the presence of 1 µg/ml doxycycline. Cells were processed for FACS sorting using affinity-purified anti-GFP antibodies and APC-coupled secondary antibodies to detect exported HASPB-N18-GFP bound on the cell surface. For a statistical analysis of three independent experiments, GFP-derived fluorescence and APC-derived cell surface staining of CHO wild-type cells expressing HASPB-N18-GFP was set to 100 %, respectively. (B) To monitor cmk1 expression, the cells were processed as described in A, and analyzed for CD8 cell surface staining using CD8 antibodies coupled to anti-mouse APC secondary antibodies.

3.3.6 Quantitative analysis of cell surface localized HASPB-N18-GFP fusion proteins exported from cmkor 1 transduced CHO wild-type and CHO K3 cell lines

To demonstrate by means of an independent method that overexpression of cmkor 1 has no positive effect regarding HASPB export from CHO K3 cells a biochemical assessment of the extracellular population of HASPB-N18-GFP in cmkor 1 transduced wild-type and K3 cell lines were performed. As shown in Fig. 32, panel A, lanes 1 and 3, the expression levels were comparable between the various cell lines. Importantly, there was no difference in the HASPB-N18-GFP cell surface staining between CHO wild-type cells (Fig. 32A lane 2, upper panel) and CHO K3 cells (Fig. 32, A lane 4, upper panel), when compared to their cmkor 1 transduced cell lines (Fig. 32A, lanes 2 and 4 middle and lower panel). This result was confirmed by a quantitative analysis of HASPB-N18-GFP cell surface exposure in the various cell lines (Fig. 32, panel B). As expected, HASPB-N18-GFP export in CHO K3 cells was largely reduced to about 60% compared to CHO wild-type cells. However, the expression of the chemokine orphan receptor 1 did neither restore HASPB-N18-GFP export from CHO K3 nor block export of HASPB-N18-GFP from CHO wild-type cells. This observation is in line with previous findings described in sections 3.3.3, 3.3.5 and 3.3.6, and confirms that the defect in the mutant CHO K3 cell line regarding HASPB export does not result from cmkor 1 downregulation. The chemokine orphan receptor 1 seems not to be an essential component of the HASPB export pathway. Since only one integration site was found (section 3.3.1), this does not rule out the possibility of other integration sites of the retrovirus causing the perturbed HASPB membrane translocation in CHO K3 cells.

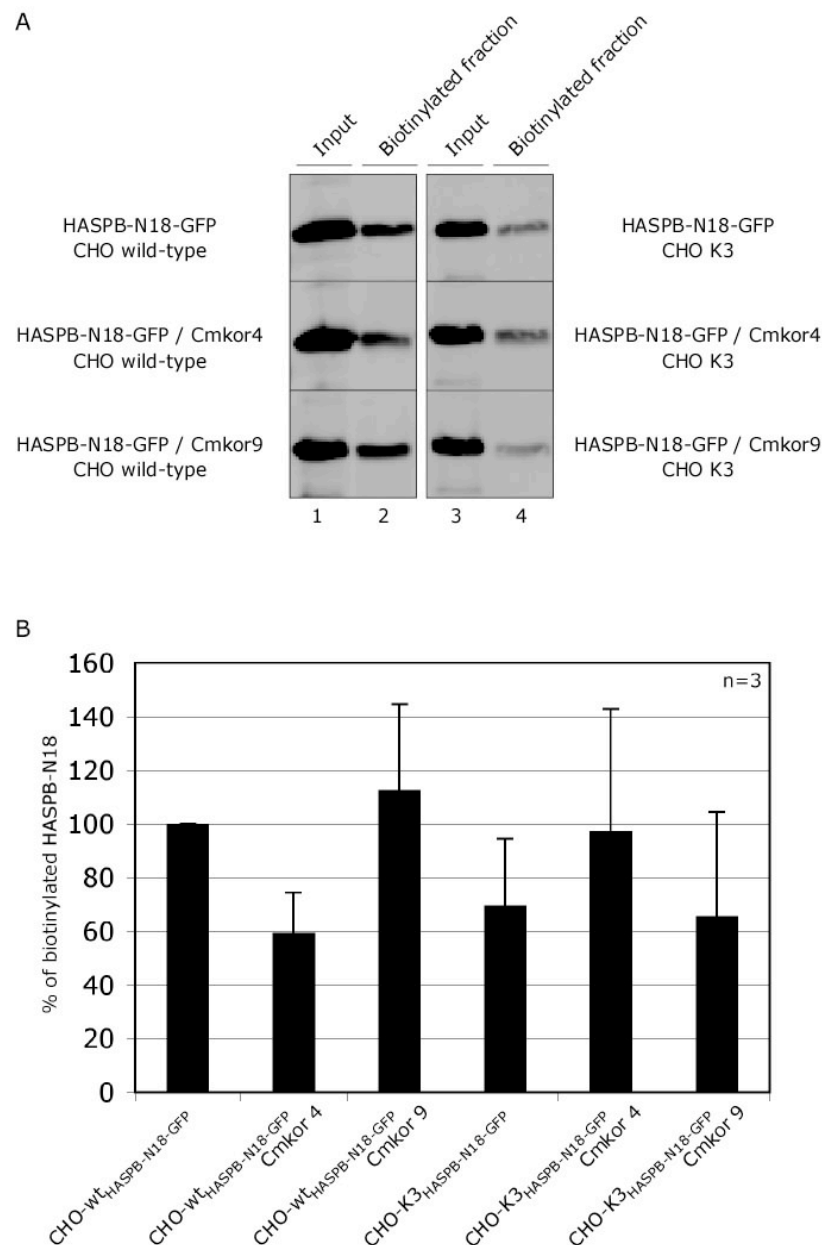


Fig. 32 Quantitative analysis of HASPB-N18-GFP export from cmkor 1 transduced CHO wild-type and K3 cells as well as from their parental CHO cell lines. (A) Cmkor 1 transduced CHO wild-type and K3 cells as well as their corresponding parental cell lines were treated with a membrane-impermeable biotinylation reagent. Cell lysates were generated and proteins were separated by streptavidin affinity chromatography. Input material (lanes 1 and 3; 3,8%) and streptavidin-bound proteins (biotinylated proteins, lanes 2 and 4; 50%) were separated by SDS-PAGE followed by western blotting using affinity-purified anti-GFP antibodies. (B) Quantitative analysis. For a statistical analysis of three independent experiments, HASPB-N18-GFP export from CHO wild-type cells was set to 100%, respectively.

B. The SH4 protein HASPB is released in extracellular vesicles in a palmitoylation-dependent manner

As described previously heterologous expression of an HASPB-N18-GFP fusion protein induces curvature of the plasma membrane resulting in the formation of highly dynamic, non-apoptotic tubules and plasma membrane blebs (Tournaviti et al., 2006 submitted). Plasma membrane blebs are cell protrusions generated by the osmotic pressure of the cell interior upon localized destabilization of the cortical actin meshwork at the plasma membrane (Charras et al., 2005; Cunningham, 1995; Sheetz et al., 2006). The Rho effector kinase Rock provides acto-myosin contractility required for the formation of most types of plasma membrane blebs (Leverrier and Ridley, 2001). Furthermore, diaphanous-related formins (DFRs) are actin nucleators and modulate actin dynamics governed by select small GTPases but also stabilize microtubules and coordinate F-actin and microtubule networks (Faix and Grosse, 2006). Moreover, the DFR FHOD1 functionally interacts with Rock to alter cellular F-actin and microtubule organization facilitating plasma membrane bleb formation (Gasteier et al., 2003; Gasteier et al., 2005). Together, based on these observations it is likely that the SH4 protein HASPB could be released from cells due to plasma membrane blebbing, a process promoting the shedding of plasma membrane-derived vesicles that are released into the extracellular space (Freyssinet, 2003; Hugel et al., 2005; Martinez et al., 2005). To gain insights into plasma membrane bleb formation, cell culture supernatants of various cell lines were analyzed for HASPB-containing vesicles employing Nycodenz flotation gradients.

3.4 Characterization of HASPB-mediated plasma membrane bleb formation

3.4.1 Heterologous expression of an HASPB-N18-GFP fusion protein induces curvature of the plasma membrane resulting in the formation of highly dynamic, non-apoptotic plasma membrane blebs

Employing confocal microscopy as described in section 3.1.4, HASPB-N18-GFP was mainly localized to the plasma membrane. Furthermore, HASPB was organized to droplet-like structures that were typically located in close proximity to the plasma membrane. By analyzing living cells using confocal microscopy, the formation of plasma membrane blebs (Tournaviti et al., 2006 submitted) was clearly visible indicating that the observed droplet-like structures were due to a fixation artefact. As illustrated in Fig. 33, panel A, formation of plasma membrane blebs was induced by heterologous expression of HASPB-N18-GFP. Furthermore, as revealed by confocal real time imaging analysis and annexin V staining experiments the plasma membrane blebs were shown to be highly dynamic as well as of non-apoptotic origin (Tournaviti et al., 2006 submitted). Importantly, the expression of the myristoylation mutant (Δ myr-HASPB-N18-GFP) as well as the palmitoylation mutant (Δ palm-HASPB-N18-GFP) did not induce curvature of the plasma membrane resulting in plasma membrane bleb formation (Fig. 33, panel B and C). In agreement with previous findings (section 3.1.4) Δ myr-HASPB-N18-GFP was found mainly in the cytosol and Δ palm-HASPB-N18-GFP was localized on intracellular membranes in a perinuclear position.

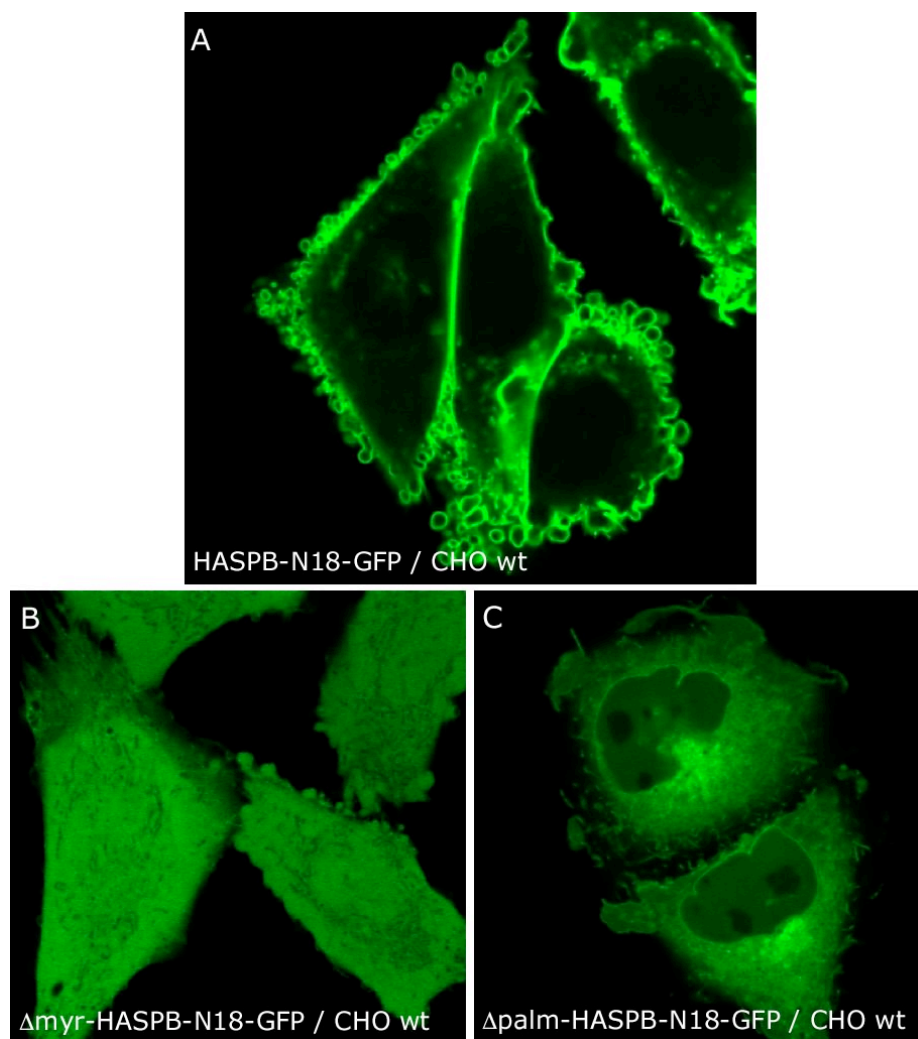


Fig. 33 Subcellular distribution of HASPB-GFP fusion proteins as determined by live confocal microscopy. Cells were grown in 8-chamber plates in the presence of 1 μ g/ml doxycycline for 48 hours at 37°C. GFP-derived fluorescence was viewed with a Zeiss LSM 510 confocal microscope. (A) HASPB-N18-GFP; (B) Δ myr-HASPB-N18-GFP; (C) Δ palm-HASPB-N18-GFP

3.4.2 *The Leishmania protein HASPB can be found in extracellular vesicles following ultracentrifugation of cell culture supernatants from growing HASPB-N18-GFP expressing cells*

To investigate whether plasma membrane blebbing might lead to the shedding of plasma membrane-derived HASPB-containing vesicles that are released into the extracellular space, cell culture supernatants of growing

CHO cells expressing HASPB-N18-GFP were ultracentrifuged in order to sediment their contents.

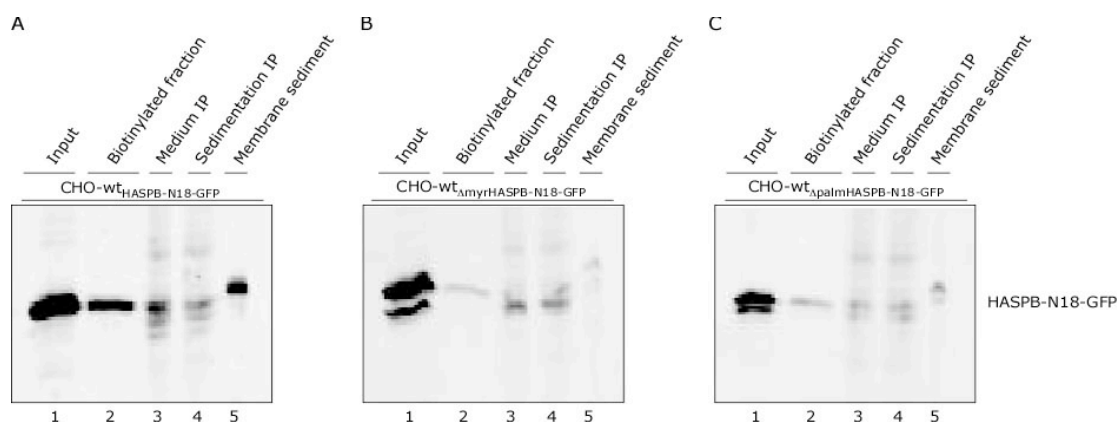


Fig. 34 Biochemical analysis of cell culture supernatants from growing CHO cells expressing HASPB-GFP fusion proteins. Cells were grown in six-well plates in the presence of 1 μ g/ml for 48 hours at 37°C. For the biochemical analysis of exported HASPB-GFP the cell surface biotinylation assay was used and the experiment was conducted exactly as described in the 'Material and Methods' section. Input material (lanes 1 of A, B and C; 3,8%) and streptavidin-bound proteins (biotinylated proteins, lanes 2 of A, B and C, 50%) are shown. Additionally, cell culture supernatants of HASPB-GFP expressing CHO cells were centrifuged (lanes 5 of A, B and C; 100%) at 100,000 g for 1 hour (membrane sediment). The resulting supernatants (lanes 4 of A, B and C, 50%) as well as cell culture supernatants from growing CHO cells (lanes 3 of A, B and C; 50%) were subjected to immunoprecipitation using affinity purified anti-GFP antibodies. All samples were separated by SDS-PAGE followed by western blotting using affinity-purified anti-GFP antibodies. (A) HASPB-N18-GFP; (B) Δ myr-HASPB-N18-GFP; (C) Δ palm-HASPB-N18-GFP

As shown in Fig. 34, panel A, most of the extracellular HASPB-N18-GFP population was found to be associated with the cell surface of CHO cells (lane 2) with only a minor portion being found in the cell culture supernatant (lane 3). However, extracellular material derived from HASPB-N18-GFP expressing cells was quantitatively found in the membrane sediment (lane 5). Only small amounts were detectable in the supernatants following ultracentrifugation of the medium (Fig. 34A, lane 4). The control proteins, both acylation mutants, Δ myr-HASPB-N18-GFP (Fig. 34B) and Δ palm-HASPB-N18-GFP (Fig. 34C), were compared with HASPB-N18-GFP. As expected,

both mutants could neither be detected on the cell surface (Fig. 34,B and C, lanes 2) nor in the cell culture supernatants (Fig. 34,B and C, lanes 3). Furthermore, no extracellular material was found in the membrane sediments of Δ myr-HASPB-N18-GFP (Fig. 34,panel B, lane 5) and Δ palm-HASPB-N18-GFP (Fig. 34, panel C, lane 5) expressing CHO cells and in the supernatants following ultracentrifugation of the medium (Fig. 34,B and C, lanes 4), respectively. Taken together, these results indicate that HASPB can be found in extracellular vesicles obtained following ultracentrifugation of cell culture supernatants.

3.4.3 Flotation of HASPB-containing vesicles in Nycodenz gradients

In order to discriminate aggregates from vesicles containing HASPB, the sedimentable material (section 3.4.2) was analyzed in Nycodenz flotation gradients. This membrane sediment was dissolved in Nycodenz to obtain a 40% Nycodenz solution as load in the bottom of the centrifuge tube (Fig. 35A, fraction (#) 3). A 30% and 0% Nycodenz solution (Fig. 35A, fraction (#) 2 and fraction (#) 1) were layered on top of the load fraction in order to achieve a 0%/30% interphase to recover and concentrate vesicles. As illustrated in Fig. 35B, lane 2, the majority of the HASPB-N18-GFP fusion protein was found in the 0%/30% interphase (fraction 1) containing a density of ~ 1.14 g/ml. Since aggregates have a higher density, HASPB seems to be associated with low-density vesicles. Together, these results strongly suggest that the sedimentable material (membrane sediment) contains HASPB-associated vesicles that are released to the extracellular space.

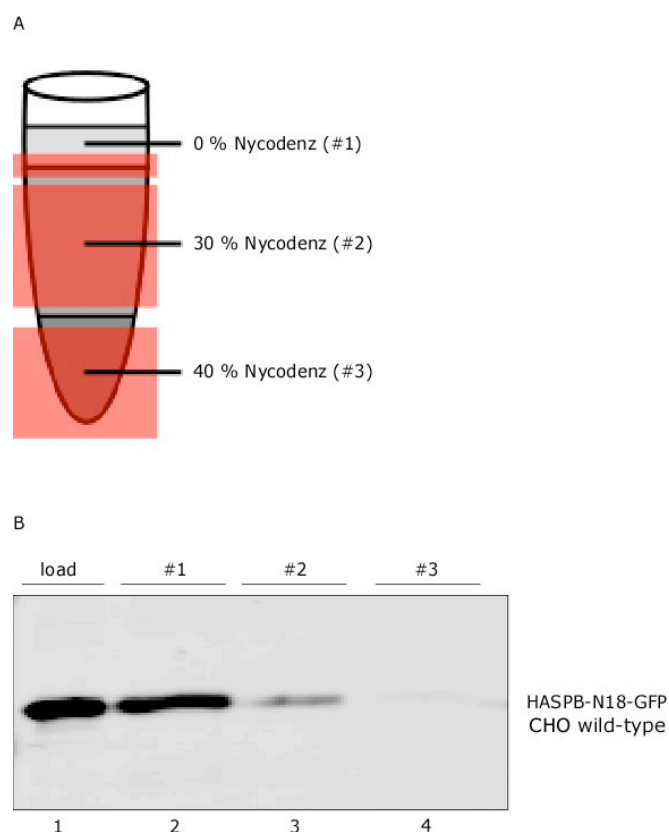


Fig. 35 Analysis of HASPB-N18-GFP-containing vesicles in Nycodenz gradients.

(A) Schematic description of Nycodenz gradients. CHO cells expressing HASPB-N18-GFP were grown in 10 cm plates in the presence of 1 $\mu\text{g/ml}$ doxycycline for 48 hours at 37°C. Cell culture supernatants were centrifuged at 100,000 g for 1 hour. The membrane sediments were mixed with 80% Nycodenz to give a 40% load sample (fraction (#) 3). This fraction was overlaid with 30% (fraction (#) 2) and 0% Nycodenz solutions (fraction (#) 1). The gradient was centrifuged at 48,000 rpm (218,438 g) for 4 hours followed by fractionation as indicated. (B) Analysis of cell culture supernatants from HASPB-N18-GFP-expressing CHO cells employing Nycodenz flotation gradients. Proteins in each fraction were precipitated using TCA. The samples (lanes 2-4; 100%, load, lane 1; 0,1%) were separated by SDS-PAGE followed by western blotting using affinity-purified anti-GFP antibodies.

3.4.4 Characterization of the floated material using different exosomes markers

Vesicles found in the extracellular space might be derived through the release of exosomes or by plasma membrane shedding/blebbing of microvesicles (section 1.3.5) (Freyssinet, 2003; Hugel et al., 2005; Martinez et al., 2005; Stoorvogel et al., 2002). In the latter case the plasma membrane forms evaginations resulting in vesicles pinching off the cell. By contrast, exosomes are derived from MVBs (**multi vesicular bodies**) that are formed through invaginations of endosomal membranes (Greco et al., 2001; Thery et al., 2002). MVBs consist of three **endosomal sorting complexes required for transport**, so called ESCRT I-III and represent endocytic intermediates (Greco et al., 2001; Thery et al., 2002). They release vesicles termed as exosomes into the extracellular space upon fusion with the plasma membrane. To monitor HASPB-containing vesicles regarding their origin, the HASPB-containing vesicle fraction was characterized with different exosomes markers (Stoorvogel et al., 2002). As expected, extracellular vesicles were found in fractions obtained from CHO wild-type (Fig. 36, lane 2, upper panel) and CHO K3 cells (Fig. 36, lane 6, upper panel), respectively. In agreement with previous findings (section 3.4.2) since Δ palm-HASPB-N18-GFP was absent from the membrane sediment, no extracellular vesicles were detectable (Fig. 36, lane 10, upper panel). As illustrated in Fig. 36 two MVB-pathway components were found in vesicle fractions derived from CHO wild-type, CHO K3 and CHO Δ palm-HASPB-N18-GFP. TSG101 (Babst et al., 2000; Garrus et al., 2001) (Fig. 36, lanes 2, 6 and 10, middle panel), the mammalian homolog to Vps23, one of the major components of the ESCRT-1 complex and Alix (Chatellard-Causse et al., 2002; Pisitkun et al., 2004) (Fig. 36, lanes 2, 6 and 10, lower panel), an ESCRT-III binding partner, were detectable.

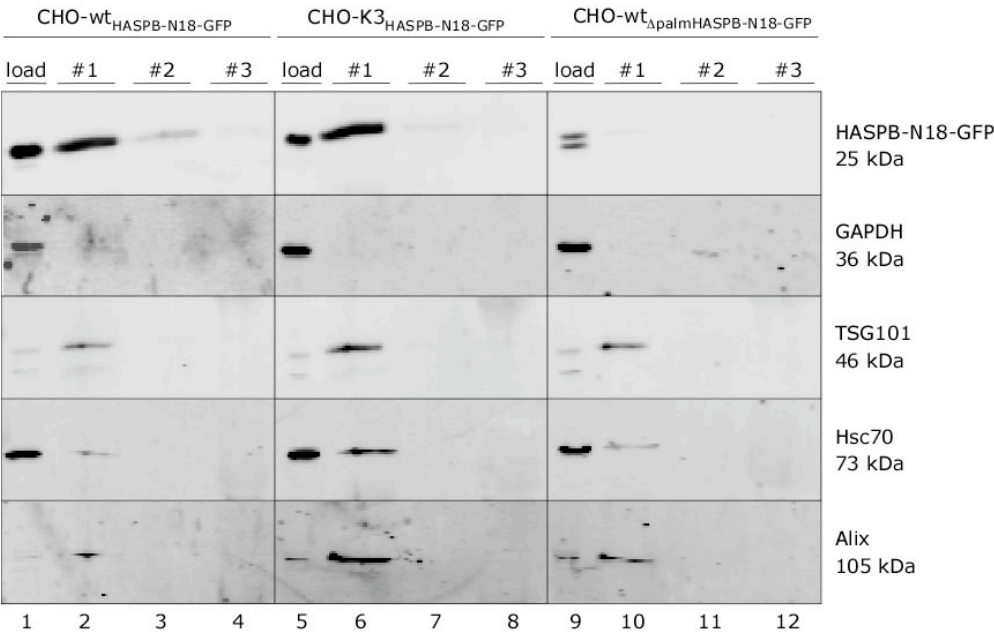


Fig. 36 Detection of various exosomes markers in HASPB-containing vesicle fractions.

CHO cells expressing HASPB-N18-GFP and Δ palm-HASPB-N18-GFP as well as CHO K3 mutant cells were grown in 10 cm plates in the presence of 1 μ g/ml doxycycline for 48 hours at 37°C. Cell culture supernatants were subjected to centrifugation at 100,000 g. Vesicles in the resulting membrane sediments were concentrated by flotation in a Nycodenz step gradient as described in the ‘Material and Methods’ section. To verify exosomes, antibodies against TSG101 (Garrus et al., 2001) and Alix (Chatellard-Causse et al., 2002) were used. To detect exosomes-released proteins and cytosolic proteins, antibodies directed against Hsc70 (Whetstone and Lingwood, 2003) and GAPDH (Elbashir et al., 2001) were used. Three fractions were generated and analyzed for each cell line: #1 (lanes 2, 6 and 10); #2 (lanes 3, 7 and 11); #3 (lanes 4, 8 and 12). The samples (fractions, 100%; load, lanes 1, 5 and 9, 0,1%) were separated by SDS-PAGE following western blotting using the antibodies indicated.

Importantly, these markers were enriched in the vesicle fractions. Furthermore, Hsc 70 (Whetstone and Lingwood, 2003) (Fig. 36, lanes 2, 6 and 10, fourth panel), a chaperone of the heat shock family and a typically exosomes-released protein was also, but to a much lower extent, present in these vesicle fractions. Quantitatively more amounts were found in the input fraction (lanes 1, 5 and 9, fourth panel). In contrast, a cytosolic housekeeping enzyme essential for glycolysis, GAPDH (Elbashir et al., 2001) (Fig. 36, lanes 1, 5 and 9, second panel) was only detectable in the input fraction. Interestingly,

TSG101, Hsc70 and Alix were enriched in the vesicle fraction obtained from CHO K3 cells compared to CHO wild-type cells and CHO cells expressing the palmitoylation mutant. This suggests that CHO K3 cells produce substantially more amounts of vesicles rather than vesicles containing quantitatively more HASPB. In summary, these results are consistent with HASPB-containing vesicles being released by the MVB machinery, i.e. HASPB-N18-GFP might be exported in exosomes.

3.4.5 HASPB-N18-GFP is localized in the lumen of extracellular vesicles as revealed by protease protection experiments

To this point the experiments suggest that HASPB is exported via vesicles being released by the MVB machinery. To verify the localization of HASPB-N18-GFP in these vesicles protease protection experiments were performed.

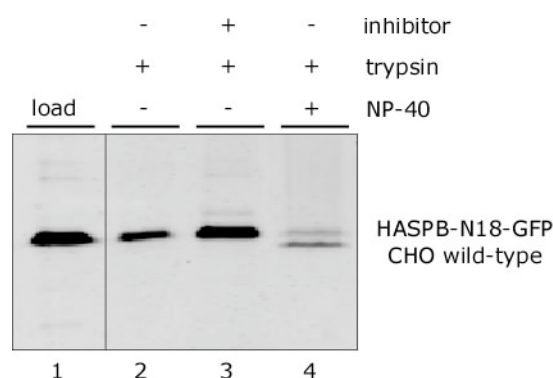


Fig. 37 Protease protection experiments of HASPB-containing vesicles. CHO cells expressing HASPB-N18-GFP were grown in 10 cm plates in the presence of 1 μ g/ml doxycycline for 48 hours at 37°C. Cell culture supernatants were centrifuged at 100,000 g for 1 hour and the resulting membrane sediments were subjected to protease treatment in absence (lanes 1-3) and presence of detergent (lane 4), respectively. Samples (lanes 1-4, 100%) were separated by SDS-PAGE followed by western blotting using affinity-purified anti-GFP antibodies.

Upon addition of the protease only small parts of the HASPB-N18-GFP fusion protein were digested (Fig. 37, compare lane 1, input material, with lane 2). As control, HASPB-N18-GFP remained protected when directly adding the

protease inhibitor together with the protease (Fig. 37, lane 3). Importantly, the protected protein was accessible by the protease only upon treatment of the vesicles with detergent (Fig. 37, lane 4). Together, this experiment demonstrates that HASPB-N18-GFP is associated with the inner leaflet of the vesicle membrane suggesting that HASPB-N18-GFP is initially located on the inner leaflet of the plasma membrane from where it is delivered into vesicles being released by the MVB sorting machinery into the extracellular space.

3.4.6 Quantitative analysis of extracellular vesicles containing various HASPB reporter molecules

In order to confirm the presence of other HASPB reporter molecules in extracellular vesicles, Nycodenz flotation gradients were performed. As shown in Fig. 38A, lane 2, besides HASPB-N18-GFP derived from CHO wild-type cells (upper panel), HASPB-N18-GFP derived from CHO K3 cells (second panel from top) and HASPB-GFP full length (lower panel) expressed from CHO wild-type cells were found in extracellular vesicles as well. Compared to the membrane sediments (Fig. 38A, lane 5), the enrichment of the various reporter molecules in the vesicle fractions was clearly visible. The controls, both acylation mutants (Δ palm-HASPB-N18-GFP and Δ myr-HASPB-N18-GFP) (Fig. 38A, lane 2, third and fourth panel from top) as well as GFP alone (Fig. 38A, lane 2, fifth panel from top) were absent from the vesicle fractions. Not surprisingly, no material was detectable in the membrane sediments (Fig. 38A, lane 5 in each panel). In agreement, the quantitative analysis of extracellular vesicles containing the various reporter molecules (Fig. 38, panel B) confirmed this result. Interestingly, a pronounced amount of extracellular HASPB-containing vesicles was observed for CHO K3 cells compared to CHO wild-type and CHO cells expressing HASPB-GFP full length, respectively. This observation is in line with the result obtained in section 3.4.4 indicating that CHO K3 cells produce quantitatively more amounts of vesicles that are released into the extracellular space.

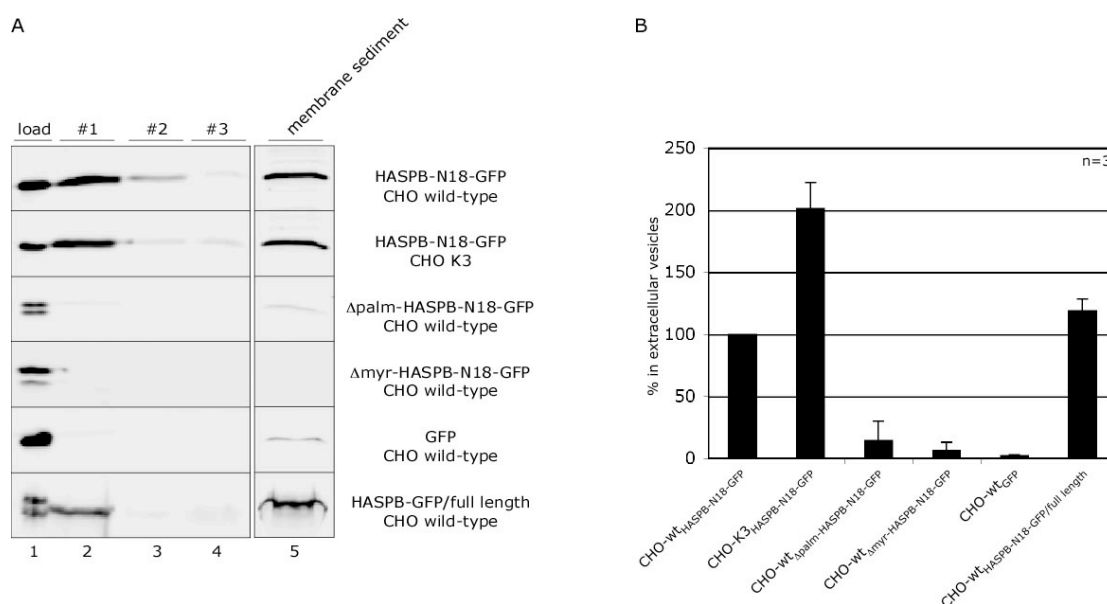


Fig. 38 Analysis of extracellular vesicles containing various HASPB reporter molecules employing Nycodenz flotation gradients. (A) CHO cells expressing various reporter molecules were grown in 10 cm plates in the presence of 1 μ g/ml doxycycline for 48 hours at 37°C. The corresponding cell culture supernatants were centrifuged at 100,000 g for 1 hour (membrane sediment, lanes 5). The resulting membrane sediments were subjected to Nycodenz flotation gradients as described in the 'Material and Methods' section and proteins in each fraction were precipitated using TCA. The samples (lanes 2-4, 100%; load, lane 1, 0,1%) were separated by SDS-PAGE followed by western blotting using affinity-purified anti-GFP antibodies. (B) Quantitative analysis of extracellular vesicles containing various HASPB reporter molecules. HASPB-N18-GFP-containing vesicles were set to 100%.

3.4.7 Quantitative analysis of extracellular vesicles containing FGF-2 and Galectin-1

As described previously galectin counter receptors promote the directional transport of Galectin-1 across the plasma membrane (Seelenmeyer et al., 2005). Furthermore, galectins have been shown to accumulate directly below the plasma membrane followed by an export mechanism that appears to involve the formation of membrane-bound vesicles that pinch off before being released into the extracellular space (Cooper and Barondes, 1990; Hughes, 1999; Mehul and Hughes, 1997; Sato et al., 1993). This mechanism distinguishes Galectin-1 export from FGF-2 export, as there is no evidence

that this protein is packaged into such vesicles (Cooper and Barondes, 1990; Hughes, 1999; Mehul and Hughes, 1997; Sato et al., 1993). In correspondence to Galectin-1, FGF-2 was shown to translocate to the outer surface of the plasma membrane by direct translocation across the plasma membrane (Schäfer et al., 2004; Zehe et al., 2006). The secreted FGF-2 population then accumulates in large HSPG-containing protein clusters on the extracellular surface of the plasma membrane (Engling et al., 2002; Zehe et al., 2006). As currently available, these large protein clusters were propagated to be exovesicles suggesting that vesicle shedding represent a mechanism for the release of biologically active FGF-2 from viable cells (Taverna et al., 2003). To assess the relevance of Galectin-1 and FGF-2 export in the context of the presence of extracellular vesicles in cell culture supernatants from CHO cells, cell lines expressing the corresponding proteins were analyzed regarding extracellular vesicles employing Nycodenz flotation gradients. As shown in Fig. 39A, lane 2, only HASPB-N18-GFP could be found in extracellular vesicles. Other unconventionally secreted proteins such as FGF-2 and Galectin-1 were absent from the vesicle fractions (Fig. 39A, lane 2, second and third panel). Not surprisingly, a similarly result was observed in the membrane sediments (Fig. 39A, lanes 5). In agreement, the control proteins (Δ palm-HASPB-N18-GFP and GFP alone) (Fig. 39A, lanes 2 and 5, fourth and fifth panel) were not detectable in these fractions. A quantitative analysis (Fig. 39, panel B) of extracellular vesicles containing FGF-2 and Galectin-1 provided additional indications that only HASPB-N18-GFP was found in extracellular vesicles. This observation confirms previous findings, indicating that only the SH4 protein HASPB is delivered into vesicles that are released into the extracellular space.

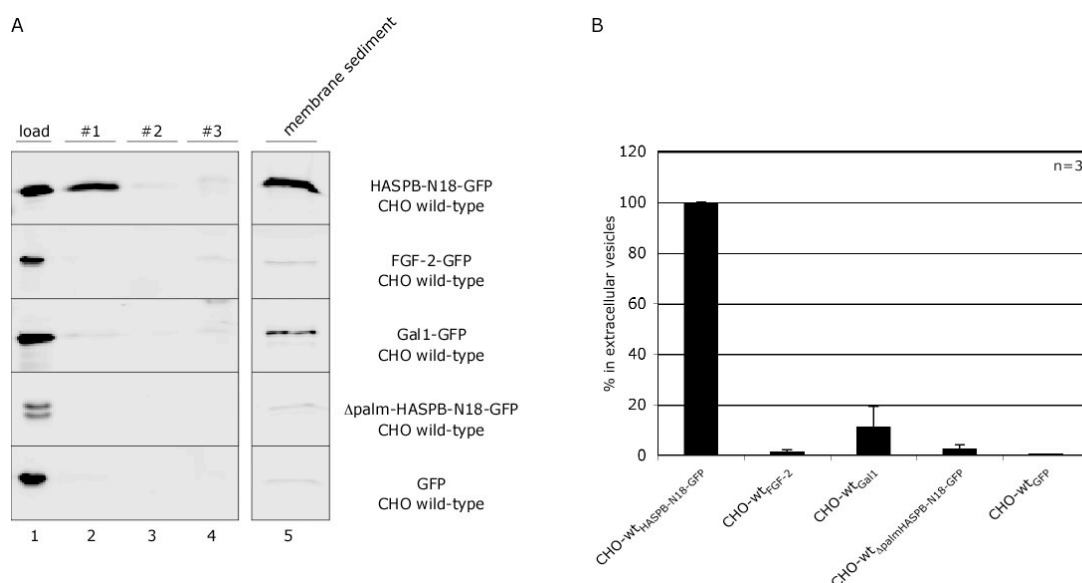


Fig. 39 Analysis of extracellular vesicles containing FGF-2 and Galectin-1 employing Nycodenz flotation gradients. (A) Cell culture supernatants from CHO cells expressing HASPB-N18-GFP, FGF-2-GFP, Galectin-1-GFP, Δ palm-HASPB-N18-GFP and GFP were subjected to Nycodenz flotation gradients as described in the 'Material and Methods' section. Proteins in each fraction were precipitated using TCA. The samples (lanes 2-4; 100%; load, lane 1; 0,1%) were separated by SDS-PAGE followed by western blotting using affinity-purified anti-GFP antibodies. (B) Quantitative analysis of extracellular vesicles containing FGF-2-GFP and Galectin-1-GFP. HASPB-N18-GFP-containing vesicles were set to 100%.

3.4.8 Extracellular HASPB-containing vesicles have an apparent density similar to that of exosomes

To validate the notion that HASPB might be exported via exosomes, the buoyant density was determined and compared with the reported density of exosomes ranging from 1.14 to 1.18 g/ml (Heijnen et al., 1999). In order to achieve a more precise separation of vesicles derived from different origins continuous sucrose gradients were performed (Fig. 40, panel B).

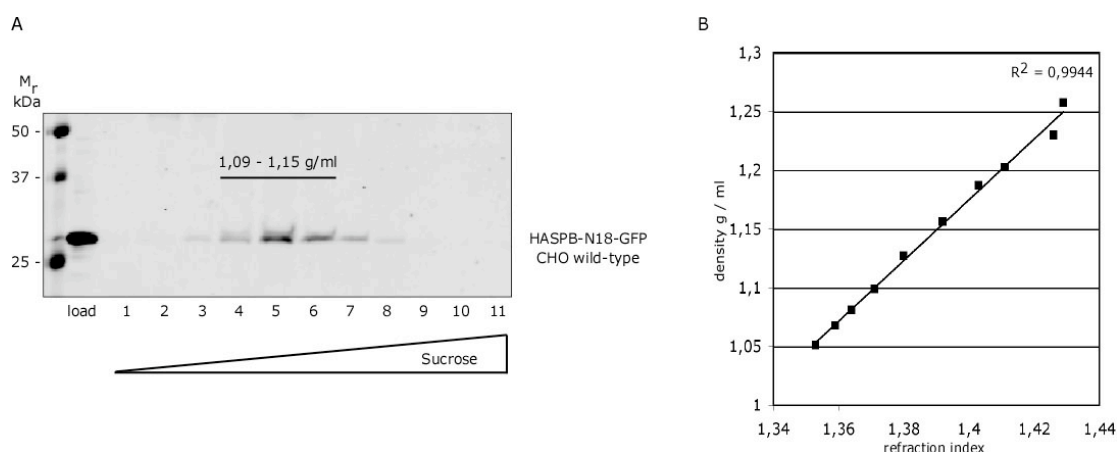


Fig. 40 Analysis of HASPB-containing vesicles in continuous sucrose gradients.

(A) CHO cells expressing HASPB-N18-GFP were grown in 10 cm plates in the presence of 1 μ g/ml doxycycline for 48 hours at 37°C. Cell culture supernatants were centrifuged at 100,000 g for 1 hour. The membrane sediments were dissolved and subjected to a continuous sucrose gradient at 26,000 rpm (65,000 g) for 16 hours. Proteins in each fraction (lanes 1-11) were precipitated using TCA, separated by SDS-PAGE and analyzed by western blotting for the presence of HASPB-N18-GFP using affinity-purified anti-GFP antibodies. (B) The linearity of the gradient was shown by the refractive index on the x-axis and the density on the y-axis.

As illustrated in Fig. 40, panel A, HASPB-containing vesicles were present in fractions equilibrating at densities of ~ 1.13 g/ml and ~ 1.15 g/ml (fraction 5 and 6) on the sucrose gradient. This observation is consistent with the exosomal density of ~ 1.15 g/ml (Heijnen et al., 1999). Taken together, the experiment indicates that HASPB-containing vesicles might represent exosomes that are released into the extracellular space upon fusion of MVBs with the plasma membrane.

3.5 The role of Rock kinase on HASPB-N18-GFP-induced plasma membrane blebbing and vesicle-associated HASPB-N18-GFP

3.5.1 HASPB-N18-GFP mediated plasma membrane blebbing is blocked in the presence of Rock inhibitor

Heterologous expression of HASPB-N18-GFP fusion protein induces curvature of the plasma membrane resulting in the formation of plasma membrane blebs (Fig. 33) (Tournaviti et al., 2006 submitted). Plasma membrane blebs are cell protrusions generated by the osmotic pressure of the cell interior upon localized destabilization of the cortical actin meshwork at the plasma membrane (Charras et al., 2005; Cunningham, 1995; Sheetz et al., 2006). These reorganizations of the plasma membrane require the membrane association of the SH4 domain in HASPB depend on the integrity of F-actin as well as microtubule architecture and are regulated by the activities of Rock kinase and Myosin-II ATPase (Tournaviti et al., 2006 submitted). Since HASPB-induced plasma membrane blebs are highly dynamic and display distinct kinetics during bleb formation and retraction (Tournaviti et al., 2006 submitted) it has to be clarified whether this process may promote the shedding of plasma membrane-derived HASPB-containing vesicles that are released into the extracellular space. To investigate whether extracellular vesicles were still detectable in the absence of plasma membrane blebbing, it was crucial to block plasma membrane bleb formation. In this regard, the cells were treated with Rock inhibitor (Coleman et al., 2001; Leverrier and Ridley, 2001) and analyzed employing confocal microscopy. As illustrated in Fig. 41, panel B, plasma membrane blebbing was completely blocked in presence of Rock inhibitor (Y-27632). In contrast, under control condition, the formation of plasma membrane blebs distributed over the whole plasma membrane was clearly visible (Fig. 41, panel A).

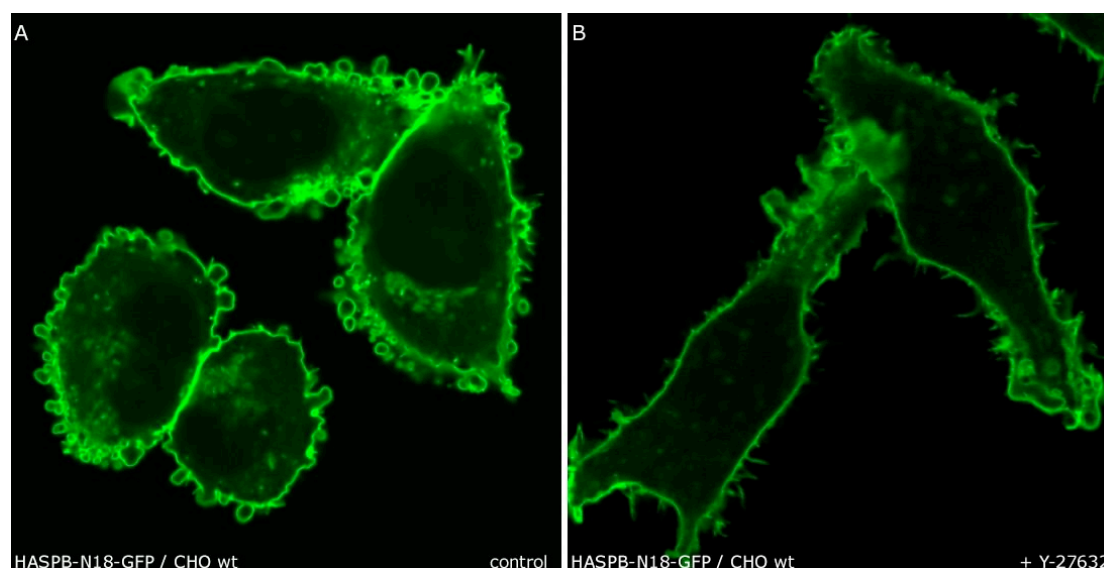


Fig. 41 HASPB-N18-GFP induced plasma membrane bleb formation is blocked in the presence of Rock inhibitor as determined by live confocal microscopy. CHO cells expressing HASPB-N18-GFP were grown in 8-chamber plates in the presence of 1 $\mu\text{g/ml}$ doxycycline for 48 hours at 37°C. GFP-derived fluorescence in presence and absence of 90 μM Rock inhibitor (Y27632) for 2 hours was viewed with a Zeiss 510 confocal microscope. (A) HASPB-N18-GFP without Y-27632 (control) (B) HASPB-N18-GFP with 90 μM Y-27632

3.5.2 Levels of HASPB-containing extracellular vesicles only partially decrease in the presence of Rock inhibitor

To further assess whether the prevention of plasma membrane blebbing by Rock inhibitor has an impact on the vesicle-associated HASPB population, HASPB-N18-GFP expressing CHO cells were analyzed in the presence and absence of Rock inhibitor employing Nycodenz flotation gradients. CHO cells expressing HASPB-N18-GFP were treated with Rock inhibitor for 30 minutes to block plasma membrane bleb formation. Subsequently the cells were incubated for two hours in the presence and absence of Rock inhibitor. As control, cells expressing HASPB-N18-GFP were not at all treated with Rock inhibitor. As shown in Fig. 42A, lane 2, upper panel, a reduction of HASPB-containing vesicles in the presence of Rock inhibitor could be observed (Fig. 42A, lane 2, middle panel). Similarly, extracellular material found in the

membrane sediments was notably reduced in the presence of Rock inhibitor (Fig. 42A, lanes 5).

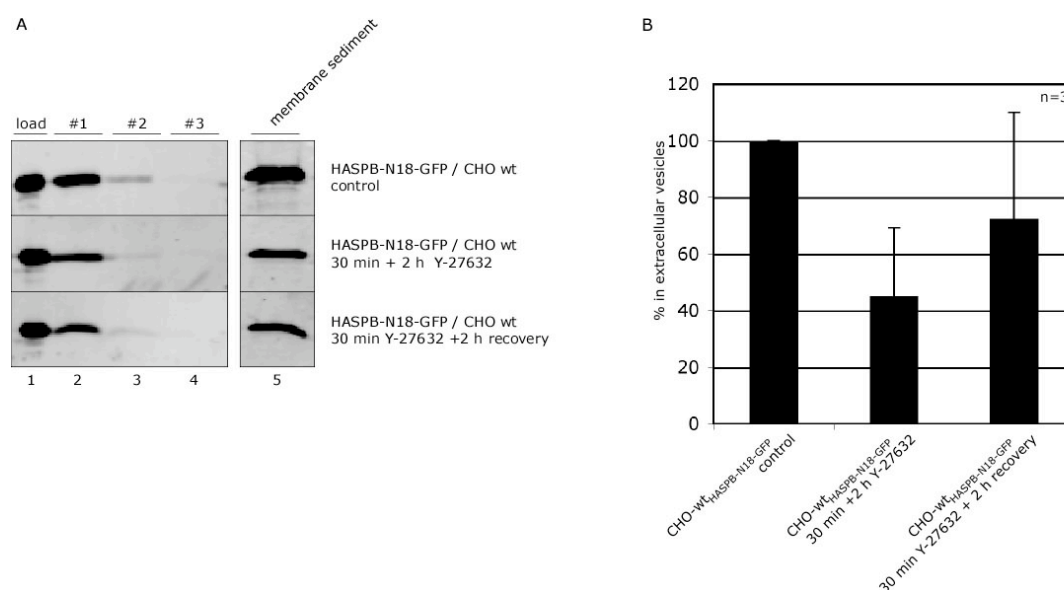


Fig. 42 Levels of HASPB-containing extracellular vesicles in the presence and absence of Rock inhibitor employing Nycodenz flotation gradients. (A) CHO cells expressing HASPB-N18-GFP were grown in 10 cm plates in the presence of 1 μ g/ml doxycycline for 48 hours at 37°C (control). In parallel, cells were treated for 30 min with 90 μ M Rock inhibitor (Y-27632) followed by a treatment of 2 hours in absence (recovery) and presence of Y-27632. Cell culture supernatants were then centrifuged at 100,000 g for 1 hour (lanes 5; 100%). The resulting membrane sediments were subjected to Nycodenz flotation gradients. Proteins in each fraction were precipitated using TCA and samples (lanes 2-4; 100%; load, lane 1; 0.1%) were separated by SDS-PAGE followed by western blotting using affinity-purified anti-GFP antibodies. (B) Quantitative analysis of HASPB-containing extracellular vesicles in absence and presence of Y-27632. HASPB-N18-GFP-containing vesicles in the absence of Rock inhibitor were set to 100% (control).

A quantitative analysis of HASPB-containing extracellular vesicles confirmed these data. Consistently, the presence of Rock inhibitor resulted in a decrease of HASPB-containing vesicles to about 50% (Fig. 42, panel B). Surprisingly, HASPB-containing vesicles were notably increased when the cells were treated only for 30 minutes with Rock inhibitor followed by incubation for two hours in absence of the inhibitor as recovery (Fig. 42, panel B). This suggests that plasma membrane blebbing, at least partially, leads to shedding of

plasma membrane-derived HASPB-containing vesicles into the cell culture supernatants of CHO cells. Hence, in contrast to the complete prevention of HASPB-mediated plasma membrane blebbing in presence of Rock inhibitor as observed by confocal microscopy, HASPB-containing vesicles were still detectable. Together, these findings confirm the presence of a HASPB-containing vesicle population that does not result from plasma membrane blebbing leading to the shedding of plasma membrane-derived vesicles into the extracellular space.

3.6 Characterization of Src, Fyn, Yes and Lck regarding plasma membrane blebbing and extracellular vesicles

3.6.1 Plasma membrane blebs are also induced by Src, Fyn, Yes and Lck

HASPB contains an N-terminal SH4 domain that becomes dually acylated by myristoylation of glycine 2 and palmitoylation of cysteine 5 (Denny et al., 2000). These posttranslational modifications are essential for HASPB targeting to the cell surface of *Leishmania* parasites (Denny et al., 2000; Pimenta et al., 1994) as well as of mammalian cells (Denny et al., 2000). Furthermore, the membrane association of the SH4 domain in HASPB induces curvature of the plasma membrane resulting in the formation of plasma membrane blebs (Tournaviti et al., 2006 submitted). Moreover, as demonstrated so far, it has been well documented that HASPB is detectable in extracellular vesicles being released by the MVB sorting machinery. Based on these observations, it was crucial to investigate whether the SH4 domains of plasma membrane-targeted protooncogenes of the Src kinase family (Bijlmakers and Marsh, 2003) induce plasma membrane blebbing in a fashion similar to HASPB. These proteins become myristoylated at glycine 2 and, with Src at exception, palmitoylated at cysteine 3 (Fig. 43).

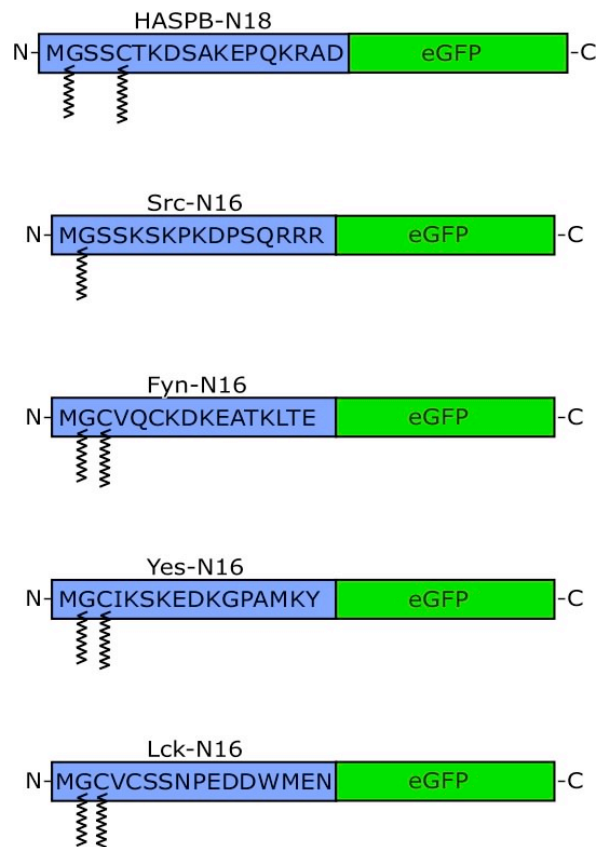


Fig. 43 Schematic description of SH4 proteins. Overview about various SH4-containing reporter constructs.

Similar to HASPB-expressing CHO cells analogous stable CHO cell lines expressing the SH4 domains of Src, Fyn, Yes and Lck were analyzed employing live imaging (performed by Stella Tournaviti) (Fig. 44). Interestingly, coincident with HASPB (Fig. 44, panel A), Yes, a typical representative of the Src kinase family, induced curvature of the plasma membrane of CHO cells resulting in the formation of plasma membrane blebs (Fig. 44, panel B).

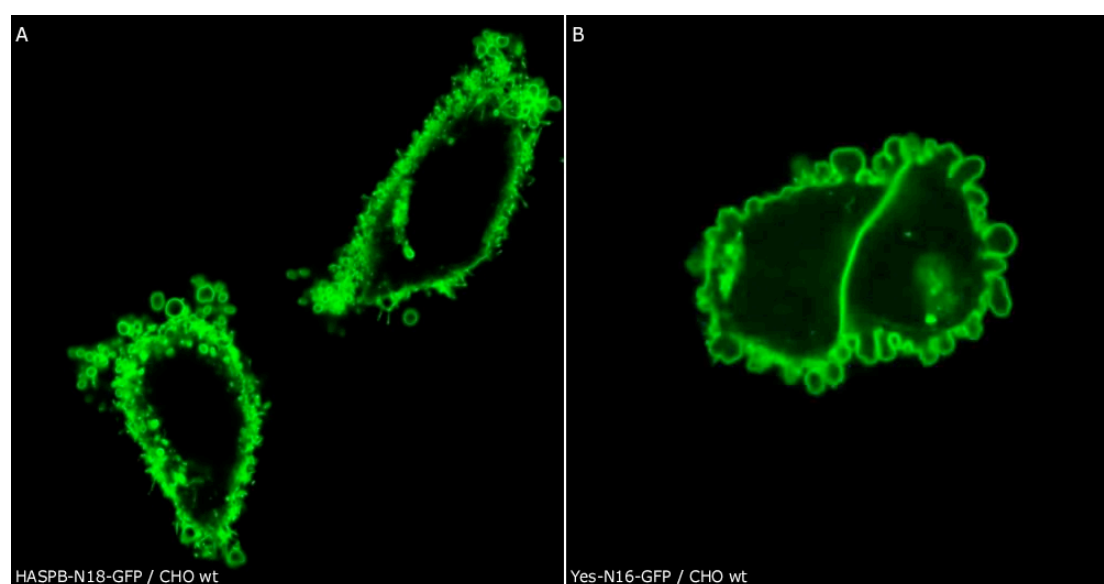


Fig. 44 Analysis of plasma membrane blebs induced by HASPB-N18-GFP and Yes-N16-GFP employing live confocal microscopy. CHO cells expressing HASPB-N18-GFP and Yes-N16-GFP, respectively, were grown in 8-chamber plates in the presence of 1 $\mu\text{g/ml}$ doxycycline for 48 hours at 37°C. GFP-derived fluorescence was viewed with a Zeiss LSM 510 confocal microscope. (A) HASPB-N18-GFP; (B) Yes-N16-GFP

3.6.2 Quantitative analysis of extracellular vesicles containing Src, Fyn, Yes and Lck

To evaluate the notion that the SH4 proteins of the Src-family might be present in extracellular vesicles since they are able to induce plasma membrane blebbing, membrane sediments obtained from cell culture supernatants of CHO cells expressing Src, Fyn, Yes and Lck were analyzed employing Nycodenz flotation gradients. In agreement with previous findings, HASPB-N18-GFP was found in extracellular vesicles as shown in Fig. 45, panel A, lanes 2 and 5. By contrast, the amount of Src-, Fyn-, Yes- and Lck-containing extracellular vesicles was notably reduced compared to the amount of HASPB-containing extracellular vesicles (Fig. 45, panel A, lanes 2). Similarly, less Src-, Fyn-, Yes- and Lck-containing extracellular material was detectable in the membrane sediments (Fig. 45, panel A, lanes 5). As

expected, Δ palm-HASPB-N18-GFP was absent from these fractions (Fig. 45, panel A, lanes 2 and 5, lower panel).

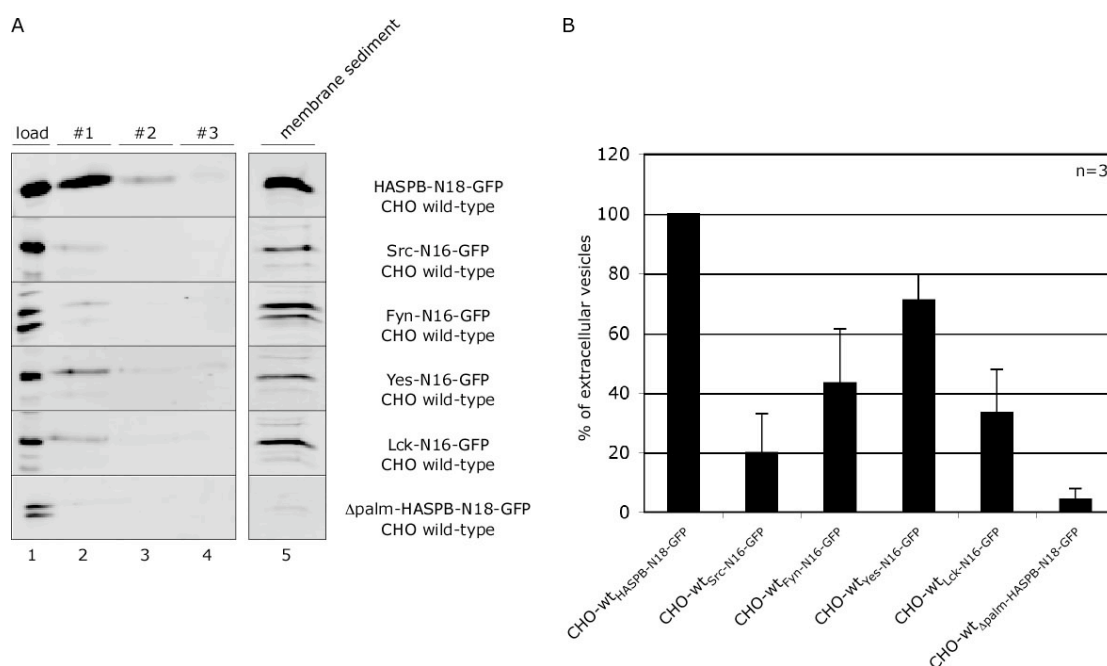


Fig. 45 Levels of extracellular vesicles containing Src, Fyn, Yes and Lck employing Nycodenz flotation gradients. (A) CHO cells expressing HASPB-, Src-, Fyn-, Yes-, Lck- and Δ palm-GFP fusion proteins were grown in 10 cm plates in the presence of 1 μ g/ml doxycycline for 48 hours at 37°C. The corresponding cell culture supernatants were centrifuged at 100,000 g for 1 hour and the resulting membrane sediments (lanes 5, 100%) were subjected to Nycodenz flotation gradients at 48,000 rpm for 4 hours. Proteins in each fraction were precipitated using TCA and samples (lanes 2-4, 100%; load, lane 1, 0.1%) were separated by SDS-PAGE followed by western blotting using affinity-purified anti-GFP antibodies. (B) Quantitative analysis of extracellular vesicles containing Src, Fyn, Yes and Lck. HASPB-N18-GFP containing vesicles were set to 100%.

In agreement, a quantitative analysis of extracellular vesicles containing Src, Fyn, Yes and Lck confirmed this result (Fig. 45, panel B). Compared to HASPB-containing vesicles normalized to the corresponding load and set to 100%, Src-, Fyn-, Yes- and Lck-containing extracellular vesicles were largely reduced to about ~20-70% as compared to wild-type levels. These data provide evidence for the presence of HASPB in extracellular vesicles suggesting that extracellular vesicles containing Src, Fyn, Yes and Lck might

be due to plasma membrane blebbing, a process promoting the shedding of plasma membrane-derived vesicles that are released into the extracellular space.

3.6.3 The extracellular vesicle populations containing Src, Fyn, Yes and Lck are notably reduced in presence of Rock inhibitor compared to the HASPB-containing vesicle population

To assess whether extracellular vesicles containing Src, Fyn, Yes and Lck are reflecting membrane-bound vesicles pinching off the cell due to plasma membrane blebbing, CHO cells expressing these proteins were treated with Rock inhibitor. Using this approach the Src-, Fyn-, Yes- and Lck-containing vesicle populations were expected to be absent from vesicle fractions employing Nycodenz flotation gradients since plasma membrane bleb formation was completely blocked in the presence of Rock inhibitor as revealed by confocal microscopy. Consistent with previous findings the HASPB-N18-GFP fusion protein was the most prominent protein found in extracellular vesicles (Fig. 46A, lane 2, first panel from top). As expected, the amount of extracellular HASPB-containing vesicles was reduced in the presence of Rock inhibitor (Fig. 46B, lane 2, first panel from top, compare Fig. 42). This observation was in line with the result obtained from Src, Fyn, Yes and Lck. Similarly, the amount of extracellular vesicles containing Src, Fyn, Yes and Lck was reduced in the presence of Rock inhibitor (compare Fig. 46, panel A and B).

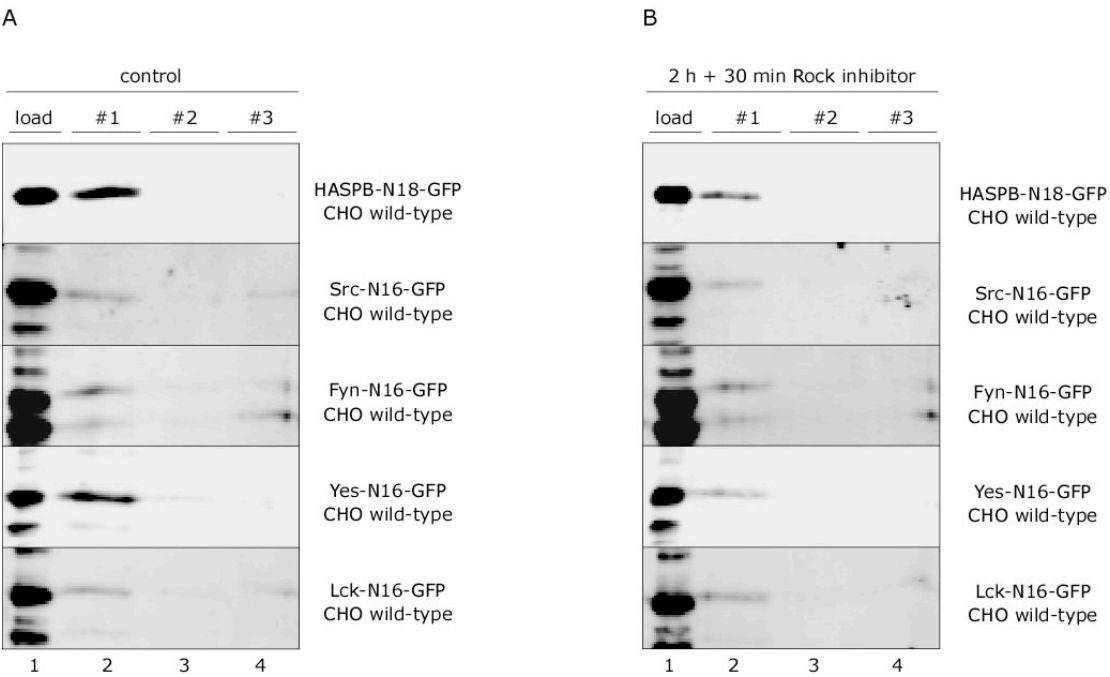


Fig. 46 Biochemical analysis of extracellular vesicles containing Src, Fyn, Yes and Lck in the absence and presence of Rock inhibitor. CHO cells expressing HASPB-, Src-, Fyn-, Yes- and Lck-GFP fusion proteins were grown in the presence of 1 µg/ml doxycycline for 48 hours at 37°C. In parallel, cells were cultured in the presence of Rock inhibitor. Membrane sediments obtained following ultracentrifugation of the cell culture supernatants were analyzed employing Nycodenz flotation gradients. The experiment was conducted exactly as described in the ‘Material and Methods’ section. Proteins in each fraction were precipitated using TCA and samples (lanes 2-4, 100%; load, lanes 1, 0.1%) were separated by SDS-PAGE following western blotting using affinity-purified anti-GFP antibodies.

Importantly, a quantitative analysis of extracellular vesicles containing the various SH4 proteins revealed that the extracellular vesicle populations containing Src, Fyn, Yes and Lck were notably reduced compared to the HASPB-containing vesicle population in the presence of Rock inhibitor (Fig. 47, compare blue bars with red bars). Indeed, HASPB-containing vesicles were only reduced to about 90% as compared to Src-, Fyn-, Yes- and Lck-containing vesicles with to about 0-40% in the presence of Rock inhibitor. Overall, in correspondence with the observation obtained in section 3.5.2 and 3.6.2, plasma membrane blebbing leads to shedding of plasma membrane-derived vesicles containing the various SH4 proteins that are released into the extracellular space. Importantly, only in case of Src, Fyn, Yes and Lck these

vesicle populations were notably reduced by prevention of plasma membrane blebbing in presence of Rock inhibitor. Together, these findings confirm that only the SH4 protein HASPB is delivered into vesicles being released by the MVB sorting machinery and that these vesicles are not derived from plasma membrane blebbing leading to the shedding of plasma membrane-derived vesicles into the extracellular space.

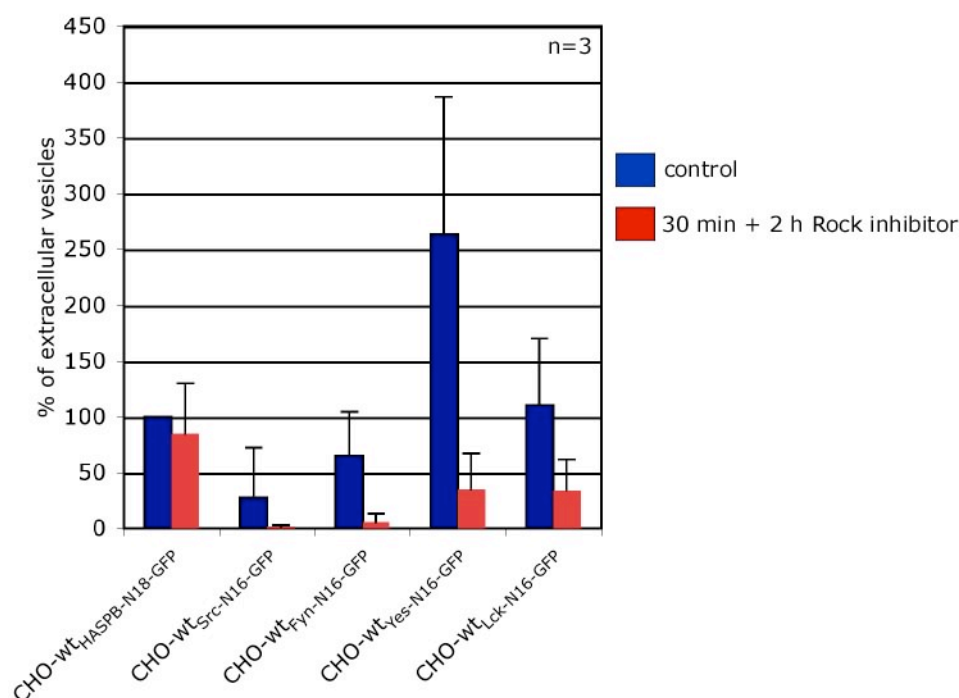


Fig. 47 Quantitative analysis of extracellular vesicles containing Src, Fyn, Yes and Lck in the absence and presence of Rock inhibitor. The experiments were exactly conducted as described in the legend of Fig. 46. HASPB-N18-GFP containing vesicles were set to 100%.

3.7 Characterization of HASPB-containing vesicles derived from HeLa cell lines

3.7.1 HASPB-N18-GFP mediated plasma membrane blebbing is notably reduced in HeLa cells compared to CHO cells

To test the functional requirement of proteins involved in the MVB machinery regarding HASPB-containing extracellular vesicles, an antisense RNA approach was planned. Since the CHO genome is not fully sequenced the human HeLa cell line was used. To investigate whether HeLa cells were able to induce plasma membrane curvature resulting in the formation of plasma membrane blebs, confocal microscopy was performed. Consistent with the phenotype observed in sections 3.4.1 and 3.6.1 heterologous expression of HASPB-N18-GFP in CHO cells resulted in the formation of highly dynamic plasma membrane blebs (Fig. 48, panel B). By contrast, plasma membrane blebbing in HeLa cells expressing HASPB-N18-GFP was notably reduced (Fig. 48, panel A).

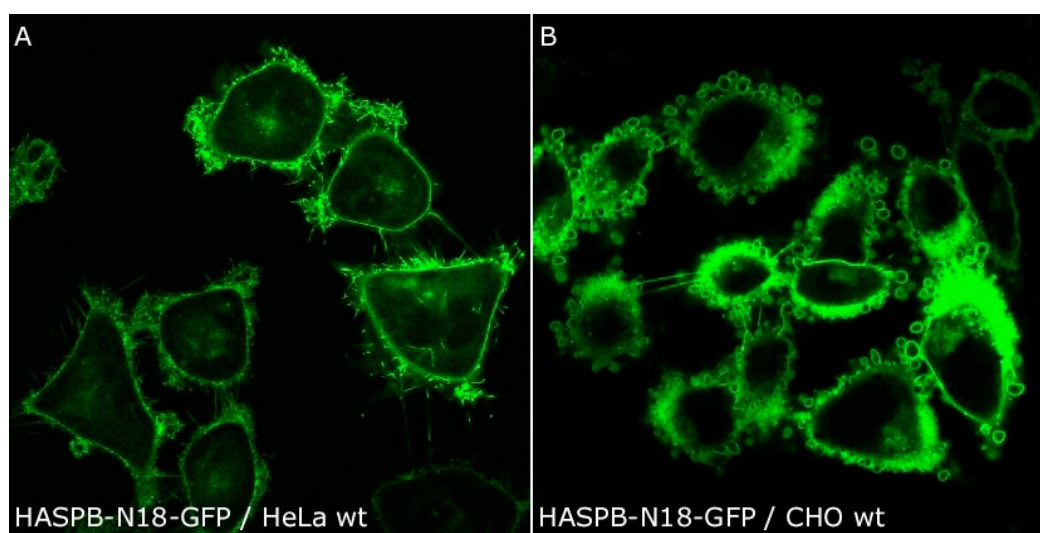


Fig. 48 Analysis of HASPB-mediated plasma membrane blebbing in HeLa and CHO cells as analyzed by live confocal microscopy. HeLa cells and CHO cells both expressing HASPB-N18-GFP were grown in 8-chamber plates in the presence of 1 μ g/ml doxycycline for 48 hours at 37°C. GFP-derived fluorescence was viewed with a Zeiss 510 confocal microscope. (A) HeLa cells expressing HASPB-N18-GFP; (B) CHO cells expressing HASPB-N18-GFP

3.7.2 Flotation of HASPB-containing extracellular vesicles derived from HeLa cells in Nycodenz gradients

To validate the notion that HASPB being expressed in HeLa cells is exported via vesicles, Nycodenz flotation gradients were performed. In correspondence with the observation obtained from CHO cells regarding HASPB-containing extracellular vesicles a similarly pronounced effect was observed for HeLa cells (Fig. 49A, lanes 2, compare upper and lower panel). Interestingly, a quantitative analysis of extracellular vesicles containing HASPB, which has been expressed in both cell lines, revealed that the amount of HASPB-containing extracellular vesicles derived from HeLa cells was reduced to about 40% as compared to the amount derived from CHO cells (Fig. 49, panel B). This result was expected since HASPB-mediated plasma membrane blebbing was largely reduced in HeLa cells. Consequently, less amounts of HASPB-containing extracellular vesicles were detectable. This observation confirms previous findings indicating that a substantial amount of HASPB-containing extracellular vesicles are a consequence of plasma membrane blebbing, a process promoting the shedding of plasma membrane-derived HASPB-containing vesicles being released into the extracellular space.

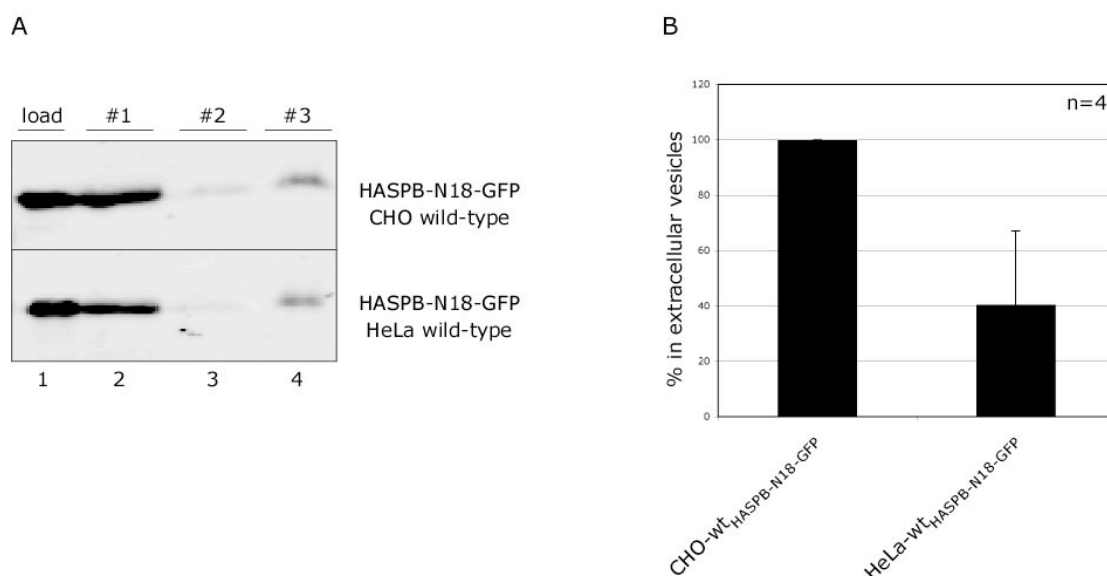


Fig. 49 Levels of HASPB-N18-GFP-containing extracellular vesicles derived from CHO and HeLa cells employing Nycodenz flotation gradients. (A) CHO and HeLa cells expressing HASPB-N18-GFP were grown in 10 cm plates in the presence of 1 μ g/ml doxycycline for 48 hours at 37°C. Cell culture supernatants were centrifuged at 100,000 g for 1 hour. The resulting membrane sediments were subjected to Nycodenz flotation gradients as described in the 'Material and Methods' section. Following precipitation of the proteins, the samples (lanes 2-4, 100%; load, lanes 1, 0.1%) were separated by SDS-PAGE followed by western blotting using affinity-purified anti-GFP antibodies. (B) Quantitative analysis of extracellular vesicles from CHO and HeLa cells expressing HASPB-N18-GFP. HASPB-containing vesicles derived from CHO cells were set to 100%.

3.7.3 *HASPB-containing extracellular vesicles derived from HeLa cells have an apparent density similar to that of exosomes*

To confirm the concept that HASPB-containing extracellular vesicles derived from CHO and HeLa cells, respectively, are of the same origin the buoyant density was analyzed employing continuous sucrose gradients (Fig. 50, panel B).

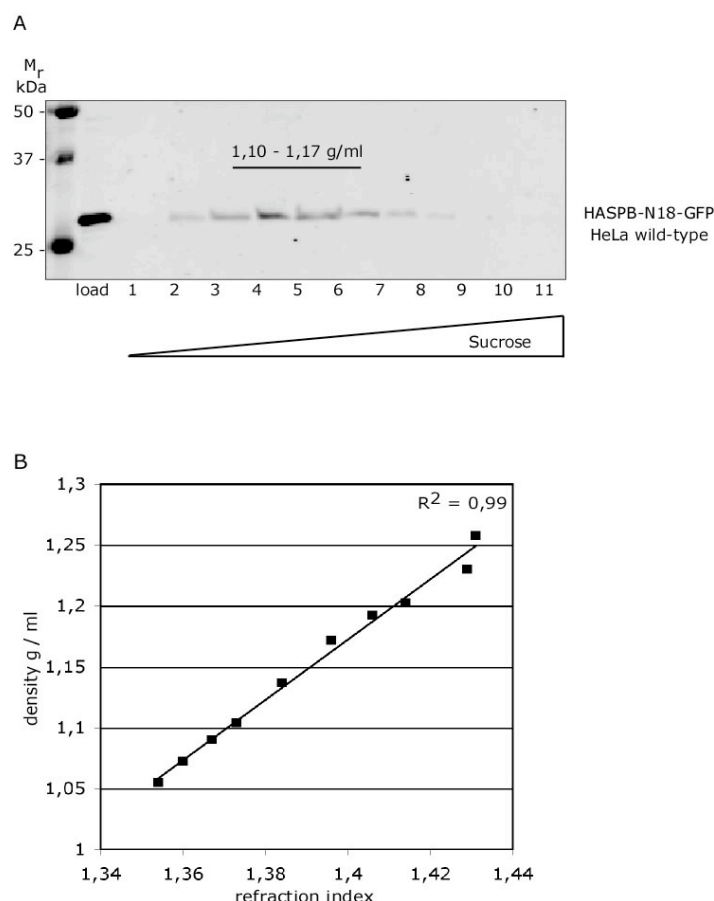


Fig. 50 Analysis of HASPB-containing extracellular vesicles derived from HeLa cells employing continuous sucrose gradients. (A) HeLa cells expressing HASPB-N18-GFP were grown in 10 cm plates in the presence of 1 μ g/ml doxycycline for 48 hours at 37°C. Cell culture supernatants were centrifuged at 100,000 g for 1 hour. The Membrane sediments were dissolved and subjected to a continuous sucrose gradient at 26,000 rpm (65,000 g) for 16 hours. Proteins in each fraction were precipitated using TCA and samples (lanes 1-11, 100%; load, lane 1, 0.1%) were separated by SDS-PAGE and analyzed by western blotting for the presence of HASPB-N18-GFP using affinity-purified anti-GFP antibodies. (B) The linearity of the gradient was shown by the refractive index on the x-axis and the density on the y-axis.

As expected, the density of HASPB-containing extracellular vesicles derived from HeLa cells was consistent with the density revealed for HASPB-containing extracellular vesicles derived from CHO cells (Fig. 40, panel A). Indeed, the density of 1.13 g/ml of extracellular vesicles containing HASPB, which has been expressed in HeLa cells (Fig. 50, panel A) is similar to the exosomal density range of ~1.14 g/ml to ~1.18 g/ml (Heijnen et al., 1999). Together, HASPB-N18-GFP fusion proteins are exported from HASPB

expressing HeLa cells as well as from CHO cells via vesicles of similar origin. Moreover, it is likely that these vesicles might represent exosomes that are released by the MVB sorting machinery into the extracellular space.

3.7.4 Confocal images of extracellular vesicles containing various reporter molecules

To investigate whether HASPB-containing extracellular vesicles could be visualized based on the GFP-derived fluorescence of the fusion proteins, membrane sediments obtained following ultracentrifugation of cell culture supernatants from various cell lines were analyzed employing confocal microscopy. As expected, HASPB-containing extracellular vesicles derived from CHO cells were found as shown by the green dots in Fig. 51, panel B. Not surprisingly, extracellular vesicles were observed from HeLa cells expressing HASPB-N18-GFP (Fig. 51, panel A) and from CHO K3 cells (Fig. 51, panel C) as well. The six-fold magnification revealed clearly the presence of these HASPB-containing vesicles (Fig. 51, panel K, L and M) derived from the corresponding cell lines. Consistent with previous findings, quite less amounts of extracellular vesicles containing Src, Fyn, Yes and Lck were detectable (Fig. 51, panel G-J). Furthermore, no extracellular vesicles containing the control proteins, the acylation mutants (Δ palm-HASPB-N18-GFP and Δ myr-HASPB-N18-GFP) (Fig. 51, panel D and E) and GFP alone (Fig. 51, panel F), respectively, were visible. These observations are in line with the biochemical data indicating that only the SH4 protein HASPB is delivered into vesicles being released by the MVB sorting machinery into the extracellular space.

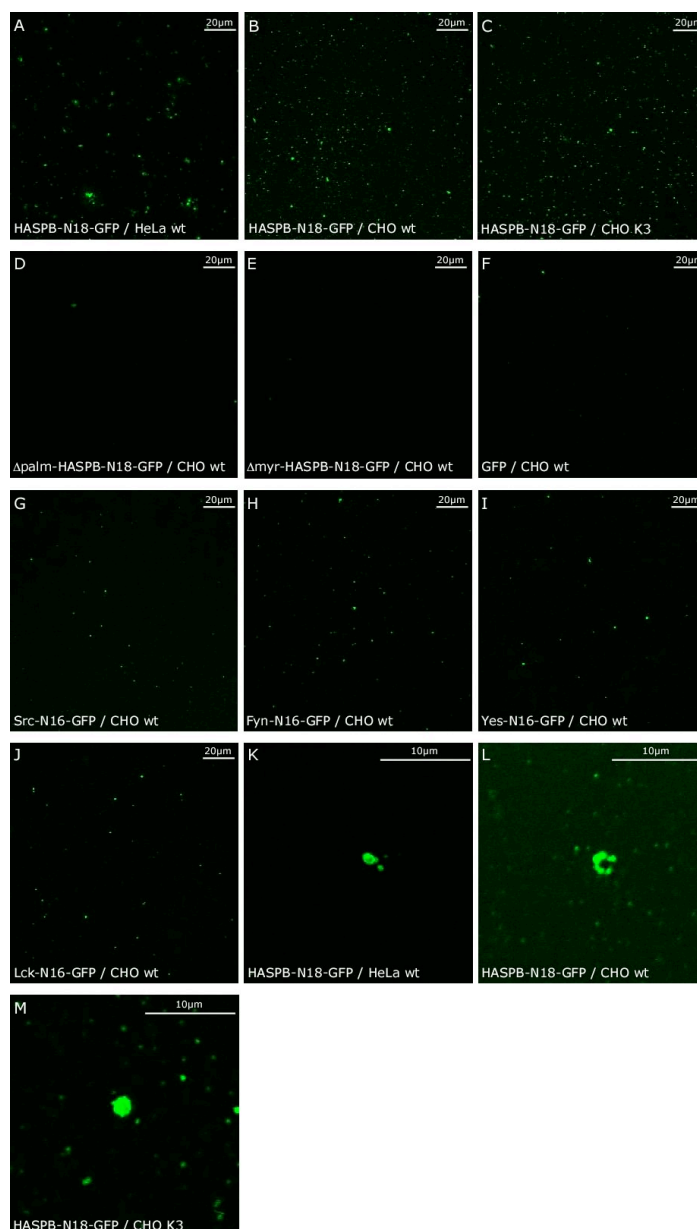


Fig. 51 Visualization of extracellular vesicles containing various reporter molecules employing confocal microscopy. Membrane sediments from various cell lines were diluted in PBS and subjected to poly-lysine coated coverslips. GFP-derived fluorescence was viewed with a Zeiss LSM 510 confocal microscope. (A) HeLa cells expressing HASPB-N18-GFP; (B) CHO cells expressing HASPB-N18-GFP; (C) CHO K3 cells expressing HASPB-N18-GFP; (D) CHO cells expressing Δ palm-HASPB-N18-GFP; (E) CHO cells expressing Δ myr-HASPB-N18-GFP; (F) CHO cells expressing GFP; (G) CHO cells expressing Src-N16-GFP; (H) CHO cells expressing Fyn-N16-GFP; (I) CHO cells expressing Yes-N16-GFP; (J) CHO cells expressing Lck-N16-GFP; (K) HeLa cells expressing HASPB-N18-GFP, six-fold magnification; (L) CHO cells expressing HASPB-N18-GFP, six-fold magnification; (M) CHO K3 cells expressing HASPB-N18-GFP, six-fold magnification.

3.7.5 Ultrastructural analysis of extracellular vesicles employing electron microscopy

To further confirm the presence of extracellular vesicles, an ultrastructural analysis was performed in collaboration with Prof. Zentgraf (DKFZ). Microsections of membrane sediments obtained following ultracentrifugation of cell culture supernatants from CHO wild-type and CHO K3 cells, respectively, were analyzed by electron microscopy.

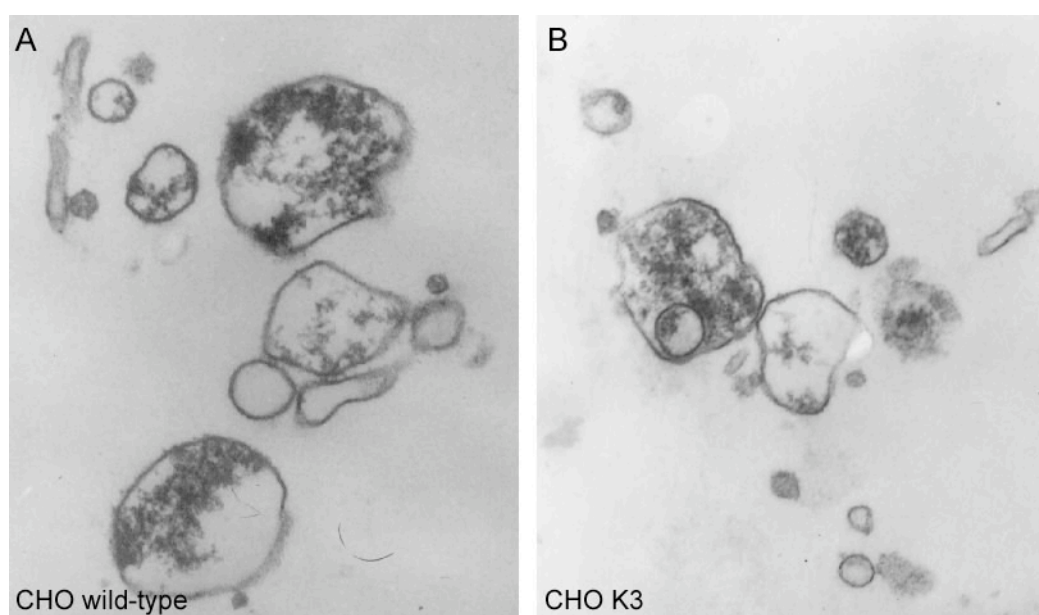


Fig. 52 Ultrastructural analysis of extracellular vesicles employing electron microscopy. CHO wild-type and CHO K3 cells were grown in 10 cm plates in presence of 1 µg/ml doxycycline for 48 hours at 37 °C. Cell culture supernatants were centrifuged at 100.000 g for 1 hour. The resulting membrane sediments were fixed in 2% glutar aldehyde and sodium cacodylate buffer for 30 min at 4°C. Following repeating washing steps for 30 min using ethanol, samples were embedded in Epon 812 (Ciba). After generating microsections, the staining was performed using uranyl acetate and lead citrate. (A) CHO wild-type; (B) CHO K3.

As illustrated in Fig. 52, extracellular vesicles derived from CHO wild-type (Fig. 52, panel A) and CHO K3 cells (Fig. 52, panel B) were characterized by a diameter between 80 and 300 nm. This range in size indicates that there exist two populations of extracellular vesicles. One subpopulation, consisting

of vesicles with a diameter of up to 100 nm might represent exosomes. Interestingly, this observation corresponds to the reported size for exosomes containing diameters between 40 and 100 nm (Stoorvogel et al., 2002). The subpopulation of vesicles with a diameter larger than 100 nm might be a consequence of plasma membrane blebbing, a process promoting the shedding of plasma membrane-derived vesicles that are released into the extracellular space.

3.8 Supplementary Figures

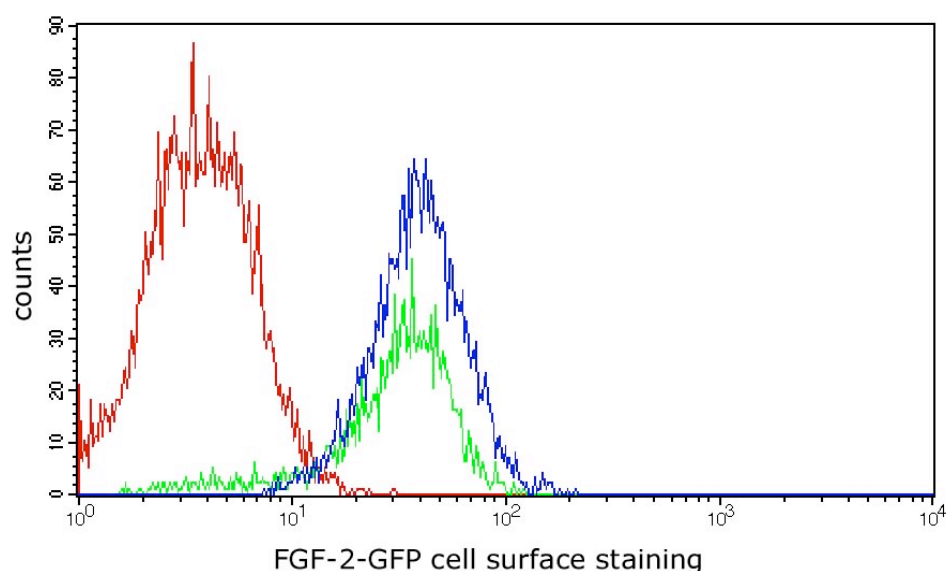
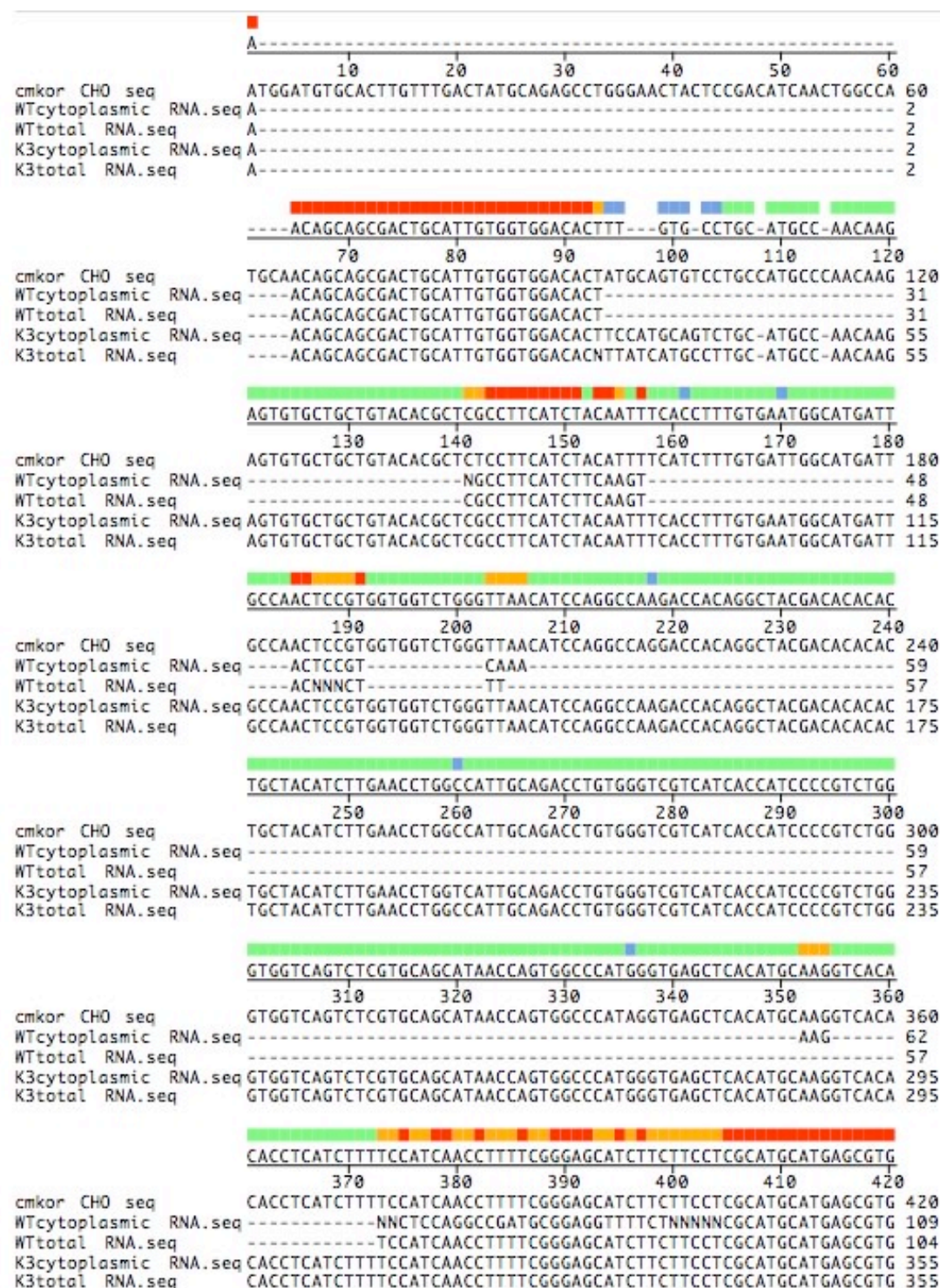






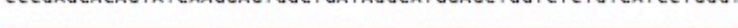

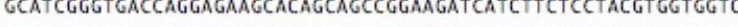
Fig. 53 Intercellular spreading of FGF-2-GFP expressing CHO cells as analyzed by FACS. Intercellular spreading was monitored by growing CHO_{MCAT-TAM2} cells ('CHO wild-type') with CHO_{MCAT-TAM2} cells retrovirally transduced with the FGF-2-GFP construct in a mixed culture. FGF-2-GFP expression was induced by 1 μ g/ml doxycycline for 48 hours at 37°C. CHO_{MCAT-TAM2} cells and CHO_{MCAT-TAM2} cells expressing FGF-2-GFP were gated based on GFP fluorescence and APC-derived fluorescence of CHO_{MCAT-TAM2} cells (green curve) and CHO_{MCAT-TAM2} cells expressing FGF-2-GFP (blue curve) was measured as depicted in the histogram. Autofluorescence was measured using CHO_{MCAT-TAM2} cells treated with antibodies.

Fig. 54 Alignment of the cmkor 1 sequence mus musculus vs cmkor 1 sequence human. Two primer pairs were designed flanking regions with different homologies (purple and blue box).

| | | | |
|-------|------|---|------|
| Query | 1 | ATGGATGTGCACTTGTGTTGACTATGCAGAGCCTGGCAACTACTCTGACATCAACTGGCCA | 60 |
| Sbjct | 10 | ATGGATGTGCACTTGTGTTGACTATGCAGAGCCTGGGAAGTACTCCGACATCAACTGGCCA | 69 |
| Query | 61 | TGTAACAGCAGCGACTGCATTGTGGTGGACACTGTGCAGTGTCCCACCATGCCTAACAAAG | 120 |
| Sbjct | 70 | TGCAACAGCAGCGACTGCATTGTGGTGGACACTATGCAGTGTCTGCCATGCCCAACAAG | 129 |
| Query | 121 | AACGTGCTTCTGTATACCTCTCCTTCATCTACATTTTCATCTTCGTGATCGGGCATGATT | 180 |
| Sbjct | 130 | AGTGTGCTGCTGTACACGCTCTCCTTCATCTACATTTTCATCTTTGTGATTGGCATGATT | 189 |
| Query | 181 | GCCAACTCTGTGGTGGTCTGGGTGAATATCCAGGCTAAGACCACAGGCTACGACACGCAC | 240 |
| Sbjct | 190 | GCCAACTCCGTGGTGGTCTGGGTAAACATCCAGGCCAGGACCACAGGCTACGACACACAC | 249 |
| Query | 241 | TGCTACATCTTGAACCTGGCCATTGCAGACCTGTGGGTGTCATCACCATCCCCGTCTGG | 300 |
| Sbjct | 250 | TGCTACATCTTGAACCTGGCCATTGCAGACCTGTGGGTGTCATCACCATCCCCGTCTGG | 309 |
| Query | 301 | GTGGTCAGTCTCGTGCAGCATAACCACTGGCCCATGGGGGAGCTCACATGCAAGATCACA | 360 |
| Sbjct | 310 | GTGGTCAGTCTCGTGCAGCATAACCACTGGCCCATAGGTGAGCTCACATGCAAGGTACA | 369 |
| Query | 361 | CACCTCATTTTCTCCATCAACCTCTTTGGGAGCATCTTCTTCTCTCGCTGCATGAGCGTG | 420 |
| Sbjct | 370 | CACCTCATCTTTTCCATCAACCTTTTGGGAGCATCTTCTTCTCTCGCATGCATGAGCGTG | 429 |
| Query | 421 | GACCGCTATCTCTCCATCACCTACTTCACCGGCACCTCCAGCTATAAGAAGAAGATGGTA | 480 |
| Sbjct | 430 | GACCGCTATCTCTCCATCACCTACTTCGCCAGCACCTCTAGCTATAAGAAGAAGATGGCG | 489 |
| Query | 481 | CGCCGTGTTGTATGCATCTTGGTGTGGCTGCTGGCCTTCTTTGTGTCCCTGCCTGATACC | 540 |
| Sbjct | 490 | CGCCGTGTTGTCTGCATCTTGGTGTGGCTGCTGGCCTTCTTTGTGTCTCTGCCCGATACC | 549 |
| Query | 541 | TACTACCTGAAGACGGTCACATCTGCTTCCAACAAATGAGACCTACTGCAGGTCTTCTAC | 600 |
| Sbjct | 550 | TACTAOCCTGAAGACGGTCACATCTGCTTCTAACAAACGAGACCTACTGCCGGTCTTCTAC | 609 |
| Query | 601 | CCCGAGCACAGCATCAAGGAGTGGCTGATCGGCATGGAGCTGGTCTCTGTCTCTTGGGC | 660 |
| Sbjct | 610 | CCCGAGCACAGTATCAAGGAGTGGCTGATAGGCATGGAGCTGGTCTCTGTCTCTTGGGT | 669 |
| Query | 661 | TTTGCTGTCCCTTCACTATCATTTGCCATCTTCTACTTCCTGCTCGCTAGAGCCATGTCA | 720 |
| Sbjct | 670 | TTTGCCATTCCCTTCAACATCATTTGCTATCTTCTACTTCCTGCTTGGCAGAGCCATGTCA | 729 |
| Query | 721 | GCATCAGGCGACACAGGAGAAGCACAGTAGCCGGAAGATCATCTTCTCCTACGTGGTGGTC | 780 |
| Sbjct | 730 | GCATCGGCTGACACAGGAGAAGCACAGCAGCCGGAAGATCATCTTCTCCTACGTGGTGGTC | 789 |
| Query | 781 | TTCTGCTATGTTGGCTGCCGTACCATTTTGTGGTTCTGCTGGACATCTTCTCCATCTTA | 840 |
| Sbjct | 790 | TTCTGCTGTGTTGGCTGCCATACCATGCCGTGGTTCTTCTGGACATCTTCTCCATCTTG | 849 |
| Query | 841 | CACTACATCCCGTTTACCTGTCAGCTGGAGAATGTGCTCTTTACAGCGTTGCATGTCACC | 900 |
| Sbjct | 850 | CACTACATTCATTACCTGCCAGCTGGAGAATGTGCTCTTACAGCGCTGCATGTCACA | 909 |
| Query | 901 | CAGTGCCTGTCTTGGTGCACCTGCTGTGTCACCCCGTGTCTACAGCTTCATCAACCGC | 960 |
| Sbjct | 910 | CAGTGCCTGTCTTGGTGCACCTGCTGTGTCACCCAGTGTCTATAGCTTCATCAACCGC | 969 |
| Query | 961 | AACTACAGGTACGAGCTGATGAAGGCCTTCATCTTCAAGTACTCGGCCAAAACAGGTCTC | 1020 |
| Sbjct | 970 | AACTACAGGTACGAGCTGATGAAGGCCTTCATTTTCAAGTACTCAGCCAAGACAGGCCTC | 1029 |
| Query | 1021 | ACCAAGCTCATTGATGCCTCCAGAGTGTGAGACAGAGTACTCTGCCCTGGAACAGAAC | 1080 |
| Sbjct | 1030 | ACCAAGCTCATCGATGCCTCCCGCGTGTGAGAGACGGAGTACTCTGCCCTGGAACAGAAC | 1089 |
| Query | 1091 | ACCAAGTGA 1099 | |
| Sbjct | 1090 | ACCAAGTGA 1098 | |

Fig. 55 Alignment of the cmkor 1 sequence mus musculus vs cmkor 1 sequence of CHO cells. CHO K3 mRNA was isolated and subjected to RT-PCR using cmkor 1-specific primers. Following cloning of the corresponding product into the pGemT vector, the cmkor 1 gene was sequenced and aligned with the cmkor 1 sequence of the mouse genome.



| | |
|-----------------------|--|
| |  |
| | <u>GACCGCTATCTCTCCATCACCTACTTCACCAGCACCTCTAGCTATAAGAAGAAGATGGCG</u> |
| | 430 440 450 460 470 480 |
| cmk0r CHO seq | GACCGCTATCTCTCCATCACCTACTTCACCAGCACCTCTAGCTATAAGAAGAAGATGGCG 480 |
| WTcytoplasmic RNA.seq | GACCGCTATCTCTCCATCACCTACTTCACCAGCACCTCTAGCTATAAGAAGAAGCTGGCG 169 |
| WTtotal RNA.seq | GACCGCTATCTCTCCATCACCTACTTCACCAGCACCTCTAGCTATAAGAAGAAGATGGCG 164 |
| K3cytoplasmic RNA.seq | GACCGCTATCTCTCCATCACCTACTTCACCAGCACCTCTAGCTATAAGAAGAAGATGGCG 415 |
| K3total RNA.seq | GACCGCTATCTCTCCATCACCTACTTCACCAGCACCTCTAGCTATAAGAAGAAGATGGCG 415 |
| |  |
| | <u>CGCCGTGTTGTCTGCATCTTGGTGTGGCTGCTGGCCTTCTTTGTGTCTCTGCCGATACC</u> |
| | 490 500 510 520 530 540 |
| cmk0r CHO seq | CGCCGTGTTGTCTGCATCTTGGTGTGGCTGCTGGCCTTCTTTGTGTCTCTGCCGATACC 540 |
| WTcytoplasmic RNA.seq | CGCCGTGTTGTCTGCATCTTGGTGTGGCTGCTGGCCTTCTTTGTGTCTCTGCCGATACC 229 |
| WTtotal RNA.seq | CGCCGTGTTGTCTGCATCTTGGTGTGGCTGCTGGCCTTCTTTGTGTCTCTGCCGATACC 224 |
| K3cytoplasmic RNA.seq | CGCCGTGTTGTCTGCATCTTGGTGTGGCTGCTGGCCTTCTTTGTGTCTCTGCCGATACC 475 |
| K3total RNA.seq | CGCCGTGTTGTCTGCATCTTGGTGTGGCTGCTGGCCTTCTTTGTGTCTCTGCCGATACC 475 |
| |  |
| | <u>TACTACCTGAAGACGGTCACATCTGCTTCTAACAACGAGACCTACTGCCGGTCCTTCTAC</u> |
| | 550 560 570 580 590 600 |
| cmk0r CHO seq | TACTACCTGAAGACGGTCACATCTGCTTCTAACAACGAGACCTACTGCCGGTCCTTCTAC 600 |
| WTcytoplasmic RNA.seq | TACTACCTGAAGACGGTCACATCTGCTTCTAACAACGAGACCTACTGCCGGTCCTTCTAC 289 |
| WTtotal RNA.seq | TACTACCTGAAGACGGTCACATCTGCTTCTAACAACGAGACCTACTGCCGGTCCTTCTAC 284 |
| K3cytoplasmic RNA.seq | TACTACCTGAAGACGGTCACATCTGCTTCTAACAACGAGACCTACTGCCGGTCCTTCTAC 535 |
| K3total RNA.seq | TACTACCTGAAGACGGTCACATCTGCTTCTAACAACGAGACCTACTGCCGGTCCTTCTAC 535 |
| |  |
| | <u>CCCGAGCACAGTATCAAGGAGTGGCTGATAGGCATGGAGCTGGTCTCTGTCATCCTGGGT</u> |
| | 610 620 630 640 650 660 |
| cmk0r CHO seq | CCCGAGCACAGTATCAAGGAGTGGCTGATAGGCATGGAGCTGGTCTCTGTCATCCTGGGT 660 |
| WTcytoplasmic RNA.seq | CCCGAGCACAGTATCAAGGAGTGGCTGATAGGCATGGAGCTGGTCTCTGTCATCCTGGGT 349 |
| WTtotal RNA.seq | CCCGAGCACAGTATCAAGGAGTGGCTGATAGGCATGGAGCTGGTCTCTGTCATCCTGGGT 344 |
| K3cytoplasmic RNA.seq | CCCGAGCACAGTATCAAGGAGTGGCTGATAGGCATGGAGCTGGTCTCTGTCATCCTGGGT 595 |
| K3total RNA.seq | CCCGAGCACAGTATCAAGGAGTGGCTGATAGGCATGGAGCTGGTCTCTGTCATCCTGGGT 595 |
| |  |
| | <u>TTTGCCATTCCCTTCACCATCATTGCTATCTTCTACTTCCTGCTTGCCAGAGCCATGTCA</u> |
| | 670 680 690 700 710 720 |
| cmk0r CHO seq | TTTGCCATTCCCTTCACCATCATTGCTATCTTCTACTTCCTGCTTGCCAGAGCCATGTCA 720 |
| WTcytoplasmic RNA.seq | TTTGCCATTCCCTTCACCATCATTGCTATCTTCTACTTCCTGCTTGCCAGAGCCATGTCA 409 |
| WTtotal RNA.seq | TTTGCCATTCCCTTCACCATCATTGCTATCTTCTACTTCCTGCTTGCCAGAGCCATGTCA 404 |
| K3cytoplasmic RNA.seq | TTTGCCATTCCCTTCACCATCATTGCTATCTTCTACTTCCTGCTTGCCAGAGCCATGTCA 655 |
| K3total RNA.seq | TTTGCCATTCCCTTCACCATCATTGCTATCTTCTACTTCCTGCTTGCCAGAGCCATGTCA 655 |
| |  |
| | <u>GCATCGGGTGACCAGGAGAAGCACAGCAGCCGGAAGATCATCTTCTCCTACGTGGTGGTC</u> |
| | 730 740 750 760 770 780 |
| cmk0r CHO seq | GCATCGGGTGACCAGGAGAAGCACAGCAGCCGGAAGATCATCTTCTCCTACGTGGTGGTC 780 |
| WTcytoplasmic RNA.seq | GCATCGGGTGACCAGGAGAAGCACAGCAGCCGGAAGATCATCTTCTCCTACGTGGNGGTC 469 |
| WTtotal RNA.seq | GCATCGGGTGACCAGGAGAAGCACAGCAGCCGGAAGATCATCTTCTCCTACGTGGTGGTC 464 |
| K3cytoplasmic RNA.seq | GCATCGGGTGACCAGGAGAAGCACAGCAGCCGGAAGATCATCTTCTCCTACGTGGTGGTC 715 |
| K3total RNA.seq | GCATCGGGTGACCAGGAGAAGCACAGCAGCCGGAAGATCATCTTCTCCTACGTGGTGGTC 715 |
| |  |
| | <u>TTCTGGTGTGTTGGCTGCCATACCATGCCGTGGTTCTTCTGGACATCTTCTCCATCTTG</u> |
| | 790 800 810 820 830 840 |
| cmk0r CHO seq | TTCTGGTGTGTTGGCTGCCATACCATGCCGTGGTTCTTCTGGACATCTTCTCCATCTTG 840 |
| WTcytoplasmic RNA.seq | TTCTGGTGTGTTGGCTGCNANNNN-----TCTTCTGGACATCTTCTCCATCTTG 519 |
| WTtotal RNA.seq | TTCTGGNNTGTTGGCTGCCATACCATGCCGTGGTTCTTCTGGACATCTTCTCCATCTTG 524 |
| K3cytoplasmic RNA.seq | TTCTGGTGTGTTGGCTGCCATACCATGCCGTGGTTCTTCTGGACATCTTCTCCATCTTG 775 |
| K3total RNA.seq | TTCTGGTGTGTTGGCTGCCATACCATGCCGTGGTTCTTCTGGACATCTTCTCCATCTTG 775 |

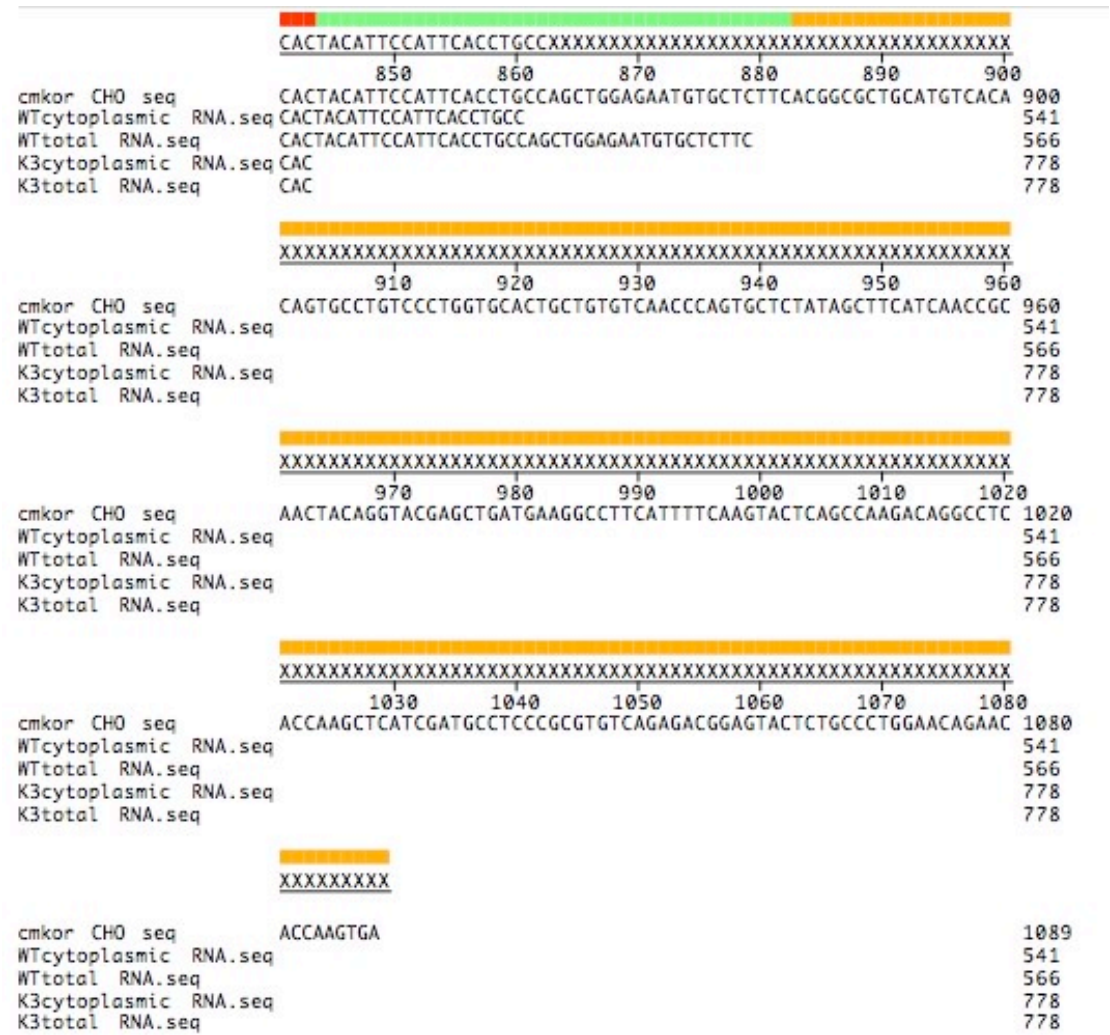


Fig. 56 Alignment of the sequenced RT-PCR products obtained from isolation of cytoplasmic and total RNA from CHO wild-type and CHO K3 cells. Cytoplasmic and total RNA isolated from CHO wild-type and CHO K3 cells were subjected to RT-PCR using cmkor 1-specific primers. The cDNA products were sequenced and aligned with the CHO cmkor 1 sequence (red parts indicate homology).

4 Discussion

Transport of most secretory proteins to the extracellular space is mediated by the ER/Golgi-dependent secretory pathway (Nickel et al., 2002; Palade, 1975; Rothman, 1994; Rothman and Wieland, 1996). In case of soluble factors, the principal targeting motifs are N-terminal signal peptides that direct classical secretory proteins to the translocation machinery of the ER (Keenan et al., 2001). However, for a number of soluble factors with defined extracellular functions, it has been demonstrated that ER/Golgi-independent routes of protein secretion exist (Cleves, 1997; Hughes, 1999; Muesch et al., 1990; Nickel, 2003; Nickel, 2005; Prudovsky et al., 2003; Rubartelli and Sitia, 1991). Among these, *Leishmania* HASPB is an unconventionally secreted protein that is a component of the surface coat of *Leishmania* parasites (Alce et al., 1999; Flinn et al., 1994; McKean et al., 2001). HASPB contains an N-terminal SH4 domain that becomes dually acylated by myristoylation of glycine 2 and palmitoylation of cysteine 5 (Denny et al., 2000). These post-translational modifications are essential for HASPB targeting to the plasma membrane and subsequent to the cell surface of *Leishmania* parasites (Denny et al., 2000; Pimenta et al., 1994) and mammalian cells (Denny et al., 2000; Stegmayer et al., 2005). Interestingly, the extreme N-terminus of HASPB consisting of 18 amino acids is sufficient for targeting a reporter molecule like GFP to the cell surface (Denny et al., 2000) suggesting that endogenous factors exist in higher eukaryotes that are exported in a mechanistically similar manner.

The specific aim of this study was to investigate the molecular mechanism of HASPB export. In this regard, especially the targeting to the plasma membrane and the identification of the subcellular site of membrane translocation of HASPB, a process that eventually allows HASPB exposure on the cell surface of eukaryotic cells was aimed. This question is of general interest since HASPB has been shown to contact intracellular membranes such as the Golgi during its biogenesis (Denny et al., 2000) suggesting that HASPB associates at least transiently with membranes of the classical

secretory pathway. Therefore, even though palmitoyltransferases have not only been localized to the Golgi but also to the ER and plasma membranes (Bijlmakers and Marsh, 2003), it is likely that Golgi membranes contain the palmitoyltransferase required for the thioester-based acylation of cysteine 5 in the N-terminal SH4 domain of HASPB. From this point on it is not clear whether fully acylated HASPB translocates across the membrane of the Golgi or whether it is first transported to the plasma membrane associated with the cytoplasmic leaflet of secretory vesicles. Even though overall cell surface expression of HASPB has been shown not to be affected by brefeldin A (Denny et al., 2000), this result does not unequivocally rule out the possibility that HASPB is traveling to the plasma membrane associated with the cytoplasmic leaflet of TGN-derived secretory vesicles. It is also possible that transfer to the plasma membrane involves an intermediate step, in which HASPB might be transported from the TGN to the endosomal system from where it might get access to the plasma membrane.

A. Direct transport across the plasma membrane of mammalian cells of Leishmania HASPB as revealed by a CHO export mutant

Based on the uncertainties discussed above the aim was to establish an experimental system that allows for a quantitative analysis of HASPB cell surface expression under conditions where defined steps in HASPB biogenesis are blocked. In particular, it was necessary to develop experimental conditions where dual acylation of the N-terminal SH4 domain of HASPB occurs normally, but HASPB export to the outer leaflet of the plasma membrane is blocked. In this regard, CHO cells were used as a model system as they are well suited for the generation of random somatic mutants. To efficiently mutate CHO cells expressing HASPB-N18-GFP in a doxycycline-dependent manner, retroviral insertion mutagenesis was used. Employing this mutagenesis strategy using CD4 as a cell surface marker, mutated cells were efficiently enriched by FACS and the isolation of clonal CHO mutants with the

desired phenotype was successful. One of these obtained mutants, referred to as K3, has been characterized in detail in the current study.

4.1 Transduced CHO cells stably expressing HASPB-N18-GFP export the fusion protein to the cell surface

A general model system in which HASPB-GFP fusion proteins are expressed from a retroviral vector containing a doxycycline/transactivator-sensitive element was developed. Following transduction of CHO_{MCAT-TAM2} cells (Engling et al., 2002; Seelenmeyer et al., 2003) that constitutively express both an ecotropic retrovirus receptor and a doxycycline-sensitive transactivator, individual GFP-positive cells were isolated by several rounds of FACS sorting. Clonal cell lines genetically modified with HASPB-N18-GFP or other control constructs were found to express the reporter molecules in a doxycycline-dependent manner at similar levels. As revealed by confocal microscopy (Fig. 14, page 100), the N-terminal targeting motif directs the HASPB-N18-GFP reporter molecule to the plasma membrane. While the palmitoylation mutant (Δ palm-HASPB-N18-GFP) showed a perinuclear staining, both Δ myr-HASPB-N18-GFP and non-tagged GFP were characterized by cytoplasmic staining. Following translocation to the surface of *Leishmania* parasites, HASPs remain membrane-anchored via their N-terminal acyl chains. Based on a robust and efficient FACS-based assay (Fig. 15, page 102) (Engling et al., 2002; Seelenmeyer et al., 2003), it was possible to quantitatively assess the amount of HASPB-N18-GFP released to the extracellular space in living cells. This allowed specific detection of secreted HASPB-N18-GFP with affinity-purified anti-GFP antibodies under native conditions based on flow cytometry. In this way, GFP-derived fluorescence was used to normalize the overall expression of the reporter molecule under various experimental conditions, whereas the secreted population could be exclusively detected on the cell surface with antibodies coupled to a second fluorophore such as allophycocyanin. These data were confirmed by a biochemical assessment of the extracellular population of

HASPB-N18-GFP in wild-type versus control cells using a membrane-impermeable biotinylation reagent and streptavidin-based immunopurification of factors exposed on the cell surface (Fig. 16, page 103). Since dual acylation of HASPB-N18-GFP is a critical determinant for plasma membrane targeting and export, carbonate extraction analysis (Fig. 17, page 105) were performed to test the overall membrane association. In combination with the cell surface biotinylation assay these data provide evidence that HASPB-N18-GFP is targeted to the plasma membrane where it is stably associated and finally translocated to the extracellular space.

4.2 HASPB-N18-GFP expressed in CHO K3 mutant cells is stably associated with the plasma membrane, but gets exported to reduced levels as compared to CHO wild-type cells

In order to establish a genetic screening procedure to identify potential molecular components of the HASPB export machinery, a FACS-based assay was developed to identify and isolate export-deficient CHO mutant cells. HASPB-N18-GFP-expressing and non-expressing cells present in a mixed culture could be distinguished from each other regarding HASPB-N18-GFP cell surface staining. As a consequence an identification and isolation of export-deficient CHO mutant cells based on FACS sorting was possible. As noted above, to efficiently mutate CHO cells expressing HASPB-N18-GFP in a doxycycline-dependent manner, retroviral insertion mutagenesis was used. Employing the mutagenesis strategy using CD4 as a cell surface marker to enrich mutated cells by FACS, a HASPB-N18-GFP mutant CHO cell line (K3) could be isolated. It is characterized by a negative HASPB-N18-GFP export phenotype, and, quite important for the strategy used, positive for CD4 cell surface staining (Fig. 19, page 109).

In the context of this work, it was most critical to isolate CHO mutants that do not have any defect in the HASPB-N18-GFP sequence itself. Sequence analysis (Fig. 20, page 111) of both HASPB-N18-GFP in CHO wild-type cells

and in the mutant CHO K3 cell line documented that this was not the case. The negative HASPB-N18-GFP export phenotype by which the clonal CHO K3 cell line was isolated could be confirmed by both FACS-based cell surface staining experiments and a biochemical assessment of HASPB-N18-GFP export using a membrane-impermeable biotinylation reagent (Fig. 21, page 113). Both methods consistently demonstrated that HASPB-N18-GFP cell surface expression in CHO K3 cells is greatly reduced to ~10-30% of the population found on the cell surface of CHO wild-type cells. As shown by GFP-derived fluorescence determined by FACS and by western blotting, the expression level of HASPB-N18-GFP does not differ significantly between CHO K3 and wild-type cells. Thus, it could be concluded that the process of HASPB-N18-GFP membrane translocation is perturbed in the mutant cell line. Since the N-terminal targeting sequence in CHO K3 mutant cells is identical compared to CHO cells, however its membrane translocation seems to be affected it was most critical to investigate, whether the isolated mutant has any defect in the co-and/or post-translational processing of HASPB. In regard to the genetic system used, mutants that are still capable of adding both myristate and palmitate to the SH4 domain of HASPB would be interesting. In case of CHO K3 cells, this was shown to be the case by carbonate extraction experiments to probe overall membrane association of HASPB-N18-GFP. Furthermore employing metabolic labeling experiments, the incorporation of [³H]-labeled myristate and palmitate into HASPB-N18-GFP was demonstrated when expressed in CHO K3 cells. These experiments (Fig. 22, page 115) unequivocally demonstrated that HASPB-N18-GFP is processed normally in CHO K3 mutant cells resulting in a membrane association that is indistinguishable from HASPB-N18-GFP expressed in CHO wild-type cells. Based on the perturbed HASPB-N18-GFP membrane translocation in the mutant CHO K3 cell line, it was then crucial to analyze whether the steady-state distribution of the reporter molecule is changed in CHO K3 cells as compared to wild-type cells. As demonstrated by confocal microscopy and subcellular fractionation (Fig. 23, page 117), in both cell lines the majority of the HASPB-N18-GFP population localizes to the plasma membrane. Intriguingly, an FGF-2-GFP as well as a Galectin-1-GFP fusion protein is secreted equally well from the CHO K3 mutant cell line and the parental CHO

wild-type cells, demonstrating that the disrupted factor in K3 cells is a specific component of the HASPB export pathway.

4.3 The integration of the retrovirus into the genome of CHO K3 cells does not cause the perturbed HASPB membrane translocation

In the context of this work it was most critical to identify the integration site of the retrovirus. As revealed by a LAM-PCR (Fig. 26, page 121), it was possible to identify and sequence the region flanked by the integration of the retrovirus. As illustrated in the alignment with the mouse genome the chemokine orphan receptor 1 (cmkor 1) was identified on chromosome 1 of the mouse genome. The retrovirus integrated into an intron flanked by two exons suggesting that cmkor 1 might get translated based on splicing reactions. However, integration into a non-coding region might also result in mRNA transcripts leading to affected translation of a desired protein. Cmkor 1 belongs to a family of G-protein coupled receptors, all of which transmit extracellular stimuli to intracellular signals (Tilakaratne and Sexton, 2005). Since there is only sparse information about its functions and its ligands, it was of interest to investigate whether downregulation or disruption of the receptor caused the observed phenotype of the mutant CHO K3 cell line. To perform RNA interference the cmkor 1 gene in CHO cells was cloned and sequenced. As shown by the antisense RNA approach (Fig. 29, page 126) using three different siRNA oligos cmkor 1 could not get downregulated in CHO wild-type cells. In contrast, cmkor 1 mRNA was detectable in CHO K3 cells as revealed by sequencing of RT-PCR products obtained from total and cytoplasmic RNA isolation (Suppl. Fig. 56, pages 167-170). Together, these findings suggest that there might exist other non-identified integration sites of the retrovirus causing the perturbed HASPB membrane localization in the mutant CHO K3 cell line.

In parallel to the RNAi experiments a possible contribution of the chemokine orphan receptor 1 on the HASPB perturbed membrane translocation in CHO

K3 cells was analyzed by overexpression of the *cmk1* gene in CHO wild-type and CHO K3 cells. *cmk1* was cloned into a vector containing both an IRES element and CD8 as cell surface marker. An IRES (internal ribosome entry site) allows translation initiation of multiple proteins from a single transcript (Jang et al., 1988; Liu et al., 2000). Following transduction *cmk1* expressing cells were efficiently enriched by FACS based on CD8-derived cell surface staining. HASPB-N18-GFP export from *cmk1* transduced CHO wild-type and CHO K3 cells was analyzed based on flow cytometry (Fig. 31, page 130) and the biochemical biotinylation assay (Fig. 32, page 132). Export of HASPB-N18-GFP could be neither restored to wild-type levels in case of CHO K3 cells nor get reduced or enhanced in CHO wild-type cells due to an overexpression of the *cmk1* gene. This observation confirms previous findings, indicating that *cmk1* expression is not affected in CHO K3 cells. This suggests that other non-identified integration sites of the retrovirus resulting in disruption of a gene could cause the perturbed HASPB membrane localization in CHO K3 cells.

In summary, these studies show that the mutant CHO K3 cell line has a direct defect in the molecular machinery promoting membrane translocation of HASPB. Importantly, the perturbed HASPB membrane translocation was not caused by disruption of the *cmk1* gene. The subcellular distribution of the reporter molecule was unchanged comparing wild-type and K3 cells, with HASPB-N18-GFP detected in both cases as a plasma membrane-resident protein. As cell surface exposure of the reporter was largely reduced in the mutant cell line, the plasma membrane was identified as the subcellular site of membrane translocation of HASPB-N18-GFP (Stegmayer et al., 2005). Thus, along with the angiogenic growth factors FGF-1 and FGF-2 (Prudovsky et al., 2002; Schäfer et al., 2004) as well as Galectin-1 (Seelenmeyer et al., 2005), a lectin of the extracellular matrix, HASPB represents another example of an unconventional secretory protein that is translocated directly across the plasma membrane of mammalian cells in order to be exposed to the extracellular space.

Finally, a two-step process for the overall biogenesis of HASPB can be described. This process is defined by acylation-dependent targeting to the

inner leaflet of the plasma membrane followed by translocation across the plasma membrane, resulting in a membrane-anchored lipoprotein on the surface of both parasites and mammalian cells.

B. The SH4 protein HASPB is released in extracellular vesicles in a palmitoylation-dependent manner

As discussed previously, HASPB is transiently associated with, and most likely palmitoylated at, the Golgi followed by plasma membrane targeting in a brefeldin A-insensitive manner (Denny et al., 2000).

Based on these observations HASPB trafficking appears to be distinct from all known classes of plasma membrane-targeted proteins carrying dual acylation motifs at their N-termini (Bijlmakers and Marsh, 2003). The routes of only two acylated proteins belonging to the Src-family of receptor tyrosine kinases (RTK) have been studied at the molecular level. The Src kinase Lck is palmitoylated at the Golgi followed by brefeldin A-sensitive transport to the plasma membrane (Bijlmakers and Marsh, 1999; Bijlmakers and Marsh, 2003). The plasma membrane targeted N-terminal acylated protein Fyn does not appear to contact intracellular membranes but rather is directly targeted from the cytoplasm to the plasma membrane. Consistently, brefeldin A does not affect Fyn targeting (Bijlmakers and Marsh, 2003; van't Hof and Resh, 1999). In contrast to these well characterized SH4 containing proteins regarding their export, less is known about the trafficking of Yes and Src. Yes is the closest relative to the prototypical family member, Src, with the two proteins sharing more than 80% homology (Sukegawa et al., 1987). Importantly, it is noteworthy that Src becomes only myristoylated in its N-terminal SH4 domain (Bijlmakers and Marsh, 2003). Moreover, both proteins are expressed ubiquitously (Thomas and Brugge, 1997). Yes is localized to the cytoplasmic leaflet of intracellular membranes and is hypothesized to control virion trafficking, since it has been shown to be involved in WNV (West Nile Virus) assembly and egress (Hirsch et al., 2005). Src represents a component of the MAP kinase pathway and localizes usually to the plasma membrane. Furthermore, Src is also found at other locations in

the cell such as focal adhesion sites (Rohrschneider, 1980), on endosomes (Kaplan et al., 1992) and synaptic vesicles (Linstedt et al., 1992). As indicated above, current knowledge about HASPB targeting to the plasma membrane does not fit with any of these examples. Interestingly, the extensive induction of non-apoptotic highly dynamic plasma membrane blebbing has been reported as a novel and conserved activity of SH4 domains derived from the HASPB proteins of *Leishmania* parasites as well as the prototypic Src kinases Src, Fyn, Yes and Lck (Tournaviti et al., 2006 submitted). These reorganizations of the plasma membrane require the membrane association of the SH4 domain depend on the integrity of F-actin as well as microtubule architecture and are regulated by the activities of Rock kinase and Myosin-II ATPase (Tournaviti et al., 2006 submitted). Furthermore as revealed by RNAi analysis, the actin and microtubule regulating diaphanous related formin (DRF) FHOD1 has been identified as a factor that facilitates plasma membrane bleb formation (Tournaviti et al., 2006 submitted).

Based on these observations it is likely that plasma membrane-associated SH4 proteins could be released from cells as a result of plasma membrane blebbing, a process promoting the shedding of plasma membrane-derived vesicles that are released into the extracellular space (Freyssinet, 2003; Hugel et al., 2005; Martinez et al., 2005). In case of HASPB as a major component for virulence in *Leishmania* (Alce et al., 1999; Flinn et al., 1994; McKean et al., 2001; Rangarajan et al., 1995), alternative secretory mechanisms could contribute to the effectiveness of these parasites to invade vertebrate hosts. To gain insights into plasma membrane blebbing and its consequences concerning HASPB export, cell culture supernatants were analyzed for the presence of HASPB-containing vesicles. The various experimental conditions resulted in a new export pathway for HASPB-N18-GFP that has been characterized in more detail in the current study.

4.4 HASPB-N18-GFP-expressing CHO cell lines induce bleb formation and release HASPB-containing vesicles into the extracellular space

Heterologous expression of a HASPB-N18-GFP fusion protein induces curvature of the plasma membrane resulting in the formation of highly dynamic, non-apoptotic tubules and plasma membrane blebs (Fig. 33, page 135) (Tournaviti et al., 2006 submitted). Plasma membrane blebs are cell protrusions generated by the osmotic pressure of the cell interior upon localized destabilization of the cortical actin meshwork at the plasma membrane (Charras et al., 2005; Cunningham, 1995; Sheetz et al., 2006). Based on this observed phenotype cell culture supernatants from CHO cells were analyzed for the presence of the reporter molecule employing ultracentrifugation (Fig. 34, page 136). Indeed, the HASPB-N18-GFP fusion protein was found in the resulting membrane sediment. To verify whether HASPB is exported via vesicles the membrane sediment was floated into a Nycodenz gradient. Employing Nycodenz flotation gradients, a 0%/30% interphase was generated in order to discriminate aggregates from vesicles. Importantly, HASPB was found in the low-density vesicle fraction (Fig. 35, page 138). Interestingly, TSG101 and Alix, two proteins necessarily required in critical steps in the MVB sorting pathway were also detectable in this HASPB-containing fraction (Fig. 36, page 140).

Multivesicular bodies (MVBs) represent endocytic intermediates and are formed from sorting (early) endosomes. During this process maturing MVBs accumulate internal vesicles that have been internalized through endocytosis (Raiborg et al., 2003). These luminal vesicles are formed through invagination and pinching-off the endosome membrane (Katzmann et al., 2001). Besides other functions one possible fate of MVBs occurs when their limiting membrane fuses with the plasma membrane, resulting in the release of the internal vesicles, which are now termed exosomes (Denzler et al., 2000). For the sorting and multivesicular body formation three separate heteromeric protein complexes called ESCRT-I, ESCRT-II and ESCRT-III are required (Raiborg et al., 2003). These protein complexes are transiently recruited from

the cytoplasm to the endosomal membrane where they function sequentially in the sorting of transmembrane proteins into the MVB pathway and in the formation of MVB vesicles. Initially the ESCRT-I protein binds to endosomal cargo and is required for the activation of ESCRT-II. ESCRT-II in turn initiates the oligomerization of at least four small coiled coil proteins resulting in the formation of a large endosome-associated structure, the ESCRT-III complex. ESCRT-III seems to function in the concentration of MVB cargo (Katz et al., 2002). Finally, after protein sorting has been completed a multimeric AAA-type ATPase, Vps4, binds to ESCRT-III and disassembles the ESCRT-III complex in an ATP-dependent manner. The Vps4-dependent dissociation of the ESCRT machinery is currently the final distinguishable step of cargo sorting and is a prerequisite for vesicle formation (Katzmann et al., 2001; Wendland, 2002).

TSG101 (Garrus et al., 2001), the mammalian homolog to Vps 23, is a member of the ESCRT-I complex involved in recognition of cargo by MVBs and Alix (Chatellard-Causse et al., 2002) functions as an ESCRT-III binding partner. Since these proteins were enriched in the HASPB-N18-GFP-containing vesicle fractions HASPB was hypothesized to get exported in vesicles being released by the MVB sorting machinery. Staining of the exosomes-released protein Hsc 70 (Whetstone and Lingwood, 2003) in this fraction as well as the absence of a cytosolic housekeeping enzyme, GAPDH (Bown et al., 2002), in the corresponding fraction provided additional evidence of the proposed pathway. In this regard, the localization of HASPB in extracellular vesicles was of interest. HASPB-N18-GFP was found to be mainly present on the inner leaflet of the vesicle membrane as revealed by protease protection experiments (Fig. 37, page 141). The digestion of the reporter molecule was only visible in presence of a detergent. Consistent with HASPB-N18-GFP found in extracellular vesicles HASPB-GFP full length was detectable in the vesicle fraction to the same extent. Intriguingly, twice the amount of HASPB was found in extracellular vesicles derived from CHO K3 cells as compared to CHO wild-type cells. This observation was expected since HASPB in the mutant CHO K3 cell line is accumulated on the inner leaflet of the plasma membrane resulting in an increased amount of HASPB-N18-GFP in extracellular vesicles. However, based on the pronounced

presence of TSG101, Alix and Hsc 70 in the vesicle fractions of CHO K3 cells documented that the mutant CHO K3 cell line produces more amounts of vesicles rather than vesicles containing quantitatively more HASPB. At this stage the reason for this observation is not known. Interestingly, an FGF-2-GFP as well as a Galectin-1-GFP fusion protein was not found in extracellular vesicles suggesting that only the SH4 protein HASPB gets access to the MVB machinery releasing HASPB-containing vesicles into the extracellular space. The similarity between HASPB-containing vesicles and exosomes was supported by analysis of the buoyant densities. As revealed by continuous sucrose gradients (Fig. 40, page 146) the densities in the peak fractions of 1.13 g/ml and 1.15 g/ml of HASPB-containing vesicles are consistent with the reported exosomal density of 1.15 g/ml (Heijnen et al., 1999). In agreement with previous findings as described in the first part of the discussion there exist two independent extracellular HASPB populations, a cell surface localized HASPB-N18-GFP population and, in addition, a population of vesicle-associated HASPB-N18-GFP.

4.5 The Rock inhibitor blocks the formation of blebs but only partially reduces the amount of HASPB-containing vesicles

Since Rock is one of many effectors for the Rho GTPases regulating the organization of the actin cytoskeleton, it controls actomyosin filament assembly and myosin contractile activity necessary for bleb formation (Coleman et al., 2001; Leverrier and Ridley, 2001). To assess the relevance of plasma membrane blebbing in the context of the detection of HASPB-containing extracellular vesicles, CHO cells expressing HASPB-N18-GFP were treated with Rock inhibitor (Y-27632). As revealed by confocal microscopy (Fig. 41, page 148) HASPB-mediated plasma membrane bleb formation was blocked in presence of Rock inhibitor. By contrast, a parallel experiment employing Nycodenz flotation gradients (Fig. 42, page 149) revealed that HASPB-containing extracellular vesicles were still detectable.

Together, these observations strongly suggest that the amount of HASPB-containing extracellular vesicles found in the cell culture supernatants of CHO cells is only partially derived from plasma membrane blebbing, a process promoting the shedding of plasma membrane-derived vesicles that are released into the extracellular space.

4.6 Src, Fyn, Yes and Lck mediate plasma membrane blebbing, however less amounts of the reporter molecules compared to HASPB are found in extracellular vesicles

As noted above, the export routes of other SH4-containing proteins were distinguishable from the HASPB export pathway (Bijlmakers and Marsh, 2003; Denny et al., 2000; Hirsch et al., 2005; Sukegawa et al., 1987; Thomas and Brugge, 1997; van't Hof and Resh, 1999). By contrast, the extensive induction of non-apoptotic highly dynamic plasma membrane blebbing has been reported as a novel and conserved activity of SH4 domains derived from the HASPB protein of *Leishmania* parasites as well as the prototypic Src kinases Src, Fyn, Yes and Lck (Tournaviti et al., 2006 submitted). Based on these observations, it was most crucial to analyze whether Src-, Fyn-, Yes- and Lck-containing extracellular vesicles could be detected in cell culture supernatants from Src, Fyn, Yes and Lck expressing CHO cells. As revealed by confocal microscopy (Fig. 44, page 152) and Nycodenz flotation gradients (Fig. 45, page 153), in contrast to the extensive plasma membrane bleb formation, Src, Fyn-, Yes- and Lck-containing vesicles were reduced to ~20-70% as compared to HASPB-containing vesicles. In agreement with previous findings (section 4.5) plasma membrane bleb formation was blocked in presence of Rock inhibitor. Interestingly, employing Nycodenz flotation gradients, the amount of extracellular vesicles containing Src, Fyn, Yes and Lck was reduced to a manifold as compared to HASPB-containing vesicles in presence of Rock inhibitor (Figs. 46, 47, page 155,156). Notably these vesicles were the result of plasma membrane bleb formation leading to the

shedding of plasma membrane-derived vesicles that are released into the extracellular space. These findings provide evidence that the targeting motif lies within the SH4 domain of only HASPB, resulting in its export in vesicles being released by the MVB sorting machinery into the extracellular space.

4.7 HASPB-N18-GFP expressed in HeLa cell lines can be found associated with extracellular vesicles, however plasma membrane blebbing is largely reduced

To further assess that HASPB is localized in extracellular vesicles being released by the MVB sorting machinery, RNA interference experiments should be performed. For this purpose the human HeLa cell line was used and characterized employing the various experimental approaches since its genome is fully sequenced. Intriguingly, HeLa cells expressing HASPB-N18-GFP showed a notably reduced plasma membrane blebbing as revealed by confocal microscopy (Fig. 48, page 157). By contrast, HASPB-containing vesicles were found in cell culture supernatants from HeLa cells employing Nycodenz flotation gradients (Fig. 49, page 159). In this regard, a study with HeLa cells would be even more interesting, as there are no additional HASPB-containing extracellular vesicles that are derived from plasma membrane blebbing leading to the shedding of plasma membrane-derived vesicles into the extracellular space. The similarity between HASPB-containing extracellular vesicles derived from HeLa and CHO cells was supported by an analysis of their densities, corresponding to the exosomal density of 1.15 g/ml (Fig. 50, page 160, Fig. 40, page 146) (Heijnen et al., 1999). As revealed by confocal microscopy (Fig. 51, page 162), HASPB-containing vesicles were clearly visible only for CHO wild-type, CHO K3 and HeLa cells expressing HASPB-N18-GFP. Moreover, employing electron microscopy (Fig. 52, page 163) extracellular vesicles derived from CHO wild-type and CHO K3 cells, respectively, ranged in sizes with diameters between 80 nm and 300 nm. Based on this observation, there might exist two subpopulations of extracellular vesicles with different origins. Vesicles with a

diameter up to 100 nm might represent exosomes, since their size correspond to the reported size of 40-100 nm for exosomes (Stoorvogel et al., 2002). By contrast, the subpopulation containing vesicles with a diameter larger than 100 nm could be caused by plasma membrane blebbing, a process promoting the shedding of plasma membrane-derived vesicles that are released into the extracellular space.

In summary, this study shows that the *Leishmania* SH4 protein HASPB can be found associated with extracellular vesicles indicating that there exists an alternative secretory mechanism for HASPB. Indeed, as revealed by Nycodenz flotation gradients with membrane sediments obtained from ultracentrifugation of cell culture supernatants, HASPB is enriched in extracellular vesicles. As revealed by protease protection experiments HASPB is located in the lumen of these vesicles. Colocalization experiments with different exosomes markers further confirmed that HASPB is exported via vesicles being released by the MVB sorting machinery. Furthermore, the HASPB-containing extracellular vesicle population was shown to be of intracellular origin since other SH4 proteins such as Src, Fyn, Yes and Lck mediate plasma membrane blebbing similar to HASPB but are not quantitatively detectable in extracellular vesicles. Interestingly, this observation was confirmed by results obtained from HeLa cells expressing HASPB-N18-GFP. HASPB is found in extracellular vesicles however HASPB-mediated plasma membrane blebbing is notably reduced in these cells. As revealed by sucrose gradients, HASPB-containing extracellular vesicles derived from CHO as well as from HeLa cells have an apparent density similar to that of exosomes. Moreover, employing electron microscopy extracellular vesicles range in sizes with diameters between 80 and 300 nm that are consistent with the reported exosomal size containing diameters of 40 to 100 nm (Stoorvogel et al., 2002). Together, these findings lead to explore the concept that HASPB is exported via vesicles, potentially representing exosomes being released by the MVB sorting machinery into the extracellular space.

4.8 Models for the unconventional secretion of HASPB

Leishmania HASPB is a lipoprotein that is exported to the extracellular space from both *Leishmania* parasites and mammalian cells via an unconventional secretory pathway (Denny et al., 2000). The HASPB primary structure differs from all other unconventional secretory proteins as it contains an N-terminal SH4 domain commonly found in Src kinases that is a substrate for N-terminal protein acylation (Resh, 1999; Resh, 2004). Combining the data presented in the current study, two export models for HASPB can be proposed. As shown in Fig. 57, after synthesizing on free ribosomes in the cytoplasm, the protein gets cotranslationally myristoylated at its N-terminal SH4 domain. A second acylation step involves palmitoylation at cysteine 5 by the enzyme palmitoyl acyltransferase. HASPB palmitoylation mutants (Δ palm-HASPB-N18-GFP, C5A) localize to Golgi membranes, as shown in Figs. 14 (page 100) and 33 (page 135), suggesting that the putative palmitoylacyltransferase is a resident enzyme of the Golgi apparatus (Denny et al., 2000; Stegmayer et al., 2005). Dual acylation of the SH4 domain of HASPB mediates stable membrane association of the molecule to the Golgi. Following transient association with the Golgi, HASPB is transported to the inner leaflet of the plasma membrane. As illustrated in Fig. 57, it is currently unclear how this transport step is mediated. However, in principle there are three options: i) HASPB might be transported to the plasma membrane associated with the cytoplasmic leaflet of secretory vesicles, ii) HASPB might be targeted first to endosomal structures followed by translocation to the plasma membrane or iii) HASPB transport from the Golgi to the plasma membrane might not at all rely on transport vesicles. In any case, palmitoylation of HASPB is strictly required for plasma membrane targeting as palmitoylation-deficient mutants of HASPB are efficiently retained at the level of the Golgi (Denny et al., 2000; Stegmayer et al., 2005). The final localization of HASPB is characterized by its stable association with the outer leaflet of the plasma membrane with the protein moiety being exposed to the extracellular space. Based on this model, HASPB must translocate across at least one membrane during its biogenesis pathway. In case intracellular HASPB transport would rely on vesicular

intermediates, membrane translocation could occur at any membrane during its transport to the cell surface, e.g. the Golgi, the plasma membrane and, potentially, secretory or endosomal vesicles. However, from the data presented, membrane translocation was shown to occur at the level of the plasma membrane rather than at intracellular sites (Stegmayer et al., 2005).

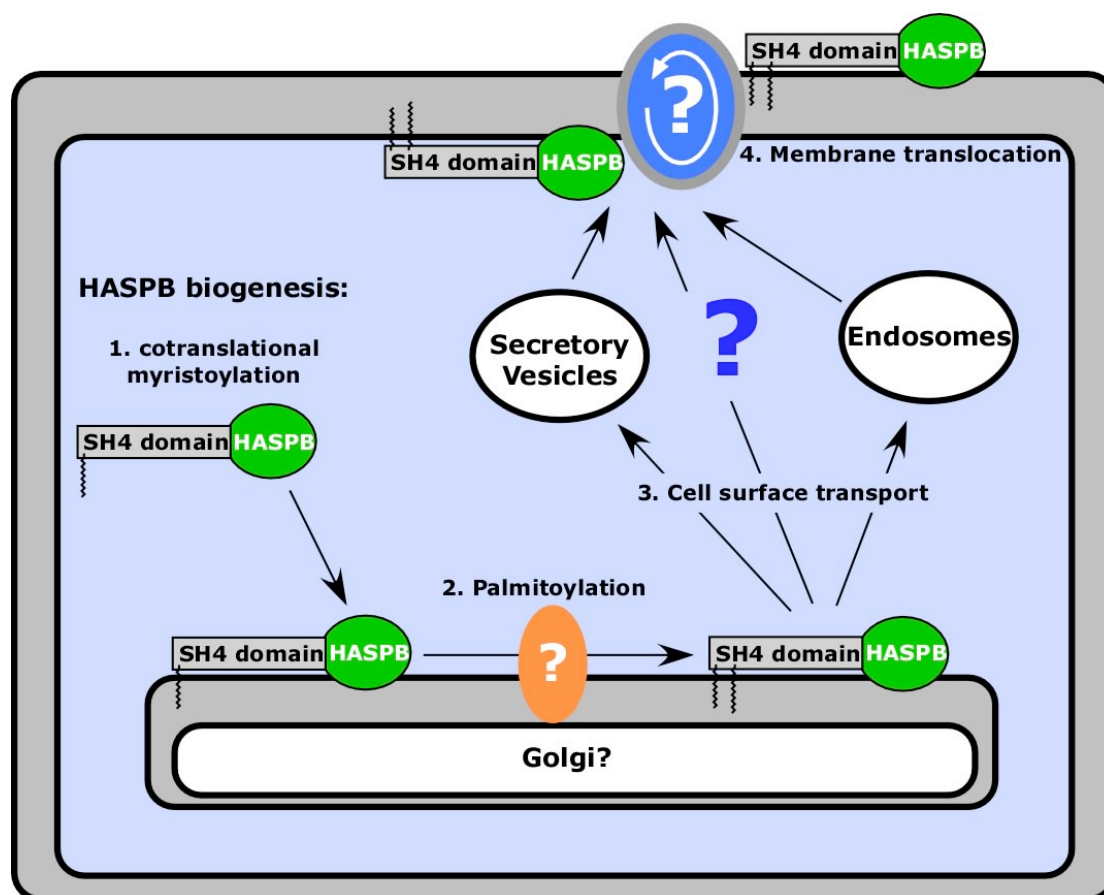


Fig. 57 Biogenesis and export of HASPB as discussed in the first chapter (chapter A).

For details, see main text.

Based on the findings discussed in the second chapter (chapter B), HASPB is exported via vesicles being released by the MVB sorting machinery. Multivesicular bodies or multivesicular endosomes (MVBs/MVEs) are endosomal compartments that contain multiple vesicles, which derive from a delimiting membrane by inward budding. The formation of MVBs is initiated at the early endosomal state as a result of the inward budding of the endosomal delimiting membrane. During the maturation of early endosomes to late

endosomes, tens or even hundreds of vesicles accumulate in their lumen. As discussed previously one option is the fusion of the MVB limiting membrane with the plasma membrane that results in export of vesicles, termed exosomes into the extracellular space (Denzer et al., 2000; Katzmann et al., 2001; Katzmann et al., 2003; Raiborg et al., 2003; Stoorvogel et al., 2002). As indicated in Fig. 58 during this process, HASPB ends up as intraluminal protein associated with the inner leaflet of the vesicle membrane. In this model HASPB does not translocate across any membrane confirming the results discussed in the first chapter, i.e. the presence of membrane-resident transporters in the plasma membrane promote membrane translocation of HASPB to the outer cell surface (Stegmayer et al., 2005).

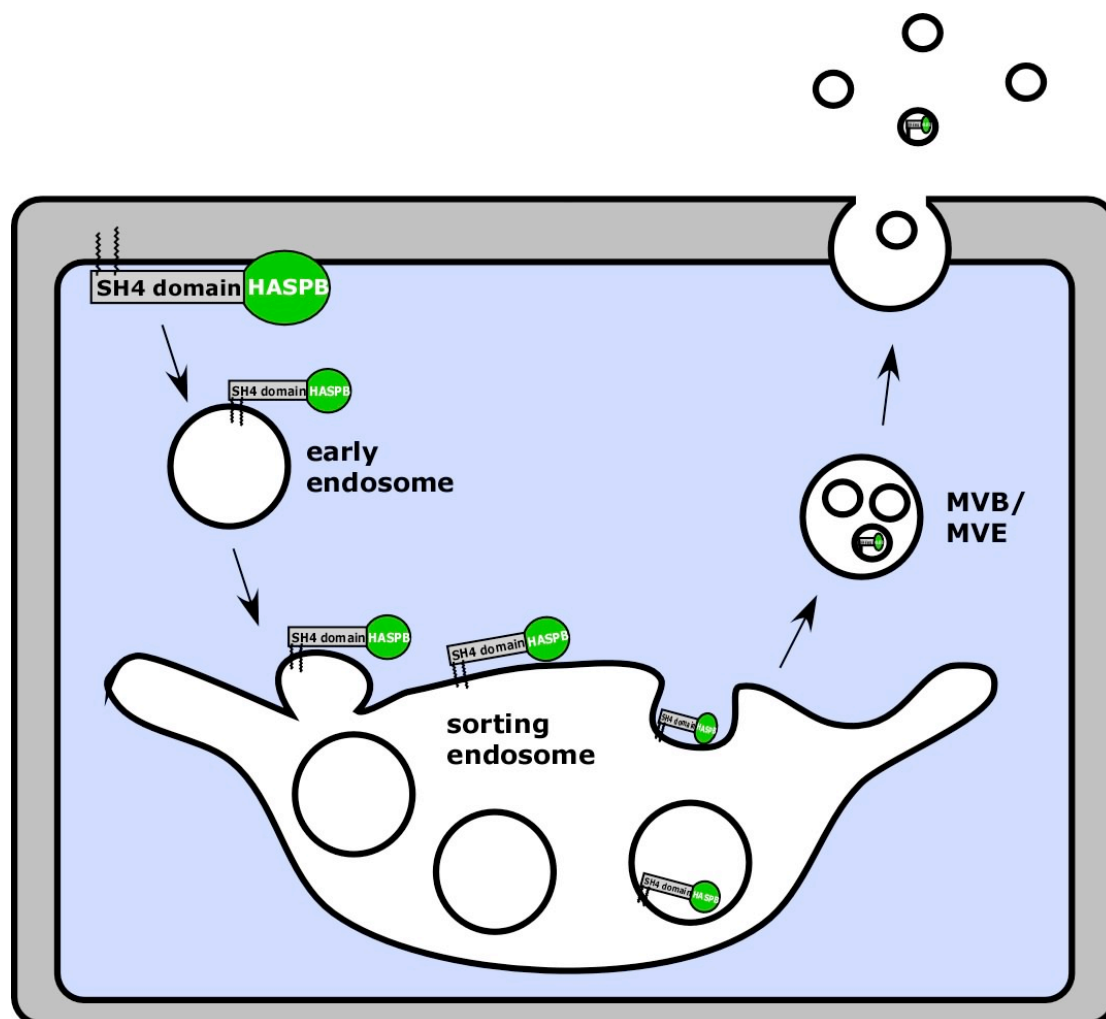


Fig. 58 Vesicle-associated export represented as exosomes as discussed in the second chapter (chapter B). For details, see main text.

The sorting of transmembrane proteins into topologically distinct limiting and intraluminal membranes has been proposed to serve several important functions: i) transmembrane proteins in the intraluminal membrane will be susceptible to degradation by lysosomal hydrolases, ii) intraluminal vesicles might represent storage vehicles for transmembrane proteins that are to be released from the cell in a regulated manner in these vesicles or iii) receptor signaling is, at least in principle, possible from the limiting membrane of MVBs, but not from the membranes of intraluminal vesicles. These findings suggest that sorting into MVBs can determine both the delivery of transmembrane proteins to lysosomes and the extracellular space, and also the ability of endocytosed receptors to transmit signals (Futter et al., 1996; Kleijmeer et al., 2001; Mullock et al., 1998; Stoorvogel et al., 2002).

In specialized cell types, for example antigen-presenting cells, exosomes have attracted interest as vehicles of immunomodulation (Stoorvogel et al., 2002; Thery et al., 2002). Furthermore it has been postulated that exosome-like vesicles might act as carriers for morphogens (Greco et al., 2001). In melanocytes and hemotopoietic cells, MVBs serve as intermediates in the formation of secretory lysosomes, such as melanosomes, MHCII compartments and lytic granules (Blott and Griffiths, 2002). Exosomes may be used by tumoral cells to invade normal tissue, and by pathogens such as prions and HIV to maximize their spreading in between cells (van Niel et al., 2006).

Since HASPs are critical determinants of both virulence and parasite survival within the vertebrate host (Alce et al., 1999; Flinn et al., 1994; McKean et al., 2001; Nugent et al., 2004; Rangarajan et al., 1995), HASPB might use this alternative secretory mechanism to efficiently invade their vertebrate hosts. HASPB is recognized by human sera collected in endemic regions with high specificity and sensitivity (Jensen et al., 1999) and shows promise as a target vaccine antigen for visceral leishmaniasis (Stager et al., 2003; Stager et al., 2000). Recent data have demonstrated that *L. donovani* HASPB is able to protect against infection *in vivo* via a novel immune mechanism involving natural antibodies and complement (Stager et al., 2003). Since it was unclear whether the cell surface localization of HASPB contributes to this immune response, recent findings have clearly demonstrated, that proteins in this

location are presented preferentially to the immune system *in vivo* (Prickett et al., 2006). Furthermore, as recently published *L.major* VPS4 mutants (VPS4^{E235Q}) accumulated the mutated protein around vesicular structures of the endocytic system and showed a defect in transport to the MVT-lysosome (Besteiro et al., 2006). This observation is quite similar to what has been observed in yeast and mammalian Vps4 mutants, suggesting a conserved role for this protein in MVB architecture from the early branching kinetoplastid flagellate lineage to mammals (Besteiro et al., 2006). Based on these observations export of HASPB via extracellular vesicles might serve to present the protein to the immune system by an alternative pathway.

In conclusion, the unconventionally secreted *Leishmania* protein HASPB, found in the extracellular space, is exported via two independent secretory mechanisms. HASPB is either directly exported across the plasma membrane or via extracellular vesicles. In the first case translocation across the plasma membrane seems to occur via plasma membrane-resident transporters potentially acting as flippases since HASPB is stably anchored in the membrane due to its dual acylation. In the second model, transport across the plasma membrane, representing the barrier for export, is mediated via vesicles being released by the MVB sorting machinery into the extracellular space. In the forthcoming years, light should be shed on the mechanisms regulating these export pathways, so that methods can be designed to interfere with unconventional secretion of HASPB. With this advance, much more could be discovered on how this unconventionally secreted protein functions in physiological and pathological situations.

References

- Ahle, S., Mann, A., Eichelsbacher, U., and Ungewickell, E. (1988). Structural relationships between clathrin assembly proteins from the Golgi and the plasma membrane. *EMBO J* 7, 919-929 issn: 0261-4189.
- Albritton, L. M., Tseng, L., Scadden, D., and Cunningham, J. M. (1989). A putative murine ecotropic retrovirus receptor gene encodes a multiple membrane-spanning protein and confers susceptibility to virus infection. *Cell* 57, 659-666.
- Alce, T. M., Gokool, S., McGhie, D., Stager, S., and Smith, D. F. (1999). Expression of hydrophilic surface proteins in infective stages of *Leishmania donovani*. *Mol Biochem Parasitol* 102, 191-196.
- Allouche, M., and Bikfalvi, A. (1995). The role of fibroblast growth factor-2 (FGF-2) in hematopoiesis. *Prog Growth Factor Res* 6, 35-48.
- Andrei, C., Dazzi, C., Lotti, L., Torrisi, M. R., Chimini, G., and Rubartelli, A. (1999). The secretory route of the leaderless protein interleukin 1beta involves exocytosis of endolysosome-related vesicles. *Mol Biol Cell* 10, 1463-1475.
- Andrei, C., Margiocco, P., Poggi, A., Lotti, L. V., Torrisi, M. R., and Rubartelli, A. (2004). Phospholipases C and A2 control lysosome-mediated IL-1 beta secretion: Implications for inflammatory processes. *Proc Natl Acad Sci U S A* 101, 9745-9750.
- Austin, C., Hinners, I., and Tooze, S. A. (2000). Direct and GTP-dependent interaction of ADP-ribosylation factor 1 with clathrin adaptor protein AP-1 on immature secretory granules. *J Biol Chem* 275, 21862-21869.
- Babst, M. (2005). A protein's final ESCRT. *Traffic* 6, 2-9.
- Babst, M., Katzmann, D. J., Snyder, W. B., Wendland, B., and Emr, S. D. (2002). Endosome-associated complex, ESCRT-II, recruits transport machinery for protein sorting at the multivesicular body. *Dev Cell* 3, 283-289.
- Babst, M., Odorizzi, G., Estepa, E. J., and Emr, S. D. (2000). Mammalian tumor susceptibility gene 101 (TSG101) and the yeast homologue, Vps23p, both function in late endosomal trafficking. *Traffic* 1, 248-258.
- Bache, K. G., Brech, A., Mehlum, A., and Stenmark, H. (2003). Hrs regulates multivesicular body formation via ESCRT recruitment to endosomes. *J Cell Biol* 162, 435-442.
- Backhaus, R., Zehe, C., Wegehingel, S., Kehlenbach, A., Schwappach, B., and Nickel, W. (2004). Unconventional protein secretion: membrane translocation of FGF-2 does not require protein unfolding. *J Cell Sci* 117, 1727-1736.
- Baird, A. (1994). Fibroblast growth factors: activities and significance of non-neurotrophin neurotrophic growth factors. *Curr Opin Neurobiol* 4, 78-86.
- Baird, A., Schubert, D., Ling, N., and Guillemin, R. (1988). Receptor- and heparin-binding domains of basic fibroblast growth factor. *Proc Natl Acad Sci U S A* 85, 2324-2328.
- Balch, W. E. (1990). Molecular dissection of early stages of the eukaryotic secretory pathway. *Curr Opin Cell Biol* 2, 634-641.

- Barlowe, C. (1998). COPII and selective export from the endoplasmic reticulum. *Biochim Biophys Acta* 1404, 67-76.
- Barlowe, C., d'Enfert, C., and Schekman, R. (1993). Purification and characterization of SAR1p, a small GTP-binding protein required for transport vesicle formation from the endoplasmic reticulum. *J Biol Chem* 268, 873-879.
- Barondes, S. H., Cooper, D. N., Gitt, M. A., and Leffler, H. (1994). Galectins. Structure and function of a large family of animal lectins. *J Biol Chem* 269, 20807-20810.
- Basilico, C., and Moscatelli, D. (1992). The FGF family of growth factors and oncogenes. *Adv Cancer Res* 59, 115-165.
- Bennett, H. S. (1956). The concepts of membrane flow and membrane vesiculation as mechanisms for active transport and ion pumping. *J Biophys Biochem Cytol* 2, 99-103.
- Bentham, M., Mazaleyrat, S., and Harris, M. (2006). Role of myristoylation and N-terminal basic residues in membrane association of the human immunodeficiency virus type 1 Nef protein. *J Gen Virol* 87, 563-571.
- Besteiro, S., Williams, R. A., Morrison, L. S., Coombs, G. H., and Mottram, J. C. (2006). Endosome sorting and autophagy are essential for differentiation and virulence of *Leishmania major*. *J Biol Chem* 281, 11384-11396.
- Bhatia, A., Daifalla, N. S., Jen, S., Badaro, R., Reed, S. G., and Skeiky, Y. A. (1999). Cloning, characterization and serological evaluation of K9 and K26: two related hydrophilic antigens of *Leishmania chagasi*. *Mol Biochem Parasitol* 102, 249-261.
- Bhatnagar, R. S., and Gordon, J. I. (1997). Understanding covalent modifications of proteins by lipids: where cell biology and biophysics mingle. *Trends Cell Biol* 7, 14-20.
- Bielli, A., Haney, C. J., Gabreski, G., Watkins, S. C., Bannykh, S. I., and Aridor, M. (2005). Regulation of Sar1 NH2 terminus by GTP binding and hydrolysis promotes membrane deformation to control COPII vesicle fission. *J Cell Biol* 171, 919-924.
- Bijlmakers, M. J., and Marsh, M. (1999). Trafficking of an acylated cytosolic protein: newly synthesized p56(lck) travels to the plasma membrane via the exocytic pathway. *J Cell Biol* 145, 457-468.
- Bijlmakers, M. J., and Marsh, M. (2003). The on-off story of protein palmitoylation. *Trends Cell Biol* 13, 32-42.
- Bikfalvi, A., Klein, S., Pintucci, G., Quarto, N., Mignatti, P., and Rifkin, D. B. (1995). Differential modulation of cell phenotype by different molecular weight forms of basic fibroblast growth factor: possible intracellular signaling by the high molecular weight forms. *J Cell Biol* 129, 233-243.
- Bikfalvi, A., Klein, S., Pintucci, G., and Rifkin, D. B. (1997). Biological roles of fibroblast growth factor-2. *Endocr Rev* 18, 26-45.
- Bishop, N., Horman, A., and Woodman, P. (2002). Mammalian class E vps proteins recognize ubiquitin and act in the removal of endosomal protein-ubiquitin conjugates. *J Cell Biol* 157, 91-101.
- Blobel, G., and Dobberstein, B. (1975a). Transfer of proteins across membranes. I. Presence of proteolytically processed and unprocessed nascent immunoglobulin light chains on membrane-bound ribosomes of murine myeloma. *J Cell Biol* 67, 835-851.
- Blobel, G., and Dobberstein, B. (1975b). Transfer to proteins across membranes. II. Reconstitution of functional rough microsomes from heterologous components. *J Cell Biol* 67, 852-862.

- Blott, E. J., and Griffiths, G. M. (2002). Secretory lysosomes. *Nat Rev Mol Cell Biol* 3, 122-131.
- Bock, J. B., Matern, H. T., Peden, A. A., and Scheller, R. H. (2001). A genomic perspective on membrane compartment organization. *Nature* 409, 839-841.
- Bohlen, P., Baird, A., Esch, F., Ling, N., and Gospodarowicz, D. (1984). Isolation and partial molecular characterization of pituitary fibroblast growth factor. *Proc Natl Acad Sci U S A* 81, 5364-5368.
- Bonatti, S., Migliaccio, G., and Simons, K. (1989). Palmitylation of viral membrane glycoproteins takes place after exit from the endoplasmic reticulum. *J Biol Chem* 264, 12590-12595.
- Bonifacino, J. S., and Glick, B. S. (2004). The mechanisms of vesicle budding and fusion. *Cell* 116, 153-166.
- Bordier, C. (1987). The promastigote surface protease of *Leishmania*. *Parasitol Today* 3, 151-153.
- Borgese, N., Mok, W., Kreibich, G., and Sabatini, D. D. (1974). Ribosomal-membrane interaction: in vitro binding of ribosomes to microsomal membranes. *J Mol Biol* 88, 559-580.
- Brewer, C. F., Miceli, M. C., and Baum, L. G. (2002). Clusters, bundles, arrays and lattices: novel mechanisms for lectin-saccharide-mediated cellular interactions. *Curr Opin Struct Biol* 12, 616-623.
- Brittingham, A., Morrison, C. J., McMaster, W. R., McGwire, B. S., Chang, K. P., and Mosser, D. M. (1995). Role of the *Leishmania* surface protease gp63 in complement fixation, cell adhesion, and resistance to complement-mediated lysis. *J Immunol* 155, 3102-3111.
- Brodsky, F. M. (1988). Living with clathrin: its role in intracellular membrane traffic. *Science* 242, 1396-1402 issn: 0036-8075.
- Bruhl, H., Wagner, K., Kellner, H., Schattenkirchner, M., Schlondorff, D., and Mack, M. (2001). Surface expression of CC- and CXC-chemokine receptors on leucocyte subsets in inflammatory joint diseases. *Clin Exp Immunol* 126, 551-559.
- Bucci, C., Parton, R. G., Mather, I. H., Stunnenberg, H., Simons, K., Hoflack, B., and Zerial, M. (1992). The Small GTPase rab5 Functions as a Regulatory Factor in the Early Endocytic Pathway. *Cell* 70, 715-728.
- Burgess, W. H., and Maciag, T. (1989). The heparin-binding (fibroblast) growth factor family of proteins. *Annu Rev Biochem* 58, 575-606.
- Burgess, W. H., Shaheen, A. M., Ravera, M., Jaye, M., Donohue, P. J., and Winkles, J. A. (1990). Possible dissociation of the heparin-binding and mitogenic activities of heparin-binding (acidic fibroblast) growth factor-1 from its receptor-binding activities by site-directed mutagenesis of a single lysine residue. *J Cell Biol* 111, 2129-2138.
- Charras, G. T., Yarrow, J. C., Horton, M. A., Mahadevan, L., and Mitchison, T. J. (2005). Non-equilibration of hydrostatic pressure in blebbing cells. *Nature* 435, 365-369.
- Chatellard-Causse, C., Blot, B., Cristina, N., Torch, S., Missotten, M., and Sadoul, R. (2002). Alix (ALG-2-interacting protein X), a protein involved in apoptosis, binds to endophilins and induces cytoplasmic vacuolization. *J Biol Chem* 277, 29108-29115.
- Chou, M. T., Wang, J., and Fujita, D. J. (2002). Src kinase becomes preferentially associated with the VEGFR, KDR/Flk-1, following VEGF stimulation of vascular endothelial cells. *BMC Biochem* 3, 32.

- Christofori, G., and Luef, S. (1997). Novel forms of acidic fibroblast growth factor-1 are constitutively exported by beta tumor cell lines independent from conventional secretion and apoptosis. *Angiogenesis* 1, 55-70.
- Clapham, D. E., and Sneyd, J. (1995). Intracellular calcium waves. *Adv Second Messenger Phosphoprotein Res* 30, 1-24.
- Clark, R., and Griffiths, G. M. (2003). Lytic granules, secretory lysosomes and disease. *Curr Opin Immunol* 15, 516-521.
- Cleves, A. E. (1997). Protein transports: the nonclassical ins and outs. *Curr Biol* 7, R318-320.
- Cleves, A. E., Cooper, D. N., Barondes, S. H., and Kelly, R. B. (1996). A new pathway for protein export in *Saccharomyces cerevisiae*. *J Cell Biol* 133, 1017-1026.
- Coleman, M. L., Sahai, E. A., Yeo, M., Bosch, M., Dewar, A., and Olson, M. F. (2001). Membrane blebbing during apoptosis results from caspase-mediated activation of ROCK I. *Nat Cell Biol* 3, 339-345.
- Cooper, D. N., and Barondes, S. H. (1990). Evidence for export of a muscle lectin from cytosol to extracellular matrix and for a novel secretory mechanism. *J Cell Biol* 110, 1681-1691.
- Cosson, P., and Letourneur, F. (1994). Coatamer interaction with di-lysine endoplasmic reticulum retention motifs. *Science* 263, 1629-1631.
- Coulson, R. M., and Smith, D. F. (1990). Isolation of genes showing increased or unique expression in the infective promastigotes of *Leishmania major*. *Mol Biochem Parasitol* 40, 63-75.
- Croft, S. L., Snowden, D., and Yardley, V. (1996). The activities of four anticancer alkyllysophospholipids against *Leishmania donovani*, *Trypanosoma cruzi* and *Trypanosoma brucei*. *J Antimicrob Chemother* 38, 1041-1047.
- Crowley, K. S., Reinhart, G. D., and Johnson, A. E. (1993). The signal sequence moves through a ribosomal tunnel into a noncytoplasmic aqueous environment at the ER membrane early in translocation. *Cell* 73, 1101-1115.
- Cunningham, C. C. (1995). Actin polymerization and intracellular solvent flow in cell surface blebbing. *J Cell Biol* 129, 1589-1599.
- Cupers, P., Veithen, A., Kiss, A., Baudhuin, P., and Courtoy, P. J. (1994). Clathrin polymerization is not required for bulk-phase endocytosis in rat fetal fibroblasts. *J-Cell-Biol* 127, 725-735 issn: 0021-9525.
- Dahl, J. P., Binda, A., Canfield, V. A., and Levenson, R. (2000). Participation of Na,K-ATPase in FGF-2 Secretion: Rescue of Ouabain- Inhibitable FGF-2 Secretion by Ouabain-Resistant Na,K-ATPase alpha Subunits. *Biochemistry* 39, 14877-14883.
- Dalbey, R. E., and Von Heijne, G. (1992). Signal peptidases in prokaryotes and eukaryotes--a new protease family. *Trends Biochem Sci* 17, 474-478.
- Davey, R. A., Hamson, C. A., Healey, J. J., and Cunningham, J. M. (1997). In vitro binding of purified murine ecotropic retrovirus envelope surface protein to its receptor, MCAT-1. *J Virol* 71, 8096-8102.
- Davies, C. R., Kaye, P., Croft, S. L., and Sundar, S. (2003). Leishmaniasis: new approaches to disease control. *Bmj* 326, 377-382.

- Deichaite, I., Casson, L. P., Ling, H. P., and Resh, M. D. (1988). In vitro synthesis of pp60v-src: myristylation in a cell-free system. *Mol Cell Biol* 8, 4295-4301.
- Denny, P. W., Gokool, S., Russell, D. G., Field, M. C., and Smith, D. F. (2000). Acylation-dependent protein export in *Leishmania*. *J Biol Chem* 275, 11017-11025.
- Denzer, K., Kleijmeer, M. J., Heijnen, H. F., Stoorvogel, W., and Geuze, H. J. (2000). Exosome: from internal vesicle of the multivesicular body to intercellular signaling device. *J Cell Sci* 113 Pt 19, 3365-3374.
- Depierre, J. W., and Dallner, G. (1975). Structural aspects of the membrane of the endoplasmic reticulum. *Biochim Biophys Acta* 415, 411-472.
- Dingwall, C., and Laskey, R. (1992). The nuclear membrane. *Science* 258, 942-947.
- Dunphy, J. T., Greentree, W. K., Manahan, C. L., and Linder, M. E. (1996). G-protein palmitoyltransferase activity is enriched in plasma membranes. *J Biol Chem* 271, 7154-7159.
- Elbashir, S. M., Harborth, J., Lendeckel, W., Yalcin, A., Weber, K., and Tuschl, T. (2001). Duplexes of 21-nucleotide RNAs mediate RNA interference in cultured mammalian cells. *Nature* 411, 494-498.
- Elliott, G., and O'Hare, P. (1997). Intercellular trafficking and protein delivery by a herpesvirus structural protein. *Cell* 88, 223-233.
- Engling, A., Backhaus, R., Stegmayer, C., Zehe, C., Seelenmeyer, C., Kehlenbach, A., Schwappach, B., Wegehingel, S., and Nickel, W. (2002). Biosynthetic FGF-2 is targeted to non-lipid raft microdomains following translocation to the extracellular surface of CHO cells. *J Cell Sci* 115, 3619-3631.
- Ensoli, B., Buonaguro, L., Barillari, G., Fiorelli, V., Gendelman, R., Morgan, R. A., Wingfield, P., and Gallo, R. C. (1993). Release, uptake, and effects of extracellular human immunodeficiency virus type 1 Tat protein on cell growth and viral transactivation. *J Virol* 67, 277-287.
- Eriksson, A. E., Cousens, L. S., Weaver, L. H., and Matthews, B. W. (1991). Three-dimensional structure of human basic fibroblast growth factor. *Proc Natl Acad Sci U S A* 88, 3441-3445.
- Faham, S., Hileman, R. E., Fromm, J. R., Linhardt, R. J., and Rees, D. C. (1996). Heparin structure and interactions with basic fibroblast growth factor. *Science* 271, 1116-1120.
- Faham, S., Linhardt, R. J., and Rees, D. C. (1998). Diversity does make a difference: fibroblast growth factor-heparin interactions. *Curr Opin Struct Biol* 8, 578-586.
- Faix, J., and Grosse, R. (2006). Staying in shape with formins. *Dev Cell* 10, 693-706.
- Fallon, J. F., Lopez, A., Ros, M. A., Savage, M. P., Olwin, B. B., and Simandl, B. K. (1994). FGF-2: apical ectodermal ridge growth signal for chick limb development. *Science* 264, 104-107.
- Ferguson, M. A., Brimacombe, J. S., Cottaz, S., Field, R. A., Guthrie, L. S., Homans, S. W., McConville, M. J., Mehlert, A., Milne, K. G., Ralton, J. E., and et al. (1994). Glycosyl-phosphatidylinositol molecules of the parasite and the host. *Parasitology* 108 Suppl, S45-54.
- Ferrara, N. (1999). Role of vascular endothelial growth factor in the regulation of angiogenesis. *Kidney Int* 56, 794-814.
- Fevrier, B., Vilette, D., Laude, H., and Raposo, G. (2005). Exosomes: a bubble ride for prions? *Traffic* 6, 10-17.

- Flieger, O., Engling, A., Bucala, R., Lue, H., Nickel, W., and Bernhagen, J. (2003). Regulated secretion of macrophage migration inhibitory factor is mediated by a non-classical pathway involving an ABC transporter. *FEBS Lett* **551**, 78-86.
- Flinn, H. M., Rangarajan, D., and Smith, D. F. (1994). Expression of a hydrophilic surface protein in infective stages of *Leishmania major*. *Mol Biochem Parasitol* **65**, 259-270.
- Flinn, H. M., and Smith, D. F. (1992). Genomic organisation and expression of a differentially-regulated gene family from *Leishmania major*. *Nucleic Acids Res* **20**, 755-762.
- Florkiewicz, R. Z., Anchin, J., and Baird, A. (1998). The inhibition of fibroblast growth factor-2 export by cardenolides implies a novel function for the catalytic subunit of Na⁺,K⁺-ATPase. *J Biol Chem* **273**, 544-551.
- Florkiewicz, R. Z., Majack, R. A., Buechler, R. D., and Florkiewicz, E. (1995). Quantitative export of FGF-2 occurs through an alternative, energy- dependent, non-ER/Golgi pathway. *J Cell Physiol* **162**, 388-399.
- Florkiewicz, R. Z., and Sommer, A. (1989). Human basic fibroblast growth factor gene encodes four polypeptides: three initiate translation from non-AUG codons. *Proc Natl Acad Sci U S A* **86**, 3978-3981.
- Franke, E. D., McGreevy, P. B., Katz, S. P., and Sacks, D. L. (1985). Growth cycle-dependent generation of complement-resistant *Leishmania* promastigotes. *J Immunol* **134**, 2713-2718.
- Freyssinet, J. M. (2003). Cellular microparticles: what are they bad or good for? *J Thromb Haemost* **1**, 1655-1662.
- Fujiki, Y., Hubbard, A. L., Fowler, S., and Lazarow, P. B. (1982). Isolation of intracellular membranes by means of sodium carbonate treatment: application to endoplasmic reticulum. *J Cell Biol* **93**, 97-102.
- Futter, C. E., Gibson, A., Allchin, E. H., Maxwell, S., Ruddock, L. J., Odorizzi, G., Domingo, D., Trowbridge, I. S., and Hopkins, C. R. (1998). In polarized MDCK cells basolateral vesicles arise from clathrin-gamma-adaptin-coated domains on endosomal tubules. *J Cell Biol* **141**, 611-623.
- Futter, C. E., Pearse, A., Hewlett, L. J., and Hopkins, C. R. (1996). Multivesicular endosomes containing internalized EGF-EGF receptor complexes mature and then fuse directly with lysosomes. *J Cell Biol* **132**, 1011-1023.
- Gal, S., and Raikhel, N. V. (1993). Protein sorting in the endomembrane system of plant cells. *Curr Opin Cell Biol* **5**, 636-640.
- Garrus, J. E., von Schwedler, U. K., Pornillos, O. W., Morham, S. G., Zavitz, K. H., Wang, H. E., Wettstein, D. A., Stray, K. M., Cote, M., Rich, R. L., *et al.* (2001). Tsg101 and the vacuolar protein sorting pathway are essential for HIV-1 budding. *Cell* **107**, 55-65.
- Gasteier, J. E., Madrid, R., Krautkramer, E., Schroder, S., Muranyi, W., Benichou, S., and Fackler, O. T. (2003). Activation of the Rac-binding partner FHOD1 induces actin stress fibers via a ROCK-dependent mechanism. *J Biol Chem* **278**, 38902-38912.
- Gasteier, J. E., Schroeder, S., Muranyi, W., Madrid, R., Benichou, S., and Fackler, O. T. (2005). FHOD1 coordinates actin filament and microtubule alignment to mediate cell elongation. *Exp Cell Res* **306**, 192-202.
- Gilmore, R. (1993). Protein translocation across the endoplasmic reticulum: a tunnel with toll booths at entry and exit [comment]. *Cell* **75**, 589-592 issn: 0092-8674.

- Gleizes, P. E., Noaillac-Depeyre, J., Amalric, F., and Gas, N. (1995). Basic fibroblast growth factor (FGF-2) internalization through the heparan sulfate proteoglycans-mediated pathway: an ultrastructural approach. *Eur J Cell Biol* 66, 47-59.
- Goerlich, D., Prehn, S., Hartmann, E., Kalies, K. U., and Rapoport, T. A. (1992). A Mammalian Homolog of SEC61p and SECYp Is Associated with Ribosomes and Nascent Polypeptides during Translocation. *Cell* 71, 489-503.
- Goldberg, J. (1998). Structural basis for activation of ARF GTPase: mechanisms of guanine nucleotide exchange and GTP-myristoyl switching. *Cell* 95, 237-248.
- Goldberg, J. (1999). Structural and functional analysis of the ARF1-ARFGAP complex reveals a role for coatamer in GTP hydrolysis. *Cell* 96, 893-902.
- Goldberg, J. (2000). Decoding of sorting signals by coatamer through a GTPase switch in the COPI coat complex. *Cell* 100, 671-679.
- Goletz, S., Hanisch, F. G., and Karsten, U. (1997). Novel alphaGalNAc containing glycans on cytokeratins are recognized invitro by galectins with type II carbohydrate recognition domains. *J Cell Sci* 110 (Pt 14), 1585-1596.
- Gonzalo, S., and Linder, M. E. (1998). SNAP-25 palmitoylation and plasma membrane targeting require a functional secretory pathway. *Mol Biol Cell* 9, 585-597.
- Gospodarowicz, D., Ferrara, N., Schweigener, L., and Neufeld, G. (1987). Structural characterization and biological functions of fibroblast growth factor. *Endocr Rev* 8, 95-114.
- Greco, V., Hannus, M., and Eaton, S. (2001). Argosomes: a potential vehicle for the spread of morphogens through epithelia. *Cell* 106, 633-645.
- Gruenberg, J., and Clague, M. J. (1992). Regulation of intracellular membrane transport. *Curr Opin Cell Biol* 4, 593-599.
- Gruenberg, J., and Stenmark, H. (2004). The biogenesis of multivesicular endosomes. *Nat Rev Mol Cell Biol* 5, 317-323.
- Hartmann, E., Rapoport, T. A., and Lodish, H. F. (1989). Predicting the orientation of eukaryotic membrane-spanning proteins. *Proc Natl Acad Sci U S A* 86, 5786-5790.
- He, J., and Baum, L. G. (2004). Presentation of galectin-1 by extracellular matrix triggers T cell death. *J Biol Chem* 279, 4705-4712.
- Heijnen, H. F., Schiel, A. E., Fijnheer, R., Geuze, H. J., and Sixma, J. J. (1999). Activated platelets release two types of membrane vesicles: microvesicles by surface shedding and exosomes derived from exocytosis of multivesicular bodies and alpha-granules. *Blood* 94, 3791-3799.
- Helms, J. B., and Rothman, J. E. (1992). Inhibition by Brefeldin A of a Golgi membrane enzyme that catalyses exchange of a guanine nucleotide bound to ARF. *Nature* 360, 352-354.
- Henrick, K., Bawumia, S., Barboni, E. A., Mehul, B., and Hughes, R. C. (1998). Evidence for subsites in the galectins involved in sugar binding at the nonreducing end of the central galactose of oligosaccharide ligands: sequence analysis, homology modeling and mutagenesis studies of hamster galectin-3. *Glycobiology* 8, 45-57.
- High, S., and Dobberstein, B. (1992). Mechanisms that determine the transmembrane disposition of proteins. *Curr Opin Cell Biol* 4, 581-586.

- High, S., Gorlich, D., Wiedmann, M., Rapoport, T. A., and Dobberstein, B. (1991). The identification of proteins in the proximity of signal-anchor sequences during their targeting to and insertion into the membrane of the ER. *J Cell Biol* 113, 35-44.
- Hirsch, A. J., Medigeschi, G. R., Meyers, H. L., DeFilippis, V., Fruh, K., Briese, T., Lipkin, W. I., and Nelson, J. A. (2005). The Src family kinase c-Yes is required for maturation of West Nile virus particles. *J Virol* 79, 11943-11951.
- Hoffmann, M. K. (1980). Antigen-specific induction and regulation of antibody synthesis in cultures of human peripheral blood mononuclear cells. *Proc Natl Acad Sci U S A* 77, 1139-1143.
- Hong, W., and Tang, B. L. (1993). Protein trafficking along the exocytotic pathway. *Bioessays* 15, 231-238.
- Huflejt, M. E., Jordan, E. T., Gitt, M. A., Barondes, S. H., and Leffler, H. (1997). Strikingly different localization of galectin-3 and galectin-4 in human colon adenocarcinoma T84 cells. Galectin-4 is localized at sites of cell adhesion. *J Biol Chem* 272, 14294-14303.
- Hugel, B., Martinez, M. C., Kunzelmann, C., and Freyssinet, J. M. (2005). Membrane microparticles: two sides of the coin. *Physiology (Bethesda)* 20, 22-27.
- Hughes, R. C. (1997). The galectin family of mammalian carbohydrate-binding molecules. *Biochem Soc Trans* 25, 1194-1198.
- Hughes, R. C. (1999). Secretion of the galectin family of mammalian carbohydrate-binding proteins. *Biochim Biophys Acta* 1473, 172-185.
- Hurley, J. H., and Emr, S. D. (2006). The ESCRT complexes: structure and mechanism of a membrane-trafficking network. *Annu Rev Biophys Biomol Struct* 35, 277-298.
- Ilgoutz, S. C., and McConville, M. J. (2001). Function and assembly of the Leishmania surface coat. *Int J Parasitol* 31, 899-908.
- Jackson, A., Friedman, S., Zhan, X., Engleka, K. A., Forough, R., and Maciag, T. (1992). Heat shock induces the release of fibroblast growth factor 1 from NIH 3T3 cells. *Proc Natl Acad Sci U S A* 89, 10691-10695.
- Jackson, A., Tarantini, F., Gamble, S., Friedman, S., and Maciag, T. (1995). The release of fibroblast growth factor-1 from NIH 3T3 cells in response to temperature involves the function of cysteine residues. *J Biol Chem* 270, 33-36.
- Jahn, R., and Grubmuller, H. (2002). Membrane fusion. *Curr Opin Cell Biol* 14, 488-495.
- Jahn, R., and Sudhof, T. C. (1999). Membrane fusion and exocytosis. *Annu Rev Biochem* 68, 863-911.
- Jang, S. K., Krausslich, H. G., Nicklin, M. J., Duke, G. M., Palmenberg, A. C., and Wimmer, E. (1988). A segment of the 5' nontranslated region of encephalomyocarditis virus RNA directs internal entry of ribosomes during in vitro translation. *J Virol* 62, 2636-2643.
- Jensen, A. T., Gasim, S., Moller, T., Ismail, A., Gaafar, A., Kemp, M., el Hassan, A. M., Kharazmi, A., Alce, T. M., Smith, D. F., and Theander, T. G. (1999). Serodiagnosis of Leishmania donovani infections: assessment of enzyme-linked immunosorbent assays using recombinant L. donovani gene B protein (GBP) and a peptide sequence of L. donovani GBP. *Trans R Soc Trop Med Hyg* 93, 157-160.

- Johnson, D. E., and Williams, L. T. (1993). Structural and functional diversity in the FGF receptor multigene family. *Adv Cancer Res* 60, 1-41.
- Jones, A. L., and Fawcett, D. W. (1966). Hypertrophy of the agranular endoplasmic reticulum in hamster liver induced by phenobarbital (with a review on the functions of this organelle in liver). *J Histochem Cytochem* 14, 215-232.
- Joshi, P. B., Sacks, D. L., Modi, G., and McMaster, W. R. (1998). Targeted gene deletion of *Leishmania major* genes encoding developmental stage-specific leishmanolysin (GP63). *Mol Microbiol* 27, 519-530.
- Joubert, R., Caron, M., Avellana-Adalid, V., Mornet, D., and Bladier, D. (1992). Human brain lectin: a soluble lectin that binds actin. *J Neurochem* 58, 200-203.
- Kaplan, K. B., Swedlow, J. R., Varmus, H. E., and Morgan, D. O. (1992). Association of p60c-src with endosomal membranes in mammalian fibroblasts. *J Cell Biol* 118, 321-333.
- Katz, M., Shtiegman, K., Tal-Or, P., Yakir, L., Mosesson, Y., Harari, D., Machluf, Y., Asao, H., Jovin, T., Sugamura, K., and Yarden, Y. (2002). Ligand-independent degradation of epidermal growth factor receptor involves receptor ubiquitylation and Hgs, an adaptor whose ubiquitin-interacting motif targets ubiquitylation by Nedd4. *Traffic* 3, 740-751.
- Katzmann, D. J., Babst, M., and Emr, S. D. (2001). Ubiquitin-dependent sorting into the multivesicular body pathway requires the function of a conserved endosomal protein sorting complex, ESCRT-I. *Cell* 106, 145-155.
- Katzmann, D. J., Stefan, C. J., Babst, M., and Emr, S. D. (2003). Vps27 recruits ESCRT machinery to endosomes during MVB sorting. *J Cell Biol* 162, 413-423.
- Keenan, R. J., Freymann, D. M., Stroud, R. M., and Walter, P. (2001). The signal recognition particle. *Annu Rev Biochem* 70, 755-775.
- Keller, P., and Simons, K. (1997). Post-Golgi biosynthetic trafficking. *J Cell Sci* 110 (Pt 24), 3001-3009.
- Kirchhausen, T. (2000). Three ways to make a vesicle. *Nat Rev Mol Cell Biol* 1, 187-198.
- Kleijmeer, M., Ramm, G., Schuurhuis, D., Griffith, J., Rescigno, M., Ricciardi-Castagnoli, P., Rudensky, A. Y., Ossendorp, F., Melief, C. J., Stoorvogel, W., and Geuze, H. J. (2001). Reorganization of multivesicular bodies regulates MHC class II antigen presentation by dendritic cells. *J Cell Biol* 155, 53-63.
- Knuepfer, E., Stierhof, Y. D., McKean, P. G., and Smith, D. F. (2001). Characterization of a differentially expressed protein that shows an unusual localization to intracellular membranes in *Leishmania major*. *Biochem J* 356, 335-344.
- Kopitz, J., von Reitzenstein, C., Burchert, M., Cantz, M., and Gabius, H. J. (1998). Galectin-1 is a major receptor for ganglioside GM1, a product of the growth-controlling activity of a cell surface ganglioside sialidase, on human neuroblastoma cells in culture. *J Biol Chem* 273, 11205-11211.
- Kyte, J., and Doolittle, R. F. (1982). A simple method for displaying the hydropathic character of a protein. *J Mol Biol* 157, 105-132.
- Laemmli, U. K., Beguin, F., and Gujer-Kellenberger, G. (1970). A factor preventing the major head protein of bacteriophage T4 from random aggregation. *J Mol Biol* 47, 69-85.

- Landriscina, M., Soldi, R., Bagala, C., Micucci, I., Bellum, S., Tarantini, F., Prudovsky, I., and Maciag, T. (2001). S100a13 participates in the release of fibroblast growth factor 1 in response to heat shock in vitro. *J Biol Chem* 276, 22544-22552.
- LaVallee, T. M., Tarantini, F., Gamble, S., Carreira, C. M., Jackson, A., and Maciag, T. (1998). Synaptotagmin-1 is required for fibroblast growth factor-1 release. *J Biol Chem* 273, 22217-22223.
- Lawyer, F. C., Stoffel, S., Saiki, R. K., Myambo, K., Drummond, R., and Gelfand, D. H. (1989). Isolation, characterization, and expression in *Escherichia coli* of the DNA polymerase gene from *Thermus aquaticus*. *J Biol Chem* 264, 6427-6437.
- Lecellier, C. H., Vermeulen, W., Bachelierie, F., Giron, M. L., and Saib, A. (2002). Intra- and intercellular trafficking of the foamy virus auxiliary bet protein. *J Virol* 76, 3388-3394.
- Lee, C., and Chen, L. B. (1988). Dynamic behavior of endoplasmic reticulum in living cells. *Cell* 54, 37-46.
- Lee, M. C., Miller, E. A., Goldberg, J., Orci, L., and Schekman, R. (2004). Bi-directional protein transport between the ER and Golgi. *Annu Rev Cell Dev Biol* 20, 87-123.
- Letourneur, F., Gaynor, E. C., Hennecke, S., Demolliere, C., Duden, R., Emr, S. D., Riezman, H., and Cosson, P. (1994). Coatamer is essential for retrieval of dilysine-tagged proteins to the endoplasmic reticulum. *Cell* 79, 1199-1207.
- Leverrier, Y., and Ridley, A. J. (2001). Apoptosis: caspases orchestrate the ROCK 'n' bleb. *Nat Cell Biol* 3, E91-93.
- Lewis, M. J., and Pelham, H. R. (1992). Ligand-induced redistribution of a human KDEL receptor from the Golgi complex to the endoplasmic reticulum. *Cell* 68, 353-364.
- Liang, X., Lu, Y., Wilkes, M., Neubert, T. A., and Resh, M. D. (2004). The N-terminal SH4 region of the Src family kinase Fyn is modified by methylation and heterogeneous fatty acylation: role in membrane targeting, cell adhesion, and spreading. *J Biol Chem* 279, 8133-8139.
- Liekens, S., Neyts, J., De Clercq, E., Verbeken, E., Ribatti, D., and Presta, M. (2001). Inhibition of fibroblast growth factor-2-induced vascular tumor formation by the acyclic nucleoside phosphonate cidofovir. *Cancer Res* 61, 5057-5064.
- Lindquist, S. (1986). The heat-shock response. *Annu Rev Biochem* 55, 1151-1191.
- Lindstedt, R., Apodaca, G., Barondes, S. H., Mostov, K. E., and Leffler, H. (1993). Apical secretion of a cytosolic protein by Madin-Darby canine kidney cells. Evidence for polarized release of an endogenous lectin by a nonclassical secretory pathway. *J Biol Chem* 268, 11750-11757.
- Linstedt, A. D., Vetter, M. L., Bishop, J. M., and Kelly, R. B. (1992). Specific association of the proto-oncogene product pp60c-src with an intracellular organelle, the PC12 synaptic vesicle. *J Cell Biol* 117, 1077-1084.
- Lippincott-Schwartz, J. (1993). Bidirectional membrane traffic between the endoplasmic reticulum and Golgi apparatus. *Trends Cell Biol* 3, 81-88.
- Lippincott-Schwartz, J., Yuan, L. C., Bonifacino, J. S., and Klausner, R. D. (1989). Rapid redistribution of Golgi proteins into the ER in cells treated with brefeldin A: evidence for membrane cycling from Golgi to ER. *Cell* 56, 801-813.
- Liu, F. T., and Rabinovich, G. A. (2005). Galectins as modulators of tumour progression. *Nat Rev Cancer* 5, 29-41.

- Liu, X., Constantinescu, S. N., Sun, Y., Bogan, J. S., Hirsch, D., Weinberg, R. A., and Lodish, H. F. (2000). Generation of mammalian cells stably expressing multiple genes at predetermined levels. *Anal Biochem* 280, 20-28.
- Logan, A., Frautschy, S. A., and Baird, A. (1991). Basic fibroblast growth factor and central nervous system injury. *Ann N Y Acad Sci* 638, 474-476.
- Lukyanov, P., Furtak, V., and Ochieng, J. (2005). Galectin-3 interacts with membrane lipids and penetrates the lipid bilayer. *Biochem Biophys Res Commun* 338, 1031-1036.
- Lutomski, D., Fouillit, M., Bourin, P., Mellottee, D., Denize, N., Pontet, M., Bladier, D., Caron, M., and Joubert-Caron, R. (1997). Externalization and binding of galectin-1 on cell surface of K562 cells upon erythroid differentiation. *Glycobiology* 7, 1193-1199.
- Maizel, A., Tassetto, M., Filhol, O., Cochet, C., Prochiantz, A., and Joliot, A. (2002). Engrailed homeoprotein secretion is a regulated process. *Development* 129, 3545-3553.
- Mandinova, A., Soldi, R., Graziani, I., Bagala, C., Bellum, S., Landriscina, M., Tarantini, F., Prudovsky, I., and Maciag, T. (2003). S100A13 mediates the copper-dependent stress-induced release of IL-1{alpha} from both human U937 and murine NIH 3T3 cells. *J Cell Sci Pt*.
- Marshall, M. (1995). Interactions between Ras and Raf: key regulatory proteins in cellular transformation. *Mol Reprod Dev* 42, 493-499.
- Martinez, M. C., Tesse, A., Zobairi, F., and Andriantsitohaina, R. (2005). Shed membrane microparticles from circulating and vascular cells in regulating vascular function. *Am J Physiol Heart Circ Physiol* 288, H1004-1009.
- Martinez-Menarguez, J. A., Geuze, H. J., Slot, J. W., and Klumperman, J. (1999). Vesicular tubular clusters between the ER and Golgi mediate concentration of soluble secretory proteins by exclusion from COPI- coated vesicles. *Cell* 98, 81-90.
- Matsuoka, K., Orci, L., Amherdt, M., Bednarek, S. Y., Hamamoto, S., Schekman, R., and Yeung, T. (1998). COPII-coated vesicle formation reconstituted with purified coat proteins and chemically defined liposomes. *Cell* 93, 263-275.
- McAvoy, J. W., Chamberlain, C. G., de longh, R. U., Richardson, N. A., and Lovicu, F. J. (1991). The role of fibroblast growth factor in eye lens development. *Ann N Y Acad Sci* 638, 256-274.
- McConville, M. J., Turco, S. J., Ferguson, M. A., and Sacks, D. L. (1992). Developmental modification of lipophosphoglycan during the differentiation of *Leishmania major* promastigotes to an infectious stage. *Embo J* 11, 3593-3600.
- McKean, P. G., Denny, P. W., Knuepfer, E., Keen, J. K., and Smith, D. F. (2001). Phenotypic changes associated with deletion and overexpression of a stage-regulated gene family in *Leishmania*. *Cell Microbiol* 3, 511-523.
- McKean, P. G., Trenholme, K. R., Rangarajan, D., Keen, J. K., and Smith, D. F. (1997). Diversity in repeat-containing surface proteins of *Leishmania major*. *Mol Biochem Parasitol* 86, 225-235.
- McNeil, P. L., Muthukrishnan, L., Warder, E., and D'Amore, P. A. (1989). Growth factors are released by mechanically wounded endothelial cells. *J Cell Biol* 109, 811-822.
- Mehul, B., and Hughes, R. C. (1997). Plasma membrane targetting, vesicular budding and release of galectin 3 from the cytoplasm of mammalian cells during secretion. *J Cell Sci* 110 (Pt 10), 1169-1178.

- Mellman, I., and Warren, G. (2000). The road taken: past and future foundations of membrane traffic. *Cell* 100, 99-112.
- Mignatti, P., Morimoto, T., and Rifkin, D. B. (1992). Basic fibroblast growth factor, a protein devoid of secretory signal sequence, is released by cells via a pathway independent of the endoplasmic reticulum-Golgi complex. *J Cell Physiol* 151, 81-93.
- Mignatti, P., and Rifkin, D. B. (1991). Release of basic fibroblast growth factor, an angiogenic factor devoid of secretory signal sequence: a trivial phenomenon or a novel secretion mechanism? *J Cell Biochem* 47, 201-207.
- Misumi, Y., Misumi, Y., Miki, K., Takatsuki, A., Tamura, G., and Ikehara, Y. (1986). Novel blockade by brefeldin A of intracellular transport of secretory proteins in cultured rat hepatocytes. *J Biol Chem* 261, 11398-11403.
- Mollenhauer, H. H., and Morre, D. J. (1991). Perspectives on Golgi apparatus form and function. *J Electron Microsc Tech* 17, 2-14.
- Morris, S. A., Ahle, S., and Ungewickell, E. (1989). Clathrin-coated vesicles. *Curr Opin Cell Biol* 1, 684-690.
- Mosser, D. M., and Brittingham, A. (1997). Leishmania, macrophages and complement: a tale of subversion and exploitation. *Parasitology* 115 Suppl, S9-23.
- Mossessova, E., Bickford, L. C., and Goldberg, J. (2003a). SNARE selectivity of the COPII coat. *Cell* 114, 483-495.
- Mossessova, E., Corpina, R. A., and Goldberg, J. (2003b). Crystal structure of ARF1*Sec7 complexed with Brefeldin A and its implications for the guanine nucleotide exchange mechanism. *Mol Cell* 12, 1403-1411.
- Mottram, J. C., Brooks, D. R., and Coombs, G. H. (1998). Roles of cysteine proteinases of trypanosomes and Leishmania in host-parasite interactions. *Curr Opin Microbiol* 1, 455-460.
- Mouta Carreira, C., LaVallee, T. M., Tarantini, F., Jackson, A., Lathrop, J. T., Hampton, B., Burgess, W. H., and Maciag, T. (1998). S100A13 is involved in the regulation of fibroblast growth factor-1 and p40 synaptotagmin-1 release in vitro. *J Biol Chem* 273, 22224-22231.
- Muesch, A., Hartmann, E., Rohde, K., Rubartelli, A., Sitia, R., and Rapoport, T. A. (1990). A novel pathway for secretory proteins? *Trends Biochem Sci* 15, 86-88.
- Mullin, K. A., Foth, B. J., Ilgutz, S. C., Callaghan, J. M., Zawadzki, J. L., McFadden, G. I., and McConville, M. J. (2001). Regulated degradation of an endoplasmic reticulum membrane protein in a tubular lysosome in Leishmania mexicana. *Mol Biol Cell* 12, 2364-2377.
- Mullock, B. M., Bright, N. A., Fearon, C. W., Gray, S. R., and Luzio, J. P. (1998). Fusion of lysosomes with late endosomes produces a hybrid organelle of intermediate density and is NSF dependent. *J Cell Biol* 140, 591-601.
- Muthukrishnan, L., Warder, E., and McNeil, P. L. (1991). Basic fibroblast growth factor is efficiently released from a cytosolic storage site through plasma membrane disruptions of endothelial cells. *J Cell Physiol* 148, 1-16.
- Naderer, T., Vince, J. E., and McConville, M. J. (2004). Surface determinants of Leishmania parasites and their role in infectivity in the mammalian host. *Curr Mol Med* 4, 649-665.

- Nakamura, N., Rabouille, C., Watson, R., Nilsson, T., Hui, N., Slusarewicz, P., Kreis, T. E., and Warren, G. (1995). Characterization of a cis-Golgi matrix protein, GM130. *J Cell Biol* 131, 1715-1726.
- Newport, J. W., and Forbes, D. J. (1987). The nucleus: structure, function, and dynamics. *Annu Rev Biochem* 56, 535-565.
- Nickel, W. (2003). The mystery of nonclassical protein secretion. *Eur J Biochem* 270, 2109-2119.
- Nickel, W. (2005). Unconventional secretory routes: direct protein export across the plasma membrane of Mammalian cells. *Traffic* 6, 607-614.
- Nickel, W., Brugger, B., and Wieland, F. T. (1998). Protein and lipid sorting between the endoplasmic reticulum and the Golgi complex. *Semin Cell Dev Biol* 9, 493-501.
- Nickel, W., Brugger, B., and Wieland, F. T. (2002). Vesicular transport: the core machinery of COPI recruitment and budding. *J Cell Sci* 115, 3235-3240.
- Nugent, P. G., Karsani, S. A., Wait, R., Tempero, J., and Smith, D. F. (2004). Proteomic analysis of *Leishmania mexicana* differentiation. *Mol Biochem Parasitol* 136, 51-62.
- Orci, L., Stannnes, M., Ravazzola, M., Amherdt, M., Perrelet, A., Sollner, T. H., and Rothman, J. E. (1997). Bidirectional transport by distinct populations of COPI-coated vesicles. *Cell* 90, 335-349.
- Orci, L., Tagaya, M., Amherdt, M., Perrelet, A., Donaldson, J. G., Lippincott-Schwartz, J., Klausner, R. D., and Rothman, J. E. (1991). Brefeldin A, a drug that blocks secretion, prevents the assembly of non-clathrin-coated buds on Golgi cisternae. *Cell* 64, 1183-1195.
- Palade, G. (1975). Intracellular aspects of the process of protein synthesis. *Science* 189, 347-358.
- Pavel, J., Harter, C., and Wieland, F. T. (1998). Reversible dissociation of coatamer: functional characterization of a beta/delta-coat protein subcomplex. *Proc Natl Acad Sci U S A* 95, 2140-2145.
- Pearse, B. M., and Robinson, M. S. (1990). Clathrin, adaptors, and sorting. *Annu Rev Cell Biol* 6, 151-171.
- Pearse, B. M., Smith, C. J., and Owen, D. J. (2000). Clathrin coat construction in endocytosis. *Curr Opin Struct Biol* 10, 220-228.
- Peitzsch, R. M., and McLaughlin, S. (1993). Binding of acylated peptides and fatty acids to phospholipid vesicles: pertinence to myristoylated proteins. *Biochemistry* 32, 10436-10443.
- Pelham, H. R. (1990). The retention signal for soluble proteins of the endoplasmic reticulum. *Trends-Biochem-Sci* 15, 483-486 issn: 0376-5067.
- Pelham, H. R. (1991). Recycling of proteins between the endoplasmic reticulum and Golgi complex. *Curr Opin Cell Biol* 3, 585-591.
- Perillo, N. L., Marcus, M. E., and Baum, L. G. (1998). Galectins: versatile modulators of cell adhesion, cell proliferation, and cell death. *J Mol Med* 76, 402-412.
- Perillo, N. L., Pace, K. E., Seilhamer, J. J., and Baum, L. G. (1995). Apoptosis of T cells mediated by galectin-1. *Nature* 378, 736-739.
- Peters, J. H., Ruhl, S., and Friedrichs, D. (1987). Veiled accessory cells deduced from monocytes. *Immunobiology* 176, 154-166.

- Peyroche, A., Paris, S., and Jackson, C. L. (1996). Nucleotide exchange on ARF mediated by yeast Gea1 protein. *Nature* **384**, 479-481.
- Pimenta, P. F., Pinto da Silva, P., Rangarajan, D., Smith, D. F., and Sacks, D. L. (1994). *Leishmania major*: association of the differentially expressed gene B protein and the surface lipophosphoglycan as revealed by membrane capping. *Exp Parasitol* **79**, 468-479.
- Pisitkun, T., Shen, R. F., and Knepper, M. A. (2004). Identification and proteomic profiling of exosomes in human urine. *Proc Natl Acad Sci U S A* **101**, 13368-13373.
- Powers, C. J., McLeskey, S. W., and Wellstein, A. (2000). Fibroblast growth factors, their receptors and signaling. *Endocr Relat Cancer* **7**, 165-197.
- Powers, T., and Walter, P. (1996). The nascent polypeptide-associated complex modulates interactions between the signal recognition particle and the ribosome. *Curr Biol* **6**, 331-338.
- Prats, H., Kaghad, M., Prats, A. C., Klagsbrun, M., Lelias, J. M., Liauzun, P., Chalon, P., Tauber, J. P., Amalric, F., Smith, J. A., and et al. (1989). High molecular mass forms of basic fibroblast growth factor are initiated by alternative CUG codons. *Proc Natl Acad Sci U S A* **86**, 1836-1840.
- Prickett, S., Gray, P. M., Colpitts, S. L., Scott, P., Kaye, P. M., and Smith, D. F. (2006). In vivo recognition of ovalbumin expressed by transgenic *Leishmania* is determined by its subcellular localization. *J Immunol* **176**, 4826-4833.
- Prudovsky, I., Bagala, C., Tarantini, F., Mandinova, A., Soldi, R., Bellum, S., and Maciag, T. (2002). The intracellular translocation of the components of the fibroblast growth factor 1 release complex precedes their assembly prior to export. *J Cell Biol* **158**, 201-208.
- Prudovsky, I., Mandinova, A., Soldi, R., Bagala, C., Graziani, I., Landriscina, M., Tarantini, F., Duarte, M., Bellum, S., Doherty, H., and Maciag, T. (2003). The non-classical export routes: FGF1 and IL-1{alpha} point the way. *J Cell Sci* **116**, 4871-4881.
- Pryer, N. K., Wuestehube, L. J., and Schekman, R. (1992). Vesicle-mediated protein sorting. *Annu Rev Biochem* **61**, 471-516.
- Rabinovich, G. A., Rubinstein, N., and Fainboim, L. (2002). Unlocking the secrets of galectins: a challenge at the frontier of glyco-immunology. *J Leukoc Biol* **71**, 741-752.
- Raiborg, C., Rusten, T. E., and Stenmark, H. (2003). Protein sorting into multivesicular endosomes. *Curr Opin Cell Biol* **15**, 446-455.
- Ramamoorthy, R., Donelson, J. E., Paetz, K. E., Maybodi, M., Roberts, S. C., and Wilson, M. E. (1992). Three distinct RNAs for the surface protease gp63 are differentially expressed during development of *Leishmania donovani* chagasi promastigotes to an infectious form. *J Biol Chem* **267**, 1888-1895.
- Raman, R., Venkataraman, G., Ernst, S., Sasisekharan, V., and Sasisekharan, R. (2003). Structural specificity of heparin binding in the fibroblast growth factor family of proteins. *Proc Natl Acad Sci U S A* **100**, 2357-2362.
- Rambourg, A., and Clermont, Y. (1990). Three-dimensional electron microscopy: structure of the Golgi apparatus. *Eur J Cell Biol* **51**, 189-200.
- Rangarajan, D., Gokool, S., McCrossan, M. V., and Smith, D. F. (1995). The gene B protein localises to the surface of *Leishmania major* parasites in the absence of metacyclic stage lipophosphoglycan. *J Cell Sci* **108** (Pt 11), 3359-3366.

- Rapoport, T. A. (1992). Transport of proteins across the endoplasmic reticulum membrane. *Science* 258, 931-936.
- Rapoport, T. A., Gorlich, D., Musch, A., Hartmann, E., Prehn, S., Wiedmann, M., Otto, A., Kostka, S., and Kraft, R. (1992). Components and mechanism of protein translocation across the ER membrane. *Antonie Van Leeuwenhoek* 61, 119-122.
- Reggiori, F., and Pelham, H. R. (2001). Sorting of proteins into multivesicular bodies: ubiquitin-dependent and -independent targeting. *Embo J* 20, 5176-5186.
- Resh, M. D. (1999). Fatty acylation of proteins: new insights into membrane targeting of myristoylated and palmitoylated proteins. *Biochim Biophys Acta* 1451, 1-16.
- Resh, M. D. (2004). Membrane targeting of lipid modified signal transduction proteins. *Subcell Biochem* 37, 217-232.
- Riley, B. B., Savage, M. P., Simandl, B. K., Olwin, B. B., and Fallon, J. F. (1993). Retroviral expression of FGF-2 (bFGF) affects patterning in chick limb bud. *Development* 118, 95-104.
- Rittig, M. G., and Bogdan, C. (2000). Leishmania-host-cell interaction: complexities and alternative views. *Parasitol Today* 16, 292-297.
- Robbins, A. R., and Roff, C. F. (1987). Isolation of mutant Chinese hamster ovary cells defective in endocytosis. *Methods Enzymol* 138, 458-470.
- Robineau, S., Chabre, M., and Antonny, B. (2000). Binding site of brefeldin A at the interface between the small G protein ADP-ribosylation factor 1 (ARF1) and the nucleotide-exchange factor Sec7 domain. *Proc Natl Acad Sci U S A* 97, 9913-9918.
- Robinson, M. S. (1987). 100-kD coated vesicle proteins: molecular heterogeneity and intracellular distribution studied with monoclonal antibodies. *J Cell Biol* 104, 887-895.
- Rocks, O., Peyker, A., Kahms, M., Verveer, P. J., Koerner, C., Lumbierres, M., Kuhlmann, J., Waldmann, H., Wittinghofer, A., and Bastiaens, P. I. (2005). An acylation cycle regulates localization and activity of palmitoylated Ras isoforms. *Science* 307, 1746-1752.
- Rogelj, S., Klagsbrun, M., Atzmon, R., Kurokawa, M., Haimovitz, A., Fuks, Z., and Vlodavsky, I. (1989). Basic fibroblast growth factor is an extracellular matrix component required for supporting the proliferation of vascular endothelial cells and the differentiation of PC12 cells. *J Cell Biol* 109, 823-831.
- Rohrschneider, L. R. (1980). Adhesion plaques of Rous sarcoma virus-transformed cells contain the src gene product. *Proc Natl Acad Sci U S A* 77, 3514-3518.
- Rot, A., and von Andrian, U. H. (2004). Chemokines in innate and adaptive host defense: basic chemokinese grammar for immune cells. *Annu Rev Immunol* 22, 891-928.
- Rothman, J. E. (1990). The reconstitution of intracellular protein transport in cell-free systems. *Harvey Lect* 86, 65-85.
- Rothman, J. E. (1994). Mechanisms of intracellular protein transport. *Nature* 372, 55-63.
- Rothman, J. E., and Orci, L. (1992). Molecular dissection of the secretory pathway. *Nature* 355, 409-415.
- Rothman, J. E., and Wieland, F. T. (1996). Protein sorting by transport vesicles. *Science* 272, 227-234.

- Rubartelli, A., Cozzolino, F., Talio, M., and Sitia, R. (1990). A novel secretory pathway for interleukin-1 beta, a protein lacking a signal sequence. *EMBO J* 9, 1503-1510.
- Rubartelli, A., and Sitia, R. (1991). Interleukin 1 beta and thioredoxin are secreted through a novel pathway of secretion. *Biochem Soc Trans* 19, 255-259.
- Rudd, C. E., Janssen, O., Prasad, K. V., Raab, M., da Silva, A., Telfer, J. C., and Yamamoto, M. (1993). src-related protein tyrosine kinases and their surface receptors. *Biochim Biophys Acta* 1155, 239-266.
- Rudnick, D. A., McWherter, C. A., Adams, S. P., Ropson, I. J., Duronio, R. J., and Gordon, J. I. (1990). Structural and functional studies of *Saccharomyces cerevisiae* myristoyl-CoA:protein N-myristoyltransferase produced in *Escherichia coli*. Evidence for an acyl-enzyme intermediate. *J Biol Chem* 265, 13370-13378.
- Rusnati, M., Urbinati, C., Tanghetti, E., Dell'Era, P., Lortat-Jacob, H., and Presta, M. (2002). Cell membrane GM1 ganglioside is a functional coreceptor for fibroblast growth factor 2. *Proc Natl Acad Sci U S A* 99, 4367-4372.
- Sacks, D. L. (1989). Metacyclogenesis in *Leishmania* promastigotes. *Exp Parasitol* 69, 100-103.
- Sacks, D. L., Barral, A., and Neva, F. A. (1983). Thermosensitivity patterns of Old vs. New World cutaneous strains of *Leishmania* growing within mouse peritoneal macrophages in vitro. *Am J Trop Med Hyg* 32, 300-304.
- Saiki, R. K., Gelfand, D. H., Stoffel, S., Scharf, S. J., Higuchi, R., Horn, G. T., Mullis, K. B., and Erlich, H. A. (1988). Primer-directed enzymatic amplification of DNA with a thermostable DNA polymerase. *Science* 239, 487-491.
- Sato, S., Burdett, I., and Hughes, R. C. (1993). Secretion of the baby hamster kidney 30-kDa galactose-binding lectin from polarized and nonpolarized cells: a pathway independent of the endoplasmic reticulum-Golgi complex. *Exp Cell Res* 207, 8-18.
- Schäfer, T., Zentgraf, H., Zehe, C., Brügger, B., Bernhagen, J., and Nickel, W. (2004). Unconventional secretion of fibroblast growth factor 2 is mediated by direct translocation across the plasma membrane of mammalian cells. *J Biol Chem* 279, 6244-6251.
- Schatz, G., and Dobberstein, B. (1996). Common principles of protein translocation across membranes. *Science* 271, 1519-1526.
- Schekman, R., and Orci, L. (1996). Coat proteins and vesicle budding. *Science* 271, 1526-1533.
- Schroeder, H., Leventis, R., Rex, S., Schelhaas, M., Nagele, E., Waldmann, H., and Silviu, J. R. (1997). S-Acylation and plasma membrane targeting of the farnesylated carboxyl-terminal peptide of N-ras in mammalian fibroblasts. *Biochemistry* 36, 13102-13109.
- Schuster, F. L., and Sullivan, J. J. (2002). Cultivation of clinically significant hemoflagellates. *Clin Microbiol Rev* 15, 374-389.
- Schwartz, S. M., and Liaw, L. (1993). Growth control and morphogenesis in the development and pathology of arteries. *J Cardiovasc Pharmacol* 21 Suppl 1, S31-49.
- Schweigerer, L., Neufeld, G., Friedman, J., Abraham, J. A., Fiddes, J. C., and Gospodarowicz, D. (1987). Capillary endothelial cells express basic fibroblast growth factor, a mitogen that promotes their own growth. *Nature* 325, 257-259.

- Seelenmeyer, C., Wegehingel, S., Lechner, J., and Nickel, W. (2003). The cancer antigen CA125 represents a novel counter receptor for galectin-1. *J Cell Sci* 116, 1305-1318.
- Seelenmeyer, C., Wegehingel, S., Tews, I., Kunzler, M., Aebi, M., and Nickel, W. (2005). Cell surface counter receptors are essential components of the unconventional export machinery of galectin-1. *J Cell Biol* 171, 373-381.
- Seetharaman, J., Kanigsberg, A., Slaaby, R., Leffler, H., Barondes, S. H., and Rini, J. M. (1998). X-ray crystal structure of the human galectin-3 carbohydrate recognition domain at 2.1-Å resolution. *J Biol Chem* 273, 13047-13052.
- Sheetz, M. P., Sable, J. E., and Dobereiner, H. G. (2006). Continuous membrane-cytoskeleton adhesion requires continuous accommodation to lipid and cytoskeleton dynamics. *Annu Rev Biophys Biomol Struct* 35, 417-434.
- Shimizu, N., Soda, Y., Kanbe, K., Liu, H. Y., Mukai, R., Kitamura, T., and Hoshino, H. (2000). A putative G protein-coupled receptor, RDC1, is a novel coreceptor for human and simian immunodeficiency viruses. *J Virol* 74, 619-626.
- Shin, J. T., Opalenik, S. R., Wehby, J. N., Mahesh, V. K., Jackson, A., Tarantini, F., Maciag, T., and Thompson, J. A. (1996). Serum-starvation induces the extracellular appearance of FGF-1. *Biochim Biophys Acta* 1312, 27-38.
- Shlomai, J. (2004). The structure and replication of kinetoplast DNA. *Curr Mol Med* 4, 623-647.
- Siegel, V. (1995). A second signal recognition event required for translocation into the endoplasmic reticulum. *Cell* 82, 167-170.
- Singer, S. J. (1990). The structure and insertion of integral proteins in membranes. *Annu Rev Cell Biol* 6, 247-296.
- Smith, D. F., Gokool, S., Keen, J. K., McKean, P. G., and Rangarajan, D. (1994). Structure and function of infective stage proteins of *Leishmania*. *Biochem Soc Trans* 22, 286-291.
- Solimena, M., Aggujaro, D., Muntzel, C., Dirkx, R., Butler, M., De Camilli, P., and Hayday, A. (1993). Association of GAD-65, but not of GAD-67, with the Golgi complex of transfected Chinese hamster ovary cells mediated by the N-terminal region. *Proc Natl Acad Sci U S A* 90, 3073-3077.
- Söllner, T., Bennett, M. K., Whiteheart, S. W., Scheller, R. H., and Rothman, J. E. (1993). A Protein Assembly-Disassembly Pathway In Vitro That May Correspond to Sequential Steps of Synaptic Vesicle Docking, Activation, and Fusion. *Cell* 75, 409-418.
- Söllner, T. H. (2002). Vesicle tethers promoting fusion machinery assembly. *Dev Cell* 2, 377-378.
- Söllner, T. H., and Rothman, J. E. (1996). Molecular machinery mediating vesicle budding, docking and fusion. *Cell Structure And Function* Oct 21, 407-412.
- Sonnichsen, B., Watson, R., Clausen, H., Misteli, T., and Warren, G. (1996). Sorting by COP I-coated vesicles under interphase and mitotic conditions. *J Cell Biol* 134, 1411-1425.
- Stager, S., Alexander, J., Kirby, A. C., Botto, M., Rooijen, N. V., Smith, D. F., Brombacher, F., and Kaye, P. M. (2003). Natural antibodies and complement are endogenous adjuvants for vaccine-induced CD8⁺ T-cell responses. *Nat Med* 9, 1287-1292.
- Stager, S., Smith, D. F., and Kaye, P. M. (2000). Immunization with a recombinant stage-regulated surface protein from *Leishmania donovani* induces protection against visceral leishmaniasis. *J Immunol* 165, 7064-7071.

- Stamnes, M. A., and Rothman, J. E. (1993). The binding of AP-1 clathrin adaptor particles to Golgi membranes requires ADP-ribosylation factor, a small GTP-binding protein. *Cell* 73, 999-1005.
- Stegmayer, C., Kehlenbach, A., Tournaviti, S., Wegehangel, S., Zehe, C., Denny, P., Smith, D. F., Schwappach, B., and Nickel, W. (2005). Direct transport across the plasma membrane of mammalian cells of *Leishmania* HASPB as revealed by a CHO export mutant. *J Cell Sci* 118, 517-527.
- Stinchcombe, J., Bossi, G., and Griffiths, G. M. (2004). Linking albinism and immunity: the secrets of secretory lysosomes. *Science* 305, 55-59.
- Stoorvogel, W., Kleijmeer, M. J., Geuze, H. J., and Raposo, G. (2002). The biogenesis and functions of exosomes. *Traffic* 3, 321-330.
- Sudhof, T. C. (2004). The synaptic vesicle cycle. *Annu Rev Neurosci* 27, 509-547.
- Sukegawa, J., Semba, K., Yamanashi, Y., Nishizawa, M., Miyajima, N., Yamamoto, T., and Toyoshima, K. (1987). Characterization of cDNA clones for the human c-yes gene. *Mol Cell Biol* 7, 41-47.
- Sutton, R. B., Fasshauer, D., Jahn, R., and Brunger, A. T. (1998). Crystal structure of a SNARE complex involved in synaptic exocytosis at 2.4 Å resolution. *Nature* 395, 347-353.
- Szebenyi, G., and Fallon, J. F. (1999). Fibroblast growth factors as multifunctional signaling factors. *Int Rev Cytol* 185, 45-106.
- Tajima, S., Lauffer, L., Rath, V. L., and Walter, P. (1986). The signal recognition particle receptor is a complex that contains two distinct polypeptide chains. *J Cell Biol* 103, 1167-1178.
- Takel, K., McPherson, P. S., Schmid, S. L., and De Camilli, P. (1995). Tubular membrane invaginations coated by dynamin rings are induced by GTP- γ S in nerve terminals. *Nature* 374, 186-190.
- Tarantini, F., Gamble, S., Jackson, A., and Maciag, T. (1995). The cysteine residue responsible for the release of fibroblast growth factor-1 resides in a domain independent of the domain for phosphatidylserine binding. *J Biol Chem* 270, 29039-29042.
- Tarantini, F., LaVallee, T., Jackson, A., Gamble, S., Carreira, C. M., Garfinkel, S., Burgess, W. H., and Maciag, T. (1998). The extravesicular domain of synaptotagmin-1 is released with the latent fibroblast growth factor-1 homodimer in response to heat shock. *J Biol Chem* 273, 22209-22216.
- Taverna, S., Gherzi, G., Ginestra, A., Rigogliuso, S., Pecorella, S., Alaimo, G., Saladino, F., Dolo, V., Dell'Era, P., Pavan, A., *et al.* (2003). Shedding of membrane vesicles mediates fibroblast growth factor-2 release from cells. *J Biol Chem* 278, 51911-51919.
- Thery, C., Boussac, M., Veron, P., Ricciardi-Castagnoli, P., Raposo, G., Garin, J., and Amigorena, S. (2001). Proteomic analysis of dendritic cell-derived exosomes: a secreted subcellular compartment distinct from apoptotic vesicles. *J Immunol* 166, 7309-7318.
- Thery, C., Zitvogel, L., and Amigorena, S. (2002). Exosomes: composition, biogenesis and function. *Nat Rev Immunol* 2, 569-579.
- Thomas, S. M., and Brugge, J. S. (1997). Cellular functions regulated by Src family kinases. *Annu Rev Cell Dev Biol* 13, 513-609.
- Thrift, R. N., Andrews, D. W., Walter, P., and Johnson, A. E. (1991). A nascent membrane protein is located adjacent to ER membrane proteins throughout its integration and translation. *J Cell Biol* 112, 809-821.

- Tilakaratne, N., and Sexton, P. M. (2005). G-Protein-coupled receptor-protein interactions: basis for new concepts on receptor structure and function. *Clin Exp Pharmacol Physiol* 32, 979-987.
- Tournaviti, S., Hannemann, S., Terjung, S., Kitzing, T. M., Stegmayer, C., Ritzerfeld, J., Grosse, R., Nickel, W., and Fackler, O. T. (2006 submitted). SH4 Domain-induced Plasma Membrane Blebbing Implicated in 3D Cell Motility.
- Towbin, H., Staehelin, T., and Gordon, J. (1979). Electrophoretic transfer of proteins from polyacrylamide gels to nitrocellulose sheets: procedure and some applications. *Proc Natl Acad Sci U S A* 76, 4350-4354.
- Traub, L. M., Bannykh, S. I., Rodell, J. E., Aridor, M., Balch, W. E., and Kornfeld, S. (1996). Ap 2 containing clathrin coats assemble on mature lysosomes. *Journal Of Cell Biology* Dec 135, 1801-1814.
- Trudel, C., Faure-Desire, V., Florkiewicz, R. Z., and Baird, A. (2000). Translocation of FGF2 to the cell surface without release into conditioned media [In Process Citation]. *J Cell Physiol* 185, 260-268.
- Tsay, Y. G., Lin, N. Y., Voss, P. G., Patterson, R. J., and Wang, J. L. (1999). Export of galectin-3 from nuclei of digitonin-permeabilized mouse 3T3 fibroblasts. *Exp Cell Res* 252, 250-261.
- Turco, S. J., and Descoteaux, A. (1992). The lipophosphoglycan of *Leishmania* parasites. *Annu Rev Microbiol* 46, 65-94.
- Ungar, D., and Hughson, F. M. (2003). SNARE protein structure and function. *Annu Rev Cell Dev Biol* 19, 493-517.
- Unsicker, K., Engels, S., Hamm, C., Ludecke, G., Meier, C., Renzing, J., Terbrack, H. G., and Flanders, K. (1992). Molecular control of neural plasticity by the multifunctional growth factor families of the FGFs and TGF-beta s. *Ann Anat* 174, 405-407.
- Urlinger, S., Baron, U., Thellmann, M., Hasan, M. T., Bujard, H., and Hillen, W. (2000). Exploring the sequence space for tetracycline-dependent transcriptional activators: novel mutations yield expanded range and sensitivity. *Proc Natl Acad Sci U S A* 97, 7963-7968.
- van Niel, G., Porto-Carreiro, I., Simoes, S., and Raposo, G. (2006). Exosomes: a common pathway for a specialized function. *J Biochem (Tokyo)* 140, 13-21.
- van't Hof, W., and Resh, M. D. (1999). Dual fatty acylation of p59(Fyn) is required for association with the T cell receptor zeta chain through phosphotyrosine-Src homology domain-2 interactions. *J Cell Biol* 145, 377-389.
- Veit, M., and Schmidt, M. F. (1993). Timing of palmitoylation of influenza virus hemagglutinin. *FEBS Lett* 336, 243-247.
- Vertel, B. M., Walters, L. M., and Mills, D. (1992). Subcompartments of the endoplasmic reticulum. *Semin Cell Biol* 3, 325-341.
- Wakisaka, N., Murono, S., Yoshizaki, T., Furukawa, M., and Pagano, J. S. (2002). Epstein-barr virus latent membrane protein 1 induces and causes release of fibroblast growth factor-2. *Cancer Res* 62, 6337-6344.
- Walter, P. (1992). Protein translocation. Travelling by TRAM. *Nature* 357, 22-23.
- Walter, P., Gilmore, R., and Blobel, G. (1984). Protein translocation across the endoplasmic reticulum. *Cell* 38, 5-8.

- Walter, P., and Lingappa, V. R. (1986). Mechanism of protein translocation across the endoplasmic reticulum membrane. *Annu Rev Cell Biol* 2, 499-516.
- Warnock, D. E., Hinshaw, J. E., and Schmid, S. L. (1996). Dynamin self assembly stimulates its gtpase activity. *Journal Of Biological Chemistry* Sep 271, 22310-22314.
- Warren, G., and Malhotra, V. (1998). The organisation of the Golgi apparatus. *Curr Opin Cell Biol* 10, 493-498.
- Weber, T., Zemelman, B. V., McNew, J. A., Westermann, B., Gmachl, M., Parlati, F., Sollner, T. H., and Rothman, J. E. (1998). SNAREpins: minimal machinery for membrane fusion. *Cell* 92, 759-772.
- Wendland, B. (2002). Epsins: adaptors in endocytosis? *Nat Rev Mol Cell Biol* 3, 971-977.
- Whetstone, H., and Lingwood, C. (2003). 3'Sulfogalactolipid binding specifically inhibits Hsp70 ATPase activity in vitro. *Biochemistry* 42, 1611-1617.
- Wilcox, C., Hu, J. S., and Olson, E. N. (1987). Acylation of proteins with myristic acid occurs cotranslationally. *Science* 238, 1275-1278.
- Wilson, K. P., Black, J. A., Thomson, J. A., Kim, E. E., Griffith, J. P., Navia, M. A., Murcko, M. A., Chambers, S. P., Aldape, R. A., Raybuck, S. A., and et al. (1994). Structure and mechanism of interleukin-1 beta converting enzyme. *Nature* 370, 270-275.
- Yasuda, K., Kosugi, A., Hayashi, F., Saitoh, S., Nagafuku, M., Mori, Y., Ogata, M., and Hamaoka, T. (2000). Serine 6 of Lck tyrosine kinase: a critical site for Lck myristoylation, membrane localization, and function in T lymphocytes. *J Immunol* 165, 3226-3231.
- Ye, R. D., Wun, T. C., and Sadler, J. E. (1988). Mammalian protein secretion without signal peptide removal. Biosynthesis of plasminogen activator inhibitor-2 in U-937 cells. *J Biol Chem* 263, 4869-4875.
- Zehe, C., Engling, A., Wegehangel, S., Schafer, T., and Nickel, W. (2006). Cell-surface heparan sulfate proteoglycans are essential components of the unconventional export machinery of FGF-2. *Proc Natl Acad Sci U S A* 103, 15479-15484.
- Zhu, X., Komiya, H., Chirino, A., Faham, S., Fox, G. M., Arakawa, T., Hsu, B. T., and Rees, D. C. (1991). Three-dimensional structures of acidic and basic fibroblast growth factors. *Science* 251, 90-93.

Acknowledgement

I want to express my gratitude to Prof. Dr. rer. nat. Walter Nickel for giving me the opportunity to work in his laboratory on this interesting project as well as for his outstanding supervision, scientific enthusiasm and permanent guidance throughout my time at the BZH.

My sincere gratitude and appreciation goes to our collaboration partner Prof. Dr. Deborah Smith for giving me the possibility to work in her laboratory in London (UK) and York (UK) and for her generous support concerning the HASPB project. Especially, I want to thank Dr. Helen Price and Dr. Cristina Guerra Giraldez for being my supervisors and guides in London and York.

I want to thank Prof. Dr. rer. nat. Michael Brunner for being my second appraiser.

I want to thank Angelika Kehlenbach and Julia Lenz (AG Schwappach) for their generous help with FACS sorting.

I am grateful to Dr. Oliver Fackler for his support concerning the HASPB project and for the nice collaboration concerning the “blebbing project”.

I am deeply indebted to Dr. Claudia Seelenmeyer for her critical comments on the manuscript, for very fruitful discussions, her time spending with proofreading, for all the good and bad times together in the ‘nickellab’ and for just being a good friend.

I am very grateful to Sabine Wegehinkel for her generous help concerning laboratory issues and for her personal support in every aspect.

A special thank goes to my writing fellow Christoph Zehe for mental support, helpful discussions, so for just being there all the time.

A huge “Thank you” goes to Stella Tournaviti for her support concerning the “K3 paper” and for being a friend throughout all the time.

Special thanks go to Koen Temmermann for his great support concerning my decision to work as postdoc in Australia, for nice discussions on our balcony and for his delivery service.

I want to thank all past and present members of the ‘Nickellab’, who provided a pleasant, friendly and productive atmosphere in the lab. Without the help of Dr. Rafael Backhaus, Lucía Cespón Torrado, Antje Ebert, Dr. André Engling, Julia Ritzerfeld, Dr. Claudia Seelenmeyer, Christian Schäfer, Koen Temmerman, Stella Tournaviti, Sabine Wegehinkel, Jaz Woo and Christoph Zehe this work would have been less successful.

Additionally, I am grateful to all past and present members of the “3rd floor”, especially Dr. Britta Brügger, Barbara Schröter, and Sandra Zitzler.

An absolute special ‘thank you’ goes to my partner in life, Joachim Elzer, for his support, understanding, encouragement, listening and finally sharing good and bad times with me.

I would like to thank all my friends - especially Cornelia Paatz for ‘proofreading’ of the manuscript, for their understanding, good conversations and encouragement during all the time.

I also want express my deepest gratitude to my brothers and sisters, Dr. Christian Stegmayer, Clarissa Stegmayer and Constantin Stegmayer and their partners Christine Stegmayer, Uwe Helde and Sandra Mann for their support throughout all the time and for spending great times on the weekends at home, in Konstanz, Hamburg and Stuttgart.

My deepest gratitude goes to my parents, Dr. Gudrun Stegmayer and Dr. Hans-Michael Stegmayer for their endless support in every aspect, for paving the way for my education and for the love I received under all circumstances of my life.

Herewith I declare that this thesis is my own work and that I cited all references and help used. I consent to this thesis being deposited in and distributed by the Library of the Ruperto Carola University, Heidelberg.

November 2006